

POWER CORRECTIONS AND RAPIDITY LOGARITHMS
IN SOFT-COLLINEAR EFFECTIVE THEORY

by

Matthew Inglis-Whalen

A thesis submitted in conformity with the requirements
for the degree of Doctor of Philosophy
Graduate Department of Physics
University of Toronto

Abstract

Power Corrections and Rapidity Logarithms
in Soft-Collinear Effective Theory

Matthew Inglis-Whalen

Doctor of Philosophy

Graduate Department of Physics

University of Toronto

2022

In this thesis a recent formulation of Soft-Collinear Effective Theory is used to study power corrections to collider observables. The techniques and concepts developed here are primarily demonstrated in the context of the Drell-Yan process, but are also broadly applicable in processes involving high-energy collimated colored particles.

First, we make progress towards the resummation of power-suppressed logarithms in processes which involve the hard interaction of two jets. We identify and compute the anomalous dimensions of all the operators that contribute to two-sector processes at $O(1/q^2)$. These anomalous dimensions are necessary to resum hard processes at next-to-leading power, although an additional observable-dependent step of matching and running is necessary to complete the full resummation. We also demonstrate how the overlap subtraction prescription for loops extends to these subleading operators.

Next, we study the origin of rapidity logarithms using a formulation of Soft-Collinear Effective Theory in which infrared degrees of freedom are not explicitly separated into modes. We consider the Sudakov form factor with a massive vector boson and Drell-Yan production of lepton pairs at small transverse momentum as demonstrative examples. We find that rapidity divergences introduce a scheme dependence into the effective theory and are associated with large logarithms appearing in the soft matching conditions. This scheme dependence may be used to derive corresponding rapidity renormalization group equations.

Finally, we examine the Drell-Yan process at next-to-leading power, where we derive a factorization of the differential cross section in the small- q_T hierarchy with $q^2 \gg q_T^2 \gg \Lambda_{\text{QCD}}^2$. We show that the cross section may be written in terms of matrix elements of power-suppressed operator products which contribute to $O(q_T^2/q^2)$ coefficients of the usual parton distribution functions. The factorization formula allows power-suppressed logarithms in each of the relevant factors to be resummed. We discuss the cancellation of rapidity divergences and the overlap subtractions required to eliminate double counting at next-to-leading power.

Acknowledgements

I would like to thank Michael Luke for guiding me through this long process. When we are able to get him in the mood, it is a delight to hear Mike's many anecdotes about the various characters he has encountered over the course of his career. His expertise and guidance has been invaluable in completing this thesis, and it has been a pleasure working with him.

I have many fond memories of the long discussions held with my fellow grad-student colleagues. As my senior, Raymond Goerke was incredibly helpful in teaching me about SCET, its philosophy, and in showing me how to wield Mathematica. I thoroughly enjoyed his weekly rants about his new favourite mathematical tool or concept, and the lab is poorer for his absence. As my juniors, Aris Spourdalakis and Jyotirmoy Roy have been very patient with my frequent interruptions to hash out some new idea on the blackboard, and have proven to be very helpful as partners in the quest for new and fruitful ideas.

Getting through the stresses of grad-life would have been far less enjoyable without the camaraderie of my Toronto friends; Andrew Fleck, Patrick Harrison, Peter Hayman, thank you, let's crack open a cold one. And to my Ottawa friends I had to leave behind – Alain and Sebastian Abols, Ryan Abels, and Anthony Abraham, who neverendingly ask me when I will be inventing the first teleportation device – thanks for believing in me, I miss you guys.

I feel privileged to have gotten to this point in my studies, a point I would not have reached without the bottomless love and encouragement from my mother Sandy Inglis. She has always been there for me, and I am deeply grateful to her. Thanks Mom, I love you forever, I love you for always.

Lastly, I would like to thank my long-time partner Meaghan McManus for being by my side during this stressful period of our lives. Your struggles and triumphs along your own path in grad school have been an inspiration, and my journey would not have been possible without your unending love and support. BXOBXO.

Contents

1	Introduction	1
1.1	The Trouble with QCD	2
1.2	Drell-Yan and its Small- q_T Power Corrections	4
1.3	Contents of Thesis	6
1.3.1	Renormalization of NLP Operators	6
1.3.2	Rapidity Divergences and Logarithms	7
1.3.3	Factorization of Small- q_T Power Corrections	8
2	Effective Field Theories	9
2.1	EFT Generalities	10
2.1.1	Many Energy Scales	10
2.1.2	Logarithmic Precision Counting	11
2.1.3	The Need to Study Power Corrections	12
2.2	The 4-Fermi Effective Theory	14
2.2.1	Beyond Tree Level	16
2.2.2	Log Minimization and Summation	17
2.3	Jets and Soft-Collinear Effective Theory	19
2.3.1	Analogy to the 4-Fermi EFT	20
2.3.2	The Usual SCET Formulation	24
3	Renormalization of Dijet Operators at $1/Q^2$	27
3.1	Introduction	27
3.2	Formalism Review	28
3.2.1	Notation	29
3.2.2	Matching	31
3.3	Renormalization of Subleading Operators	35
3.3.1	Overlap Subtraction	35
3.3.2	Organization of the Calculation	35
3.3.3	Results	37
3.4	Conclusion	39
4	Rapidity Logarithms in SCET Without Modes	40
4.1	Introduction	40
4.2	The Massive Sudakov Form Factor	42

4.2.1	Soft-Collinear Factorization	43
4.2.2	Scheme Dependence Without Modes	44
4.2.3	Resummation	47
4.3	Drell-Yan at Small q_T	51
4.3.1	Factorization by Successive Matching	52
4.3.2	Matrix Elements of $T_{(0,0)}$	53
4.3.3	Resummation	57
4.4	Conclusions	58
5	Factorization of Power Corrections in the Drell-Yan Process	59
5.1	Introduction	59
5.1.1	Factorization	61
5.2	NLP Operator Products in SCET	64
5.2.1	Hard-Scale Matching	65
5.2.2	Renormalization Group Running	68
5.2.3	$T_{(i,j)}$ Definitions	69
5.2.4	Matrix Elements of Operator Products	70
5.2.5	C_{ff} at Fixed Order	80
5.2.6	Rapidity Running	83
5.3	Overlap Subtractions at NLP	85
5.3.1	Overlap Subtraction and Scheme Dependence at LP	86
5.3.2	Overlap Subtraction and Scheme Dependence at NLP	88
5.4	Conclusion	94
5.A	Summary of Matrix Elements of Hard Scattering Operators	95
5.B	Plus Distribution Identities	96
5.B.1	Single Variable Plus Distributions	96
5.B.2	Vector Plus Distributions	98
5.C	Fixed-Order Comparison	99
6	Conclusions	103
6.1	Epilogue	105
Appendices		106
A	QCD Expansion up to $O(1/Q^2)$	106
Bibliography		108

Chapter 1

Introduction

The Standard Model of particle physics (SM) is currently our best description of the fundamental building blocks of Nature. This $SU(3)_C \times SU(2)_L \times SU(1)_Y$ chiral gauge theory has three generations of fermionic fields for each of the quarks and leptons, and their coupling to a massive scalar field generates the fermion masses after spontaneous symmetry breaking to $SU(3)_c \times SU(1)_{\text{em}}$.

It is well known, however, that the Standard Model cannot be a complete description of matter and its interactions. Since the discovery of neutrino oscillations [1, 2] it has remained undecided whether neutrinos are Dirac or Majorana fermions [3]. It is also unknown how Einstein's theory of gravity can be merged with the Standard Model in a way that will be applicable at all energy scales [4, 5], and little is known about Dark Energy other than the fact that it exists [6, 7]. Furthermore, astronomical data has long implied the presence of a non-SM form of matter [8], and it is widely believed that this Dark Matter has a particle-based description in some as-yet-unknown extension of the Standard Model [9, 10]. Though these theoretical and cosmological issues provide no specific indication about the field-theoretical properties of physics beyond the Standard Model, recent terrestrial experiments are also finding tentative evidence that the Standard Model cannot describe all the acquired data, and together are beginning to produce a coherent picture of the nature of new physics. For example, the short-baseline MiniBooNe experiment has found excess electron-neutrinos appearing in a muon-neutrino beam [11], confirming previously measured excesses at LSND [12]. Additionally, measurements of the muon's anomalous magnetic moment $g - 2$ at Fermilab have increased [13] the already large discrepancy [14] between experiment and SM predictions. Even further, decays of B -mesons to electrons or muons at LHCb have shown evidence for lepton non-universality [15]. Though none of these experiments individually cross the discovery threshold, in combination they provide a hint that new physics perhaps lies in the lepton sector.

Measuring the coupling of leptons to the Higgs boson or other particles present in high-energy scattering experiments could further pinpoint the origin of non-SM physics. The current energy frontier is being explored by the Large Hadron Collider (LHC), which has a design center-of-mass energy of 14 TeV. The LHC has now been collecting data for over a decade, with perhaps its most important observation being the discovery of the Higgs boson during the course of its first run [16, 17]. Its second run, now complete, continued to gather important information about how the Higgs couples to matter [18]. In order to determine the properties of the Higgs, and particularly in order to determine whether these properties are predicted by the Standard Model, it is important to have a thorough and precise

understanding of how the LHC’s high-energy hadrons interact to produce the various particles seen in its detector.

Hadronic matter, being made of colored particles, is described by Quantum Chromodynamics (QCD). In this thesis, effective theories of QCD are studied and developed in order to better understand how colored particles interact, and ultimately to improve the theoretical precision of collider observables according to the Standard Model. In the following section we provide some context for these goals by briefly describing the history of QCD and, through the lens of Effective Field Theory (EFT), discussing the fundamental limitations for which types of quantities are calculable in hadronic environments. We then introduce the Drell-Yan process [19], the main observable studied in this thesis, and review recent theoretical developments which motivate a continued interest in an observable that has been well-studied for 40 years [20]. We finish this chapter with an overview of the three papers that form the main contents of this thesis.

1.1 The Trouble with QCD

By the late 1950s it appeared that the list of fundamental particles numbered in the many dozens [21], with pions, kaons, cascade particles, vector mesons, and many others making up the “particle zoo” [22]. In order to explain certain symmetries between these hadrons, it was proposed in the early 1960s that these particles were not fundamental, but rather were composed of pointlike particles called quarks [23–25]. This was first confirmed in high-energy electron-proton scattering experiments that were able to probe the internal structure of the proton [26, 27], the results of which were soon framed in the parton model of nuclear substructure [28, 29]. While these Deep Inelastic Scattering (DIS) experiments showed that protons contained spin-1/2 electromagnetically-charged quarks, it was later argued that quarks alone did not properly account for the total momentum of a proton [30]. This indirect evidence for the existence of some electromagnetically-neutral type of parton aligned perfectly with the co-developing knowledge of non-Abelian gauge theories [31–34]. In particular, it was proposed that quarks come in three distinct colors and that the color force is mediated by color-charged gluons [35], as is now described in the Standard Model by Quantum Chromodynamics. By the mid 1970s it was well accepted that the remaining momentum of a proton was accounted for by the existence of the spin-1 gluons [36]. It was not until the late 1970s, however, that the gluon was directly confirmed to exist by observing 3-jet events in electron-positron colliders [37].

The difficulty in confirming the existence of quarks and gluons is due to the phenomenon of confinement, where the overwhelming long-range attraction between colored objects ensures that quarks and gluons can never be observed in isolation. Rather, the only objects that are measurable in experiments are color-neutral bundles of quarks and gluons that we call hadrons. This disparity between the fundamental building blocks of QCD, the quarks and gluons, and the objects that are observed in experiments, the hadrons, has deep implications for the types of calculations and predictions that can be made by studying QCD without reference to experiment. For example, confinement is related to the fact that at low energies ($E \lesssim \Lambda_{QCD} \sim 300$ MeV) the coupling strength between colored particles is large. This strong coupling prevents the use of perturbation theory and so analytically extracting theoretical predictions from QCD becomes a completely intractable problem. If we could somehow calculate the partonic composition of hadrons we could establish a link between the disparate experimental and theoretical degrees of freedom, but the large coupling strength in the relevant energy regime prevents us from using

the only tool we have at our disposal to make such a calculation¹. How then are we supposed to describe the transition probabilities between the incoming and outgoing hadronic states that are prepared and measured in experiments?

Fortunately, there are ideas and tools that still allow progress to be made. Qualitatively, one often observes that low-energy dynamics need not know about high-energy physics in order for calculations at low energies to be predictive [43]. The classic example is that atomic models don't need to include information about the top quark ($M_{\text{top}} \sim 200$ GeV) or the complicated internal dynamics of the proton ($E_{\text{partons}} \sim 300$ MeV) in order to adequately describe the hydrogen atom (with energy splittings $E_{\text{kin}} \sim 10$ eV). The reverse situation is also observed: high-energy (short-distance) physical properties need not know about the intricate details of low-energy (long-distance) physics in order to be predictive; the proton's internal structure does not depend on the location of the moon or the stars.

A mathematical consequence of this decoupling of energy scales is that observables tend to factorize in the presence of large scale separations; when an observable involves two or more widely separated energy scales, the observable can often be decomposed into multiple factors, with each factor depending on only one energy scale. Consider a toy observable $\Sigma(Q, E)$ that depends on two widely separated scales $Q \gg E$, where Q is some experimentally tunable energy scale, and E is some fixed energy scale representing the internal dynamics of the system we are studying. We will discuss various examples of such systems in Chapter 2, but for now it can be useful to imagine that Q represents the center-of-mass energy of two composite particles and E represents the binding energy of each particle. In many such systems the scales Q and E will decouple, and Σ will schematically have the factorization

$$\Sigma(Q, E) = C(Q, \mu) f(E, \mu) + O\left(\frac{E}{Q}\right), \quad (1.1)$$

where μ is some arbitrary energy scale called the factorization scale. Having such a factorization is quite beneficial; if $C(Q, \mu)$ is some calculable function of Q , then even if $f(E, \mu)$ is some incalculable function of E , only one measurement of Σ is necessary in order to predict Σ for all possible experimental energies Q . This is because, when $C(Q, \mu)$ is known, then a measurement of $\Sigma(Q, E)$ also represents a measurement of $f(E, \mu)$. Since $f(E, \mu)$ remains unchanged when a new experimental energy Q' is explored, all factors of the observable $\Sigma(Q', E) = C(Q', \mu) f(E, \mu)$ are therefore known.

Effective Field Theory [44–48] is a framework that allows such factorization formulae to be derived in a straightforward manner. Though this toy example is simply meant to demonstrate some benefits of applying the techniques of EFT, it is not so different from the actual situation encountered when studying hadron scattering. Experimental setups can tune the initial-state collision energy Q of hadrons, while the internal dynamics with $E \sim \Lambda_{\text{QCD}}$ of the colliding hadrons do not depend on the energies at which they collide with one another. In EFT, the Standard Model is replaced with an effective model that does not include the high-energy dynamics, but exactly reproduces the low-energy dynamics. Hadronic matrix elements in the EFT generate non-perturbative and incalculable factors similar to $f(E, \mu)$, and a process called matching uses perturbative partonic calculations to determine matching coefficients

¹Lattice QCD [38] provides a non-perturbative numerical method for studying low-energy phenomena, but it faces the reciprocal issue encountered by perturbation theory in the sense that it cannot be used to study high-energy processes. This is because lattice methods rely on simulating the QCD vacuum on a grid with lattice spacing a ; since the maximum resolvable momentum on a grid scales like $p_{\text{max}} \sim 1/a$, a process involving a momentum transfer Q requires a grid with $N \sim Q^4$ lattice sites in 4 dimensions [39]. At nuclear energy scales $Q \sim 1$ GeV the number of gridpoints is manageable, but at the $Q \gtrsim 1$ TeV energies encountered at modern colliders the processing power is still not available. Moreover, since the grid in Lattice QCD exists in Euclidean spacetime, measuring matrix elements involving timelike separations (like parton distribution functions) introduces a host of new problems to solve, and is still an active area of research [40–42].

similar to $C(Q, \mu)$.

The incalculable factor $f(E, \mu)$ can either be measured in experiment or, in some cases, it can be determined non-perturbatively using lattice methods. However, even Lattice QCD requires externally-acquired measurements in order to fix its length and energy scales. In effect, there is no way to determine $f(E, \mu)$ without reference to experiment. Therefore, since a hadronic observable $\Sigma(Q, E)$ is composed of both perturbative factors $C(Q, \mu)$ and non-perturbative factors $f(E, \mu)$, QCD does not provide an *ab initio* method for predicting the experimental results of hadron scattering. The only calculations that can be done in QCD without reference to experiment are thus only those quantities that do not depend on non-perturbative factors. The list of such quantities is quite short; a non-exhaustive list might include the matching coefficients $C(Q, \mu)$, the anomalous dimensions $\gamma_C(\mu)$ and $\gamma_f(\mu)$ that determine how the factors change with the factorization scale μ , and sufficiently inclusive cross sections for processes involving hadron-free initial states.

In the end, EFT provides a powerful set of tools for determining the factorization structure for each observable of interest. It methodically decomposes observables into matching coefficients that only depend on a single one of the various perturbative energy scales in the problem, and encapsulates all the non-perturbative dynamics in a small set of non-perturbative functions that can be measured once and for all. QCD still has the inherent problem that hadronic observables are incalculable from first principles, but scale separation and the tools of EFT allow for QCD to achieve predictive power for factorizable processes.

1.2 Drell-Yan and its Small- q_T Power Corrections

Since it is important to study the properties of the Higgs boson, and especially its interaction with leptons, it is also important to understand similar processes that may mimic the signature of Higgs production in collider environments. One such process is the scattering of hadrons to produce a vector boson that subsequently decays into a lepton pair, also known as the the Drell-Yan (DY) process. This is shown in Fig. 1.1.

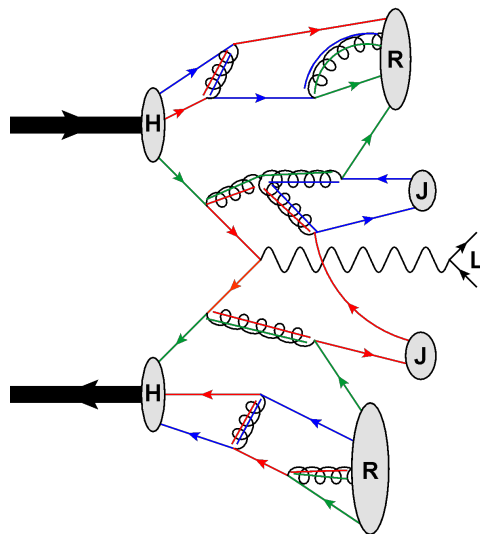


Figure 1.1: A cartoon of hadron (H) scattering, producing a lepton pair (L), jets (J), and remnants (R) of the colliding hadrons.

In the seminal work of Collins, Soper, and Sterman (CSS, [49–51]), it was rigorously proven that the leading power differential cross section for the Drell-Yan process $H_A(P_A)H_B(P_B) \rightarrow V^*(q) + X$ can be written in the factorized form

$$\frac{1}{\sigma_0} \frac{d\sigma}{dq^2 dy dq_T^2} = \sum_{ab} \int \frac{d^2 \mathbf{b}_T}{(2\pi)^2} e^{i\mathbf{b}_T \cdot \mathbf{q}_T} \int \frac{d\xi_A}{\xi_A} \frac{d\xi_B}{\xi_B} H(Q, \mu_T) \times C_a \left(\frac{x_A}{\xi_A}, \mu_T \right) C_b \left(\frac{x_B}{\xi_B}, \mu_T \right) f_{a/A}(\xi_A, \mu_T) f_{b/B}(\xi_B, \mu_T) + O\left(\frac{q_T^2}{Q^2}, \frac{\Lambda_{\text{QCD}}^2}{Q^2} \right) \quad (1.2)$$

when both $\Lambda_{\text{QCD}}^2 \ll Q^2$ and $q_T^2 \ll Q^2$. Here the sum runs over parton flavors a and b , while $Q = \sqrt{q^2}$ is the hard momentum transfer. The variables $x_{A,B} = e^{\pm y} Q / \sqrt{s}$ are roughly the fractions of the hadronic large momentum components given to the off-shell photon, and $\xi_{A,B}$ may be interpreted as the lightcone momentum fractions of the incoming hadrons given to the initial-state partons. The scale $\mu_T = 1/|\mathbf{b}_T| \sim q_T \ll Q$ is an appropriate low-energy scale for matching transverse momentum dependent parton distribution functions (TMDPDFs), with matching coefficient $C_{a,b}$, onto the PDFs $f_{i/H}(\xi, \mu)$ that are measured in Deep Inelastic Scattering experiments.

In the CSS formalism each of the perturbative factors that appear in Eq. (1.2) originates from a region of momentum space where, due to the location of propagator poles in the complex plane, the path of integration cannot be deformed to avoid every pole. The momentum regions where this occurs are called pinched singular surfaces, and factorization follows from the notion that these surfaces create non-overlapping contributions to the parton-level cross section. Each of the factors – and hence the entire differential cross section – of the leading power CSS formula are available in resummed form up to N^3LL [52–58]. Estimates for the relative sizes of N^4LL effects versus power-corrected contributions suggest that it is now more beneficial to extend the factorization and resummation programs beyond leading power. While the CSS formula has been extended to include the non-perturbative power corrections which scale like $O(\Lambda_{\text{QCD}}^2/Q^2)$ [59–63], little is known about the factorization structure of the perturbative power corrections which scale like $O(q_T^2/Q^2)$.

It has been shown in multiple ways how effective theory techniques can be used to reproduce these classic CSS results at leading power [64–67]. The relevant effective theory for jet-like observables, which includes hadron scattering, is called Soft-Collinear Effective Theory (SCET, [68–74]). The usual formulation of SCET takes a parallel approach to CSS, where each of the relevant CSS regions can be mapped onto a distinct degree of freedom (a distinct mode) in the EFT. Factorization then arises from the decoupling of these modes in the effective Lagrangian. Though EFT techniques provide a methodical framework for extending factorization formulae beyond leading power, up until recently the community’s focus has mostly been directed towards improving the precision of leading power calculations. Some recent calculations have determined the fixed order contributions from perturbative power corrections at [75, 76], but none of these achieve a factorization formula in terms of operators that can be renormalized and hence resummed.

This SCET approach to factorizing and resumming collider observables has been wildly successful, but there are certain drawbacks to its usual construction that have initiated a recent reformulation of SCET [77]. Notably, the usual formulation of SCET has different variations (e.g. SCET_I[78], SCET_{II}[79, 80], SCET₊[81]) and different sets of modes depending on the observable being studied, despite the fact that they all share the same high-energy origin of QCD interacting with a hard momentum transfer. Moreover, when constructed using modes, SCET is linked to and defined in terms of the full theory of QCD (see the

end of Section 2.3.2). This link to the full high energy theory induces hard scale dependence in the low energy effective Lagrangian. Since low energy matrix elements should be evaluated at a correspondingly low energy renormalization scale (in order to minimize the dynamically-generated logarithms involving infrared energy scales), the appearance of a high energy parameter in a low energy Lagrangian endangers the usual benefits of having a factorization formula.

These drawbacks can be alleviated by constructing a version of SCET that does not depend on the relative hierarchy of energy scales which are parametrically smaller than the hard interaction scale. The new formulation of SCET which we use in this thesis only segregates degrees of freedom based on their mutual invariant mass, and thus does not rely on modes or regions. The effective theory and the hard-scale matching is the same for all observables, and it is only when observable dependence is asserted that an observable-dependent matching process is initiated. Moreover, the new formulation is treated as a Quantum Field Theory in its own right, and is therefore required to exist independently from – and make predictions without reference to – its parent theory. Relevant limits of QCD tree-level diagrams provide the hard scattering operator basis for our new formalism, but any quantum corrections beyond tree level do not refer back to the equivalent diagrams in QCD. This is in contrast to the method of regions interpretation of SCET [82], where SCET radiative corrections are taken directly from an appropriate expansion of QCD corrections. This is also in contrast to the usual mode formulation of SCET [80], where having correlated rapidity schemes across different modes is motivated by the expected agreement of infrared and rapidity divergences in SCET when compared with QCD. Our formulation is not given any information about QCD beyond tree level, and so as expected from a low energy field theory it does not have any dynamical dependence on the hard scale. It is only when a matching calculation is performed in order to determine the appropriate Wilson coefficient that our formulation of SCET is forced to agree with QCD. Finally, since the new formulation we use here has fewer partitions of the low-energy degrees of freedom, there are fewer operators to find and renormalize in the effective Lagrangian at subleading powers. Since we wish to study power corrections to collider observables, a smaller basis of effective operators makes a full analysis more feasible.

1.3 Contents of Thesis

In Chapter 2 we outline some of the properties that make EFTs such a popular and powerful modern tool for systematically improving the precision of collider-based experimental predictions. We use the 4-Fermi Effective Field Theory as an explicit demonstration of these tools, and use this to help explain the ideas behind the new formulation of Soft-Collinear Effective Theory, which we briefly contrast with the usual SCET construction. Chapters 3, 4, and 5 then describe my original research, which I outline in the following subsections. Finally, Chapter 6 summarizes the main contents of this thesis and finishes with a discussion of possible future research topics.

1.3.1 Renormalization of NLP Operators

If an operator’s counterterm is known then its anomalous dimension can be calculated. The renormalization group can then be used to find an all-orders resummed expression that evolves the operator from the high-energy matching scale down to the next low-energy matching scale. The anomalous dimension for the leading power SCET operator O_2 was found long ago [78], and the anomalous dimensions have recently been calculated for the relevant SCET operators which are suppressed by $O(1/Q)$ in the power

counting [83]. However, the observables which we study here begin at $O(1/Q^2)$, and so all operators which are suppressed by $O(1/Q^2)$ must be determined and subsequently renormalized in order to obtain a complete resummation for any chosen observable at NLP. This is done in Chapter 3.

1.3.2 Rapidity Divergences and Logarithms

In [84] it was noted that the massive Sudakov form factor has the factorization

$$\langle p_2 | J_{\text{QCD}}^\mu | p_1 \rangle = F \left(\frac{Q^2}{M^2} \right) \bar{u}_2 \gamma^\mu u_1 = C_2(Q, \mu) \langle p_2 | O_2(\mu) | p_1 \rangle , \quad (1.3)$$

where up to one loop

$$\begin{aligned} C_2(Q, \mu) &= \left[1 + \frac{\bar{\alpha}}{2} \left(-L_Q^2 + 3L_Q + \frac{\pi^2}{6} - 8 \right) \right] , \text{ and} \\ \langle p_2 | O_2(\mu) | p_1 \rangle &= \left[1 + \frac{\bar{\alpha}}{2} \left(-L_M^2 - L_M(3 - 2L_Q) - \frac{5\pi^2}{6} + \frac{9}{2} \right) \right] \bar{u}_2 \gamma^\mu u_1 . \end{aligned} \quad (1.4)$$

On the basis of scale separation and factorization, matrix elements of effective operators are expected to only contain infrared dynamics and to only generate infrared energy scales. However, the matrix element of the effective operator O_2 depends on the scale Q^2 , which should have been integrated out of the EFT. In the conventional language of tree-level symmetries that are broken by loop effects, some authors have called this unexpected appearance of Q^2 in the EFT the collinear anomaly [64, 85, 86]. The broken symmetry here is the RPI_{III} boost invariance $p_n^- \rightarrow \beta_n p_n^-$ in the n -sector and $p_{\bar{n}}^+ \rightarrow \beta_{\bar{n}} p_{\bar{n}}^+$ in the \bar{n} -sector, which are assumed symmetries of the theory that become broken by regularizing rapidity divergences. The anomalous $\log Q^2/\mu^2$ then originates from the two terms $\log(p_n^-/\mu) + \log(p_{\bar{n}}^+/\mu)$, each of which comes from a different boost-broken sector. In the sum these reproduce the required QCD result, but the full symmetry group is broken to the subgroup generated by $\beta_n = 1/\beta_{\bar{n}}$. The same anomaly occurs when studying the Drell-Yan process at small q_T [64] and when calculating the event shape called jet broadening [85]. More generally the collinear anomaly occurs in all SCET_{II}-type observables, where the isotropic modes are only separated from the collinear modes by boosts.

The problem with the anomalous $\log(Q^2/\mu^2)$ in the effective operator's matrix element is that the logarithm is large when matching onto the next EFT at $\mu = M$. To solve this issue, the authors in [64, 84] proved that $\log F$ is linear in $\log Q^2/\mu^2$ at all orders in α_s , thus showing that the large logarithm exponentiates and therefore is under theoretical control. The authors of [80] take another approach, finding that these large logarithms come from an ambiguity in the partitioning of collinear and soft modes that lie on the same mass hyperbola. Noting that the large logarithms are associated with rapidity divergences in the radiative corrections for jet and soft functions, they define a regularization scheme similar to dimensional regularization in order to control the divergences. Exploiting the partitioning ambiguity, they then derive a rapidity RGE that sums the anomalous logarithms in the same manner as the usual RGE.

Since the mass-hyperbola ambiguity in [80] was first noted in the context of soft-collinear mode factorization, it is unclear how such a structure might arise in our formulation of SCET which does not contain explicit soft modes. After all, the rapidity divergences in the jet and soft functions of [80] cancel in the sum. This implies that perhaps the divergences, and thus the ambiguity itself, are simply artifacts

of the form of the factorization², and therefore that a different divergence-free factorization might be unable to sum rapidity logarithms. In Chapter 4 we verify without an explicit rapidity regulator that rapidity divergences in both the massive Sudakov form factor and the Drell-Yan cross section at small- q_T indeed cancel in the sum. We also show how rapidity logarithms can be summed due to an integration ambiguity which arises when summing together divergent diagrams. This integration ambiguity gives rise to a logarithm $\log(\nu^2/\mu^2)$ that is only fixed by matching onto QCD to be equal to $\log(Q^2/\mu^2)$. This provides an additional perspective on the origin of the anomalous Q^2 -dependence at leading power, and in the process also shows that boost invariance actually remains unbroken in SCET.

1.3.3 Factorization of Small- q_T Power Corrections

In the usual formulation of SCET it has been shown how power corrections can be factorized using bare functions for real emissions [91]. To achieve an equivalent renormalized factorization formula the power-suppressed radiative functions in that formalism still need to be renormalized. It is expected that their renormalization will not be straightforward, since it has been pointed out that radiative jet functions contain double counting with respect to their accompanying soft functions [92]. It therefore still needs to be determined how the requisite zero-bin subtractions beyond leading power will be incorporated into the definitions of subtracted radiative jet functions while also preserving the factorization structure found in [91].

In the formulation of SCET used in this thesis, however, there are no subleading terms in the SCET Lagrangian beyond the hard scattering operators which we find and renormalize in Chapter 3. Consequently, we do not need radiative functions to describe real emissions, and factorization is a straightforward consequence of successive matching steps at the appropriate perturbative energy scales. We demonstrate this in Chapter 5, where we show how the first q_T^2/Q^2 power corrections to Drell-Yan process can be factorized. We also introduce a prescription for removing double counting at next-to-leading power, and show how this prescription again leads to an integration ambiguity for power-suppressed rapidity divergences. All soft-scale matching coefficients are determined at $O(\alpha_s)$, but further work is required to determine all entries in the rapidity anomalous dimension matrix. Once these entries are found, a full leading-log resummation will be available for power corrections in the Drell-Yan process.

²The first signs of this can be noted by the form of the anomaly exponent in [64]. There the original factorization of the cross section into separate x_T -dependent PDFs, defined in terms of collinear modes, must be refactorized due to the collinear anomaly. The refactorized x_T -dependent PDFs have no operator definition, hinting that perhaps the original mode decomposition was not appropriate for describing the low-energy degrees of freedom. Refactorization is also a feature of the “infinity-bin” formalism of [87–90].

Chapter 2

Effective Field Theories

A comprehensive review of Effective Field Theories can be found in any of [43, 93–97]. From the classic Wilsonian perspective [38], EFTs are the field theories which result from working at a particular energy scale Λ and discarding all the dynamics and degrees of freedom with energies $E > \Lambda$. The degrees of freedom used to construct the resulting effective Lagrangian below the cutoff energy are only those relevant to the low-energy dynamics, and while these low-energy degrees of freedom can be entirely different from the degrees of freedom that existed before a cutoff was imposed, the low-energy dynamics are exactly reproduced by the effective Lagrangian when the effective coupling constants are appropriately chosen.

This picture of integrating out degrees of freedom naturally comes from Wilson’s statistical mechanics picture of placing fields on a lattice: since energy transfers on the lattice are limited to momenta $p < \pi/a$, the lattice spacing a acts as a high-energy cutoff for the theory. Zooming out from the lattice gives semigroup scaling relations between the coupling constants at different zoom levels that maintain the long-distance dynamics and correlations on the lattice.

This discrete picture of an energy-momentum cutoff is different, however, from most modern applications of EFTs in the continuum [94, 97]. While the tree-level construction is the same in both the Wilsonian and the continuum pictures – that large mass and large virtuality degrees of freedom are removed in the EFT – the treatment of radiative corrections differs. Instead of an explicit cutoff, modern calculations use dimensional regularization to suppress the contributions from high-energy degrees of freedom. All loop momenta go to infinity, and instead of removing high-energy degrees of freedom by hand, the focus of continuum EFT is ensuring that the effective Lagrangian exactly reproduces low-energy amplitudes and probabilities of the full-theory. The long-distance non-local dynamics are contained in the non-analytic dependence on infrared energy scales in matrix elements, while the short-distance effects of the neglected high-energy modes are placed in the coupling constants of local operators in the EFT.

In this continuum picture, EFTs enjoy a variety of properties that work in tandem to make the framework very powerful. In this chapter we will outline some of these properties, and hope to paint a cohesive picture for how they work together to provide an improved understanding of our universe. We then showcase how this works with the 4-Fermi Effective Field Theory as an explicit example, and proceed to describe the basic ideas of Soft-Collinear Effective Theory.

2.1 EFT Generalities

Before we explicitly discuss the mechanisms behind the factorization and resummation formulae of observables in Effective Field Theory, it should be helpful to first discuss the overall structure of observables which arises after the methods of EFT have been employed.

In Section 1.1 we wrote down a toy factorization for an observable involving two widely separated energy scales. In various important processes there can be many energy scales, so we first begin by considering the various energy scales an observable might involve. Then we note that while factorization is a useful property in and of itself, without any further input each factor will suffer from large logarithms. When combined with the renormalization group, however, an all-orders resummed form of each factor can be achieved. This resummation has the dual benefits of taming the large logarithms, and also being able to predict terms at higher orders in perturbation theory. We finish this section by discussing the uncertainties associated with the best resummations of various observables at leading power, and how these compare with the uncertainties associated with neglecting power corrections.

2.1.1 Many Energy Scales

The QCD scale Λ_{QCD} sets the energy scale below which perturbative QCD predictions may no longer be trusted. Thus, Λ_{QCD} is the lowest possible energy scale in the hierarchy of scales for any observable with hadrons in the initial or final state. In the previous chapter we discussed a simplified example where an observable factorizes into a hard factor and a soft factor, but this is often not the end of the factorization. Many observables contain additional intermediate scales corresponding to mass thresholds for propagating degrees of freedom. For instance, in semileptonic B -decays (e.g. $B \rightarrow X_c \ell \bar{\nu}_\ell$ decays, shown in Fig. 2.1 in the parton model), there are multiple perturbative mass and energy scales associated with the transition. The transition is mediated by the propagation of a virtual W boson with mass $m_W \sim 80.4$ GeV, while the natural energy scale of the initial state corresponds to the mass of the b -quark $m_b \sim 4.18$ GeV. The natural energy scale of the final hadronic state is given by the mass of the charm quark $m_c \sim 1.28$ GeV, which is parametrically smaller than either m_b or m_W and also parametrically larger than $\Lambda_{\text{QCD}} \sim 0.3$ GeV. At each of these energy thresholds the methods of EFT add a new factor to the factorization formula which depends only on that threshold scale. Explicitly, the decay width for this process can be written [98–102]

$$\Gamma(B_u \rightarrow D_u \ell \bar{\nu}_\ell) = \Gamma_0 C_W(m_W, \mu) C_b(m_b, \mu) C_c(m_c, v_B \cdot v_D, \mu) \xi_0(v_B \cdot v_D, \mu) + O\left(\frac{m_{b,c}}{m_W}, \frac{\Lambda_{\text{QCD}}}{m_W}\right). \quad (2.1)$$

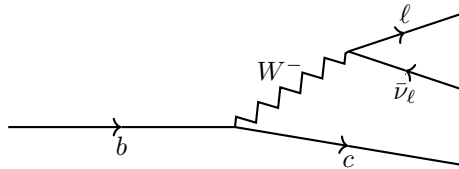


Figure 2.1: Parton-level process $b \rightarrow c \ell \bar{\nu}_\ell$.

The non-perturbative form factor $\xi_0(v_B \cdot v_D, \mu)$ is incalculable, but can be measured in laboratory experiments. The other factors are associated with each of the widely separated mass scales, and these arise naturally in EFT as a consequence of matching onto new effective theories at each mass threshold.

The factors associated with perturbative energy scales are calculable in perturbation theory and have the general form

$$C_i(m_i, \mu) = 1 + \alpha_s \left(A_1 \log \frac{m_i}{\mu} + B_1 \right) + \alpha_s^2 \left(A_2 \log^2 \frac{m_i}{\mu} + B_2 \log \frac{m_i}{\mu} + C_2 \right) + \dots \quad . \quad (2.2)$$

If $\mu \ll m_i$ or $\mu \gg m_i$ then the logarithm is large and the perturbative series in powers of $\alpha_s \ll 1$ becomes a perturbative series in powers of $\alpha_s \log m_i/\mu \sim 1$, implying that the asymptotic expansion of QCD is no longer under theoretical control. From Eq. (2.1) it is clearly not possible to set μ to a scale which keeps the logarithms small in each factor. This is an issue which is handled in a general manner in Section 2.1.2, with a further explicit example in Section 2.2.2.

2.1.2 Logarithmic Precision Counting

In each of the factorization formulae that have been written up to this point, the neglected terms are suppressed by powers of small mass ratios. For many phenomenologically important observables (e.g. event shapes [103], decay widths [104], and fiducial phase-space restricted cross sections [55, 56]) the leading power factorization formulae have been derived, and the perturbative factors at each relevant energy scale have been calculated to very high levels of precision.

Typical perturbative calculations count the number of loops (equivalently, the highest power of the coupling constant relative to tree level) that have been accounted for in Feynman diagrams contributing to the observable, giving a rough estimate of the precision achieved by the calculation. A tree-level calculation is called leading order (LO), a one-loop calculation is called next-to-leading order (NLO), etc. For example, a 3-loop calculation in a field theory with coupling constant α whose perturbative expansion begins at $O(\alpha^0)$ will include terms up to and including $O(\alpha^3)$ corrections. In QED the neglected terms would then begin at $O(\alpha_{\text{em}}^4) \sim (1/137)^4 \approx 3 \times 10^{-9}$ (ignoring the appropriate factors of $1/\pi$ and the factorial growth in the number of diagrams). Such calculations which classify their precision based on the number of loops (or the relative suppression by the coupling constant) is called a fixed order (FO) expansion.

However, when relevant energy scales in a physical process are widely separated (e.g. $Q \gg E$), diagrams will generate logarithms of the scale ratio; depending on whether or not there exist one or two types of infrared singularities in the diagrams, each power of α will be also accompanied by one or two powers of $\log(Q/E)$. With this hierarchy of scales, the effective coupling constant is $\alpha \log(Q/E)$, so that if the separation of scales is large enough, i.e. $\log(Q/E) \sim 1/\alpha$, then the asymptotic FO expansion of the observable in powers of α_i becomes unreliable.

Fortunately in such situations the separation of scales allows for a renormalization group (RG) improved representation of the observable. For any factor \mathcal{P} with double logarithms, rather than writing the FO expansion of the factor as

$$\mathcal{P}(Q, \mu) = \sum_n \alpha^n \left(p_{n,2n} \log^{2n} \frac{Q}{\mu} + p_{n,2n-1} \log^{2n-1} \frac{Q}{\mu} + \dots + p_{n,0} \right) , \quad (2.3)$$

it can be shown in RG-improved perturbation theory that the logarithm \mathcal{P} has the equivalent expansion

$$\log \mathcal{P} = \log \frac{Q}{\mu} \sum_n c_n \left(\alpha \log \frac{Q}{\mu} \right)^n + \sum_n d_n \left(\alpha \log \frac{Q}{\mu} \right)^n + \alpha_i \sum_n f_n \left(\alpha \log \frac{Q}{\mu} \right)^n . \quad (2.4)$$

The coefficients c_n , d_n , f_n , etc., of the log expansion precisely reproduce the coefficients $p_{n,m}$ of the fixed order expansion when expanded order-by-order in α .

In this form, however, it is difficult to determine the number of loops required in order to calculate each of the coefficients. A more convenient basis can be found by transmuting the log dependence into a function of the coupling constants evaluated at the relevant energy scales. Since the logarithm of the scale ratio obeys the relation

$$\log\left(\frac{Q}{\mu}\right) \sim \frac{1}{\alpha(Q)} g(\alpha(Q), \alpha(\mu)) , \quad (2.5)$$

where $g(\alpha(Q), \alpha(M))$ is determined by the beta function of the theory, the log expansion can also be rewritten in the exponentiated form

$$\mathcal{P} = \exp\left[\frac{1}{\alpha(Q)} f_0(z)\right] \exp[f_1(z)] \exp[\alpha(Q) f_2(z)] \cdots \quad (2.6)$$

where $z = \alpha(\mu)/\alpha(Q)$. At this point, it can be simply stated that the function $f_0(z)$ is entirely determined by 1-loop diagrams, the function $f_1(z)$ is entirely determined by 2-loop and 1-loop diagrams, etc. [69, 105–108]. A calculation which determines $f_0(z)$ is said to have summed the leading-log (LL) series of coefficients c_n , while the function $f_1(z)$ gives the next-to-leading-log (NLL) series d_n , and so on and so forth.

The benefits are twofold: most importantly, the exponentiated form brings the fixed order expansion under perturbative control, but it also *predicts* fixed order coefficients at all orders in α , which can later serve as a cross-check for subsequent higher-loop calculations.

These RG-improvement techniques have been applied to many observables to achieve high levels of precision. For example, $e^+e^- \rightarrow$ hadronic event shapes like thrust [109] and the C -parameter [110] have been calculated to N^3LL at leading power. The same impressive logarithmic order has been achieved at leading power in the Drell-Yan process in the endpoint region [111] and in the small- q_T region [52]. Leading-power DIS has even been analyzed up to N^4LL [112].

2.1.3 The Need to Study Power Corrections

For many observables the logarithmic precision achieved in the leading power factorization formula has reached the point where the neglected terms in the factorization formulae, the power corrections, are now the limiting entities in understanding and predicting probabilities in physical processes. For example, a N^3LL calculation of the simple scalar observable \mathcal{P} used above will have no information about the exponentiated factor $\exp[\alpha^3(Q)f_4(z)]$. If the process is mediated via QCD, and the largest energy scale in the interaction is roughly $Q \sim 1$ TeV, then $\alpha_s(Q) \sim 1/10$ and the relative uncertainty from the neglected factor is $\alpha_s^3(Q) \sim 1/1000$. Compared to the uncertainty associated with the neglected power corrections, which will be of the order E/Q , then computing the unknown function $f_4(z)$ – which would require a heroic 5-loop calculation – will only be more important for precision improvement if $E/Q < 1/1000$. Most important observables do not have such a wide scale separation.

Of course, power corrections are not been completely neglected in practice, it is only their factorization and resummation structures that are not fully understood. Indeed, the leading power factorization of an observable is only valid when a wide separation of scales $E/Q \ll 1$ exists. In the absence of such a hierarchy, as can be the case when E represents a dynamically-generated energy scale (e.g. $E \sim q_T$ for the Drell-Yan process), the fixed order cross section is under perturbative control and provides the

exact all-orders dependence on the scale ratio E/Q . In order to describe the cross section of a process across the entire phase space of possible scale hierarchies, and in order to maintain RG-improvement properties when $E/Q \ll 1$, the cross section is often written as [103, 113]

$$\hat{\sigma}_{\text{smoothed}} = \hat{\sigma}_{\text{LP}}^{\text{summed}} + (\hat{\sigma} - \hat{\sigma}_{\text{LP}}^{\text{summed}})_{\text{FO}} . \quad (2.7)$$

Here $\hat{\sigma}$ represents the partonic fixed order cross section, and $\hat{\sigma}_{\text{LP}}^{\text{summed}}$ is the RG-improved cross section at leading power when $E \ll Q$. This formula smoothly links the regions $E \ll Q$, where resummation is important and the leading power factorization allows for a resummation, with the region $E \sim Q$, where no factorization exists but the cross section is known at all orders in E/Q . The parenthesized term then represents the fixed order power corrections.

The aim of this thesis is to improve the understanding of power corrections for observables that are already well understood at leading power. In the past 30 years there has been a great deal of work done to explore the fixed order structure of power corrections in EFT. For example, FO power corrections in HQET have been explored since the early 90s [114–116], and the next-to-leading power (NLP) SCET Lagrangian was worked out shortly after SCET was first created [117]. However, just like the leading power fixed order expansion of Eq. (2.3), power corrections also have spoiled perturbative expansions from large logarithms, and it is only recently that efforts have turned towards deriving RG-improved formulae for the power corrections themselves. Before my degree began there were only a few papers concerned with the exponentiation of power corrections [83, 118], but since then there has been a growing industry of authors seeking to exponentiate various observables at NLP [75, 87–89, 119–130].

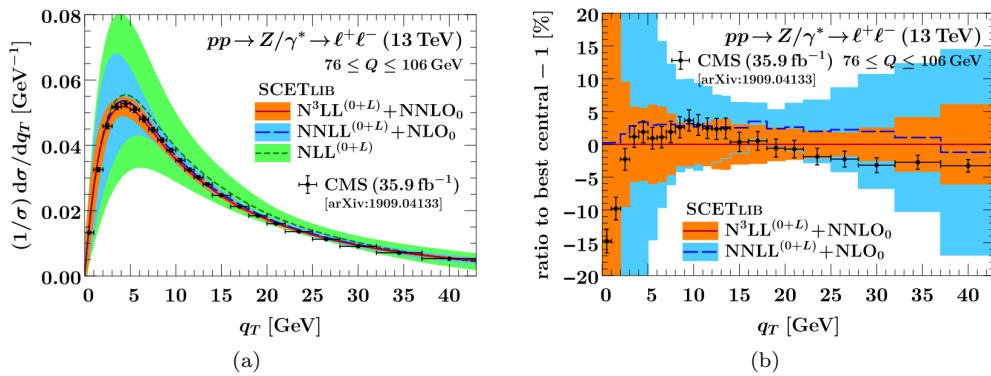


Figure 2.2: The q_T spectrum (left) and its associated uncertainties (right), where CMS fiducial cuts $p_T^{\ell_{1,2}} > 25 \text{ GeV}$ and $|\eta_{\ell_{1,2}}| < 2.5$ have been applied. Figures are taken from [55], with experimental data from [131].

In this thesis, we will focus on studying the Drell-Yan process at small q_T . Fig. 2.2 shows the q_T spectrum for the DY process¹. Fig. 2.2b shows that experimental uncertainties currently outpace theory uncertainties. A decomposition of these theory uncertainties is also shown in Fig. 2.3. There, resummation (Δ_{res}) and non-perturbative (Δ_{Λ}) contributions dominate in the peak and post-peak shoulder regions. Uncertainties associated with power corrections (Δ_{FO}), and with matching the resummed spec-

¹In [55] fiducial phase space cuts are applied to the leptonic final state according to the typical detector acceptance regions of CMS. The effects of these cuts can formally be expanded in a power series in the small ratio q_T/Q , with non-vanishing linear terms from whence they might identify “linear power corrections”. However, those authors argue that this expansion is not strictly required, and instead keep the exact, all-powers q_T/Q dependence from phase-space cuts.

trum onto the fixed order power corrections via an equation like Eq. (2.7) (Δ_{match}), dominate in the tail region. A better understanding of power corrections is thus important for increasing theoretical precision in the tail.

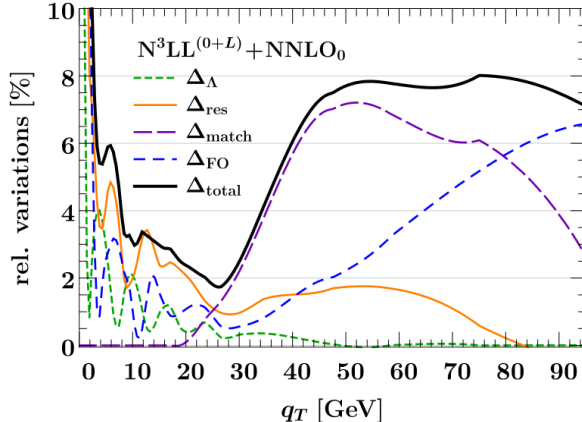


Figure 2.3: Uncertainties associated with various theory inputs. These include the uncertainties from the freeze-out energy Λ_{fr} of the QCD coupling, the uncertainties from choosing the canonical scales for the resummation scheme, uncertainties associated with the profile-scale scheme for turning off resummation in the matching of Eq. (2.7), and uncertainties associated with the fixed-order scale at which the power corrections are evaluated. Figure taken from [55], with experimental data from [131].

In fact, in other applications it can be more important to understand the tail region than the peak region. For example, in [103], the fit region for determining α_s from the thrust distribution is $6 \text{ GeV}/Q < \tau < 1/3$, while in [132] the fit region is $25 \text{ GeV}/Q < C < 0.7$. These fit regions are chosen to avoid non-perturbative effects, and correspond to the tail region of each distribution.

For the Drell-Yan process at small q_T with totally inclusive hadronic final states, the QCD portion of the cross section has power corrections that first begin to contribute at $O(q_T^2/Q^2)$. These quadratic corrections, which we will call the NLP power corrections in this thesis, have not yet been resummed, and in the main body of this thesis we take steps towards their exponentiation.

2.2 The 4-Fermi Effective Theory

In Chapter 1 we provided some examples of the mathematical structure of various observables when following the process set out by Effective Field Theory. These formulae generically have a factorized structure, where each factor depends only on a single energy scale. In this section we demonstrate the mechanism and process behind how this factorization structure is achieved using the 4-Fermi EFT as a demonstrative example.

Observables in Quantum Field Theory are generated by the interactions allowed in the Standard Model Lagrangian; for example, the hadronic decay of a B -meson into a charmed final state is mediated by the two Standard Model interaction terms

$$\begin{aligned} \mathcal{L}_{(cWb)} &= \frac{g_2}{\sqrt{2}} V_{cb} \bar{c}_L \not{W}^+ b_L \\ \mathcal{L}_{(dWu)} &= \frac{g_2}{\sqrt{2}} V_{ud}^* \bar{d}_L \not{W}^+ u_L . \end{aligned} \tag{2.8}$$

These interactions generate the transition amplitude (in Feynman gauge)

$$\begin{aligned} i\mathcal{M}_{b \rightarrow cd\bar{u}} &= \langle cd\bar{u} | b \rangle = \langle cd\bar{u} | T\{i\mathcal{L}_{(cWb)}, i\mathcal{L}_{(dWu)}\} | b \rangle + \dots \\ &= \frac{ig_2}{\sqrt{2}} V_{ud}^* \bar{u}_L^d \gamma^\alpha v_L^u \frac{-ig_{\alpha\beta}}{q^2 - m_W^2} \frac{ig_2}{\sqrt{2}} V_{cb} \bar{u}_L^c \gamma^\beta u_L^b + \dots \end{aligned} \quad (2.9)$$

where the tree-level term is included (see Fig. 2.4) and higher-loop corrections are included in the ellipses.

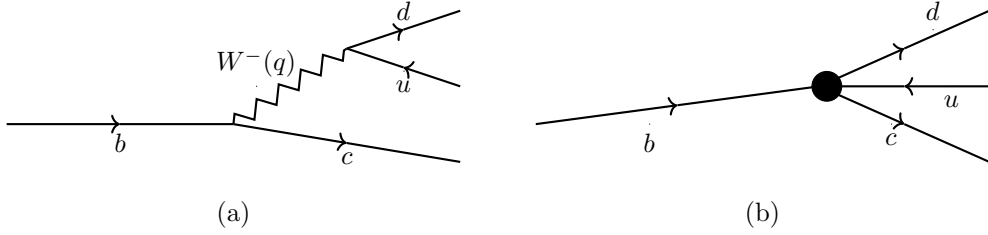


Figure 2.4: Hadronic $B \rightarrow X_c$ decay in the parton model. (a) Full-theory tree-level diagram for the parton-level process $b \rightarrow cd\bar{u}$. (b) Effective interaction for the same process when $q^2 \ll m_W^2$.

When working at energy transfers $q^2 \ll m_W^2$ (e.g. here the typical energy transfer is $q^2 \lesssim m_b^2$) the W boson cannot propagate as an external state; since the W boson cannot freely propagate, one can think of the propagator in Fig. 2.4 as contracting to a point, shown in Fig. 2.4(b). The Lagrangian of the full theory (the Standard Model) is then replaced with the effective Lagrangian

$$\mathcal{L}_{\text{eff}} = C_1 \bar{c}_L \gamma^\alpha b_L \bar{d}_L \gamma_\alpha u_L + C_2 \bar{c}_L \gamma^\alpha u_L \bar{d}_L \gamma_\alpha b_L + O\left(\frac{q^2}{m_W^2}, \frac{\Lambda_{\text{QCD}}^2}{m_W^2}\right). \quad (2.10)$$

The Wilson coefficients $C_{1,2}$ play the role of coupling constants, and the field contents of each term define the effective operators

$$O_1 = \bar{c}_L \gamma^\alpha b_L \bar{d}_L \gamma_\alpha u_L, \quad O_2 = \bar{c}_L \gamma^\alpha u_L \bar{d}_L \gamma_\alpha b_L. \quad (2.11)$$

In order to determine the Wilson coefficients $C_{1,2}$ a matching calculation – in which matrix elements are calculated in both the full theory and the effective theory – is performed, which fixes the effective couplings in terms of the coupling constants of the full theory. Since the effective operators reproduce all the low-energy dynamics of the full theory the Wilson coefficients $C_{1,2}$ are independent of the chosen external state for the matching calculation, provided that the external states lie in a configuration where the scale separation is maintained. This is quite important; though the actual process being studied is a transition between hadronic external states, matching calculations can be performed by calculating partonic matrix elements.

Matching calculations therefore involve calculating the simplest matrix elements which describe the desired parton-level process (instead of, say, the same parton-level process but with N initial-state

gluons). In the case of hadronic B -decay, then from Eq. (2.9),

$$\begin{aligned} \langle cd\bar{u} | T\{i\mathcal{L}_{(cWb)}, i\mathcal{L}_{(dWu)}\} | b \rangle &\underset{q^2 \ll m_W^2}{=} -i \frac{g_2^2}{2m_W^2} V_{ud}^* V_{cb} \bar{u}_L^d \gamma^\alpha v_L^u \bar{u}_L^c \gamma_\alpha u_L^b + O\left(\frac{q^2}{m_W^2}, \frac{\Lambda_{\text{QCD}}^2}{m_W^2}\right) \\ &\downarrow \\ \langle cd\bar{u} | i\mathcal{L}_{\text{eff}} | b \rangle + \dots &= iC_1 \bar{u}_L^d \gamma^\alpha v_L^u \bar{u}_L^c \gamma_\alpha u_L^b + iC_2 \bar{u}_L^d \gamma^\alpha v_L^b \bar{u}_L^c \gamma_\alpha u_L^u + \dots \end{aligned} \quad (2.12)$$

giving the tree-level Wilson coefficients $C_1 = -g_2^2 V_{ud}^* V_{cb} / 2m_W^2 [1 + O(g_1^2, g_2^2, g_3^2)]$ and $C_2 = O(g_1^2, g_2^2, g_3^2)$. The higher corrections to the Wilson coefficients come from loop diagrams, i.e. the g_1^2 and g_2^2 corrections come from considering electroweak loop diagrams, and the g_3^2 corrections come from QCD loops.

The matching requires that $C_2 = 0$ at tree level, making it unclear why the operator O_2 was required in the first place. From a physically motivated standpoint, the operator O_1 originated from a charged-current interaction changing the flavor of the b -quark to a c -quark. Similarly, O_2 has the appearance of a neutral-current interaction changing the flavor of a b -quark to a d -quark. In the Standard Model the unitarity of the CKM matrix ensures that no flavor-changing neutral currents exist at tree level. Since the weak bosons, and thus their associated currents, have been integrated out of the EFT, there is no similar mechanism which *a priori* prevents such a transition in the EFT and therefore O_2 must be generically included in the EFT's Lagrangian. As we will see in the next subsection O_2 is also required for the renormalization of O_1 , so we often say that O_2 is induced by renormalization.

2.2.1 Beyond Tree Level

Loop effects give a great deal of structure to the matching relation in Eq. (2.12). Loops in the full theory induce logarithms of large scale ratios which can be separated into logarithms involving only a single energy scale and an arbitrary factorization scale μ . Meanwhile, the reason factorization works at all is because EFTs entirely reproduce the infrared physics of the full theory, and as a consequence the matching coefficients depend only on the scale that was integrated out.

When calculating matrix elements in the full theory and in the effective theory, ultraviolet divergences require a regulator to be introduced. The most common regulator in modern calculations is dimensional regularization, where the spacetime dimension is analytically continued from $d = 4$ to $d = 4 - 2\epsilon$. With this regulator all continuous and discrete symmetries are preserved with the exception of scale invariance, causing coupling constants and operators to become dependent on a renormalization scale μ . After renormalization the factors in the effective Lagrangian in Eq. (2.10) then have scale dependence

$$\mathcal{L}_{\text{eff}} = C_1(\mu)O_1(\mu) + C_2(\mu)O_2(\mu) + O\left(\frac{q^2}{m_W^2}, \frac{\Lambda_{\text{QCD}}^2}{m_W^2}\right). \quad (2.13)$$

Generally speaking, observables calculated in the parton model have complicated non-analytic dependence on the various ratios $R_{ij} = m_i^2/m_j^2$ of the mass scales in the problem. Since there is a large hierarchy of scales in this process, the matching onto an effective theory entails expanding these complicated full-theory results in powers of $R_{ij} \ll 1$. The expanded non-analytic functions then reduce to logarithmic functions of the ratio, e.g.

$$i\mathcal{M}_{\text{full theory}}^{\text{1-loop}} \propto \alpha_s \log R_{ij} + O(R_{ij}). \quad (2.14)$$

For our example of hadronic B -decay, the perturbative ratios could be e.g. $R_{bW} = m_b^2/m_W^2$, $R_{cW} = m_c^2/m_W^2$, $R_{qW} = q^2/m_W^2$, etc. Since $\log m_1^2/m_2^2 = \log m_1^2/\mu^2 + \log \mu^2/m_2^2$, the full-theory matrix element separates into high-energy and low-energy pieces. For example, after expanding the QCD 1-loop matrix element for $b \rightarrow cd\bar{u}$, we might find that

$$i\mathcal{M}_{b \rightarrow cd\bar{u}}^{1\text{-loop}} \propto \alpha_s \left(A \log \frac{m_b^2}{m_W^2} + B \log \frac{m_c^2}{m_W^2} + C \log \frac{q^2}{m_W^2} \right) \quad (2.15)$$

for some constants A, B, C . This then separates into a high-energy piece and a low-energy piece as

$$i\mathcal{M}_{b \rightarrow cd\bar{u}}^{1\text{-loop}} \propto \alpha_s (A + B + C) \log \frac{\mu^2}{m_W^2} + \alpha_s \left(A \log \frac{m_b^2}{\mu^2} + B \log \frac{m_c^2}{\mu^2} + C \log \frac{q^2}{\mu^2} \right). \quad (2.16)$$

The effective theory, if properly constructed, will reproduce all the infrared physics of the full theory. Here the infrared dynamics are represented by the non-analytic functional dependence on the low-energy scales m_b^2, m_c^2, q^2 , or any other dynamically generated infrared scale. Meanwhile, the high-energy scale m_W^2 no longer exists in the effective theory (matrix elements of the operator do not generate m_W^2 dependence). Thus, in order for the effective field theory to match onto the full theory, the m_W^2 dependence must be fully accounted for by the Wilson coefficient C_W . This separation into high- and low-energy terms is how factorization arises. The matching coefficients $C_{1,2}(\mu, m_W)$ then only depend on the scales μ and m_W , and after explicit calculations of the full-theory and EFT matrix elements it can be shown that

$$\begin{aligned} C_1(\mu, m_W) &= -\frac{g_2^2}{2m_W^2} V_{ud}^* V_{cb} \left(1 - \frac{\alpha_s(\mu)}{4\pi} \log \frac{\mu^2}{m_W^2} + O(\alpha_s^2) \right) \\ C_2(\mu, m_W) &= -\frac{g_2^2}{2m_W^2} V_{ud}^* V_{cb} \left(-3 \frac{\alpha_s(\mu)}{4\pi} \log \frac{\mu^2}{m_W^2} + O(\alpha_s^2) \right). \end{aligned} \quad (2.17)$$

This finishes the 1-loop summary of matching the full theory onto the effective theory for B -decay at leading power in q^2/m_W^2 .

2.2.2 Log Minimization and Summation

While our matching procedure has successfully separated high-energy from low-energy effects, it remains to be determined what should be done with the factorization scale μ . Recall from our discussion in Section 2.1.2 that large logarithms spoil the fixed order expansion of the observable. If μ is chosen to be near the high-energy scale $\mu^2 \sim m_W^2$, then there are large logarithms in the matrix elements $\langle O_{1,2}(\mu) \rangle$. If μ is chosen to be a low-energy scale $\mu^2 \sim m_b^2, m_c^2, q^2$, then there are large logarithms in the Wilson coefficient $C_W(\mu, m_W)$.

This issue is solved through the power of the renormalization group. In dimensional regularization, the relation between a bare operator and its renormalized counterpart is written as

$$O_i^{\text{bare}} = Z_{ij}(\mu) O_j(\mu) \quad (2.18)$$

where we have allowed for operator mixing. Since the bare operator is scale invariant, we are led to the

renormalization group equation (RGE)

$$\begin{aligned} \frac{d}{d \log \mu} O_i(\mu) &= \left(-Z_{ik}^{-1}(\mu) \frac{d}{d \log \mu} Z_{kj}(\mu) \right) O_j(\mu) \\ &\equiv \gamma_{ij}(\mu) O_j(\mu) , \end{aligned} \quad (2.19)$$

where we have implicitly defined the anomalous dimension γ_{ij} . The form of this differential equation is not always so simple – in various applications the RGE can involve sums and convolutions over continuous labels, making it much more difficult to solve the RGE. In the case of hadronic B -decays, however, the 1-loop anomalous dimension matrix is well known [133, 134]

$$\gamma = \frac{\alpha_s}{2\pi} \begin{pmatrix} 1 & -3 \\ -3 & 1 \end{pmatrix} . \quad (2.20)$$

From diagonalizing the matrix and solving the RGE in the new basis of operators, it can be shown that the effective Lagrangian may be written in the resummed form

$$\mathcal{L}_{\text{eff}} = C_1(\mu_H, m_W) U_1(\mu_H, \mu) O_1(\mu) + C_2(\mu_H, m_W) U_2(\mu_H, \mu) O_2(\mu) + O\left(\frac{m_{b,c}^2}{m_W^2}, \frac{\Lambda_{\text{QCD}}^2}{m_W^2}\right) , \quad (2.21)$$

where μ_H is some hard energy scale $\mu_H \sim m_W$, and

$$\begin{aligned} U_1(\mu_H, \mu) &= \frac{1}{2} \left[\exp\left(\frac{2}{\beta_0} \log \frac{\alpha(\mu_H)}{\alpha(\mu)}\right) + \exp\left(-\frac{4}{\beta_0} \log \frac{\alpha(\mu_H)}{\alpha(\mu)}\right) \right] \\ U_2(\mu_H, \mu) &= \frac{1}{2} \left[\exp\left(\frac{2}{\beta_0} \log \frac{\alpha(\mu_H)}{\alpha(\mu)}\right) - \exp\left(-\frac{4}{\beta_0} \log \frac{\alpha(\mu_H)}{\alpha(\mu)}\right) \right] . \end{aligned} \quad (2.22)$$

Two points here should be emphasized. Firstly, the unitary evolution factors $U_i(\mu_H, \mu)$ have the same form as the summation exponent $f_1(z)$ in Eq. (2.6) (there is no $f_0(z)$ here because there are no double logs for this observable). The expansion of the evolution factors order-by-order in $\alpha_s(\mu)$ will contain large logarithms of the ratio μ^2/μ_H^2 , but the entire series has been summed and thus perturbative control has been restored. Secondly, the Wilson coefficient $C_W(\mu_H, m_W)$ can be evaluated at $\mu_H = m_W$, eliminating all large logs from that factor, while the renormalization scale μ only appears in U_i and O_i , and can thus be chosen to be a low-energy scale $\mu \sim m_{b,c}$. The matching and running procedures, in tandem, have separated the high-energy physics from the low-energy physics, and have summed the infinite series of large logarithms between these two hierarchical scales.

This process of matching and running can continue as long as there are perturbative scales that can be accessed by either the initial or the final state. In the case of inclusive $B \rightarrow X_c$ decay, both the initial and final states have invariant masses that are proportional to m_b^2 , and thus once the renormalization scale reaches $\mu \lesssim m_b$ both initial and final states are integrated out of the EFT. For other observables of interest, there could be many successively lower perturbative energy scales to explore, giving further factors and requiring further renormalization-group resummations.

2.3 Jets and Soft-Collinear Effective Theory

When quarks and gluons are produced in a high energy collision they must eventually decay to form color-neutral hadronic bound states which we observe in our detectors. Due to angular-ordering theorems which show that radiated particles become increasingly collimated as more emissions occur [135, 136], we observe the spectacular phenomenon that final state hadrons create a distinctive conelike appearance inside a detector (see Fig. 2.5). These jets of hadrons have been observed since the 1970s [36, 137], but since there is no way to calculate how quarks and gluons become hadrons, we can only empirically model the various processes which lead to the formation of hadrons from a given configuration of quark and gluon progenitors [135, 138, 139].

For carefully-chosen observables, however, EFT techniques place all hadronization effects into universal non-perturbative factors akin to $f(E)$ in Chapter 1, transmuting the problem of calculating cross sections into the problem of calculating matching coefficients at perturbative scales. The basic idea of SCET is that when studying jet-like observables the typical collimated and conelike signature of jets in colliders endows the observable with additional perturbative low-energy scales. It is in these cases, when additional infrared energy scales are widely separated from the large center-of-mass energy producing the jets, that small ratios of scales can be used to expand QCD and allow EFT techniques to be used.

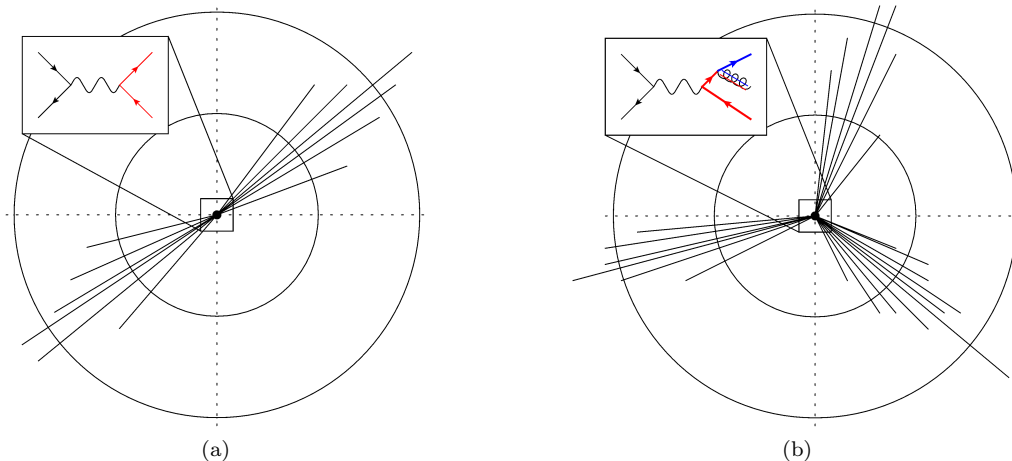


Figure 2.5: Cartoons of dijet (a) and trijet (b) events in the style of the TASSO detector at the electron-positron collider PETRA [140, 141]. Cutaways show possible short-distance interactions which generate the event.

For concreteness, picture an electron-positron collision producing two back-to-back jets, as in Fig. 2.5 (a). It is useful to first define some of the relevant kinematic quantities: after a collision with center-of-mass energy Q , one of the resulting jets will travel approximately in the $\hat{\mathbf{n}}$ direction and will draw from the interaction vertex a significant fraction of the total energy available ($E_n \sim O(Q)$). It will also have some invariant mass M and some 4-momentum $p^\mu = \sum_i p_i^\mu$, where the sum is over all the jet's constituent partons². Effective field theory is generally only useful when there is a hierarchical separation between scales so we will take $M \ll E \sim Q$. In this case, where the energy is much larger than its mass,

²The particular clustering algorithm used to define a jet is unimportant for our analysis. For observables which can be described using SCET, the observable's hierarchy of scales will enforce collimated configurations of hadrons, (e.g. $1-T \ll 1$ for thrust or $1-x \ll 1$ for endpoint DIS). If the jet algorithm itself is the observable being studied [142, 143], the kinematics here capture the relevant features of non-pathological jet definitions [144, 145].

the jet is relativistic and nearly lightlike: it is thus convenient to use a lightcone basis to represent its 4-momentum. This is often defined in terms of the components $p^- = E + \mathbf{p} \cdot \hat{\mathbf{n}}$, $p^+ = E - \mathbf{p} \cdot \hat{\mathbf{n}}$, $\mathbf{p}_T = \mathbf{p} - \hat{\mathbf{n}}(\mathbf{p} \cdot \hat{\mathbf{n}})$, giving the 4-momentum

$$p^\mu = p^+ \frac{\bar{n}^\mu}{2} + p^- \frac{n^\mu}{2} + p_\perp^\mu , \quad (2.23)$$

where $n^\mu = (1, \hat{\mathbf{n}})$, $\bar{n}^\mu = (1, -\hat{\mathbf{n}})$, and $p_\perp^2 = -\mathbf{p}_T^2$.

With this coordinate system the jet's energy-momentum relation is $M^2 = p^2 = p^+ p^- - \mathbf{p}_T^2$. Since $\hat{\mathbf{n}}$ is chosen to align very closely with the jet's direction of travel $|\mathbf{p}_T| \ll \mathbf{p} \cdot \hat{\mathbf{n}} = \sqrt{E^2 - M^2 - \mathbf{p}_T^2} \sim O(Q)$, and then from the hierarchy of scales $p^- \sim O(Q)$ and $p^+ \sim O(M^2/Q, \mathbf{p}_T^2/Q)$. The 4-momenta p_i^μ of the jet's constituents must sum to each of the jet's lightcone components so each of the parton constituents of the jet then have the scaling $p_i^- < p^- \sim O(Q)$ and $p_i^+ < p^+ \sim O(M^2/Q, \mathbf{p}_T^2/Q) \ll Q$. In this thesis we treat partons as massless, so each of their on-shell relation reads $p_i^2 = 0 = p_i^+ p_i^- - \mathbf{p}_{iT}^2$, giving the scaling $p_{iT} \sim O(M, p_T) \ll Q$.

These scaling relations for each jet constituent allow QCD Feynman diagrams that describe jet production to be expanded in a power series of the small ratio p_{iT}/E . While it has been convenient to explain these ideas through the viewpoint of jet production, these techniques are generally useful whenever there exists a collection of colored particles which are collimated. For instance, these techniques are also applicable when hadrons exist in the initial state of a reaction, since hadrons are nothing more than a tightly bound bundle of partons travelling in the same direction.

2.3.1 Analogy to the 4-Fermi EFT

Equipped with the kinematics of a jet and its constituents we now examine some Feynman diagrams in QCD which correspond to jet production. We will expand these diagrams in the appropriate kinematic regime and determine which EFT operators are required to reproduce the expanded amplitudes.

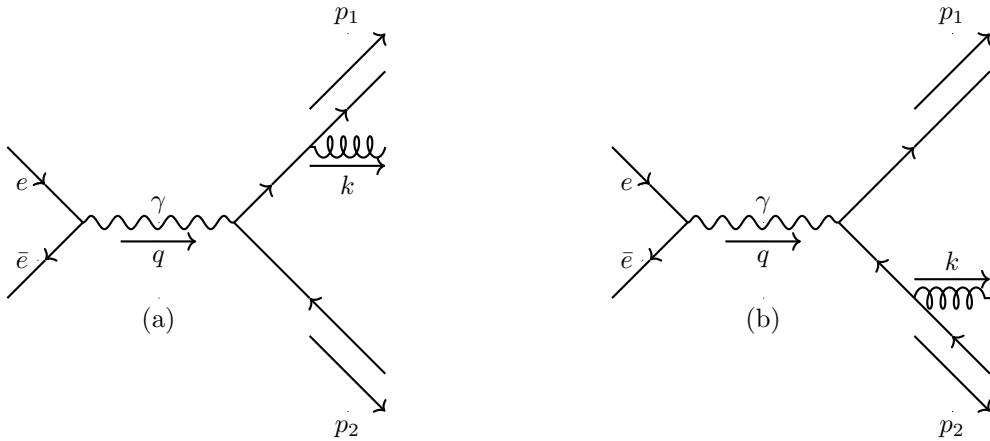


Figure 2.6: Electron-positron annihilation mediated by a virtual photon with energy transfer $q^2 = Q^2$, with a gluon emitted from either (a) the quark or (b) the antiquark.

Consider the tree level graphs for dijet production from e^+e^- annihilation with one final state gluon,

shown in Figure 2.6. The QCD portions of these graphs are

$$i\mathcal{M}_a^\mu = -igT_{cc'}^a \bar{u}_1^c \gamma^\alpha \frac{\not{p}_1 + \not{k}}{2p_1 \cdot k} \gamma^\mu v_2^{c'} \epsilon_\alpha^*, \quad i\mathcal{M}_b^\mu = igT_{cc'}^a \bar{u}_1^c \gamma^\mu \frac{\not{p}_2 + \not{k}}{2p_2 \cdot k} \gamma^\alpha v_2^{c'} \epsilon_\alpha^*. \quad (2.24)$$

In the dijet region of phase space, i.e. when $\hat{\mathbf{n}}$ defines a jet axis and the transverse momenta relative to this axis are small, then $|\mathbf{p}_{1T}| \ll Q$, $|\mathbf{p}_{2T}| \ll Q$, and $|\mathbf{k}_T| \ll Q$. There are three possible partitions of the particles which obey momentum conservation: either the quark and gluon travel in the same direction and recoil against the antiquark, or the gluon travels in the same direction as the antiquark, or the quark and antiquark travel in the same direction.

For our purposes, let us analyze the first case, where the quark and gluon become the progenitors of the jet moving in the $\hat{\mathbf{n}}$ direction (the n -jet), and the antiquark becomes the progenitor of the jet moving in the $-\hat{\mathbf{n}}$ direction (the \bar{n} -jet). We can then derive from the free-quark equations of motion that the spinors obey the expansion

$$\bar{u}(p_1) \underset{p_1 \in \bar{n}}{=} \bar{u}(p_1) \left(P_{\bar{n}} - \frac{\not{p}_{1\perp}}{p_1^-} \frac{\not{k}}{2} \right), \quad v(p_2) \underset{p_2 \in \bar{n}}{=} \left(P_{\bar{n}} - \frac{\not{p}}{2} \frac{\not{p}_{2\perp}}{p_2^+} \right) v(p_2), \quad (2.25)$$

where $P_{\bar{n}} = \not{n}\not{p}/4$ is a projection operator. These equations serve to project away the small components of the spinors in an expansion in powers of $1/p_1^- \sim 1/Q \sim 1/p_2^+$.

In this topology, let us examine the virtualities of the propagators in Fig. 2.6 (a) and (b). In Fig. 2.6 (a), the quark propagator has virtuality $(p_1 + k)^2$, which corresponds to the mass of the jet. In events where the jet mass is small compared to the energy transfer, $M^2 = (p_1 + k)^2 \ll Q^2$, this represents an infrared energy scale. This propagator thus contains no high-energy scales which need to be integrated out, so there is no expansion necessary, and the dynamics of the diagram must be reproduced exactly by the effective theory.

By contrast, in Fig. 2.6 (b), the antiquark propagator has virtuality $(p_2 + k)^2$ which corresponds to a large energy scale. To see this quickly we choose $\hat{\mathbf{n}}$ so that the net transverse momentum of each jet is precisely zero; this provides vanishing momentum components $\mathbf{p}_{2T} = 0$ and $p_2^- = 0$ for the antiquark. The virtuality of the propagator then reads $(p_2 + k)^2 = p_2^+ k^-$, and from the arguments of the previous section $k^- \sim O(Q)$ and $p_2^+ \sim O(Q)$, so $(p_2 + k)^2 \sim O(Q^2)$.

As with the $1/(q^2 - m_W^2)$ W -propagator in the 4-Fermi example, here the antiquark propagator has a large virtuality. Since a high energy scale is present, the propagator must be integrated out of the theory when $\mu < Q$. However, since $k^- p_2^+$ is not precisely equal to the high energy scale Q^2 , there are still some residual dynamics which will remain in the expanded amplitude.

To make this concrete, we examine the full propagator along with the adjacent spinor expansion. Expanding in powers of small over large momentum components, we find that

$$\frac{\not{p}_2 + \not{k}}{2p_2 \cdot k} \gamma^\alpha \left(P_{\bar{n}} - \frac{\not{p}}{2} \frac{\not{p}_{2\perp}}{p_2^+} \right) v(p_2) \epsilon_\alpha^* \xrightarrow[k \in \bar{n}, p_2 \in \bar{n}]{} P_{\bar{n}} \left(\frac{\bar{n}^\alpha}{\bar{n} \cdot k} + \dots \right) v(p_2) \epsilon_\alpha^* \quad (2.26)$$

The overall result of these expansions is that when the quark and gluon both travel in the $\hat{\mathbf{n}}$ direction, the net QCD result of graphs (a) and (b) has the expansion

$$i\mathcal{M}_{a+b}^\mu \xrightarrow[p_1, k \in \bar{n}, p_2 \in \bar{n}]{} -igT_{cc'}^a \bar{u}_1^c \left(\gamma^\alpha \frac{\not{p}_1 + \not{k}}{2p_1 \cdot k} - \frac{\bar{n}^\alpha}{\bar{n} \cdot k} \right) P_{\bar{n}} \gamma^\mu P_{\bar{n}} v_2^{c'} \epsilon_\alpha^* + \dots \quad (2.27)$$

Technical details and higher corrections for these expansions are collected in Appendix A.

To motivate the form of the operator which reproduces this expanded matrix element, let us examine the large momentum component of the propagator in each diagram. In diagram (a), the intermediate quark has a large momentum component $p_1'^-$, and after the gluon emission the final-state quark has large momentum component $p_1^- = p_1'^- - k^-$. Since k^- is large, the large momentum component of the quark changes by a large amount. In contrast, in diagram (b), the intermediate antiquark has a large momentum component $p_2'^+$, and after the gluon emission the final-state antiquark has large momentum component $p_2^+ = p_2'^+ - k^+ \sim p_2'^+$; the large momentum component of the antiquark does not change.

Thus at leading power in the $1/Q$ expansion any radiation emitted by the antiquark in the opposite direction cannot change the energy nor the direction of travel of the antiquark. From the perspective of the emitted gluon the antiquark represents an immovable color source travelling in the opposite direction at the speed of light. Such an object is represented in field theory as a Wilson line,

$$W_n(x) = \bar{\mathcal{P}} \exp \left(-ig \int_0^\infty ds \bar{n} \cdot A_n(x + \bar{n}s) e^{-0^+ s} \right). \quad (2.28)$$

In words, the Wilson line W_n – which acts as a lightlike color source for n -gluons – is given by the anti-path-ordered exponential of gluon fields along the \bar{n} direction. The path ordering simply preserves the usual color ordering of multiple gluon emissions when walking backwards along the arrows of a fermion line, and the $e^{-0^+ s}$ provides a damping factor required for convergence of the integral and precisely aligns with the usual $i\varepsilon$ prescription of the antiquark propagator.

The operator building block which reproduces the dynamics the expanded diagrams (a) and (b) is

$$\bar{\chi}_n(x) = \bar{\psi}_n(x) W_n(x) P_{\bar{n}}. \quad (2.29)$$

All emissions off the quark field in the n -direction are the same as those in QCD, while all emissions in the n -direction off the Wilson line reproduce the dynamics of QCD emissions off the antiquark, if these QCD emissions are expanded in the same kinematic regime.

The analysis is symmetric: the building block which reproduces the dynamics of both expanded diagrams (a) and (b) in the alternate case where the gluon instead travels in the \bar{n} -direction is

$$\chi_{\bar{n}}(x) = P_{\bar{n}} W_{\bar{n}}^\dagger(x) \psi_{\bar{n}}(x). \quad (2.30)$$

Together, each of these operator fragments reproduce all possibilities for quarks and antiquarks travelling in opposite directions. At leading power, the overall operator which produces small-mass dijets is

$$O_2^\mu(x) = \bar{\chi}_n(x) \gamma^\mu \chi_{\bar{n}}(x). \quad (2.31)$$

This is shown in Fig. 2.7. It can be shown that the final topology, where the quark and antiquark travel in the same direction, produces amplitudes which are strictly subleading in powers of $1/Q$.

The effective Lagrangian for SCET can thus be summarized as the usual QCD Lagrangian for each jet, augmented by effective operators for the vector current which couples the separate jet sectors. In short,

$$\mathcal{L}_{\text{QCD}} + g_{\text{em}} V_\mu \bar{\psi} \gamma^\mu \psi \longrightarrow \mathcal{L}_{\text{QCD},n} + \mathcal{L}_{\text{QCD},\bar{n}} + g_{\text{em}} V_\mu (C_2(\mu, Q) O_2^\mu(x, \mu) + \dots), \quad (2.32)$$

where g_{em} corresponds to the electromagnetic charge of the quark flavor in the current. 1-loop calculations then give both the Wilson coefficient and the anomalous dimension for O_2 up to $O(\alpha_s)$,

$$\begin{aligned} C_2(\mu, Q) &= 1 + \frac{\alpha_s C_F}{4\pi} \left(-\log^2 \frac{-Q^2}{\mu^2} + 3 \log \frac{-Q^2}{\mu^2} + \zeta_2 - 8 \right), \\ \gamma_{O_2}(\mu) &= \frac{\alpha_s C_F}{2\pi} \left(3 - 2 \log \frac{-Q^2}{\mu^2} \right). \end{aligned} \quad (2.33)$$

This provides the renormalization-group kernel needed to evolve O_2 from the hard scale $\mu_H \sim Q$ at which we match onto SCET down to μ , where the leading-log contribution is

$$\log U_H(Q, \mu) = \frac{1}{\alpha_s(Q)} \frac{8\pi C_F}{\beta_0^2} \left[1 - \frac{\alpha_s(Q)}{\alpha_s(\mu)} + \log \frac{\alpha_s(Q)}{\alpha_s(\mu)} \right]. \quad (2.34)$$

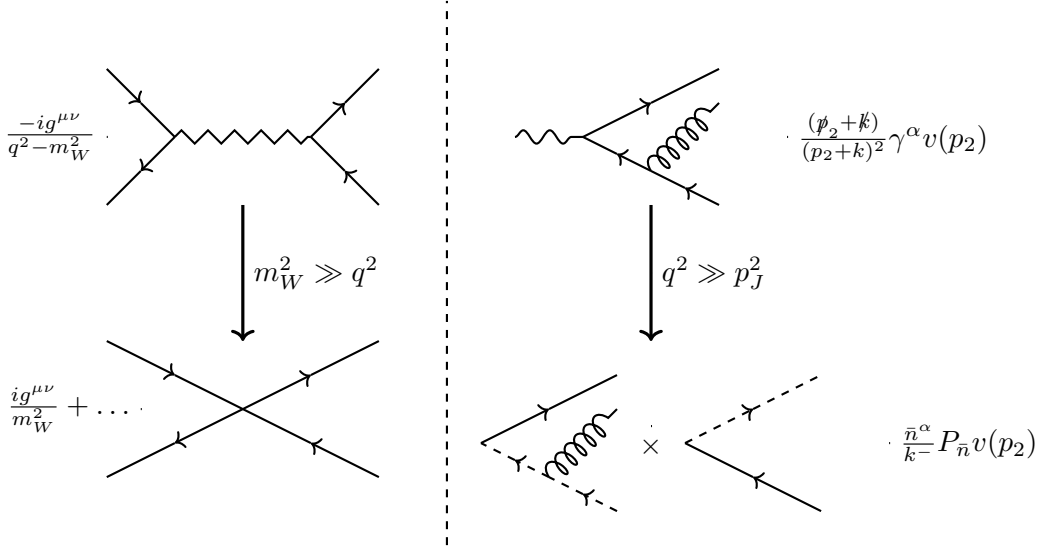


Figure 2.7: Expanding Feynman diagrams in the presence of a hierarchy of scales. In (a) a heavy W -propagator beyond the cutoff of the theory contracts to a point, leaving the 4-Fermi effective vertex. In (b) a high-virtuality antiquark propagator beyond the cutoff of the theory becomes a non-local Wilson-line propagator in SCET. Some authors take the analogy even further and depict Wilson-line emissions as emanating from the vertex, as if to signify that the antiquark had also contracted to a point.

In summary, when expanding the full-theory amplitudes relevant to either the 4-Fermi EFT or to SCET, a propagating particle in the full theory which contains a large energy scale is replaced with an effective operator in the EFT. In the 4-Fermi EFT the hierarchy of scales is known *a priori* based on the initial state's available energy. In SCET the hierarchy of scales only applies to particular regions of phase space, yet in these regions the principles of EFT still apply: matching coefficients only depend on the hard matching scale, effective operators reproduce all the infrared dynamics of the full theory, and the renormalization group can be applied to sum the large logarithms which appear as a result of the dynamically-induced scale separation.

This finishes the methodology we use in this thesis for defining the EFT for jet-like processes below the hard scale Q . Further low-energy thresholds Λ_{IR} exist for jet observables, each of which require a further matching calculation to determine the effective operators below that threshold. The resulting soft effective theories will depend on the observable, and so can only be discussed on a case-by-case basis.

Crucially, however, the version of SCET we have defined here is observable independent – as long as there is a hard interaction then between the scales $\Lambda_{\text{IR}} < \mu < Q$ the operators and matching coefficients are universal.

2.3.2 The Usual SCET Formulation

The way I have described SCET so far is different from its usual formulation. More often, external momenta of particles and the fields which create these particles are partitioned into modes, each of which are assigned scaling relations indicating the size of their lightcone components. Typical mode scalings of the lightcone components $(p^+, p^-, |\mathbf{p}_T|)$ include

$$\begin{aligned} p_{\text{hard}} &\sim Q(1, 1, 1) \\ p_{\text{hard-collinear}} &\sim Q(\lambda^2, 1, \lambda) \\ p_{\text{anti-hard-collinear}} &\sim Q(1, \lambda^2, \lambda) \\ p_{\text{soft}} &\sim Q(\lambda, \lambda, \lambda) \\ p_{\text{ultrasoft}} &\sim Q(\lambda^2, \lambda^2, \lambda^2) \\ p_{\text{Glauber}} &\sim Q(\lambda^2, \lambda^2, \lambda) . \end{aligned} \tag{2.35}$$

The exact value of $\lambda \ll 1$ depends on the observable, e.g. for the massive Sudakov form factor $\lambda = M/Q$ [84], for thrust $\lambda = \sqrt{1-T}$ [146], for the small- q_T Drell-Yan process $\lambda = q_T/Q$ [64], etc. Some observables require further scaling parameters in order to decouple the scale-dependence of modes. For instance, in endpoint DIS it has been argued [147, 148] (and counter-argued [149]) that the soft-collinear mode $p_{\text{soft-collinear}} = Q(\epsilon, \lambda^2, \sqrt{\epsilon}\lambda)$ is required to reproduce the infrared dynamics of QCD, where $\lambda = \Lambda_{\text{QCD}}/Q$ and $\epsilon = \sqrt{1-x}$. The proliferation of these modes is part of the motivation for exploring a different formulation of SCET without modes.

A long sequence of manipulations, and a detailed exposition of various transformation properties, are required to fully define the consequences of partitioning QCD fields into n modes, \bar{n} modes, soft modes, etc. [91]. In the canonical example where n , \bar{n} , and ultrasoft modes are required for a SCET_I-type observable, the QCD fields are partitioned into the appropriate modes via

$$\psi = \xi_n + \xi_{\bar{n}} + q_{us} \quad , \quad A^\mu = A_n^\mu + A_{\bar{n}}^\mu + A_{us}^\mu . \tag{2.36}$$

After applying the BPS field redefinition [71, 72, 150]

$$\begin{aligned} \xi_n &\rightarrow Y_n^\dagger \xi_n + O(\lambda) \\ A_n^\mu &\rightarrow Y_n^\dagger A_n^\mu Y_n + O(\lambda) \end{aligned} \tag{2.37}$$

where the Wilson lines $Y_{n,\bar{n}}$ create and annihilate ultrasoft fields, the SCET Lagrangian reads

$$\mathcal{L}_{\text{QCD}} + g_{\text{em}} V_\mu \bar{\psi} \gamma^\mu \psi \longrightarrow \mathcal{L}_n + \mathcal{L}_{\bar{n}} + \mathcal{L}_{us} + g_{\text{em}} V_\mu J_{\text{SCET}}^\mu \tag{2.38}$$

where [91]

$$\begin{aligned}\mathcal{L}_n &= \bar{\xi}_n \left(in \cdot D_n + i \not{D}_{n\perp} W_n^\dagger \frac{1}{i \bar{n} \cdot \partial} W_n i \not{D}_{n\perp} \right) \xi_n \\ &\quad + \frac{1}{2g^2} \text{Tr} [W_n^\dagger i D_n^\mu W_n, W_n^\dagger i D_n^\nu W_n]^2 + \text{gauge fixing + ghost fields} + O(\lambda) \\ \mathcal{L}_{us} &= \bar{q}_{us} i \not{D}_{us} q_{us} + \frac{1}{2g^2} \text{Tr} [i D_{us}^\mu, i D_{us}^\nu]^2 + \text{gauge fixing + ghost fields} \\ J_{\text{SCET}}^\mu &= C_2(Q, \mu) \bar{\xi}_n W_n Y_n^\dagger \gamma^\mu Y_{\bar{n}} W_{\bar{n}}^\dagger \xi_{\bar{n}} + O(\lambda) .\end{aligned}\tag{2.39}$$

From here the BPS field redefinition can be used to factorize each term in the SCET Lagrangian into individually gauge-invariant n , \bar{n} , and ultrasoft factors. At leading power, a convenient consequence is that all the inter-mode couplings are placed into the hard-interaction portion J_{SCET}^μ of the SCET Lagrangian. Derivations of factorization formulae are thus quite straightforward at leading power, generically producing factorization formulae for cross sections of the form

$$\begin{aligned}\sigma &\propto \int d^4x e^{-iq \cdot x} \langle X_n X_{\bar{n}} X_{us} | J^{\mu\dagger}(x) J^\nu(0) | X_n X_{\bar{n}} X_{us} \rangle \\ &\rightarrow \int d^4x e^{-iq \cdot x} \langle X_n X_{\bar{n}} X_{us} | |C_2|^2 (\bar{\xi}_n W_n Y_n^\dagger \gamma^\mu Y_{\bar{n}} W_{\bar{n}}^\dagger \xi_{\bar{n}})(x) (\bar{\xi}_{\bar{n}} W_{\bar{n}} Y_{\bar{n}}^\dagger \gamma^\nu Y_n W_n^\dagger \xi_n)(0) | X_n X_{\bar{n}} X_{us} \rangle \\ &= \gamma_{\alpha\beta}^\mu \gamma_{\rho\sigma}^\nu |C_2(Q)|^2 \int d^4x e^{-iq \cdot x} \langle X_n | (\bar{\xi}_n W_n)^\alpha(x) (W_n^\dagger \xi_n)^\sigma(0) | X_n \rangle \langle X_{\bar{n}} | (W_{\bar{n}}^\dagger \xi_{\bar{n}})^\beta(x) (\bar{\xi}_{\bar{n}} W_{\bar{n}})^\rho(0) | X_{\bar{n}} \rangle \\ &\quad \times \langle X_{us} | (Y_n^\dagger Y_{\bar{n}})(x) (Y_{\bar{n}}^\dagger Y_n)(0) | X_{us} \rangle \\ &\equiv \gamma_{\alpha\beta}^\mu \gamma_{\rho\sigma}^\nu H(Q) \int d^4x e^{-iq \cdot x} \tilde{J}^{\alpha\sigma}(x, \lambda Q) J_{\bar{n}}^{\beta\rho}(x, \lambda Q) S(x, \lambda^2 Q) \\ &= \gamma_{\alpha\beta}^\mu \gamma_{\rho\sigma}^\nu H(Q) J_n^{\alpha\sigma}(P_n, \lambda Q) \otimes J_{\bar{n}}^{\beta\rho}(P_{\bar{n}}, \lambda Q) \otimes S(P_{us}, \lambda^2 Q) ,\end{aligned}\tag{2.40}$$

where the convolution theorem has been used to write the cross section in terms of convolutions, denoted by \otimes . The energy scales in the argument of the jet functions $J_{n,\bar{n}}$ and soft function S come from the scaling of the modes which make up the function. Fierz identities and multipole expansions are then used to further simplify the structure of the cross section, but the general form still remains $H(Q) \times J_n(\lambda Q) \otimes J_{\bar{n}}(\lambda Q) \otimes S(\lambda^2 Q)$.

By matching QCD onto this usual formulation of SCET the hard, jet, and soft scales have been disentangled. Typically in EFT a matching at the hard scale will only disentangle hard dynamics, producing a factor $H(Q)$, and subsequent matching steps need to be performed to separate the various infrared energy scales. Here, the infrared dynamics have separated automatically. While this is useful, the drawback is that for a different observable – say one that depends on soft $(\lambda, \lambda, \lambda)$ or csoft modes $(\epsilon, \lambda^2, \sqrt{\epsilon}\lambda)$ – a different Lagrangian must be constructed, and a different factorization formula must be derived. In effect, a different version of SCET is required for each observable³.

The formulation of SCET used in this thesis does not classify degrees of freedom using λ -scaling, and instead partitions particles into sectors based on where their mutual interactions fall in the hierarchy

³A potential complication from having a separate version of SCET for each observable is that multi-differential cross sections – involving the simultaneous measurement of multiple observables – might prove incompatible with a SCET treatment. However, it has been shown that these joint observables can be analyzed using the formalism of SCET+ [81, 151–155], which outlines a phase space of effective theories depending on the relative hierarchy of scales from each distinct observable and which results in a continuous multi-differential spectrum.

relative to the hard cutoff scale Q^2 . Our formulation also does not depend on the specific hierarchy or relative scaling of any of the infrared energy scales, and thus can be used for any observable with a hard interaction and jet-like kinematics. Finally, we do not need to define our theory in reference to QCD. In the method of regions approach to SCET [82] the reference to QCD is quite clear, where EFT diagrams are explicitly calculated as limiting cases of full-theory diagrams. In the usual formulation of SCET the connection is less explicit, but is still used implicitly; for example, when defining rapidity regulators [80], the n , \bar{n} , and soft modes are connected through the use of the same rapidity scale ν and regulating parameter η for each mode. If these modes were truly independent then each mode would be free to choose its own rapidity parameters.

Chapter 3

Renormalization of Dijet Operators at $1/Q^2$

In this chapter, we take important steps towards the resummation of power-suppressed logarithms in processes which involve the hard interaction of two collimated collections of colored particles. Using a newly developed formalism for Soft-Collinear Effective Theory (SCET), we identify and compute the anomalous dimensions of all the operators that contribute to event shapes at order $1/Q^2$. These anomalous dimensions are necessary to resum power-suppressed logarithms in hard processes, although an additional matching step and running of observable-dependent soft functions will be necessary to complete the resummation. In contrast to standard SCET, the new formalism does not make reference to modes or λ -scaling. Since the formalism does not distinguish between collinear and ultrasoft degrees of freedom at the matching scale, fewer subleading operators are required when compared to recent similar work. We demonstrate how the overlap subtraction prescription extends to these subleading operators. The contents of this chapter appear in [77].

3.1 Introduction

Event shapes such as thrust, broadening, and the C-parameter are strong probes of the predictive power of perturbative quantum chromodynamics. Thrust [103, 109, 156] and the C-parameter [132] have been used to precisely determine α_s from e^+e^- collision data with the help of Soft-Collinear Effective Theory (SCET) [68–71]. The value of α_s determined by these event shape measurements deviates from the world average [157], and a better understanding of QCD power corrections could help understand this discrepancy.

For a concrete example, we consider the event shape thrust. Thrust is defined as

$$\tau = 1 - T = 1 - \max_{\hat{\mathbf{t}}} \sum_{i \in X} \left| \frac{\hat{\mathbf{t}} \cdot \mathbf{p}_i}{Q} \right|, \quad (3.1)$$

where $\hat{\mathbf{t}}$ is the unit vector that maximizes the weighted sum over all final state momenta X . The value of τ ranges between $1/2$ for spherically symmetric distribution of momenta in the final state to 0 for exactly collinear back-to-back jets. A corresponding observable for thrust is the cumulative thrust distribution

for $e^+e^- \rightarrow \text{jets}$. Normalizing to the Born cross section σ_0 this cumulative distribution $R(\tau)$ is given by

$$R(\tau) = \frac{1}{\sigma_0} \frac{1}{2Q^2} \sum_i L_{\mu\nu}^i \sum_X \int d^4x \langle 0 | \mathcal{J}_i^{\mu\dagger}(x) | X \rangle \theta(\tau - \hat{\tau}(X)) \langle X | \mathcal{J}_i^\nu(0) | 0 \rangle, \quad (3.2)$$

where $\hat{\tau}(X)$ is the function that computes eq. (3.1) for each final state X . The dependence on the leptonic current has been absorbed in $L_i^{\mu\nu}$, and the current $\mathcal{J}_i^\mu = e^{-iq\cdot x} \sum_{f,c} \bar{\psi}_f^c \Gamma_i^\mu \psi_f^c$ is either the vector ($\Gamma_V^\mu = \gamma^\mu$) or axial ($\Gamma_A^\mu = \gamma^\mu \gamma_5$) QCD quark current. In the limit $\tau \ll 1$ the cumulative thrust distribution can be computed in a perturbative expansion in both α_s and τ , and takes the value [158]

$$R(\tau) = 1 + \frac{\alpha_s C_F}{2\pi} (-2 \log^2 \tau - 3 \log \tau + 2\zeta_2 - 1) + \frac{\alpha_s C_F}{2\pi} \tau (2 \log \tau - 4) + O(\alpha_s^2, \tau^2). \quad (3.3)$$

For sufficiently small values of τ , the quantity $\alpha_s \log \tau$ becomes large and the validity of the asymptotic expansion in fixed-order perturbation theory breaks down. Effective field theories and renormalization group techniques can be used to resum infinite subsets of these logarithmic terms, which improves the validity of the approximation. Summing the infinite subset of Sudakov (double) logarithms, starting with the term proportional to $\alpha_s \ln^2 \tau$, is called the leading logarithm (LL) approximation, with NLL describing the summation of the terms starting with $\alpha_s \ln \tau$, and so on. SCET has enjoyed a great deal of success in summing these logarithmic terms up to $N^3 LL'$ in the thrust distribution [109, 146, 159].

However, the terms suppressed by powers of τ still limit the theoretical uncertainty in the regime where τ is small but still large enough that perturbation theory is valid, i.e. $Q\tau \gg \Lambda_{\text{QCD}}$ (also known as the “tail” region of the distribution). Power corrections have been included in thrust calculations using direct and effective field theory methods [103, 109, 156, 160, 161], however these have been at fixed-order in perturbation theory, which computes only the leading terms in the infinite subset.

In this chapter we make progress towards the goal of summing the whole series of leading logarithms suppressed by τ in the cumulative thrust distribution by computing the anomalous dimensions of all the necessary scattering operators in SCET that contribute to the $O(\alpha_s \tau)$ cumulative distribution. We use a new formalism for SCET developed in [77]. The remaining ingredient required to complete the summation is to match onto and renormalize the subleading soft functions. The soft functions in this formalism will correspond exactly to the soft functions discussed in standard SCET for event shapes, which encode the effect of low energy radiation on the event shape. They are therefore observable-dependent, in contrast to the operators we consider in this chapter, which apply to any event shape for $e^+e^- \rightarrow \text{dijets}$. A detailed analysis of soft function matching and renormalization in this formalism is currently a work in progress and so we will not discuss it further here¹.

3.2 Formalism Review

The formalism for SCET developed in [77] expanded on the work of [163], in which SCET was constructed as an effective field theory of decoupled copies of QCD interacting with each other via Wilson lines. This idea was further explicated in [164, 165] to study factorization in QCD. In [77], the formalism was modified to remove the ultrasoft sector from dijet operators in the effective theory below the matching scale, while modifying the standard “zero-bin” prescription to make the theory consistent. In this section

¹Definitions of subleading soft functions were given in [162], although the formalism of SCET used there is different from the one used here.

we briefly review the notation and formalism used in this framework for SCET and demonstrate the matching calculation onto the subleading operators.

3.2.1 Notation

Throughout this chapter we will use the usual lightcone coordinates:

$$p^\mu = n \cdot p \frac{\bar{n}^\mu}{2} + \bar{n} \cdot p \frac{n^\mu}{2} + p_\perp^\mu = p^+ \frac{\bar{n}^\mu}{2} + p^- \frac{n^\mu}{2} + p_\perp^\mu, \quad (3.4)$$

where $n^\mu = (1, \mathbf{n})$, $\bar{n}^\mu = (1, -\mathbf{n})$ and $n \cdot \bar{n} = 2$; we will also use the shorthand $p^\mu = (p^+, p^-, \mathbf{p}_\perp)$. In standard SCET specific “ λ -scaling” is assigned to each light-cone component depending on which sector the particle is in. In contrast, in this formalism there is no need to compare the relative scaling of collinear modes to soft, ultrasoft, or other modes², and so defining a λ -counting for different components of momenta will not be necessary. When matching onto the effective theory we will consider the limits of QCD in which p^+ or p^- are much less than the matching scale Q , considering all such perturbations to be of the same order. The power counting of subleading operators in this formalism is then determined entirely by their dimension, as will be made evident below. In the dijet limit, thrust scales like the hemispherical mass-squared $\tau \sim M_H^2/Q^2$ [166], so to calculate the cumulative thrust distribution up to $O(\tau)$ it is necessary to determine the subleading operators up to a suppression of $1/Q^2$.

We define the following gauge-invariant operator building-blocks which we will use to construct subleading operators, using notation familiar from existing SCET literature:

$$\begin{aligned} \chi_{n_i}(x) &= W_{n_i}^\dagger(x) P_{n_i} \psi_{n_i}(x), \\ \mathcal{B}_{n_i}^{\mu_1 \dots \mu_N}(x) &= W_{n_i}^\dagger(x) i D_{n_i}^{\mu_1}(x) \dots i D_{n_i}^{\mu_N}(x) W_{n_i}(x), \end{aligned} \quad (3.5)$$

where $P_{n_i} = \not{p}_i \not{\bar{p}}_i / 4$, and n_i are the directions of each jet. For dijets, we always work in a reference frame where $\mathbf{n}_1 = \mathbf{n}$ and $\mathbf{n}_2 = \bar{\mathbf{n}}$, such that $\bar{\mathbf{n}}_1 = \mathbf{n}_2$ and $\bar{\mathbf{n}}_2 = \mathbf{n}_1$. The Wilson lines are defined in the usual way,

$$W_{n_i}(x) = \bar{\mathcal{P}} \exp \left[-ig \int_0^\infty ds \bar{n}_i \cdot A_{n_i}^a(x + \bar{n}_i s) T^a e^{-\epsilon s} \right], \quad (3.6)$$

where $\bar{\mathcal{P}}$ denotes antipath ordering and ϵ is the Feynman pole prescription. The only distinction between these objects and their equivalents in standard SCET literature is that in the present formalism, fields are regular QCD fields with quantum numbers labeling their corresponding sector.

While the operators in the effective theory depend on the choice of a direction \mathbf{n} , they are in fact invariant under boosts along that direction; i.e. the form of the operators does not depend on which reference frame one uses to define $n^\mu = (1, 0, 0, 1)$, provided \mathbf{n} points along the same axis. Thus, following [77], we define new vectors η and $\bar{\eta}$,³

$$\eta^\mu = \sqrt{\frac{q \cdot \bar{n}}{q \cdot n}} n^\mu, \quad \bar{\eta}^\mu = \sqrt{\frac{q \cdot n}{q \cdot \bar{n}}} \bar{n}^\mu, \quad (3.7)$$

where $q^\mu = (Q/\alpha, Q\alpha, \mathbf{0})$ is the momentum transfer of the process, and in the case of $e^+e^- \rightarrow X$ it is the momentum of the virtual electroweak boson. The parameter α defines the relative boost from the

²See Section 2.3.2.

³Note that these differ by a sign from the definitions in [77], since in our case q is timelike rather than spacelike.

frame in which $n^\mu = (1, 0, 0, 1)$. The four-vectors η and $\bar{\eta}$ have been defined so that $p \cdot \eta$ and $p \cdot \bar{\eta}$ don't depend on α for any p , and are therefore useful for making this boost symmetry of the effective theory manifest.

For brevity, we define some shorthand notation to denote the displacement of fields from the interaction vertex in position space, which will be necessary for renormalization:

$$\begin{aligned}\mathcal{B}_{n_i}^{\mu_1 \dots \mu_N}(x, t) &= \mathcal{B}_{n_i}^{\mu_1 \dots \mu_N}(x + \bar{\eta}_i t/Q) \\ \chi_{n_i}(x, t) &= \chi_n(x + \bar{\eta}_i t/Q).\end{aligned}\tag{3.8}$$

Here t is dimensionless parameter that displaces the fields from the vertex at x along the \mathbf{n}_i direction.

Following the lead of [167–169] we will also find it useful to build subleading operators using a set of building blocks that project out states with definite helicity. We find that this both simplifies the structure of subleading operators but also allows us to take advantage of the compact form of matrix elements of massless QCD between states with definite helicity.

Using the standard basis for transverse polarization vectors,

$$\xi_\pm^\mu = \frac{1}{\sqrt{2}}(0, 1, \mp i, 0),\tag{3.9}$$

we define the following combinations of quark-antiquark fields,

$$\begin{aligned}J_{n\bar{n}\pm}^{ij}(x, t_1, t_2) &= \bar{\chi}_{n\pm}^i(x, t_1) \not{\epsilon}_\mp \chi_{\bar{n}\pm}^j(x, t_2) \\ J_{n0}^{ij}(x, t_1, t_2) &= \bar{\chi}_{n+}^i(x, t_1) \not{\epsilon}_0 \chi_{n+}^j(x, t_2) \\ J_{n\bar{0}}^{ij}(x, t_1, t_2) &= \bar{\chi}_{n-}^i(x, t_1) \not{\epsilon}_0 \chi_{n-}^j(x, t_2),\end{aligned}\tag{3.10}$$

where $\chi_{n_i\pm}(x) = P_\pm \chi_{n_i} = \frac{(1 \pm \gamma^5)}{2} \chi_{n_i}(x)$ (these correspond to helicity projections for massless quarks). Here and in the following equation, superscripts i and j are fundamental color indices. We will occasionally drop the second and third arguments denoting the shifts when they are not necessary, i.e. $J_{n\bar{n}\pm}^{ij}(x) \equiv J_{n\bar{n}\pm}^{ij}(x, 0, 0)$. We also define helicity projections of the gluon fields:

$$\mathcal{B}_{n_i h_1 \dots h_N}^{ij}(x, t) = \xi_{h_1 \mu_1} \dots \xi_{h_N \mu_N} \mathcal{B}_{n_i}^{ij \mu_1 \dots \mu_N}(x, t),\tag{3.11}$$

where $h_i \in \pm$ are helicity labels, and μ_i are Lorentz indices.

We would like to finish this section by noting that the power counting of an operator in this formalism is determined entirely by the total mass dimension of its constituent fields. By way of example, each field $\chi_{n_i}(x, t)$ contributes $3/2$ to the mass dimension of any operator in which it appears, while each insertion of a covariant or partial derivative contributes 1 to the mass dimension. In what follows, the leading power operator $O_2^{(0)}$ has a mass dimension of 3 , and so an operator with a mass dimension of $3 + n$ is said to be suppressed by n powers of $1/Q$ relative to the leading power operator.

3.2.2 Matching

We match the QCD current onto a series of subleading operators organized in an expansion in inverse powers of Q , the energy of the hard interaction:

$$\begin{aligned} \mathcal{J}^\mu(x) = e^{-iq \cdot x} & \left[C_2^{(0)} O_2^{(0)}(x) + \frac{1}{Q} \sum_i \int dt C_2^{(1i)}(t) O_2^{(1i)}(x, t) \right. \\ & \left. + \frac{1}{Q^2} \sum_i \int dt C_2^{(2i)}(t) O_2^{(2i)}(x, t) + \mathcal{O}\left(\frac{1}{Q^3}\right) \right], \end{aligned} \quad (3.12)$$

where, as above, q^μ is the momentum transfer of the process.

The leading power operator in eq. (3.12) is the usual leading power dijet operator. Using the building blocks defined in the previous section, it takes the form

$$O_2^{(0)}(x) = (-\xi_+^\mu J_{n\bar{n}+}^{ii}(x) - \xi_-^\mu J_{n\bar{n}-}^{ii}(x)) \quad (3.13)$$

which has matching coefficient [78, 170]

$$C_2^{(0)}(\mu) = 1 + \frac{\alpha_s C_F}{4\pi} \left(-\log^2 \frac{-Q^2 - i0^+}{\mu^2} + 3 \log \frac{-Q^2 - i0^+}{\mu^2} + \zeta_2 - 8 \right). \quad (3.14)$$

In this section we demonstrate tree-level matching from QCD onto SCET currents up to order $1/Q^2$. In [77], details of the matching calculation for $O_2^{(0)}$, $O_2^{(1\perp)}$ and $O_2^{(1a)}$ were presented using this formalism in the context of deep inelastic scattering. The details of the matching procedure for dijets are very similar, but for completeness we will include them here.

Following [77], we take advantage of the simplified form of matrix elements in massless QCD when the helicities of the external states are specified. It is especially useful to use the spinor-helicity formalism for these calculations, and we follow all of the conventions that can be found in the appendix of [77]. We first match onto a general quark-antiquark final state, denoting

$$\mathcal{M}_{q\pm} \equiv \langle p_1 \mp p_2 \pm | \mathcal{J}^\mu | 0 \rangle, \quad (3.15)$$

where the quark (p_1) and anti-quark (p_2) are forced to have opposite helicities by angular momentum conservation. The exact result in the full theory is then given by

$$\begin{aligned} \mathcal{M}_{q\pm} = & -\sqrt{p_1 \cdot \eta} \sqrt{p_2 \cdot \eta} \bar{\eta}^\mu + \sqrt{p_1 \cdot \bar{\eta}} \sqrt{p_2 \cdot \bar{\eta}} \eta^\mu \\ & - \sqrt{2} e^{i\phi(p_2)} \sqrt{p_1 \cdot \bar{\eta}} \sqrt{p_2 \cdot \eta} \xi_+^\mu + \sqrt{2} e^{-i\phi(p_2)} \sqrt{p_1 \cdot \eta} \sqrt{p_2 \cdot \bar{\eta}} \xi_-^\mu. \end{aligned} \quad (3.16)$$

We expand this to leading power in the limit where the quark is collinear to the \mathbf{n} direction while the antiquark is collinear in the opposite direction, $-\mathbf{n}$. According to the definitions in the previous section, this limit corresponds to the limit $\frac{p_1 \cdot \eta}{Q} \ll 1$ and $\frac{p_2 \cdot \bar{\eta}}{Q} \ll 1$. Using $\mathcal{M}^{(i)}$ to refer to the i^{th} order term in this power expansion, we have

$$\mathcal{M}_{q\pm}^{(0)} = -\sqrt{2} e^{\pm i\phi(p_2)} \sqrt{Q} \sqrt{p_1 \cdot \bar{\eta}} \xi_\pm^\mu. \quad (3.17)$$

As expected, this is reproduced by the leading power operator $O_2^{(0)}$ defined in eq. (3.13). At next-to-

leading power in this limit, we find

$$\mathcal{M}_{q^\pm}^{(1)} = \sqrt{Q} (\sqrt{p_2 \cdot \bar{\eta}} \eta^\mu - \sqrt{p_1 \cdot \eta} \bar{\eta}^\mu) , \quad (3.18)$$

which is reproduced by the operator

$$\begin{aligned} O_2^{(1\perp)}(x) = & -\bar{\eta}^\mu (i(\xi_+ \cdot \partial_n) J_{n\bar{n}+}(x) + i(\xi_- \cdot \partial_n) J_{n\bar{n}-}(x)) \\ & - \eta^\mu (i(\xi_+ \cdot \partial_{\bar{n}}) J_{n\bar{n}+}(x) + i(\xi_- \cdot \partial_{\bar{n}}) J_{n\bar{n}-}(x)) \end{aligned} \quad (3.19)$$

where the subscripts on the derivatives ∂_i indicate that the derivative only acts on fields in the i -sector; for example,

$$(\xi_\pm \cdot \partial_n) J_{n\bar{n}}^\pm = (\xi_\pm^\mu \partial_\mu \bar{\chi}_n^\pm) \not{\epsilon}_\mp \chi_{\bar{n}}^\pm . \quad (3.20)$$

As was noted in [77], the $O_2^{(1\perp)}$ operator can be absorbed into the leading power operator $O_2^{(0)}$ by a small rotation of \mathbf{n} , and therefore reparameterization invariance implies that the matching coefficient and anomalous dimension of this operator will be the same as the leading power operator to all orders in α_s .

There are additional subleading operators at this order in the power counting that only appear with at least one gluon in the final state, and thus we must expand the QCD matrix elements with three-body final states. However, we can take advantage of the fact that matrix elements of the operator $O_2^{(1\perp)}$ are proportional to the total perpendicular momentum of a whole sector. By choosing to match onto three body final states with zero perpendicular momentum in each sector we ensure that $O_2^{(1\perp)}$ does not contribute, which also serves to simplify the matching procedure.

The relevant diagrams in QCD for a three-body final state are shown in Fig. 3.1. For three external particles, there are three ways to combine them into back-to-back sectors. The quark and antiquark can be in different sectors, in which case the gluon can be aligned with either one. Due to the CP symmetry of QCD, these two limits are equivalent, and it will be sufficient to consider the gluon being aligned with the quark. The remaining possibility is that the gluon can be in a sector by itself with the quark and antiquark recoiling together. For brevity, we will refer to these limits by listing the sector of each particle in a superscript, so the first possibility above is the $q^n \bar{q}^n g^n$ limit, which is equivalent to the $q^n \bar{q}^n g^n$ limit, and the remaining case is the $q^n \bar{q}^n g^n$ limit.

We first consider the $q^n \bar{q}^n g^n$ limit in which case we arrange the gluon-quark system to have zero perpendicular momentum. Denoting

$$\mathcal{M}_{q^\pm g^\pm} \equiv \langle p_1 \mp p_2 \pm; k \pm' | \mathcal{J}^\mu | 0 \rangle , \quad (3.21)$$

where we note that angular momentum conservation ensures the quark and antiquark have opposite helicity, while the helicity of the gluon is independent. We find that the exact result in massless QCD for the diagrams in Fig. 3.1 is

$$\begin{aligned} \mathcal{M}_{g^\pm q^\pm} &= -\sqrt{2}g T^a \frac{\sqrt{p_1 \cdot \bar{\eta}}}{\sqrt{p_2 \cdot \eta}} \left((\bar{\eta}^\mu - \eta^\mu) - \sqrt{2}e^{\mp i\phi(k)} \frac{\sqrt{p_1 \cdot \bar{\eta}}}{\sqrt{p_1 \cdot \eta}} \xi_\mp^\mu + \sqrt{2}e^{\pm i\phi(k)} \frac{\sqrt{p_1 \cdot \bar{\eta}}}{\sqrt{p_1 \cdot \eta}} \xi_\pm^\mu \right) \\ \mathcal{M}_{g^\pm q^\mp} &= -2g e^{\mp i\phi(k)} T^a \frac{\sqrt{p_2 \cdot \eta}}{\sqrt{p_1 \cdot \eta}} \xi_\pm^\mu . \end{aligned} \quad (3.22)$$

The leading-power terms of eq. (3.22) in the $q^n \bar{q}^n g^n$ limit are already reproduced by the three-body

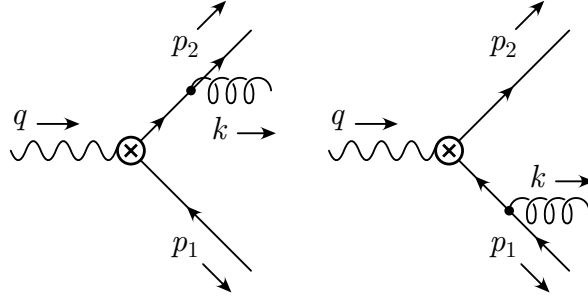


Figure 3.1: QCD graphs contributing to three-body final states.

matrix elements of the leading power operator $O_2^{(0)}$. Expanding to next-to-leading power in this limit we have

$$\begin{aligned}\mathcal{M}_{g^\pm q^\pm}^{(1)} &= -\sqrt{2}gT^a \sqrt{\frac{p_1 \cdot \bar{\eta}}{Q}} (\bar{\eta}^\mu - \eta^\mu) \\ \mathcal{M}_{g^\pm q^\mp}^{(1)} &= 0,\end{aligned}\quad (3.23)$$

and we find that this is reproduced by the operator

$$O_2^{(1a)}(x, t) = (\bar{\eta}^\mu - \eta^\mu) \left(\mathcal{B}_{n-}^{ij}(x, t) J_{n\bar{n}+}^{ij}(x) + \mathcal{B}_{n+}^{ij}(x, t) J_{n\bar{n}-}^{ij}(x) \right) \quad (3.24)$$

where $C_2^{(1a)}(t, \mu) = \delta(t) + \mathcal{O}(\alpha_s)$. Note that we've included the shift parameter t to displace some fields from the interaction vertex. Despite the fact that matching at tree-level sets $t = 0$, a general t will be necessary in order to renormalize this operator, as discussed in the following section.

Now we can match at next-to-next-to-leading power in the $q^n \bar{q}^n g^n$ limit onto operators suppressed by factors of $1/Q^2$. Care must be taken in this limit when performing a matching calculation, since momentum conservation relates the three small parameters, i.e. $p_1 \cdot \eta$, $p_2 \cdot \bar{\eta}$, and $k \cdot \eta$ are not independent. The leading power operator $O_2^{(0)}$ has matrix elements that can be expanded in $p_1 \cdot \eta$ and $k \cdot \eta$, and the higher-power terms must be included consistently to match at $1/Q^2$ (such ambiguities do not appear at $1/Q$). Expanding eq. (3.22) in the $q^n \bar{q}^n g^n$ limit to second order in the power counting and subtracting the corresponding matrix elements of all lower-power effective operators, the lowest-power terms are

$$\begin{aligned}\mathcal{M}_{g^\pm q^\pm}^{(2)} &= 2gT^a \left(\frac{e^{\mp i\phi(k)} \sqrt{p_1 \cdot \eta}}{\sqrt{Q}} \xi_\mp^\mu - \frac{e^{\pm i\phi(k)} \sqrt{k \cdot \eta} \sqrt{p_1 \cdot \bar{\eta}}}{\sqrt{Q} \sqrt{k \cdot \bar{\eta}}} \xi_\pm^\mu \right) \\ \mathcal{M}_{g^\pm q^\mp}^{(2)} &= 0.\end{aligned}\quad (3.25)$$

These terms are reproduced in the effective theory by introducing the operators

$$\begin{aligned}O_2^{(2a_1)}(x, t) &= \left(\xi_+^\mu J_{n\bar{n}+}^{ij}(x) \mathcal{B}_{n-}^{ij}(x, t) + \xi_-^\mu J_{n\bar{n}-}^{ij}(x) \mathcal{B}_{n-}^{ij}(x, t) \right) \\ O_2^{(2a_2)}(x, t) &= \left(\xi_-^\mu J_{n\bar{n}+}^{ij}(x, t, 0) \mathcal{B}_{n-}^{ij}(x) + \xi_+^\mu J_{n\bar{n}-}^{ij}(x, t, 0) \mathcal{B}_{n+}^{ij}(x) \right)\end{aligned}\quad (3.26)$$

where $C_2^{(2a_1)}(t, \mu) = 2i\theta(t) + \mathcal{O}(\alpha_s)$ and $C_2^{(2a_2)}(t, \mu) = -2i\theta(t) + \mathcal{O}(\alpha_s)$.

There will also be operators at this order in the $q^n \bar{q}^n g^n$ limit formed by acting total perpendicular derivatives on lower-power operators, in analogy with the relationship between $O_2^{(1\perp)}$ and $O_2^{(0)}$. As in that case, the operators with total perpendicular derivatives can always be absorbed into their lower-

power counterparts by slight rotation of \mathbf{n} and must therefore share the same anomalous dimension as their lower-power counterparts. In this chapter we choose to focus only on the operators with new anomalous dimensions and so it will be sufficient to match onto states with zero total perpendicular momentum.

The $q^n \bar{q}^n g^{\bar{n}}$ limit is completely analogous to the $q^n \bar{q}^n g^n$ limit and so we won't repeat the details. One can match onto the equivalent operators with n -collinear gluon fields replaced by \bar{n} -collinear gluon fields and they will have the same matching coefficient and anomalous dimension as the $q^n \bar{q}^n g^n$ limit operators.

The $q^n \bar{q}^n g^{\bar{n}}$ limit, where the gluon is in a sector by itself with the quark and antiquark in the other sector, requires different types of operators. The exact result in QCD, now considering a configuration where the quark and antiquark have zero total perpendicular momentum, is

$$\begin{aligned} \mathcal{M}_{g^\pm q^\pm} &= \sqrt{2}g \frac{\sqrt{p_1 \cdot \eta}}{\sqrt{p_2 \cdot \bar{\eta}}} \frac{Q}{k \cdot \eta} e^{\mp i\phi(p_2)} \left((\bar{\eta}^\mu - \eta^\mu) \right. \\ &\quad \left. - \frac{\sqrt{2}e^{\mp i\phi(p_2)} \sqrt{p_1 \cdot \eta}}{\sqrt{p_1 \cdot \bar{\eta}}} \xi_\mp^\mu + \frac{\sqrt{2}e^{\pm i\phi(p_2)} \sqrt{p_1 \cdot \bar{\eta}}}{\sqrt{p_1 \cdot \eta}} \xi_\pm^\mu \right) \\ \mathcal{M}_{g^\pm q^\mp} &= \sqrt{2}g \frac{\sqrt{p_1 \cdot \eta}}{\sqrt{p_2 \cdot \bar{\eta}}} \frac{Q}{k \cdot \eta} e^{\pm i\phi(p_2)} \left((\bar{\eta}^\mu - \eta^\mu) \right. \\ &\quad \left. - \frac{\sqrt{2}e^{\mp i\phi(p_2)} \sqrt{p_2 \cdot \bar{\eta}}}{\sqrt{p_2 \cdot \eta}} \xi_\mp^\mu + \frac{\sqrt{2}e^{\pm i\phi(p_2)} \sqrt{p_2 \cdot \eta}}{\sqrt{p_2 \cdot \bar{\eta}}} \xi_\pm^\mu \right). \end{aligned} \quad (3.27)$$

Expanding eq. (3.27) up to lowest power in the $q^n \bar{q}^n g^{\bar{n}}$ limit we find

$$\begin{aligned} \mathcal{M}_{g^\pm q^\pm}^{(0)} &= 2g \sqrt{\frac{p_1 \cdot \bar{\eta}}{p_2 \cdot \bar{\eta}}} \xi_\pm^\mu \\ \mathcal{M}_{g^\pm q^\mp}^{(0)} &= -2g \sqrt{\frac{p_2 \cdot \bar{\eta}}{p_1 \cdot \bar{\eta}}} \xi_\pm^\mu \end{aligned} \quad (3.28)$$

which is reproduced by the operator

$$\begin{aligned} O_2^{(1c)}(x, t) &= \left(\xi_+^\mu J_{n0}^{ij}(x, 0, t) \mathcal{B}_{\bar{n}+}^{ij}(x) - \xi_-^\mu J_{n0}^{ij}(x, t, 0) \mathcal{B}_{\bar{n}-}^{ij}(x) \right. \\ &\quad \left. - \xi_-^\mu J_{n\bar{0}}^{ij}(x, 0, t) \mathcal{B}_{\bar{n}-}^{ij}(x) - \xi_+^\mu J_{n\bar{0}}^{ij}(x, t, 0) \mathcal{B}_{\bar{n}+}^{ij}(x) \right) \end{aligned} \quad (3.29)$$

where $C_2^{(1c)}(t, \mu) = 2i\theta(t)$. There is no need to continue the expansion in the $q^n \bar{q}^n g^{\bar{n}}$ limit to higher powers, because operators with this configuration of external states can only interfere with other operators of the same configuration in the calculation of an event shape. Since the operators in eq. (3.29) are the lowest power operators in this limit and are already suppressed by $1/Q$ in eq.(3.12), they are sufficient to consider contributions to the observable at order $1/Q^2$.

This completes the matching procedure required to calculate the fixed-order cumulative thrust distribution to $O(\alpha_s \tau)$ in e^+e^- scattering. Once finished, our 1-loop resummation program is expected to capture the entire leading-logarithmic behaviour of the cumulative thrust distribution. Pushing the scope of this work to $O(\alpha_s^2 \tau)$ would require additional tree-level matching with a four-body final state. Further extending the theory to allow for hadronic initial states would require new gluon-only operators, as shown in [167–169], though it should be noted that the formalism in those references is different than the one used here.

3.3 Renormalization of Subleading Operators

The anomalous dimension of the leading power operator $O_2^{(0)}$ has been calculated to three loops [103, 171], and the anomalous dimensions of the subleading $\mathcal{O}(1/Q)$ operators $O_2^{(1a)}$ and $O_2^{(1c)}$ have been calculated to one loop [83]. Relevant to the resummation of the $\mathcal{O}(\alpha_s \tau)$ cumulative thrust distribution, there are two operators remaining that have not been renormalized: $O_2^{(2a_1)}$ and $O_2^{(2a_2)}$, and these will be the main results of this chapter. In this section, we first review the definition of the overlap subtraction procedure that is used to properly define loop integrals in this formalism, and then we will discuss the definitions and the results of the anomalous dimensions for all the operators we matched onto in the previous sections.

3.3.1 Overlap Subtraction

In order to properly define loop integrals in standard SCET, one must introduce the zero-bin subtraction prescription [172] or the equivalent, and include both collinear and ultrasoft degrees of freedom in the loops. Formally, the zero-bin removes the overlap of each collinear sector with the ultrasoft sector so as to not double-count degrees of freedom.

In this formalism ultrasoft degrees of freedom are not included separately from collinear degrees of freedom in the effective theory, so the subtraction prescription must be modified in order to correctly remove the double-counting, as discussed in [77]. Formally, rather than subtract the overlap of each collinear sector with the ultrasoft sector, one subtracts the overlap between the two collinear sectors. For the calculations we perform here there is little distinction between the two procedures since in each case the zero-bin, overlap, and ultrasoft amplitudes are equal.

We note that for the operators discussed in this chapter the overlap subtraction amounts to dividing by the vacuum expectation value of light-like Wilson lines:

$$\frac{\langle X | O^{(i)}(x) | 0 \rangle}{\langle 0 | \frac{1}{d_{\mathbf{R}}} \text{tr} W_{\bar{n}}^{\mathbf{R}\dagger}(x) W_n^{\mathbf{R}}(x) | 0 \rangle}, \quad (3.30)$$

where each Wilson line is directed along one of the jets and lives in a representation determined by the field content of the operator in the numerator, and where $d_{\mathbf{R}}$ is the dimension of the representation \mathbf{R} . For operators in which the quark and antiquark are in different sectors, the Wilson lines are in the fundamental representation and $d_{\mathbf{R}} = N_c$, while for the operators in which the quark and antiquark are in the same sector the Wilson lines are in the adjoint representation and $d_{\mathbf{R}} = N_c^2 - 1$. When eq. (3.30) is expanded in perturbation theory to NLO, it includes a diagram corresponding to the one-loop amplitude of the denominator convoluted with the tree-level amplitude of the numerator, along with a minus sign; this formula thus implements the desired subtraction.

Using eq. (3.30) to define the procedure for calculating the one-loop matrix elements of the SCET operator $O^{(i)}(x)$, we proceed to compute their ultraviolet counterterms and determine their anomalous dimensions.

3.3.2 Organization of the Calculation

To regulate the ultraviolet divergences we use the $\overline{\text{MS}}$ dimensional regularization scheme in $D = 4 - 2\epsilon$ dimensions, and to regulate the infrared divergences we use a gluon mass. This choice for an infrared

regulator provides relatively simple expressions for each loop diagram, with the tradeoff that individual diagrams may contain unregulated divergences [173]. Despite this drawback, the sum of all diagrams, including the overlap subtraction, is well-defined provided that the integrands are combined before integrating⁴. Since we are computing diagrams with an external gauge boson, we use the background field method [174] to make the counterterms gauge-invariant.

We find it most convenient to compute matrix elements in terms of the position-space variable t and then Fourier transform to a momentum space variable u before extracting the counterterms and computing the anomalous dimensions. Formally, the Fourier transformed operators are defined by

$$\mathcal{O}_2^{(j)}(x, u) = \int \frac{dt}{2\pi} e^{-iut} \mathcal{O}_2^{(j)}(x, t) \quad (3.31)$$

and matching coefficients

$$C_2^{(j)}(x, u) = \int dt e^{iut} \mathcal{O}_2^{(j)}(x, t) \quad (3.32)$$

which together satisfy

$$\int dt C_2^{(j)}(x, t) \mathcal{O}_2^{(j)}(x, t) = \int du C_2^{(j)}(x, u) \mathcal{O}_2^{(j)}(x, u). \quad (3.33)$$

Operators of the same (j) -label but different value of u mix under renormalization, so that counterterms of $\mathcal{O}_2^{(j)}(x, u)$ are non-diagonal in u . We write the relation between bare and renormalized operators as

$$\mathcal{O}_{2,bare}^{(j)}(x, u) = \int dv Z_{2(j)}(u, v) \mathcal{O}_{2,ren}^{(j)}(x, v), \quad (3.34)$$

and we find that operators of different (j) -label do not mix under renormalization.

As usual, we note that the bare operators cannot depend on the $\overline{\text{MS}}$ scale μ , so taking the logarithmic derivative of both sides of eq. (3.34) and defining the inverse counterterm via the relation

$$\int dw Z_{2(j)}^{-1}(u, w) Z_{2(j)}(w, v) = \delta(u - v) \quad (3.35)$$

we find the renormalization group equation that governs the running of $\mathcal{O}_2^{(j)}(x, u)$

$$\frac{d}{d \log \mu} \mathcal{O}_2^{(j)}(x, u) = - \int dv \gamma_2^{(j)}(u, v) \mathcal{O}_2^{(j)}(x, v) \quad (3.36)$$

where the anomalous dimension is

$$\gamma_2^{(j)}(u, v) = \int dw Z_{2(j)}^{-1}(u, w) \frac{d}{d \log \mu} Z_{2(j)}(w, v). \quad (3.37)$$

Since the combination $\int du C_2^{(j)}(\mu, u) \mathcal{O}_2^{(j)}(\mu, u)$ must be μ -independent, the Wilson coefficient $C_2^{(j)}(u)$ must flow in the opposite manner from its corresponding operator, and in the transposed form

$$\frac{d}{d \log \mu} C_2^{(j)}(u) = \int dv C_2^{(j)}(v) \gamma_2^{(j)}(v, u). \quad (3.38)$$

⁴This was the prevailing viewpoint when the paper associated with this thesis chapter was originally written. However, as we will see in Chapter 5, this viewpoint is now outdated, since an ambiguity arises from combining rapidity-divergent integrals. Accounting for this integration ambiguity, the only resulting changes to this chapter are the replacement of $\log -Q^2/\mu \rightarrow \log -\nu^2/\mu^2$, where ν is the rapidity scale.

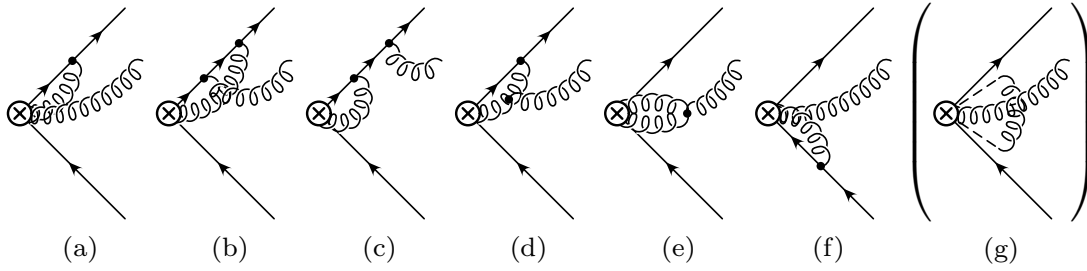


Figure 3.2: The Feynman diagrams for any operator with the $q^n \bar{q}^n g^n$ configuration. The Feynman rules for the effective vertex are determined by the structure of each operator. Diagram (g) is the overlap amplitude, and must be subtracted.

Writing the counterterm as a series in α_s ,

$$Z_{2(j)}(u, v) = \delta(u - v) + \frac{\alpha_s}{2\pi} Z_{2(j)}^{(1)}(u, v) + \mathcal{O}(\alpha_s^2) , \quad (3.39)$$

the anomalous dimension is then given by:

$$\gamma_2^{(j)}(u, v) = \frac{\alpha_s}{\pi} \left(\frac{\partial}{\partial \log \mu^2} - \epsilon \right) Z_{2(j)}^{(1)}(u, v) + \mathcal{O}(\alpha_s^2) . \quad (3.40)$$

3.3.3 Results

We first reproduce the results from [83], in which the anomalous dimensions of the operators $O_2^{(1a)}$ and $O_2^{(1c)}$ were computed.

The relevant diagrams for $O_2^{(1a)}$ operators are shown in Fig. 3.2. To find the counterterms we add together the divergent parts of the diagrams (a) – (f), subtract off the overlap diagram (g), and also include the wavefunction graphs. For $O_2^{(1c)}$ the diagrams are shown in Fig. 3.3; the counterterm is determined by adding diagrams (a) – (d), subtracting the overlap (e), and including the wavefunction graphs. After collecting all the terms and computing the anomalous dimensions according to the notation defined above we find the following results. Note that u corresponds to the fraction of the light-cone momentum $q \cdot \bar{n}$ carried by the particle that was displaced from the vertex in position space; thus, it should be understood that the anomalous dimensions below vanish unless $u \in (0, 1)$. For brevity we denote $\bar{u} = 1 - u$ and $\bar{v} = 1 - v$.

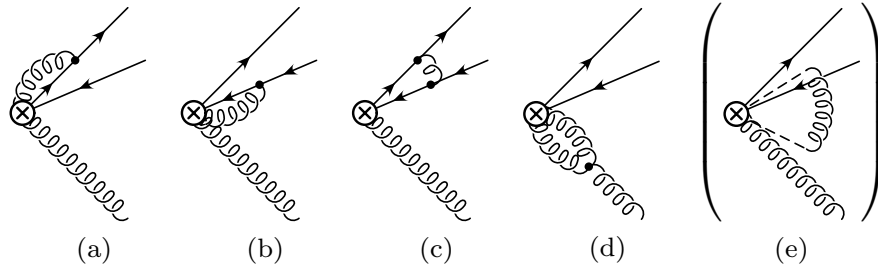


Figure 3.3: The Feynman diagrams for any operator with the $q^n \bar{q}^n g^n$ configuration. The Feynman rules for the effective vertex are determined by the structure of each operator. Diagram (e) is the overlap amplitude, and must be subtracted.

$$\begin{aligned}\gamma_{(1a)}(u, v) &= \frac{\alpha_s \delta(u - v)}{\pi} \left[C_F \left(\log \frac{-Q^2}{\mu^2} - \frac{3}{2} + \log \bar{v} \right) + \frac{C_A}{2} \left(1 + \log \frac{v}{\bar{v}} \right) \right] \\ &+ \frac{\alpha_s}{\pi} \left(C_F - \frac{C_A}{2} \right) \bar{u} \left(\frac{uv}{\bar{u}\bar{v}} \theta(1 - u - v) + \frac{uv + u + v - 1}{uv} \theta(u + v - 1) \right) \\ &+ \frac{\alpha_s}{\pi} \frac{C_A}{2} \bar{u} \left(\frac{\bar{v} - uv}{u\bar{v}} \theta(u - v) + \frac{\bar{u} - uv}{v\bar{u}} \theta(v - u) \right. \\ &\quad \left. - \frac{1}{\bar{u}\bar{v}} \left[\bar{u} \frac{\theta(u - v)}{u - v} + \bar{v} \frac{\theta(v - u)}{v - u} \right]_+ \right) \end{aligned} \tag{3.41}$$

$$\begin{aligned}\gamma_{(1c)}(u, v) &= \frac{\alpha_s \delta(u - v)}{\pi} \left[\frac{1}{2} C_F + C_A \left(\log \frac{-Q^2}{\mu^2} - 1 + \frac{1}{2} \log v\bar{v} \right) \right] \\ &- \frac{\alpha_s}{\pi} \left(C_F - \frac{C_A}{2} \right) \frac{1}{v\bar{v}} \left(v\bar{u} \theta(u - v) + u\bar{v} \theta(v - u) \right. \\ &\quad \left. + \left[\bar{u}v \frac{\theta(u - v)}{u - v} + \bar{v}u \frac{\theta(v - u)}{v - u} \right]_+ \right). \end{aligned} \tag{3.42}$$

We define the symmetric plus-distribution as

$$\begin{aligned}\left[q(u, v) \theta(u - v) + q(v, u) \theta(v - u) \right]_+ &= \lim_{\beta \rightarrow 0} \frac{d}{du} \left(\theta(u - v - \beta) \int_1^u dw q(w, v) \right. \\ &\quad \left. + \theta(v - u - \beta) \int_0^u dw q(v, w) \right) \end{aligned} \tag{3.43}$$

which satisfies

$$\begin{aligned}\int_0^1 du \left[q(u, v) \theta(u - v) + q(v, u) \theta(v - u) \right]_+ f(u) \\ = \int_0^1 du \left(q(u, v) \theta(u - v) + q(v, u) \theta(v - u) \right) (f(u) - f(v)). \end{aligned} \tag{3.44}$$

Note that we have included fewer operators than in [83], since those authors used a formalism in which ultrasoft degrees of freedom were included in the effective theory below the hard scale. Since we are using a formalism where ultrasoft degrees of freedom are not distinguished from the collinear degrees of freedom below the hard scale, some of the operators defined in that paper have no equivalents in this formalism. We also note that there are some minor errors in the coefficients of the logarithms in the diagonal terms for the equivalent results in [83]; we have confirmed that the above results, using the definition of the plus distribution (3.43), are correct.

We now come to the main result of this chapter, in which we present the results for the anomalous dimensions of the $O_2^{(2a_1)}$ and $O_2^{(2a_2)}$ operators, which have been computed for the first time here. The relevant diagrams are also given by Fig. 3.2, as the structure of the graphs will be the same for any operator in which the quark and antiquark are in different sectors. Of course, the Feynman rules to produce a gluon from the vertex is different for each operator. Computing the divergent parts of the graphs, subtracting the overlap graph, and including the wavefunction contributions, we find the

anomalous dimensions:

$$\begin{aligned} \gamma_2^{(2a_1)}(u, v) = & \frac{\alpha_s}{\pi} \delta(u - v) \left[C_F \left(\log \frac{-Q^2}{\mu^2} + \log(\bar{v}) - \frac{3}{2} \right) + \frac{C_A}{2} \left(\log \frac{v}{\bar{v}} + \frac{5}{2} \right) \right] \\ & + \frac{\alpha_s}{\pi} \left(C_F - \frac{C_A}{2} \right) \frac{1}{v\bar{v}^2} \left(\bar{u}^2 \bar{v}^2 \theta(u + v - 1) + uv(\bar{u}\bar{v} + \bar{u} + \bar{v} - 1)\theta(1 - u - v) \right) \\ & - \frac{\alpha_s}{\pi} \frac{C_A}{2} \frac{1}{v\bar{v}^2} \left(v\bar{u}^2(1 + \bar{v})\theta(u - v) + u\bar{v}^2(1 + \bar{u})\theta(v - u) \right. \\ & \quad \left. + \left[v\bar{u}^2 \frac{\theta(u - v)}{u - v} + u\bar{v}^2 \frac{\theta(v - u)}{v - u} \right]_+ \right), \end{aligned} \quad (3.45)$$

$$\begin{aligned} \gamma_2^{(2a_2)}(u, v) = & \frac{\alpha_s}{\pi} \delta(u - v) \left[C_F \left(\log \frac{-Q^2}{\mu^2} + \log(v) - \frac{3}{2} \right) + \frac{C_A}{2} \left(\log \frac{\bar{v}}{v} + \frac{5}{2} \right) \right] \\ & + \frac{\alpha_s}{\pi} \left(C_F - \frac{C_A}{2} \right) \frac{1}{\bar{v}v^2} \left(\frac{uv}{\bar{u}\bar{v}}(\bar{u} - v)(\bar{v} - u)\theta(1 - u - v) \right) \\ & - \frac{\alpha_s}{\pi} \frac{C_A}{2} \frac{1}{\bar{v}v^2} \left(\frac{v\bar{u}(\bar{v} - u)}{\bar{v}}\theta(u - v) + \frac{u\bar{v}(\bar{u} - v)}{\bar{u}}\theta(v - u) \right. \\ & \quad \left. + \left[\bar{u}v^2 \frac{\theta(u - v)}{u - v} + \bar{v}u^2 \frac{\theta(v - u)}{v - u} \right]_+ \right). \end{aligned} \quad (3.46)$$

We have used plus-distribution identities to ensure the anomalous dimensions have the form

$$\gamma_2(u, v) = \delta(u - v)W(v) + f(u, v)S(u, v), \quad (3.47)$$

where $W(v)$ is the diagonal part of the anomalous dimension, $f(u, v)$ is analytic in u and v , and $S(u, v)$ is symmetric in u and v . This property could be important to some readers, since it has previously been exploited to solve the renormalization group equation for the heavy-to-light equivalent of $O_2^{(1a)}$ in terms of Jacobi polynomials [118]. Extending these methods to the operators $O_2^{(1b)}$, $O_2^{(2a_1)}$, and $O_2^{(2a_2)}$ is outside the scope of this work.

3.4 Conclusion

We have computed the anomalous dimensions of all operators required to compute subleading corrections to event shapes such as thrust in SCET. We have used a new formalism for SCET that does not make reference to momentum modes or λ -scaling, and have demonstrated how to match onto a series of higher-dimension operators suppressed by inverse powers of the matching scale Q . These anomalous dimensions will be necessary to resum series of subleading logarithms in event shapes, such as those suppressed by powers of τ in the cumulative thrust distribution, as well as a variety of other event shapes and dijet observables. To complete this program of resummation, an additional matching step onto observable-dependent soft functions will be necessary, and we leave this for future work.

Chapter 4

Rapidity Logarithms in SCET Without Modes

In this chapter, we re-examine observables with rapidity divergences in the context of a formulation of Soft-Collinear Effective Theory in which infrared degrees of freedom are not explicitly separated into modes. We consider the Sudakov form factor with a massive vector boson and Drell-Yan production of lepton pairs at small transverse momentum as demonstrative examples. In this formalism, rapidity divergences introduce a scheme dependence into the effective theory and are associated with large logarithms appearing in the soft matching conditions. This scheme dependence may be used to derive the corresponding rapidity renormalization group equations, and rates naturally factorize into hard, soft and jet contributions without the introduction of explicit modes. Extending this formalism to study power corrections is straightforward. The contents of this chapter appear in [\[175\]](#).

4.1 Introduction

Effective Field Theory (EFT) offers an elegant framework for systematically separating the physics at different scales in a given process. When working with a cutoff μ , physics at high energy scales $\mu_H > \mu$ is integrated out of the theory, and its effects on physics at lower energy scales $\mu_S < \mu$ is taken into account with a series of effective operators of increasing dimension whose effects are suppressed by powers of the ratios of the two scales. One advantage of this approach is that observables depending on multiple scales may be systematically factorized into functions that each depend only on a single energy scale and an arbitrary factorization scale μ . Each factor may then be evaluated at its natural scale, and using renormalization group evolution (RGE) can be brought under perturbative control at an arbitrary scale μ . In multi-scale processes, the theory is matched at each relevant scale μ_i to a new effective theory where physics at scales above μ_i is integrated out, allowing physical quantities to be factorized into multiple terms, each of which depends on a single scale.

Soft-Collinear Effective Theory (SCET) [\[68–74\]](#) achieves this factorization in hard scattering processes by explicitly introducing separate fields, or modes, for each relevant scaling of the various momentum components of the field. A typical SCET factorization theorem separates physical processes into hard, collinear, and soft/ultrasoft pieces. Hard physics (above the cutoff) is incorporated as usual into the matching coefficients of operators in the effective Lagrangian, whereas the factorization of low energy

degrees of freedom occurs dynamically in the effective theory: soft, ultrasoft and collinear degrees of freedom are described by distinct fields which decouple at leading power in the SCET Lagrangian. This allows factorization theorems for many observables to be derived. Processes factorizing into collinear and ultrasoft modes, such as Deep Inelastic Scattering (DIS) in the $x \rightarrow 1$ limit, are referred to as SCET_I processes, whereas those factorizing into collinear and soft modes, such as Drell-Yan (DY) with $q_T^2 \ll q^2$, are referred to as SCET_{II} processes. More complicated processes may require additional modes, and have more complex factorization theorems; some examples are given in [81, 152, 176–178].

In [77] it was proposed that the introduction of separate modes in SCET is not necessary to factorize hard processes in QCD, and in fact complicates the theory. In general, if a theory has a number of physical scales, lowering the cutoff and constructing a new EFT at each threshold Λ_i of the theory automatically factorizes physics at different distance scales, including the factorization which results from splitting the low-energy degrees of freedom into modes. SCET is an EFT describing multiple jets of particles in which the invariant mass of pairs of particles within a jet is much less than the invariant mass of any pair of jets. The degrees of freedom of SCET in a given jet are therefore just those of QCD with a UV cutoff Λ . SCET is more complicated than many canonical EFTs such as four-fermi theory or HQET because of the interactions between the various sectors and the necessity to avoid double counting of degrees of freedom which could be consistently be assigned to more than one sector.

In the formalism presented in [77], each low invariant mass sector of the theory is described by a different copy of QCD, with interactions between sectors occurring via Wilson lines in the external current. This simplifies the EFT by reducing the number of degrees of freedom and interactions, while also making manifest the scales at which different factorizations occur. It also simplifies the structure of power corrections in the theory, since individual modes in SCET do not manifestly factorize at subleading order due to soft-collinear mixing terms in the Lagrangian¹, and these are not present in this approach. In addition, since at the matching scale Q the degrees of freedom below Q are not factorized into separate modes, there is no distinction between the EFT for SCET_I and SCET_{II} processes immediately below Q ; this distinction occurs at a lower scale where a process-dependent matching onto a soft theory is performed.

In [77], this approach was demonstrated for a simple SCET_I observable, DIS in the $x \rightarrow 1$ limit, up to subleading order in $1/Q$. The EFT, including operators up to $O(1/Q^2)$, was renormalized in this framework in [179]. It was observed in [77] that it is necessary to subtract the double-counting of low-energy degrees of freedom which are below the cutoff in different sectors. This is required to reproduce the correct cross section at tree level, and is analogous to zero-bin subtraction in SCET [172]. Without this overlap subtraction, ultraviolet divergences in the EFT would be sensitive to the infrared scales of the theory, so the EFT could not be consistently renormalized.

In this chapter we consider SCET_{II} observables in the same framework. Soft-collinear factorization in SCET_{II} is quite different from ultrasoft-collinear factorization in SCET_I; since the invariant mass of ultrasoft degrees of freedom is parametrically smaller than that of collinear degrees of freedom, ultrasoft-collinear factorization automatically occurs in SCET_I as the renormalization scale of the EFT is lowered. For example, in DIS the SCET Lagrangian is run from Q down to an intermediate scale $Q\sqrt{1-x}$, at which point the Operator Product Expansion (OPE) of the external current and its conjugate is matched onto a parton distribution function (PDF), effectively integrating the collinear degrees of freedom out of the theory. The matching conditions onto the PDF are the usual jet functions of SCET.

¹This factorization was demonstrated at subleading power in [91].

In contrast, soft-collinear factorization is not achieved by lowering the cutoff of the theory, because soft and collinear degrees of freedom have the same invariant mass. In the standard SCET formalism with distinct collinear and soft modes, soft-collinear factorization is required to sum rapidity logarithms of the form $\alpha_s \ln \frac{\mu}{Q} \ln \frac{\mu}{M}$ which arise in SCET_{II} processes, where Q , M and μ are the hard, soft and renormalization scales, respectively. Without resummation, these show up as large logarithms in the matching condition at the scale $\mu \sim M$. Individual soft and collinear graphs contain rapidity divergences which are unregulated in dimensional regularization. In order to define the individual graphs, an additional regulator (examples include the δ regulator [173], the analytic regulator [180, 181], the η -regulator [80, 182], or the pure rapidity regulator [76]) must be introduced, which allows soft and collinear terms to be factorized in a scheme dependent manner. The scheme dependence introduced by the choice of regulator allows a set of rapidity renormalization group (RRG) evolution equations to be derived which sum rapidity logarithms [80, 84, 108, 173, 182, 183].

Since the formalism in [77] does not factorize collinear and soft degrees of freedom in the SCET Lagrangian, it is not immediately clear how soft-collinear factorization arises in this approach. As we will show in this chapter, rapidity logarithms arise because at the loop level there is an ambiguity in defining the sum of individually divergent contributions from the different sectors of the theory, and the scheme dependence of this ambiguity is analogous to the rapidity cutoff usually introduced to factorize soft and collinear modes in SCET. The ambiguity and corresponding resummation occurs in the matching conditions onto the soft theory, so does not affect the running in the intermediate EFT.

In the next section, we illustrate this with the simplest SCET_{II} process, the massive Sudakov form factor. In the subsequent section we consider the Drell-Yan (DY) process at $q_T^2 \ll q^2$. Our conclusions are presented in Sec. 4.4.

4.2 The Massive Sudakov Form Factor

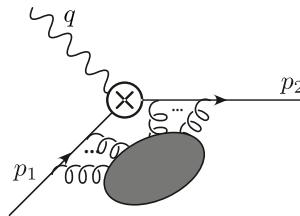


Figure 4.1: The massive Sudakov form factor.

The massive Sudakov form factor provides a simple example of a physical quantity with rapidity logarithms [184]. In a theory with a vector boson of mass M the vector form factor $F(Q^2/M^2)$ is defined by

$$\langle p_2 | j^\mu | p_1 \rangle = F \left(\frac{Q^2}{M^2} \right) \bar{u}_2 \gamma^\mu u_1 \quad (4.1)$$

where

$$j^\mu(x) = \bar{\psi}(x) \gamma^\mu \psi(x), \quad (4.2)$$

and $q^\mu = p_2^\mu - p_1^\mu$ and $Q^2 \equiv -q^2 = 2p_1 \cdot p_2$. The one-loop QCD calculation gives

$$F\left(\frac{Q^2}{M^2}\right) = 1 + \frac{\bar{\alpha}}{2} \left(-L_{Q/M}^2 + 3L_{Q/M} - \frac{4\pi^2}{6} - \frac{7}{2} \right) \quad (4.3)$$

where $\bar{\alpha} \equiv \alpha_s C_F / (2\pi)$ and $L_{Q/M} \equiv \log(Q^2/M^2)$. The large logarithms of Q^2/M^2 in the fixed-order expansion indicate that for $Q^2 \gg M^2$, perturbation theory is not well behaved and must be resummed. This is achieved by splitting $F(Q^2/M^2)$ into separate factors, each of which depends only on a single dynamical scale as well as an arbitrary factorization scale; consistency of the factorization formula to all orders in α_s then places sufficient constraints on the perturbative series to allow resummation of the logarithmically enhanced terms to any order in the leading-log expansion.

4.2.1 Soft-Collinear Factorization

First we review the standard SCET approach to factorization for this quantity. In this standard framework, the EFT below $\mu = Q$ is SCET_{II} [173] with contributions from n -collinear, \bar{n} -collinear and soft (or mass) modes, $p_n \sim Q(\lambda^2, 1, \lambda)$, $p_{\bar{n}} \sim Q(1, \lambda^2, \lambda)$ and $p_s \sim Q(\lambda, \lambda, \lambda)$, where $\lambda \sim M/Q$. Matching from QCD onto SCET factors out at the hard matching coefficient at the scale $\mu = Q$, giving

$$F\left(\frac{Q^2}{M^2}\right) = \left[1 + \frac{\bar{\alpha}}{2} \left(-L_Q^2 + 3L_Q + \frac{\pi^2}{6} - 8 \right) \right] \left[1 + \frac{\bar{\alpha}}{2} \left(-L_M^2 - L_M(3 - 2L_Q) - \frac{5\pi^2}{6} + \frac{9}{2} \right) \right] \quad (4.4)$$

where $L_Q = \log(Q^2/\mu^2)$ and $L_M = \log(M^2/\mu^2)$. The first factor is the hard matching coefficient

$$C_2(\mu) = 1 + \frac{\bar{\alpha}}{2} \left(-L_Q^2 + 3L_Q + \frac{\pi^2}{6} - 8 \right) \quad (4.5)$$

from the QCD current to the leading SCET current, and is independent of the infrared scale M , while the second factor is the matrix element of the vector current in the effective theory.

As discussed in [84], the matrix element of the vector current in SCET is problematic, as it has a logarithmic dependence on the ultraviolet scale Q , which is above the cutoff of the EFT. Typically in an EFT, logarithms of ultraviolet scales are replaced by logarithms of the cutoff, which allows them to be summed using RGE techniques. As noted in [64], the scale Q enters the EFT because the contributions to the loop graph from individual modes are not separately well-defined, so even though Q is not a dynamical scale associated to any single mode, the sum of the graphs re-introduces Q into the result (this was dubbed the “collinear anomaly” in [64]). As a result, integrating the massive gauge boson out of the theory at $\mu = M$ gives matching conditions onto the soft theory containing logarithms of Q/M which are not resummed by the usual RGE evolution.

Rapidity logarithms are resummed in SCET by exploiting an additional scheme dependence in the theory, beyond the choice of renormalization scale μ . In SCET_{II} processes with rapidity logarithms, individual collinear and soft graphs are not well-defined; only the sum is. In order to regulate the individual soft and collinear contributions, an additional regulator must be added to the theory. Using, for example, the rapidity regulator of [80], individual soft and collinear contributions are separately well-defined, and the form factor factorizes into individual hard, soft and jet functions,

$$F\left(\frac{Q^2}{M^2}\right) = C_2(\mu) S\left(\frac{M}{\nu}, \frac{M}{\mu}\right) J_n\left(\frac{p_2^-}{\nu}, \frac{M}{\mu}\right) J_{\bar{n}}\left(\frac{p_1^+}{\nu}, \frac{M}{\mu}\right) \quad (4.6)$$

where p_1^+ and p_2^- are the large light-cone components of p_1^μ and p_2^μ satisfying $p_1^+ p_2^- = Q^2$, and, to one loop,

$$\begin{aligned} J_n\left(\frac{p_2^-}{\nu}, \frac{M}{\mu}\right) &= 1 + \bar{\alpha} \left[L_M \left(\log \frac{p_2^-}{\nu} - \frac{3}{4} \right) - \frac{\pi^2}{6} + \frac{9}{8} \right] \\ J_{\bar{n}}\left(\frac{p_1^+}{\nu}, \frac{M}{\mu}\right) &= 1 + \bar{\alpha} \left[L_M \left(\log \frac{p_1^+}{\nu} - \frac{3}{4} \right) - \frac{\pi^2}{6} + \frac{9}{8} \right] \\ S\left(\frac{M}{\nu}, \frac{M}{\mu}\right) &= 1 + \frac{\bar{\alpha}}{2} \left[L_M^2 - 4L_M \log \frac{M}{\nu} - \frac{\pi^2}{6} \right]. \end{aligned} \quad (4.7)$$

The rapidity scale ν defines a scheme-dependent way to separate soft and collinear contributions. While the individual soft and jet functions depend on ν , their product is ν -independent, thus allowing a renormalization group equation (the rapidity renormalization group) to be derived. Each of the terms may then be evolved from its natural rapidity scale in ν , summing the rapidity logarithms.

Similar results have also been derived in the collinear anomaly formalism [64, 85, 185], in which the product of $J_n J_{\bar{n}} S$ in Eq. (4.6) is re-factorized as the product of two functions: an anomaly exponent F in which the rapidity logarithms appear and a remainder function W independent of the hard scale.

4.2.2 Scheme Dependence Without Modes

In the formalism introduced in [77], there are no explicit modes, so rapidity logarithms are not resummed by exploiting the scheme dependent separation into soft and collinear degrees of freedom. Instead, as we now discuss, the contributions from the individual n and \bar{n} sectors of the theory, along with the corresponding overlap subtraction, are individually divergent, and the scheme dependence in defining their sum allows rapidity logarithms to be summed.

In this formalism, the incoming and outgoing states are each described by two decoupled copies of QCD. Each sector interacts with the other sector as a lightlike Wilson line, contained in the hard external current, since gluons with sufficient momentum to deflect the worldline of the other sector have been integrated out of the theory. While the theory is frame-independent, for simplicity we work in the Breit frame and label the sectors by the light-like directions $n^\mu = (1, 0, 0, 1)$ and $\bar{n}^\mu = (1, 0, 0, -1)$, with the light-cone coordinates of a four-vector p^μ defined as $p^+ \equiv p \cdot n$, $p^- \equiv p \cdot \bar{n}$. The incoming quark is in the \bar{n} -sector, $p_1^+ \gg (p_1^-, |p_{1\perp}|)$, while the outgoing is in the n -sector, $p_2^- \gg (p_2^+, |p_{2\perp}|)$.

At leading order, the hard QCD current matches onto the scattering operator O_2 via the matching relation

$$j^\mu(x) \rightarrow j_{\text{SCET}}^\mu = C_2(\mu) O_2^\mu(x) + O\left(\frac{1}{Q}\right), \quad (4.8)$$

where $C_2(\mu)$ is given in Eq. (4.5), and the neglected subleading operators are known up to order $1/Q^2$ when there are two sectors [179]. The operator $O_2^\mu(x)$ is defined as

$$O_2^\mu(x) = [\bar{\psi}_n(x_n) \bar{W}_n(x_n)] P_n \gamma^\mu P_{\bar{n}} [W_{\bar{n}}^\dagger(x_{\bar{n}}) \psi_{\bar{n}}(x_{\bar{n}})] \quad (4.9)$$

where the fields ψ_n and $\psi_{\bar{n}}$ are QCD quark fields in the two sectors, and

$$P_n = \frac{\not{n} \not{\bar{n}}}{4}, \quad P_{\bar{n}} = \frac{\not{\bar{n}} \not{n}}{4}. \quad (4.10)$$

The square brackets separate the field content of each sector. The (un)barred Wilson lines are (outgoing)

incoming, and are defined [164, 186, 187]) as

$$\begin{aligned}\bar{W}_n(x) &= P \exp \left(ig \int_{-\infty}^0 ds \bar{n} \cdot A_n(x + \bar{n}s) e^{s0^+} \right) \\ W_{\bar{n}}^\dagger(x) &= P \exp \left(ig \int_0^\infty ds n \cdot A_{\bar{n}}(x + ns) e^{-s0^+} \right)\end{aligned}\tag{4.11}$$

where again the subscript in the gluon fields $A_{n,\bar{n}}^\mu$ labels the sector. Note that we are using the labelling convention that $W_{\bar{n}}^\dagger$ is a Wilson line along the n direction, coupling to fields in the \bar{n} sector.

Finally, consistently expanding the QCD amplitude in powers of $1/Q$ also means that the energy-momentum conserving delta function must also be expanded, giving

$$\delta_{\text{SCET}}(Q; p_n, p_{\bar{n}}) \equiv 2\delta(p_n^- - Q^-)\delta(p_{\bar{n}}^+ - Q^+)\delta(\mathbf{p}_{nT} + \mathbf{p}_{\bar{n}T} - \mathbf{q}_T) + \dots\tag{4.12}$$

where p_n and $p_{\bar{n}}$ are the total momenta in the n and \bar{n} sectors, respectively. This is achieved by multipole expanding the x^μ dependence of the current in Eq. (4.9), where we have defined

$$x_n^\mu \equiv x^+ \frac{\bar{n}^\mu}{2} + x_\perp^\mu, \quad x_{\bar{n}}^\mu \equiv x^- \frac{n^\mu}{2} + x_\perp^\mu.\tag{4.13}$$

Multipole expanding the energy-momentum conserving delta function has no effect on the renormalization of O_2 since the sectors are decoupled, but ensures correct power counting when calculating production rates, as we will see in the next section for Drell-Yan production.

As described in [77], this theory double counts quarks and gluons whose momentum is below the cutoff of both sectors, and the effects of this double counting must be explicitly subtracted from diagrams. This ‘overlap subtraction’ is similar to the familiar zero-bin subtraction in SCET [172], or the equivalent soft subtraction prescription discussed in [188–190]. At tree level it is required to ensure that external states are not double counted in the rate. At one loop this corresponds to subtracting the overlap graph in Fig. 4.2(c), which is equivalent to either the n - or \bar{n} -sector graph, but with the quark propagator replaced by the corresponding lightlike Wilson line. Formally this corresponds to dividing matrix elements of O_2 by the vacuum expectation value of Wilson lines,

$$\langle p_2 | O_2(x) | p_1 \rangle_{\text{subtracted}} = \frac{\langle p_2 | O_2(x) | p_1 \rangle}{\frac{1}{N_C} \text{Tr} \langle 0 | W_{\bar{n}}^\dagger(x) \bar{W}_n(x) | 0 \rangle}.\tag{4.14}$$

This prescription means that the one-loop matrix element of O_2 is given by the combination

$$\mathcal{M}_1 = \Gamma_n + \Gamma_{\bar{n}} - \Gamma_{\text{sub}} - 2\frac{\Gamma_\psi}{2},\tag{4.15}$$

where the Γ_i represent the one-loop n -sector, \bar{n} -sector, and overlap subtraction graphs in Fig. 4.2(a), (b) and (c), and Γ_ψ is the wavefunction renormalization contribution,

$$\Gamma_\psi = \frac{1}{2} \bar{\alpha} \mathcal{M}_0 \left(\frac{1}{\epsilon} - L_M - \frac{1}{2} \right)\tag{4.16}$$

where $\mathcal{M}_0 = \bar{u}_2 P_{\bar{n}} \gamma^\mu P_{\bar{n}} v_1$ and we work in $d = 4 - 2\epsilon$ dimensions.

As described in [77] (and, in a different context, [83, 173, 189]), while the terms Γ_n , $\Gamma_{\bar{n}}$ and Γ_{sub} are all individually divergent even when the theory is regulated in dimensional regularization, adding

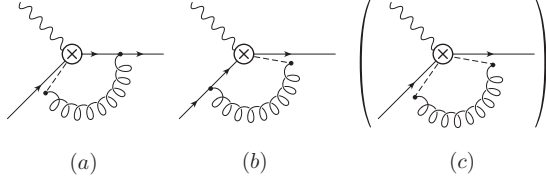


Figure 4.2: Renormalization of O_2 . Diagram (c) is the overlap subtraction. In (a), the gluon is in the n sector; in (b), it is in the \bar{n} sector. In (c), the dashed lines represent Wilson lines $W_{n,\bar{n}}$, depending on their direction.

together the individual graphs before doing the final momentum integral results in a finite answer in d dimensions:

$$\mathcal{M}_1 = \frac{\bar{\alpha}}{2} \mathcal{M}_0 \left[\frac{2}{\epsilon^2} + \left(\frac{1}{\epsilon} - L_M \right) (3 - 2L_Q) - L_M^2 - \frac{5\pi^2}{6} + \frac{9}{2} \right]. \quad (4.17)$$

After adding the appropriate counterterm, this reproduces the second line in Eq. (4.4). This result was used in [77] to define the one-loop renormalization of O_2 in this formalism.

However, one must be careful here, because naïvely adding together divergent graphs is not a well-defined procedure. In particular, adding the integrands before performing the final integration corresponds to only one possible scheme to define the sum of the divergent graphs. We can illustrate this scheme dependence by doing the k^+ integrals for $\Gamma_{n,\bar{n},\text{sub}}$ by contours for each graph and then doing the $(d-2)$ -dimensional k_\perp integrals, but leaving the divergent k^- integrals unevaluated. This gives for the n -sector graph, Fig. 4.2 (a),

$$\Gamma_n = C_\epsilon \int_0^{p_2^-} \frac{dk^-}{-k^-} \left(1 - \frac{k^-}{p_2^-} \right)^{1-\epsilon} \quad (4.18)$$

where

$$C_\epsilon \equiv \bar{\alpha} \mathcal{M}_0 \left(\frac{\mu^2 e^{\gamma_E}}{M^2} \right)^\epsilon \Gamma(\epsilon). \quad (4.19)$$

The \bar{n} -sector graph gives

$$\begin{aligned} \Gamma_{\bar{n}} &= C_\epsilon \left[\frac{1}{1-\epsilon} + \int_0^\infty \frac{p_1^+ dk^-}{M^2} \frac{1 - \left(\frac{p_1^+ k^-}{M^2} \right)^{-\epsilon}}{1 - \frac{p_1^+ k^-}{M^2}} \right] \\ &= C_\epsilon \left[\frac{1}{1-\epsilon} + \pi \csc(\pi\epsilon) (-1 + i0^+)^{-\epsilon} + \int_0^\infty \frac{p_1^+ dk^-}{M^2} \frac{1}{1 - \frac{p_1^+ k^-}{M^2}} \right] \end{aligned} \quad (4.20)$$

and finally the overlap subtraction graph gives

$$\Gamma_{\text{sub}} = C_\epsilon \int_0^\infty \frac{dk^-}{-k^-}. \quad (4.21)$$

The n -sector and \bar{n} -sector graphs are divergent as $k^- \rightarrow 0$ and $k^- \rightarrow \infty$, respectively. When the graphs are added together before doing the final integral, these divergences are canceled by the overlap graph, giving the result in Eq. (4.17). However, the individual terms Γ_i each arise from loops containing distinct particles in the EFT (n - and \bar{n} -collinear gluons and their overlap), so we are free to individually rescale the momenta in the individual integrals before combining them. For example, rescaling the integration

variable in $\Gamma_{\bar{n}}$ by $k^- \rightarrow \frac{\zeta^2}{Q^2} k^-$ will instead give the sum of the three graphs

$$\begin{aligned} I_n + I_{\bar{n}} - I_{\text{sub}} &= \int_0^{p_2^-} \left[\frac{1}{-k^-} \left(1 - \frac{k^-}{p_2^-} \right)^{1-\epsilon} + \frac{\zeta^2 p_1^+}{M^2 Q^2} \frac{1}{1 - \frac{k^- \zeta^2 p_1^+}{M^2 Q^2}} + \frac{1}{k^-} \right] dk^- \\ &\quad + \int_{p_2^-}^{\infty} \left[\frac{\zeta^2 p_1^+}{M^2 Q^2} \frac{1}{1 - \frac{k^- \zeta^2 p_1^+}{M^2 Q^2}} + \frac{1}{k^-} \right] dk^- \\ &= 1 + \log \frac{M^2}{\zeta^2} + i\pi + \left(1 - \frac{\pi^2}{6} \right) \epsilon + O(\epsilon^2) \equiv I(\zeta) \end{aligned} \quad (4.22)$$

which gives the ζ -dependent matrix element

$$\mathcal{M}_1 = \frac{\bar{\alpha}}{2} \mathcal{M}_0 \left[\frac{2}{\epsilon^2} + \left(\frac{1}{\epsilon} - L_M \right) (3 - 2L_\zeta) - L_M^2 - \frac{5\pi^2}{6} + \frac{9}{2} \right] \quad (4.23)$$

where $L_\zeta = \log(\zeta^2/\mu^2)$. Choosing $\zeta = Q$ corresponds to the naïve result (Eq. (4.17)), but leaving ζ free makes the scheme dependence manifest. This also underscores the fact that SCET has no dynamical dependence on the scale Q , which has been integrated out of the theory: the Q dependence in the naïve matrix element is in fact ζ dependence, which parameterizes the scheme-dependence of the rapidity divergent integrals. A similar calculation was performed with massless gluons in [189] where the authors noted that the scaleless SCET integrals had the scale Q inserted by hand; any other scale ζ could similarly be inserted by hand, but the choice $\zeta = Q$ was “justified *a posteriori* by the requirement that SCET reproduce the IR divergences of QCD”.

This simple one-loop example demonstrates how rapidity logarithms of the hard scale Q enter into the EFT: they are not logarithms of Q in matrix elements, but rather logarithms of some dimensionful scheme parameter which defines how individually rapidity divergent graphs in different sectors are added together. The scheme dependence of the matrix element in Eq. (4.23) suggests that we introduce a corresponding scheme dependence in the one-loop matching coefficient from QCD onto SCET,

$$C_2(\mu) \rightarrow C_2(\mu, \zeta) = 1 + \frac{\bar{\alpha}}{2} \left(-L_Q^2 + 3L_Q + 2L_M L_{Q/\zeta} + \frac{\pi^2}{6} - 8 \right) \quad (4.24)$$

where $L_{Q/\zeta} \equiv \log Q^2/\zeta^2$, so that physical quantities are independent of ζ . However, as we will discuss in detail in the next section, the Wilson coefficient C_2 must be independent of the infrared scale M , which requires choosing $\zeta = Q$ at the matching scale $\mu = Q$, eliminating the nonanalytic dependence on M in Eq. (4.24). Thus, it would seem that there is no freedom to choose ζ in SCET, since it is fixed to $\zeta = Q$ by the requirement that the scales M and Q factorize. However, the fact that logarithms of Q in matrix elements of O_2 are in fact logarithms of a scheme parameter allows us to sum rapidity logarithms in low-energy matrix elements. Since the ζ -scheme defined in this section was introduced for illustrative purposes and is not obviously defined beyond the simple one-loop graphs considered here, we will discuss resummation of rapidity logarithms with a well-defined regulator in the next section.

4.2.3 Resummation

There are a number of regulators in the literature which regulate rapidity divergences [51, 76, 80, 173, 180, 191]; the most instructive for our purposes is to use a version of the δ -regulator [173]. In its original

formulation, quark propagators and Wilson lines were both modified by adding a quark mass term to the Lagrangian and using the new quark propagator to derive the new Wilson line propagator. Here we leave quark and gluon propagators unchanged and simply redefine the Wilson lines by shifting the pole prescription $i0^+ \rightarrow -\delta_n + i0^+$ for both the \bar{W} and W^\dagger in Eq. (4.11), and we allow each sector label n_i to have a separate value of δ (i.e. $\delta_{\bar{n}}$ in the \bar{n} -sector and δ_o in the overlap between the sectors²). With this modification, the n -sector graph becomes

$$\Gamma_n^\delta = \bar{\alpha} \mathcal{M}_0 \left[\left(\frac{1}{\epsilon} - L_M \right) \left(\log \frac{\delta_n}{p_2^-} + 1 \right) - \frac{\pi^2}{6} + 1 \right], \quad (4.25)$$

and the \bar{n} sector gives the same result but with $\delta_n \rightarrow \delta_{\bar{n}}$ and $p_2^- \rightarrow p_1^+$. The overlap graph contributes

$$\Gamma_{\text{sub}}^\delta = \bar{\alpha} \mathcal{M}_0 \left[-\frac{1}{\epsilon^2} + \left(\frac{1}{\epsilon} - L_M \right) \log \frac{\delta_o^2}{\mu^2} + \frac{L_M^2 + \frac{\pi^2}{6}}{2} \right], \quad (4.26)$$

so that together with the wavefunction graphs we find

$$\mathcal{M}_1^\delta = \frac{\bar{\alpha}}{2} \mathcal{M}_0 \left[\frac{2}{\epsilon^2} + \left(\frac{1}{\epsilon} - L_M \right) \left(3 - 2 \log \frac{\nu^2}{\mu^2} \right) - L_M^2 + \frac{9}{2} - \frac{5\pi^2}{6} \right], \quad (4.27)$$

where the parameter ν , defined by

$$\frac{\delta_n \delta_{\bar{n}}}{\delta_o^2} \equiv \frac{Q^2}{\nu^2}, \quad (4.28)$$

plays a role analogous to ζ in the previous section. We can take the regulators δ_i to zero while keeping ν fixed, and the scheme-dependence of the rapidity log is then reflected in the ν dependence of the result.³ We note that Q as introduced here is not a dynamical scale in the EFT, but simply serves to define the dimensionful parameter ν .

Setting $\nu = Q$ in Eq. (4.27) gives the naïve result, Eq. (4.17). More generally, the scheme dependence of the matrix element in Eq. (4.27) requires a corresponding scheme dependence in the Wilson coefficient of O_2 so that physical quantities are independent of ν . We must be careful, however, in defining the rapidity scheme. It is a general feature of EFTs that Wilson coefficients do not have nonanalytic dependence on infrared scales; otherwise, the EFT would not factorize the physics of short and long distance scales. At scales μ parametrically larger than M , this can only be achieved by choosing $\nu = Q$; otherwise the Wilson coefficient $C_2(\mu)$ would contain a factor of $L_M \log Q^2/\nu^2$, which is sensitive to the IR scale M . As with the ζ -scheme in the previous section, it would therefore seem that there is no freedom to choose the rapidity regulator in SCET, since it is fixed to $\nu = Q$ by the requirement that the scales M and Q factorize. However, after running the theory down to the scale $\mu = \mu_S \sim M$, the gluon mass is no longer an infrared scale, and we are then free to run ν from $\nu_H \equiv Q$ to $\nu_S = M$ when calculating the matching conditions onto the free theory, summing the rapidity logarithms in the matching condition at μ_S .

After running the matching coefficient C_2 from $\mu = Q$ down to $\mu_S \sim M$, we integrate out the massive gluon and match O_2 onto a free theory,

$$O_2^\mu(x) \rightarrow C_S O_S^\mu(x) \quad (4.29)$$

²This differs from the prescription in [77], where the overlap Wilson lines had the same value of δ as the corresponding sector.

³The scheme dependence in taking the $\delta_i \rightarrow 0$ limit was also stressed in [66].

where

$$O_S^\mu(x) = \bar{\psi}(x) P_{\bar{n}} \gamma^\mu P_{\bar{n}} \psi(x) \quad (4.30)$$

and the ψ 's are free fermions. However, the resulting matching coefficient

$$C_S = 1 + \frac{\bar{\alpha}}{2} \left[-L_M \left(3 - 2 \log \frac{\nu_H^2}{\mu_S^2} \right) - L_M^2 - \frac{5\pi^2}{6} + \frac{9}{2} \right] \quad (4.31)$$

contains a large rapidity logarithm. To resum this, we must effectively run the matching condition C_S in rapidity from ν from $\nu = \nu_H$ to $\nu = \nu_S \sim \mu_S$ before integrating out the gluon, which we do by running the operator O_2 in rapidity at the matching scale μ_S . We define

$$C_2 O_2^\mu(x)|_{\mu=\mu_S} = C_2(\mu_S) V_J \left(\frac{\mu_S}{M}, \frac{\nu}{Q} \right) O_2^\mu(x, \nu) \quad (4.32)$$

where $O_2^\mu(x, \nu)$ denotes $O_2(\mu_S)$ defined with $\nu \neq Q$, and at one loop,

$$V_J \left(\frac{\mu}{M}, \frac{\nu}{Q} \right) = 1 + \bar{\alpha} L_M \log \frac{Q^2}{\nu^2}. \quad (4.33)$$

The fact that the Q dependence of O_2 factorizes according to Eq. (4.32) means that the logarithm of Q in Eq. (4.33) exponentiates. Explicitly, differentiating Eq. (4.32) with respect to $\log \nu$ gives the equation

$$\frac{d}{d \log \nu} V_J = \left(-\langle O_2^\mu(x, \nu) \rangle^{-1} \frac{d}{d \log \nu} \langle O_2^\mu(x, \nu) \rangle \right) V_J \equiv \gamma_\nu^J V_J \quad (4.34)$$

where

$$\gamma_\nu^J = -2\bar{\alpha} L_M. \quad (4.35)$$

This has the solution

$$\log V_J \left(\frac{\mu_S}{M}, \frac{\nu_S}{Q} \right) = \int_Q^{\nu_S} \frac{d\nu}{\nu} \gamma_\nu^J = \bar{\alpha}(\mu_S) \log \frac{M^2}{\mu_S^2} \log \frac{Q^2}{\nu_S^2} \quad (4.36)$$

which corresponds to running the rapidity scale from $\nu = Q$ to ν_S .

Having resummed the large rapidity logarithms into V_J , the heavy gauge boson is then integrated out, and Eqs. (4.29) and (4.31) become

$$O_2^\mu(x, \nu_S) \rightarrow C_S \left(\frac{\mu_S}{M}, \frac{\nu_S}{\mu_S} \right) O_S(x) \quad (4.37)$$

and

$$C_S \left(\frac{\mu}{M}, \frac{\nu}{\mu} \right) = 1 + \frac{\bar{\alpha}}{2} \left[-L_M \left(3 - 2 \log \frac{\nu^2}{\mu^2} \right) - L_M^2 - \frac{5\pi^2}{6} + \frac{9}{2} \right] \quad (4.38)$$

which has no large logarithms at $\mu \sim \nu \sim M$. We can then combine all of these steps to obtain the resummed factorization formula

$$F \left(\frac{Q^2}{M^2} \right) = U_2(\mu_S, \mu_H) C_2(\mu_H) V_J \left(\frac{\mu_S}{M}, \frac{\nu_S}{Q} \right) C_S \left(\frac{\mu_S}{M}, \frac{\nu_S}{\mu_S} \right) \quad (4.39)$$

where

$$\begin{aligned}\log U_2(\mu_S, \mu_H) &= \int_{\mu_H}^{\mu_S} \frac{d\mu}{\mu} \gamma_2^{LL}(\mu) \\ &= \frac{4C_F^2}{\beta_0^2} \left[\frac{1}{\bar{\alpha}(\mu_H)} - \frac{1}{\bar{\alpha}(\mu_S)} - \frac{1}{\bar{\alpha}(Q)} \log \left(\frac{\bar{\alpha}(\mu_S)}{\bar{\alpha}(\mu_H)} \right) \right]\end{aligned}\quad (4.40)$$

is the usual leading-log renormalization group evolution of C_2 [105–107], and

$$\gamma_2^{LL}(\mu) = 2\bar{\alpha}(\mu) \log \frac{Q^2}{\mu^2} \equiv \Gamma_{\text{cusp}}[\bar{\alpha}] \log \frac{Q^2}{\mu^2} . \quad (4.41)$$

This reproduces the results of [80], with the caveat that, since this formalism explicitly performs the RRG at the scale $\mu = \mu_S \sim M$, logarithms of μ/M which are resummed in the expression $\log \frac{\alpha_s(\mu)}{\alpha_s(M)}$ in $\log V_J$ in [182] do not require resummation here.

While Eq. (4.39) is equivalent to the factorization formula in Eq. (4.6), it arises differently in this form of the EFT. In Eq. (4.6), the J_i are matrix elements of collinear fields; here V_J corresponds to the rapidity evolution factor of $O_2(x, \nu)$. The assignment of factors of L_M and constants to O_J and O_S also differs from that of Eq. (4.7), and more closely resembles the refactorized form of [85, 185], but the particular arrangement of these terms is irrelevant for summing logarithms since α_s is evaluated at the same scale in both the soft and jet functions in SCET_{II} processes. We could also choose to define separate rapidity scales for each sector, $\nu_n \equiv p_1^+ \delta_o / \delta_n$ and $\nu_{\bar{n}} \equiv p_2^- \delta_o / \delta_{\bar{n}}$, which would then allow us to write V_J as the product of two separate factors, in direct analogy with the two jet functions of Eq. (4.7); however, this is not necessary for the present case, where the rapidity scales always appear as the product $\nu_n \nu_{\bar{n}} = \nu^2$.

There are also some important differences between the rapidity running of $O_2(x, \nu)$ and the rapidity renormalization group of [80]. In [80], separate soft and collinear contributions to O_2 are defined and separately run in rapidity space; the regularization scheme is defined so that the product of soft and collinear factors is regulator-independent. In our case, matrix elements of operators in the EFT have explicit dependence on the rapidity regulator, which is canceled by the regulator dependence of the corresponding Wilson coefficient $C_2 V_J$ in the EFT. In addition, since the rapidity regulator introduces sensitivity to the matching scale $\mu_S \ll Q$ into the Wilson coefficient of O_2 , the variation of ν is performed at the matching scale μ_S , not at a higher scale. There is a physical reason for this: unlike the renormalization group running of O_2 in μ , rapidity running is not universal in SCET, but depends on the particular process of interest. In Drell-Yan at low q_T^2 , for example, and as discussed in the next section, the rapidity logarithms arise in the matching conditions of products of O_2 onto products of parton distribution functions, and are distinct from the rapidity logarithms in Eq. (4.32). Thus, in this formalism, in which the same SCET Lagrangian may be used to calculate a variety of observables with different rapidity logarithms (or none at all), rapidity logarithms arise in low-energy matching coefficients and are resummed at the appropriate matching scale.

This is also apparent from Eq. (4.36): the resummed rapidity logarithms are all multiplied by factors of $\alpha_s(\mu_S)$, so rapidity evolution naturally occurs at the low matching scale. This is also the case using the usual SCET RRG formalism: although in [80] it was shown that one can evolve along any path in the (μ, ν) plane to obtain the resummed factorization formula, performing rapidity running away from $\mu = \mu_S$ requires an additional resummation of the large logarithms L_M in the rapidity anomalous dimensions of the jet and soft functions in order to achieve an equivalent result.

Just as in the usual RRG formalism, consistency of the factorization (4.39) places constraints on the rapidity anomalous dimension γ_ν^J . In [80] these constraints were derived using independence of path in the (μ, ν) plane; we obtain analogous results by requiring consistency between evolving to two different soft scales μ_S which differ by order 1. The difference in V_J evaluated at two different soft scales μ_S and μ'_S is of order $\log Q^2/M^2$, and so contains a large logarithm of Q . Since the overall variation of the form factor with respect to μ_S must vanish, and since matrix elements of O_2 are independent of Q , this large variation of V_J must be compensated for in the running of $C_2(\mu)$. This means that the change in $C_2 V$ resulting from varying μ_S by an amount of order 1 is Q independent, which implies

$$\frac{d}{d \log Q} \frac{d}{d \log \mu} (\log U_2 + \log V_J) = 0. \quad (4.42)$$

Since $\frac{d \log U_2}{d \log \mu} = \gamma_2^{LL}$ and $\frac{d \log V_J}{d \log Q} = -\frac{d \log V_J}{d \log \nu} = -\gamma_\nu^J$, this immediately gives the relation

$$\frac{d \gamma_2^{LL}}{d \log Q} = \frac{d \gamma_\nu^J}{d \log \mu} = 2\Gamma_{\text{cusp}}. \quad (4.43)$$

4.3 Drell-Yan at Small q_T

A somewhat more involved process with rapidity logarithms is Drell-Yan (DY) scattering, $N_1(p)N_2(\bar{p}) \rightarrow \gamma^* + X \rightarrow (\ell\bar{\ell}) + X$, with $q_T^2 \ll q^2$, where q^μ and q_T^μ are the total and transverse momenta of the final state leptons, respectively. In standard SCET, this is a SCET_{II} process in which the product of two hard external currents may be written in terms of a convolution of transverse-momentum dependent parton distribution functions (TMDPDFs) or beam functions [64, 66, 80, 192–194] with n -collinear, \bar{n} -collinear and soft modes, which individually exhibit rapidity divergences. By running the TMDPDFs using both the usual μ -renormalization group and its counterpart in rapidity space, logarithms associated with ultraviolet divergences and rapidity divergences may both be summed. If $q_T \equiv \sqrt{\mathbf{q}_T^2} \gg \Lambda_{\text{QCD}}$, an additional expansion may then be performed in powers of Λ_{QCD}/q_T , allowing the product of TMDPDFs to be matched onto the usual parton distribution functions (PDFs).

Proceeding in an analogous fashion to the previous section, in our formalism the QCD current is first matched at the hard matching scale onto the corresponding SCET current in a theory with n and \bar{n} sectors with the appropriate overlap subtractions. Again, there is no distinction between SCET_I and SCET_{II} at the hard matching scale, since amplitudes are expanded in powers of p^+ , \bar{p}^- , p_\perp and \bar{p}_\perp , with no hierarchy assumed between these scales. The EFT is then evolved via the RGE until a scale $\mu = \mu_S \sim q_T$, at which point the product of currents is matched onto a convolution of PDFs in the soft theory below $\mu = \mu_S$. However, the rate given by this product of currents has an integration ambiguity similar to that discussed in the previous section, and so rapidity logarithms arise when evaluating the matching conditions onto the soft theory. These may be summed by first matching the product of the currents at $\mu = \mu_S$ onto a nonlocal operator equivalent to a convolution of TMDPDFs, which is then run in rapidity space before matching onto PDFs.

4.3.1 Factorization by Successive Matching

The DY process is mediated in SCET by the dijet current, defined by the matching relation

$$\begin{aligned} j^\mu(x) &= C_2(\mu) O_2^\mu(x) + \dots \\ &= C_2(\mu) [\bar{\psi}_{\bar{n}}(x_{\bar{n}}) \bar{W}_{\bar{n}}(x_{\bar{n}})] P_n \gamma^\mu P_n [\bar{W}_n^\dagger(x_n) \psi_n(x_n)] + \dots \end{aligned} \quad (4.44)$$

where the ellipses denote power corrections, and

$$\bar{W}_n^\dagger(x) = \bar{P} \exp \left[-ig \int_{-\infty}^0 ds \bar{n} \cdot A_n(x + \bar{n}s) e^{s0^+} \right]. \quad (4.45)$$

We have denoted the dijet operator as O_2 as in the previous section, but in this case both the quark and antiquark are incoming, so the two Wilson lines are also incoming. As in the previous section, the coordinates x_n and $x_{\bar{n}}$ give the expanded energy-momentum conserving delta functions in Eq. (4.12), which gives the correct power counting for $q_T^2 \ll q^2$. The differential cross section for DY is then proportional to the sum over states

$$\sum_X \langle N_1(p) N_2(\bar{p}) | O_2^{\mu\dagger} | X \rangle \langle X | O_{2\mu} | N_1(p) N_2(\bar{p}) \rangle. \quad (4.46)$$

Following the standard derivation, we perform the sum over states in Eq. (4.46), then fcolor- and spinor-Fierz the product of currents into the form [49, 64, 195, 196]

$$O_2^{\mu\dagger}(x) O_{2\mu}(0) = -\frac{1}{N_c} \left[\bar{\chi}_n(x_n) \frac{\not{n}}{2} \chi_n(0) \right] \left[\bar{\chi}_{\bar{n}}(0) \frac{\not{n}}{2} \chi_{\bar{n}}(x_{\bar{n}}) \right] \quad (4.47)$$

where $\chi_n \equiv \bar{W}_n^\dagger \psi_n$, $\bar{\chi}_n = \bar{\psi}_n \bar{W}_n$, and similar for $\chi_{\bar{n}}$. We have neglected terms which vanish when taking color- and spin-averaged matrix elements. The differential rate may then be written

$$\begin{aligned} d\sigma &= \frac{4\pi\alpha^2}{3q^2s} \frac{d^4q}{(2\pi)^4} (-g_{\mu\nu}) |C_2(\mu)|^2 \int d^4x e^{-iq \cdot x} \langle N_1(p) N_2(\bar{p}) | O_2^{\mu\dagger}(x) O_2^\nu(0) | N_1(p) N_2(\bar{p}) \rangle \\ &= \frac{4\pi\alpha^2}{3N_c q^2 s} dq^+ dq^- d^2\mathbf{q}_T |C_2(\mu)|^2 \langle N_1(p) N_2(\bar{p}) | T_{(0,0)}(q^-, q^+, \mathbf{q}_T) | N_1(p) N_2(\bar{p}) \rangle \end{aligned} \quad (4.48)$$

where $s = (p + \bar{p})^2$, and the non-local operator

$$\begin{aligned} T_{(0,0)}(q^+, q^-, \mathbf{q}_T) &= \int \frac{d\xi_1 d\xi_2}{(2\pi)^d} d^{d-2} \mathbf{x}_T e^{-i\xi_1 q^-} e^{-i\xi_2 q^+} e^{i\mathbf{q}_T \cdot \mathbf{x}_T} \\ &\times \left[\bar{\chi}_n(\bar{n}\xi_1 + \mathbf{x}_T) \frac{\not{n}}{2} \chi_n(0) \right] \left[\bar{\chi}_{\bar{n}}(0) \frac{\not{n}}{2} \chi_{\bar{n}}(n\xi_2 + \mathbf{x}_T) \right] \end{aligned} \quad (4.49)$$

is the Fourier transform of the product of position-space TMDPDFs (defined here in d dimensions). This has the same form as Equation (9) of [64], although in our case the theory in which $T_{(0,0)}$ is defined does not have separate collinear and soft modes. Note that at this stage the introduction of $T_{(0,0)}$ is no more than notation, since it is equivalent to the product of currents in Eq. (4.47); it will be useful when summing rapidity logarithms. Typically in SCET one then factorizes $T_{(0,0)}$ into the product of two TMDPDFs, each of which is then individually renormalized (and individually ill-defined without

the introduction of a rapidity regulator). Here we do not further factorize $T_{(0,0)}$, but instead treat it as a single object which has the convolution included as part of its definition.

If $q_T \sim \Lambda_{\text{QCD}}$, the differential rate is given by the nonperturbative matrix element of $T_{(0,0)}$ in Eq. (4.48). Here we will focus on the hierarchy $q_T \gg \Lambda_{\text{QCD}}$, which allows us to perform an additional matching at the scale $\mu = q_T$ of $T_{(0,0)}$ onto a product of two parton distribution functions,

$$T_{(0,0)}(q^-, q^+, \mathbf{q}_T) \rightarrow \int \frac{dz_1}{z_1} \frac{dz_2}{z_2} C_{(0,0)}(z_1, z_2, \mathbf{q}_T, \mu) O_q \left(\frac{q^-}{z_1} \right) O_{\bar{q}} \left(\frac{q^+}{z_2} \right) + O \left(\frac{1}{q_T^2} \right) \quad (4.50)$$

where

$$\begin{aligned} O_q(\ell^-) &= \frac{1}{2\pi} \int d\xi e^{-i\xi\ell^-} \bar{\psi}_n(\bar{n}\xi) \frac{\not{\ell}}{2} W(\bar{n}\xi, 0) \psi_n(0) \\ O_{\bar{q}}(\ell^+) &= \frac{1}{2\pi} \int d\xi e^{-i\xi\ell^+} \bar{\psi}_{\bar{n}}(0) \frac{\not{\ell}}{2} W(0, n\xi) \psi_{\bar{n}}(n\xi) \end{aligned} \quad (4.51)$$

are the usual unpolarized lightcone distribution operators as used in Deep Inelastic Scattering [78], whose hadronic matrix elements are the parton distribution functions

$$\begin{aligned} \langle N(P) | O_q(\ell^-) | N(P) \rangle &= f_{q/N} \left(\frac{\ell^-}{P^-} \right) \\ \langle N(P) | O_{\bar{q}}(\ell^+) | N(P) \rangle &= f_{\bar{q}/N} \left(\frac{\ell^+}{P^+} \right). \end{aligned} \quad (4.52)$$

The matching coefficient $C_{(0,0)}(\omega_1, \omega_2, \mathbf{q}_T, \mu)$ may be calculated by evaluating matrix elements of both sides of Eq. (4.50) between perturbative quark and gluon states.

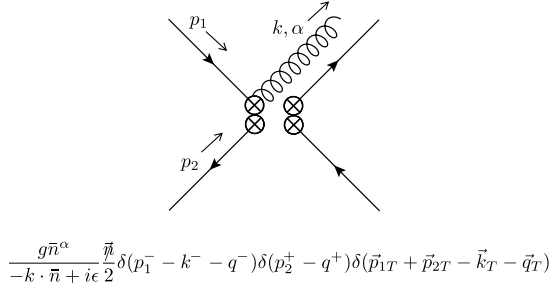


Figure 4.3: One-gluon Feynman rule (n -sector) for the left $T_{(0,0)}(q^-, q^+, \mathbf{q}_T)$ vertex.

4.3.2 Matrix Elements of $T_{(0,0)}$

At tree level, $T_{(0,0)}$ has the spin-averaged parton-level matrix element

$$\begin{aligned} \overline{\mathcal{M}}_0 &\equiv \frac{1}{4} \sum_{\text{spins}} \langle p_1 p_2 | T_{(0,0)}(q^-, q^+, \mathbf{q}_T) | p_1 p_2 \rangle \\ &= \delta(\bar{z}_1) \delta(\bar{z}_2) \delta(\mathbf{q}_T - \mathbf{p}_{1T} - \mathbf{p}_{2T}) + O(\alpha_s) \end{aligned} \quad (4.53)$$

where p_1 is the momentum of the incoming quark in the n -sector, p_2 the momentum of the antiquark in the \bar{n} -sector, and $\bar{z}_1 \equiv 1 - z_1 \equiv 1 - q^-/p_1^-$, $\bar{z}_2 \equiv 1 - z_2 \equiv 1 - q^+/p_2^+$. The parton-level matrix elements

of O_q and $O_{\bar{q}}$ manifestly factorize, since the n and \bar{n} sectors are decoupled:

$$\langle p_1, p_2 | O_q(k^-) O_{\bar{q}}(k^+) | p_1, p_2 \rangle = \langle p_1 | O_q(k^-) | p_1 \rangle \langle p_2 | O_{\bar{q}}(k^+) | p_2 \rangle \quad (4.54)$$

and, to one loop, we have the familiar spin-averaged matrix element

$$\frac{1}{2} \sum_{\text{spins}} \langle p_1 | O_q(z p_1^-) | p_1 \rangle = \delta(1-z) - \frac{\bar{\alpha}}{\epsilon} \left[\frac{1+z^2}{1-z} \right]_+ \quad (4.55)$$

where the infrared divergent term is the usual one-loop Altarelli-Parisi splitting kernel.

Expanding Eq. (4.53) in powers of \mathbf{p}_{iT}/q_T and comparing with Eq. (4.55) gives the tree-level matching condition

$$C_{(0,0)}^{(0)}(z_1, z_2, \mathbf{q}_T, \mu) = \delta(1-z_1)\delta(1-z_2)\delta(\mathbf{q}_T) \quad (4.56)$$

where

$$C_{(0,0)}(z_1, z_2, \mathbf{q}_T, \mu) \equiv C_{(0,0)}^{(0)}(z_1, z_2, \mathbf{q}_T, \mu) + \bar{\alpha} C_{(0,0)}^{(1)}(z_1, z_2, \mathbf{q}_T, \mu) + O(\alpha_s^2). \quad (4.57)$$

To calculate the matching at one loop, we need the matrix element of $T_{(0,0)}$ between quark states given by the diagrams in Fig. 4.4, along with the analogous graphs with \bar{n} -sector gluons coupling to the antiquark lines. The overlap graphs are obtained from the n - (or equivalently \bar{n}) sector graphs by replacing the quark propagators with the corresponding lightlike Wilson lines. Since we are working at leading order in $1/q$ we may set the external transverse momenta \mathbf{p}_{1T} and \mathbf{p}_{2T} to zero.

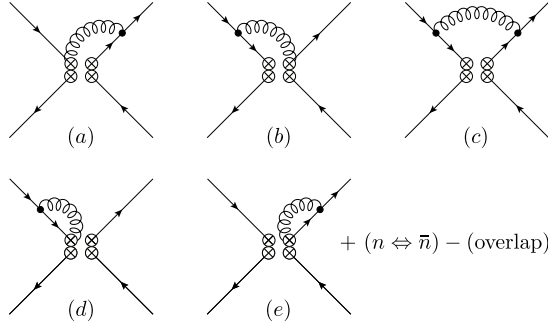


Figure 4.4: One-loop graphs contributing to $\langle p_1 p_2 | T_{(0,0)} | p_1 p_2 \rangle$.

Away from $\bar{z}_1 = \bar{z}_2 = 0$, only graphs (a-c) and the corresponding \bar{n} -sector graphs contribute, and the individual graphs are well-defined. The only component of the gluon loop momentum k^μ not fixed by energy-momentum conservation is k^- , so the loop integral is easily done using contour integration⁴. We use the distributional relation in d dimensions,

$$\frac{1}{\mathbf{q}_T^2} = -\frac{S_{2-2\epsilon}}{2\epsilon} \mu^{-2\epsilon} \delta(\mathbf{q}_T) + \left[\frac{1}{\mathbf{q}_T^2} \right]_+^\mu \quad (4.58)$$

⁴Note that these are not cut graphs, but the poles from the light quark propagators are on the opposite side of the real axis from the pole from the gluon propagator, so the k^- integral picks out only the pole at $k^2 = 0$.

where $S_d = 2\pi^{d/2}/\Gamma(d/2)$, and $\left[\frac{1}{\mathbf{q}_T^2}\right]_+^\mu$ denotes a $(d-2)$ -dimensional plus distribution, defined as

$$\begin{aligned} [g(\mathbf{p}_T)]_+^\mu &= g(\mathbf{p}_T), \quad |\mathbf{p}_T| > 0, \quad \text{and} \\ \int_{|\mathbf{p}_T| \leq \mu} d^{d-2} \mathbf{p}_T [g(\mathbf{p}_T)]_+^\mu &= 0. \end{aligned} \quad (4.59)$$

(Note that Eq. (4.58) is independent of μ .) After renormalization we take the limit $d-2 \rightarrow 2$, which recovers the 2-dimensional plus distribution definition of [67]. This gives for the spin-averaged n -sector graphs

$$\overline{\mathcal{M}}_{1n}(\bar{z}_1 \neq 0) = \frac{\bar{\alpha}}{\pi} f_\epsilon \left(-\frac{S_{2-2\epsilon}}{2\epsilon} \mu^{-2\epsilon} \delta(\mathbf{q}_T) + \left[\frac{1}{\mathbf{q}_T^2} \right]_+^\mu \right) \delta(\bar{z}_2) \frac{2 - 2\bar{z}_1 + \bar{z}_1^2(1-\epsilon)}{\bar{z}_1}, \quad (4.60)$$

where $f_\epsilon = \pi^\epsilon \mu^{2\epsilon} e^{\epsilon \gamma_E}$, while the \bar{n} graphs yields the same under the switch $\bar{z}_2 \leftrightarrow \bar{z}_1$. We can therefore write the spin-averaged one-loop matrix element of $T_{(0,0)}$ as the sum of contributions away from $\bar{z}_1 = \bar{z}_2 = 0$ and some unknown contribution at this point,

$$\begin{aligned} \overline{\mathcal{M}}_1 &= \frac{\bar{\alpha}}{\pi} f_\epsilon \left(-\frac{S_{2-2\epsilon}}{2\epsilon} \mu^{-2\epsilon} \delta(\mathbf{q}_T) + \left[\frac{1}{\mathbf{q}_T^2} \right]_+^\mu \right) \\ &\quad \times \left(A \delta(\bar{z}_1) \delta(\bar{z}_2) + \delta(\bar{z}_2) \left[\frac{2 - 2\bar{z}_1 + \bar{z}_1^2(1-\epsilon)}{\bar{z}_1} \right]_+ + \delta(\bar{z}_1) \left[\frac{2 - 2\bar{z}_2 + \bar{z}_2^2(1-\epsilon)}{\bar{z}_2} \right]_+ \right) \end{aligned} \quad (4.61)$$

then calculate the contributions to the constant A from graphs (a-c) by integrating the individual graphs with respect to \bar{z}_1 and \bar{z}_2 before doing the loop integrals. The gluon momentum k^- is then no longer fixed by the delta functions, and just as in the previous section, the integrals defining A in Eq. (4.61) contain rapidity divergences and are not individually well-defined.

As in the case of the massive Sudakov form factor, it is instructive to follow the naïve scheme of performing the integrals for all graphs except for the k^- integral. In this case, the contributions to A from graphs (a-c) and their counterparts in the \bar{n} and overlap sectors are

$$\begin{aligned} A_n &= \int_0^{p_1^-} \frac{dk^-}{k^-} \left[2 - 2 \frac{k^-}{p_1^-} + \left(\frac{k^-}{p_1^-} \right)^2 (1-\epsilon) \right] \\ A_{\bar{n}} &= \int_{\frac{q_T^2}{p_2^+}}^{\infty} \frac{dk^-}{k^-} \left[2 - 2 \left(\frac{q_T^2}{k^- p_2^+} \right) + (1-\epsilon) \left(\frac{q_T^2}{k^- p_2^+} \right)^2 \right] \\ A_o &= 2 \int_0^{\infty} \frac{dk^-}{k^-} \end{aligned} \quad (4.62)$$

where $\hat{s} \equiv p_1^- p_2^+ = q^2/(z_1 z_2)$. Proceeding as in the previous section, we can rescale the integration variable $k^- \rightarrow \zeta^2 k^- / \hat{s}$ in the $A_{\bar{n}}$ integral in Eq. (4.62) to obtain the scheme-dependent sum

$$A(\zeta) \equiv A_n + A_{\bar{n}} - A_o = 2 \log \frac{\zeta^2}{q_T^2} - 3 - \epsilon. \quad (4.63)$$

Again, we see that the SCET calculation has no dynamical dependence on the hard scale \hat{s} ; rather, it arises as one possible choice of scheme needed to evaluate the sum of divergent integrals.

As in the previous section, we can make the individual graphs well-defined with an appropriate regulator. Modifying the position-space Wilson lines to include the δ -regulator, the n -sector contributes

$$\overline{\mathcal{M}}_{1n}^\delta = \frac{\bar{\alpha}}{\pi} f_\epsilon \left(-\frac{S_{2-2\epsilon}}{2\epsilon} \mu^{-2\epsilon} \delta(\mathbf{q}_T) + \left[\frac{1}{\mathbf{q}_T^2} \right]_+^\mu \right) \delta(\bar{z}_2) \left(\frac{2(1-\bar{z}_1)}{\bar{z}_1 + \frac{\delta_n}{p_1}} + \bar{z}_1(1-\epsilon) \right). \quad (4.64)$$

Converting to distribution form using

$$\frac{1}{\bar{z} + \delta} = -\delta(\bar{z}) \log \delta + \left[\frac{1}{\bar{z}} \right]_+ + O(\delta) \quad (4.65)$$

gives

$$\overline{\mathcal{M}}_{1n}^\delta = \bar{\alpha} \delta(\bar{z}_2) \left\{ \left(\frac{\delta(\mathbf{q}_T)}{\epsilon} - \frac{1}{\pi} \left[\frac{1}{\mathbf{q}_T^2} \right]_+^\mu \right) \left(\delta(\bar{z}_1) \left[\frac{3}{2} - 2 \log \frac{p_1^-}{\delta_n} \right] - \left[\frac{1+z_1^2}{\bar{z}_1} \right]_+ \right) + \bar{z}_1 \delta(\mathbf{q}_T) \right\} \quad (4.66)$$

The \bar{n} -sector graphs are the same as above but with $p_1^- \rightarrow p_2^+$ and $z_1 \leftrightarrow z_2$, and the calculation of the overlap graphs gives

$$\overline{\mathcal{M}}_{1o}^\delta = 2 \frac{\bar{\alpha}}{\pi} f_\epsilon \delta(\bar{z}_1) \delta(\bar{z}_2) \frac{1}{q_T^2} \log \frac{q_T^2}{\delta_o^2}. \quad (4.67)$$

In d dimensions,

$$\frac{\log \frac{q_T^2}{\mu^2}}{q_T^2} = -\frac{S_{2-2\epsilon}}{2\epsilon^2} \mu^{-2\epsilon} \delta(\mathbf{q}_T) + \left[\frac{\log \frac{\mathbf{q}_T^2}{\mu^2}}{\mathbf{q}_T^2} \right]_+^\mu \quad (4.68)$$

and so

$$\begin{aligned} \overline{\mathcal{M}}_{1o}^\delta &= \bar{\alpha} \delta(\bar{z}_1) \delta(\bar{z}_2) \left[\delta(\mathbf{q}_T) \left(-\frac{2}{\epsilon^2} + \frac{2 \log \frac{\delta_o^2}{\mu^2}}{\epsilon} + \frac{\pi^2}{6} \right) \right. \\ &\quad \left. - \frac{2}{\pi} \log \frac{\delta_o^2}{\mu^2} \left[\frac{1}{\mathbf{q}_T^2} \right]_+^\mu + \frac{2}{\pi} \left[\frac{\log \frac{\mathbf{q}_T^2}{\mu^2}}{\mathbf{q}_T^2} \right]_+^\mu \right] \end{aligned} \quad (4.69)$$

Combining all the above yields the net contribution to matrix elements of $T_{(0,0)}$ from single-gluon emissions into the final state

$$\begin{aligned} \overline{\mathcal{M}}_{1g}^\delta &= \bar{\alpha} \left(\delta(\bar{z}_1) \delta(\bar{z}_2) \delta(\mathbf{q}_T) \left(\frac{2}{\epsilon^2} + \frac{3 - 2 \log \frac{\nu^2}{\mu^2}}{\epsilon} - \frac{\pi^2}{6} \right) \right. \\ &\quad - \frac{\delta(\mathbf{q}_T)}{\epsilon} \left(\delta(\bar{z}_1) \left[\frac{1+z_2^2}{\bar{z}_2} \right]_+ + \delta(\bar{z}_2) \left[\frac{1+z_1^2}{\bar{z}_1} \right]_+ \right) \\ &\quad + \left((1+z_2^2) \delta(\bar{z}_1) \left[\frac{1}{\bar{z}_2} \right]_+ + (1+z_1^2) \delta(\bar{z}_2) \left[\frac{1}{\bar{z}_1} \right]_+ \right) \frac{1}{\pi} \left[\frac{1}{\mathbf{q}_T^2} \right]_+^\mu \\ &\quad \left. + \delta(\mathbf{q}_T) (\bar{z}_2 \delta(\bar{z}_1) + \bar{z}_1 \delta(\bar{z}_2)) - 2 \delta(\bar{z}_1) \delta(\bar{z}_2) \frac{1}{\pi} \left[\frac{\log \frac{\mathbf{q}_T^2}{\nu^2}}{\mathbf{q}_T^2} \right]_+^\mu \right) \end{aligned} \quad (4.70)$$

where, as with the form factor calculation, we have taken the limit $\delta_{n,\bar{n},o} \rightarrow 0$, again holding the ratio $\delta_n \delta_{\bar{n}} / \delta_o^2 \equiv q^2/\nu^2$ fixed, which defines the scheme for regulating the rapidity divergences. The virtual graphs are scaleless, so do not contribute in this scheme.

The divergences in the first line in Eq. (4.70) are canceled by the counterterm for O_2 if $\nu^2 = q^2$, which imposes the scheme $\nu = q$ when matching from QCD onto SCET. The divergence in the second line is equal to the infrared divergence in the matrix elements of O_q and $O_{\bar{q}}$ in Eq. (4.55) and cancels in the matching conditions at $\mu = q_T$, leaving the one-loop result

$$\begin{aligned} C_{(0,0)}^{(1)}(z_1, z_2, \mathbf{q}_T, \mu) = & \left((1 + z_2^2) \delta(\bar{z}_1) \left[\frac{1}{\bar{z}_2} \right]_+ + (1 + z_1^2) \delta(\bar{z}_2) \left[\frac{1}{\bar{z}_1} \right]_+ \right) \frac{1}{\pi} \left[\frac{1}{\mathbf{q}_T^2} \right]_+^\mu \\ & + 2\delta(\bar{z}_1)\delta(\bar{z}_2) \log \frac{q^2}{\mu^2} \frac{1}{\pi} \left[\frac{1}{\mathbf{q}_T^2} \right]_+^\mu - 2\delta(\bar{z}_1)\delta(\bar{z}_2) \frac{1}{\pi} \left[\frac{\log \frac{\mathbf{q}_T^2}{\mu^2}}{\mathbf{q}_T^2} \right]_+^\mu \\ & + \delta(\mathbf{q}_T) \left(\bar{z}_2 \delta(\bar{z}_1) + \bar{z}_1 \delta(\bar{z}_2) - \frac{\pi^2}{6} \delta(\bar{z}_1)\delta(\bar{z}_2) \right) \end{aligned} \quad (4.71)$$

where $\bar{\omega}_{1,2} \equiv 1 - \omega_{1,2}$. The rapidity logarithm depends on the ultraviolet scale q^2 only because of the choice of scheme parameter $\nu^2 = q^2$. As in the previous section, we may resum the leading order rapidity logarithms by running the scheme parameter ν from $\nu_H^2 = q^2$ to $\nu_S^2 = q_T^2$, as will be discussed in the next section.

4.3.3 Resummation

The rapidity renormalization group equations for $T_{(0,0)}$, which resum the large logarithms of q^2/q_T^2 in $C_{(0,0)}$, arise from the independence of $C_{(0,0)}$ on the scheme parameter ν . Since matrix elements of $T_{(0,0)}$ have no dynamical dependence on q^2 , we can write, proceeding analogously to Eq. (4.32),

$$\begin{aligned} T_{(0,0)}(q^+, q^-, \mathbf{q}_T, \nu^2 = q^2)|_{\mu=q_T} = & \int \frac{d\omega_1}{\omega_1} \frac{d\omega_2}{\omega_2} d^2 \mathbf{p}_T V_{(0,0)} \left(\omega_1, \omega_2, \mathbf{p}_T, \frac{q^2}{\nu^2} \right) \\ & \times T_{(0,0)} \left(\frac{q^+}{\omega_1}, \frac{q^-}{\omega_2}, \mathbf{q}_T - \mathbf{p}_T, \nu^2 \right) \end{aligned} \quad (4.72)$$

and, from Eq. (4.70), at one loop

$$V_{(0,0)}(\omega_1, \omega_2, \mathbf{p}_T, \nu) = \delta(\bar{\omega}_1)\delta(\bar{\omega}_2) \left(\delta(\mathbf{p}_T) + 2\bar{\alpha} \log \frac{q^2}{\nu^2} \frac{1}{\pi} \left[\frac{1}{\mathbf{p}_T^2} \right]_+^\mu \right) + \dots \quad (4.73)$$

Eq. (4.72) plays the role of a SCET factorization theorem in this analysis, although here it just reflects the fact that $T_{(0,0)}$ is the only operator at leading order contributing to the cross section, so the cross section must be expressible as a linear combination of $T_{(0,0)}$'s (with different arguments). Since Eq. (4.72) is independent of ν , we perform the standard manipulations and find

$$\begin{aligned} \frac{d}{d \log \nu} V_{(0,0)}(\mathbf{p}_T, \nu) = & \int d^2 \mathbf{k}_T \left(-4\bar{\alpha} \frac{1}{\pi} \left[\frac{1}{(\mathbf{p}_T - \mathbf{k}_T)^2} \right]_+^\mu \right) V_{(0,0)}(\mathbf{k}_T, \nu) \\ \equiv & \gamma_\nu^{(0,0)}(\mathbf{p}_T) \otimes V_{(0,0)}(\mathbf{p}_T, \nu) \end{aligned} \quad (4.74)$$

where the two dimensional convolution is defined as

$$f(\mathbf{p}_T) \otimes g(\mathbf{p}_T, \dots) \equiv \int d^2 \mathbf{k}_T f(\mathbf{p}_T - \mathbf{k}_T, \dots) g(\mathbf{k}_T, \dots). \quad (4.75)$$

We have made use of the fact that at one loop the anomalous dimension is diagonal in each of the ω_i , and defined $V_{(0,0)}(\omega_1, \omega_2, \mathbf{p}_T, \nu) \equiv \delta(\bar{\omega}_1)\delta(\bar{\omega}_2)V_{(0,0)}(\mathbf{p}_T, \nu)$. $V_{(0,0)}$ therefore obeys the same form of rapidity renormalization group equation as a beam function in the usual SCET formalism. The all-orders solution for V and the complications associated with evaluating distributions at canonical scales has been discussed in detail in [67].

This gives the resummed formula for the low-scale matching condition

$$C_{(0,0)}(z_1, z_2, \mathbf{q}_T, \mu_S) = V(\mathbf{q}_T, \mu_S, \nu_S) \otimes C_{(0,0)}(z_1, z_2, \mathbf{q}_T, \mu_S, \nu_S) \quad (4.76)$$

and the final factorized and resummed expression for the DY cross section reads

$$\begin{aligned} \frac{d^4\sigma}{dq^+dq^-d^2\mathbf{q}_T} &= \frac{4\pi\alpha^2}{3N_c q^2 s} |U_2(\mu_S, \mu_H)C_2(\mu_H)|^2 \\ &\times \int \frac{dz_1}{z_1} \frac{dz_2}{z_2} V(\mathbf{q}_T, \mu_S, \nu_S) \otimes C_{(0,0)}(z_1, z_2, \mathbf{q}_T, \mu_S, \nu_S) f_q\left(\frac{\xi_1}{z_1}\right) f_{\bar{q}}\left(\frac{\xi_2}{z_2}\right) \end{aligned} \quad (4.77)$$

where $\xi_1 = q^-/P_1^-$, $\xi_2 = q^+/P_2^+$, $\mu_H = \nu_H = q$, $\mu_S = \nu_S = q_T$, and U_2 is defined in Eq. (4.40).

4.4 Conclusions

In this chapter we have demonstrated how to apply SCET to processes involving rapidity divergences without explicitly separating the low energy degrees of freedom into separate modes. We have shown that the anomalous appearance of the hard scale Q in the effective theory below Q in SCET_{II}-type problems arises from a scheme dependence in the effective theory. This scheme dependence is common for both SCET_I and SCET_{II} processes, with the only distinction between these types of processes being whether the matching coefficient onto the soft theory exhibits a large logarithmic enhancement (SCET_{II}) or not (SCET_I); the intermediate effective theory is the same until we reach the matching scale at which the process dependence arises. The free scheme parameter can be exploited to derive evolution equations for matching coefficients, yielding a method for the summation of the large rapidity logarithms which appear in the soft matching coefficients of SCET_{II} processes.

The factorizations and resummations presented in this chapter are well known in the standard SCET formalism, and we reproduce the results here. However, reducing the number of distinct fields in the theory simplifies the structure of the theory and significantly reduces the number of Feynman diagrams and operators required for a given calculation. In particular, we expect the calculation of power corrections in SCET, which have been recently of much interest [76, 119, 120, 123], to be significantly simplified. The matching and anomalous dimensions of power-suppressed contributions to the dijet current were calculated in this formalism in [179]; Fierz-rearranged products $T_{(i,j)}$ of these subleading operators, analogous to $T_{(0,0)}$, may be constructed and their rapidity logarithms resummed by exploiting the scheme dependence of the rapidity regulator. However, as pointed out in [76], at subleading orders in $1/Q$ the δ -regulator is not sufficient to regulate all the rapidity divergences and another regulator, such as the pure rapidity regulator presented in that reference, is required. Work on this subject is in progress.

Chapter 5

Factorization of Power Corrections in the Drell-Yan Process

In this chapter, we examine the Drell-Yan process at next-to-leading power (NLP) in Soft-Collinear Effective Theory. Using an approach with no explicit soft or collinear modes, we discuss the factorization of the differential cross section in the small- q_T hierarchy with $q^2 \gg q_T^2 \gg \Lambda_{\text{QCD}}^2$. We show that the cross section may be written in terms of matrix elements of power-suppressed operators $T_{(i,j)}$, which contribute to $O(q_T^2/q^2)$ coefficients of the usual PDFs. We derive a factorization for this observable at NLP which allows the large logarithms in each of the relevant factors to be resummed. We discuss the cancellation of rapidity divergences and the overlap subtractions required to eliminate double counting at next-to-leading power. The contents of this chapter appear in [197].

5.1 Introduction

The Drell-Yan (DY) process $N_1(P_1)N_2(P_2) \rightarrow \gamma^*(q) + X \rightarrow (\ell\bar{\ell}) + X$ has been extensively studied in perturbative QCD [51, 198, 199]. In the limiting case that the transverse momentum q_T of the lepton pair is parametrically larger than Λ_{QCD} and smaller than its invariant mass $\sqrt{q^2}$, the cross section may be written as [49]

$$\frac{1}{\sigma_0} \frac{d\sigma}{dq^2 dy dq_T^2} = \sum_{a,b} \int \frac{dz_1}{z_1} \frac{dz_2}{z_2} C_{f\bar{f}}^{ab}(z_1, z_2, q^2, q_T^2) f_{a/N_1}\left(\frac{\xi_1}{z_1}\right) f_{b/N_2}\left(\frac{\xi_2}{z_2}\right) + O\left(\frac{\Lambda_{\text{QCD}}^2}{q_T^2}\right), \quad (5.1)$$

where q^μ is the four-momentum of the lepton pair, $\xi_1 \equiv q^-/P_1^-$, $\xi_2 \equiv q^+/P_2^+$, $y = \log(q^-/q^+)/2$, and P_1^- and P_2^+ are the large light-cone components of the incoming hadron momenta. The sum is over parton types a, b , and the f_i are the usual parton distribution functions (PDFs). In this chapter we only study the quark-induced process for a single flavour of quark, so we define $C_{f\bar{f}} \equiv C_{f\bar{f}}^{q\bar{q}}$.

The coefficient function $C_{f\bar{f}}$ may be expanded in powers of q_T^2/q^2 ,

$$C_{f\bar{f}}(z_1, z_2, q^2, q_T^2) = C_{f\bar{f}}^{(0)}(z_1, z_2, q^2, q_T^2) + \frac{1}{q^2} C_{f\bar{f}}^{(2)}(z_1, z_2, q^2, q_T^2) + \dots. \quad (5.2)$$

where each subsequent term is suppressed by increasing powers of q_T^2/q^2 .

Since they depend on two parametrically different scales q^2 and q_T^2 , the fixed-order perturbative expansions for each $C_{f\bar{f}}^{(n)}$ contain large logarithms of q_T^2/q^2 which can spoil the behavior of perturbation theory and need to be resummed. The resummation of the leading power (LP) term $C_{f\bar{f}}^{(0)}$ has been extensively studied in the literature, using both perturbative QCD techniques [49, 200–210] and effective field theory methods [64, 65, 67, 148]. Factorization theorems allow $C_{f\bar{f}}^{(0)}$ to be written as a product of separate terms depending on distinct scales, each of which may be resummed to arbitrary order using a variety of renormalization group (RG) or related techniques. The most recent analyses achieve a resummation up to $N^3LL+NNLO$ order [52–58]. However, much less is known about the factorization and resummation properties of the first power correction $C_{f\bar{f}}^{(2)}$. $C_{f\bar{f}}$ has been computed in QCD at fixed-order in perturbation theory up to N^2LO [211, 212], but an all-orders RG resummation at next-to-leading power (NLP) has not been performed.

Soft-Collinear Effective Theory (SCET) [68–74] is an effective field theory (EFT) which provides a systematic framework in which to study power corrections in hard QCD processes. There has been much recent work studying power corrections to various processes, with applications including beam thrust [119], Drell-Yan production near threshold [120], threshold Higgs production from gluon fusion [121], Higgs production and decay [122], the energy-energy correlator in $\mathcal{N} = 4$ SYM [123] and Higgs to diphoton decays [87–89]. Power corrections have also been studied using non-EFT QCD techniques [75, 124–129].

The DY process at small q_T^2 is typically referred to as a SCET_{II} process, characterized by collinear and soft modes in the EFT, and exhibiting rapidity logarithms in matrix elements. Rapidity logarithms are large logarithms in matrix elements which arise in SCET due to divergences in individual diagrams at large values of the rapidity of one of the particles. These divergences cancel between graphs with different modes, but the final result contains large finite logarithms of the hard scale of the scattering which cannot be resummed using usual RG techniques. Rapidity divergences require an additional regulator beyond dimensional regularization, and various techniques have been successfully employed to handle the rapidity resummation, including off-the-light-cone techniques [49], the rapidity renormalization group [80], the collinear anomaly framework [64], the exponential regulator [191] and the recently proposed pure rapidity regulator [76, 123]. The latter regulator has been recently used [76] to calculate the small- q_T DY cross section by expanding the QCD graphs in the soft and collinear limits, where it correctly treats the power-law rapidity divergences arising at NLP. The connection between rapidity renormalization in SCET_{II} and the usual renormalization group equation (RGE) in SCET_I was discussed in [213].

In this chapter we study power corrections to DY production using the version of SCET developed in [77, 175, 179]. In this approach the degrees of freedom in the EFT are not analyzed using the method of regions [82] in which they are explicitly separated into soft, collinear, ultrasoft, and possibly additional modes. Instead, states are separated into distinct sectors, where the relative invariant mass of particles within each sector is less than the renormalization scale μ of the EFT, but the relative invariant mass of different sectors is larger than the renormalization scale. As with the mode expansion, particles of the same type but in different sectors are described by different fields; however, interactions within a sector are described by QCD, while interactions between sectors are mediated via the external current, which is expanded in inverse powers of the hard matching scale. Factorization of different modes (soft-collinear, ultrasoft-collinear, and others) does not occur explicitly in the Lagrangian since different modes in a given sector are described by the same fields, but instead arises through the usual EFT process of integrating out degrees of freedom and matching onto a new EFT at appropriate threshold scales.

This reduces the number of separate fields in the Lagrangian and therefore simplifies the formalism, both conceptually and practically. One immediate feature is that subleading terms in the effective Lagrangian coupling different modes and violating manifest factorization are not present in this approach. In addition, rather than deriving a factorization theorem in terms of jet and soft functions which are individually well-defined and renormalized at the appropriate scale, the rate is simply expressed in terms of bilocal products of operators in the EFT which may be run both in the renormalization scale μ as well as the rapidity scale ν . Similar to the situation at LP discussed in [175], we show here that the DY cross section naturally factorizes into hard matching coefficients, rapidity evolution factors, soft matching coefficients and parton distribution functions, and give expressions for the first three quantities up to NLP at one loop. The complete resummation of rapidity logarithms is left for a future work.

Consistency of this theory requires that double counting of degrees of freedom between the two sectors is consistently subtracted, similar to the usual zero-bin subtraction [172] in SCET. This procedure of overlap subtraction is necessary for the theory to be well-defined, and is implicit in all matrix elements. Furthermore, as discussed in detail in [175], the scheme-dependence of this subtraction allows rapidity logarithms to be summed using techniques similar to [76, 80] without having manifest factorization of soft and collinear modes in the effective Lagrangian. At subleading powers this subtraction is nontrivial, requiring contributions from multiple operators as well as subleading corrections to the leading power subtraction. While these subtractions vanish using an appropriately chosen regulator, the interplay of these subtraction terms explains patterns of rapidity divergence cancellation between different operators, similar to the nontrivial cancellations of rapidity and endpoint divergences at NLP seen in other approaches [87–89].

QCD proofs of factorization in hard scattering processes require that the effects of the exchange of soft gluons in the Glauber regime relevant to small angle parton scattering cancel in the relevant observable [51, 198, 199, 214, 215]. Glauber modes have been the subject of much recent interest in SCET [177], and a consistent treatment of gluons in the Glauber regime has been shown to be necessary to ensure that operator statements in SCET are independent of the external states [178]. Investigation of these effects in the formalism presented here are beyond the scope of this thesis, but we will assume that gluons in the Glauber regime do not introduce factorization-violating effects in the context of this calculation.

In Section 5.1.1 we sketch the ingredients of the calculation and the approach to factorization in this formalism. We present the one-loop calculations of the various pieces in Section 5.2, and compare our fixed-order results with the unsummed QCD result. In Section 5.3 we consider the cross section with no rapidity regulator to demonstrate the cancellation of rapidity divergences between different operators and their respective overlap subtractions across different regions of phase space. We present our conclusions in Section 5.4. A few details of plus distributions used here are given in the appendices, as well as a comparison to a recent one-loop analysis [76] of power corrections to the DY process.

5.1.1 Factorization

In the SCET formalism introduced in [77, 175, 179] there are no explicit soft, collinear or ultrasoft modes, so factorization does not arise explicitly from a Lagrangian mode expansion, but instead by integrating out ultraviolet degrees of freedom at the relevant matching scales. In this section we briefly review the approach of [175] to DY scattering and introduce its extension to subleading power. Precise definitions of quantities appearing in this section will be given in Section 5.2.

The cross section for the electromagnetic Drell-Yan production process, $N_1 N_2 \rightarrow \gamma^* + X \rightarrow (\ell\bar{\ell}) + X$ is given in QCD by

$$d\sigma = \frac{4\pi\alpha^2}{3q^2s} \frac{d^4q}{(2\pi)^4} \int d^d x e^{-iq \cdot x} (-g_{\mu\nu}) \langle N_{12} | J_{\text{QCD}}^{\mu\dagger}(x) J_{\text{QCD}}^{\nu}(0) | N_{12} \rangle, \quad (5.3)$$

where $q^2 = (p_\ell + p_{\bar{\ell}})^2$ is the invariant mass of the lepton pair, $s = (P_1 + P_2)^2$ is the invariant mass of the incoming hadrons, the initial hadronic state is $|N_{12}\rangle = |N_1(P_1)N_2(P_2)\rangle$, and the vector QCD current J_{QCD}^{μ} is

$$J_{\text{QCD}}^{\mu}(x) = \bar{\psi}(x) \gamma^{\mu} \psi(x) \quad (5.4)$$

for a single flavor of light quark. The extension to electroweak currents is straightforward [49, 64].

For $q_T^2 \ll q^2$, perturbative corrections to the cross section in Eq. (5.3) contain powers of logarithms of q_T^2/q^2 , which can spoil the apparent convergence of perturbation theory. SCET provides a systematic approach to resumming these terms. At the renormalization scale $\mu = \mu_H \sim \sqrt{q^2} \gg q_T$, hard interactions are integrated out of the theory and QCD is matched onto SCET. In the formalism used here, SCET consists of two decoupled QCD sectors, denoted by the lightlike vectors n^μ and \bar{n}^μ , with total momenta p_n^μ and $p_{\bar{n}}^\mu$; the sectors are distinguished by the power counting

$$p_n^2, p_{\bar{n}}^2 \ll q^2, p_n \cdot p_{\bar{n}} \sim q^2. \quad (5.5)$$

Interactions between the sectors are mediated by the external current J_{SCET}^{μ} , which is written as a sum of operators of increasing dimension¹

$$J_{\text{SCET}}^{\mu}(x) = \sum_i \frac{1}{q_L^{[i]}} C_2^{(i)}(\mu) O_2^{(i)\mu}(x, \mu), \quad (5.6)$$

where an operator $O_2^{(i)}$ has mass dimension $[i]$ in excess of the leading-power operator $O_2^{(0)}$. We have defined $q_L^2 \equiv q^+ q^-$, and for brevity we will not explicitly include the μ dependence of operators in subsequent equations unless required for clarity. It is convenient to expand in inverse powers of q_L^2 rather than $q^2 = q_L^2 - q_T^2$ so that the hard scale of the EFT is independent of the infrared (IR) scale q_T^2 . This expansion has been performed up to $O(1/q_L^2)$ [77, 78, 83, 118, 216], the details of which are summarized in Section 5.2.1. The SCET expansion for the differential cross section is then given in SCET by

$$\frac{d\sigma}{dq^2 dy dq_T^2} = \frac{4\pi\alpha^2}{3q^2s} (-g_{\mu\nu}) \int \frac{d\Omega_T}{2} \int \frac{d^d x}{(2\pi)^d} \sum_{ij} \frac{H_{(i,j)}(\mu)}{q_L^{[i]+[j]}} e^{-iq \cdot x} \langle N_{12} | O_2^{(i)\mu\dagger}(x) O_2^{(j)\nu}(0) | N_{12} \rangle, \quad (5.7)$$

where $H_{(i,j)}(\mu) \equiv C_2^{(i)\dagger}(\mu) C_2^{(j)}(\mu)$ and the final angular integral $d\Omega_T$ corresponds to the angular integral in the transverse momentum \mathbf{q}_T . Since we have not subdivided the degrees of freedom of SCET into separate soft and collinear modes, there is no expansion of the SCET Lagrangian beyond that in Eq. (5.6); in particular, there are no power corrections arising from soft-collinear mixing terms in the Lagrangian [73, 74, 117, 150, 217, 218]. This simplifies the analysis of power corrections considerably.

While matrix elements of the operator products in Eq. (5.7) may be directly evaluated between

¹Subleading operators are also labeled by continuous indices, so the discrete sums over operators also include integrals, which we neglect for simplicity in this section.

partons in perturbation theory, it is convenient to perform a Fierz rearrangement to write the operator product as a convolution of transverse momentum dependent distribution operators (whose hadronic matrix elements are generally referred to as TMDPDFs), one in the n -sector and one in the \bar{n} -sector. This is a standard procedure at leading power [64, 199]; at subleading powers a similar procedure may be used to express the basis of operator products as convolutions of power-suppressed distribution operators,

$$\int \frac{d^d x}{2(2\pi)^d} (-g_{\mu\nu}) e^{-iq \cdot x} O_2^{(i)\mu\dagger}(x) O_2^{(j)\nu}(0) = \sum_{k,\ell} \frac{1}{N_c} K_{(k,\ell)}^{(i,j)} T_{(k,\ell)}(q^-, q^+, \mathbf{q}_T) + \text{spin-dependent}, \quad (5.8)$$

where each $T_{(i,j)}$ relevant to this calculation will be defined explicitly in Section 5.2. Rewriting the operator products in terms of the operators $T_{(i,j)}$ is simply a change of operator basis, and not a matching condition or expansion in SCET, and so introduces no new perturbative corrections. Typically in SCET this Fierz rearrangement is performed to write the operator product in a form which manifestly factorizes into jet and soft functions; since this factorization is not needed here this change of basis is not strictly necessary, but it is included here for easier comparison with other approaches.

At $O(\alpha_s)$ matrix elements of the $T_{(i,j)}$'s at small q_T are insensitive to the cutoff scale q_L and so running the scattering operators $O_{2,(i)}$ from $\mu_H \sim q_L$ to $\mu_S \sim q_T$ sums the usual renormalization group logarithms of q_L^2/q_T^2 in the rate. If $q_T \sim \Lambda_{\text{QCD}}$, matrix elements of each $T_{(i,j)}$ are nonperturbative quantities which would have to be either modeled or extracted from experiment. In the scaling of interest here, $q_T \gg \Lambda_{\text{QCD}}$, each $T_{(i,j)}$ may be further expanded in powers $\Lambda_{\text{QCD}}^2/q_T^2$, allowing the operator product in Eq. (5.7) to be matched onto the usual light-cone distribution operators whose hadronic matrix elements are the parton distribution functions. This expansion corresponds to matching SCET onto a soft theory of completely decoupled sectors of QCD at the scale $\mu_S \sim q_T$, and at leading twist takes the form

$$T_{(k,\ell)}(q^-, q^+, \mathbf{q}_T, \mu_S) \rightarrow \int \frac{dz_1}{z_1} \frac{dz_2}{z_2} C_{S,(k,\ell)}(z_1, z_2, \mathbf{q}_T, \mu_S) O_q \left(\frac{q^-}{z_1}, \mu_S \right) O_{\bar{q}} \left(\frac{q^+}{z_2}, \mu_S \right), \quad (5.9)$$

where the various $C_{S,(k,\ell)}$ are matching coefficients and the hadronic matrix elements of the light-cone quark and antiquark distribution operators $O_{q,\bar{q}}$ are the usual spin-averaged parton distribution functions

$$\begin{aligned} f_{q/N_1}(\zeta_1) &= \langle N_1(P_1) | O_q(\zeta_1 P_1^-) | N_1(P_1) \rangle \\ f_{\bar{q}/N_2}(\zeta_2) &= \langle N_2(P_2) | O_{\bar{q}}(\zeta_2 P_2^+) | N_2(P_2) \rangle, \end{aligned} \quad (5.10)$$

with $P_i^- \equiv P_i \cdot \bar{n}$ and $P_i^+ \equiv P_i \cdot n$. Combining these matching steps gives an expression for the DY cross section for a single quark flavor of the form

$$\frac{d\sigma}{dq^2 dy dq_T^2} = \sigma_0 \int \frac{dz_1}{z_1} \frac{dz_2}{z_2} C_{f\bar{f}}(z_1, z_2, q_L^2, q_T^2) f_{q/N_1} \left(\frac{\xi_1}{z_1} \right) f_{\bar{q}/N_2} \left(\frac{\xi_2}{z_2} \right) + \dots \quad (5.11)$$

where $\sigma_0 = 4\pi\alpha^2/(3N_c q^2 s)$, $\xi_1 = q^-/P_1^-$, $\xi_2 = q^+/P_2^+$, and $C_{f\bar{f}}$ has the partially factorized form

$$C_{f\bar{f}}(z_1, z_2, q_L^2, q_T^2) = \int \frac{d\Omega_T}{2} \sum_{ijk\ell} K_{(k,\ell)}^{(i,j)} \left(\frac{1}{q_L} \right)^{[i]+[j]} H_{(i,j)}(\mu_S) C_{S,(k,\ell)}(z_1, z_2, \mathbf{q}_T, \mu_S). \quad (5.12)$$

However, in this form the matching coefficients C_S still contain large logarithms of q_T^2/q_L^2 which are not

resummed by the usual renormalization group evolution. These rapidity logarithms arise because the graphs renormalizing matrix elements of $T_{(i,j)}$ in SCET are separately divergent in each sector, even in d dimensions, and the divergences only cancel in the sum. These graphs therefore require the introduction of an additional regulator beyond dimensional regularization, and the rapidity divergences are reflected in logarithms of the (scheme-dependent) rapidity scale. While a number of regulators have been used at leading power [76, 80, 173, 180, 191], the “pure rapidity regulator” introduced in [76, 86] is particularly convenient for studying power corrections, as it properly regulates the power divergences in phase space integrals arising at NLP.

In this chapter we use a version of the pure rapidity regulator appropriate for our formalism which introduces separate scheme-dependence for the n - and \bar{n} -sectors, denoted by the parameters ν_n and $\nu_{\bar{n}}$. Rapidity logarithms are summed by running the operators $T_{(i,j)}$ from $\nu_{n,\bar{n}}^H = q_L$ to $\nu_{n,\bar{n}}^S = \mu \sim q_T$. Under rapidity renormalization the operators $T_{(i,j)}$ can mix, leading generically to rapidity renormalization group running of the form

$$T_{(i,j)}(q^-, q^+, \mathbf{q}_T, \mu_S, \nu_{n,\bar{n}}^H) = \sum_{k,\ell} \int \frac{d\omega_1}{\omega_1} \frac{d\omega_2}{\omega_2} d^2 \mathbf{p}_T V_{(i,j),(k,\ell)}(\omega_1, \omega_2, \mathbf{p}_T, \mu_S, \nu_{n,\bar{n}}^H, \nu_{n,\bar{n}}^S) \times T_{(k,\ell)}\left(\frac{q^-}{\omega_1}, \frac{q^+}{\omega_2}, \mathbf{q}_T - \mathbf{p}_T, \mu_S, \nu_{n,\bar{n}}^S\right), \quad (5.13)$$

where by $\nu_{n,\bar{n}}$ we denote depends on both ν_n and $\nu_{\bar{n}}$ separately, and the large logarithms of $\nu_{n,\bar{n}}^H / \nu_{n,\bar{n}}^S$ have been resummed in the rapidity evolution factors $V_{(i,j),(k,\ell)}$. Combining all these steps gives the DY cross section in Eq. (5.11), where $C_{f\bar{f}}$ now has the fully factorized form

$$C_{f\bar{f}}(z_1, z_2, q_L^2, q_T^2) = \int \frac{d\Omega_T}{2} \int \frac{d\omega_1}{\omega_1} \frac{d\omega_2}{\omega_2} \sum_{ijkk'\ell\ell'} \frac{H_{(i,j)}(\mu_S) K_{(k,\ell)}^{(i,j)}}{q_L^{[i]+[j]}} \times \int d^2 \mathbf{p}_T V_{(k,\ell),(k',\ell')}(\omega_1, \omega_2, \mathbf{p}_T, \mu_S, \nu_{n,\bar{n}}^H, \nu_{n,\bar{n}}^S) \times C_{S,(k',\ell')}\left(\frac{z_1}{\omega_1}, \frac{z_2}{\omega_2}, \mathbf{q}_T - \mathbf{p}_T, \mu_S, \nu_{n,\bar{n}}^S\right). \quad (5.14)$$

In this chapter the fixed-order $O(\alpha_s)$ contributions to each of the factors in Eq. (5.14) which are required to determine the fixed-order cross section at NLP are calculated. The $O(\alpha_s)$ anomalous dimensions of the relevant hard matching coefficients may be found in the literature [83, 179], and here we also calculate the $O(\alpha_s)$ off-diagonal entries for the rapidity evolution kernels $\gamma_{(k,\ell),(0,0)}$ which mix the various subleading operators $T_{(k,\ell)}$ into the leading operator $T_{(0,0)}$ with an NLP coefficient. The calculation of the one-loop entries which mix the subleading operators amongst themselves is left for future work. Additionally, in most phenomenological applications, q_T resummation is performed for the Fourier conjugate of q_T (b -space); here we will work in q_T space, where the SCET operators we are using are defined. Fourier transforming our results to b -space may be useful for future applications.

5.2 NLP Operator Products in SCET

In this section the $O(\alpha_s)$ ingredients that contribute to $C_{f\bar{f}}$ at next to leading power in SCET are calculated. We begin by summarizing the hard-scale matching of the QCD current onto SCET scat-

tering operators, and then proceed by Fierz-rearranging products of these scattering operators into a smaller basis of operators. The matrix elements of these operators are calculated using the pure rapidity regulator, and the final result is compared to the corresponding fixed order result from QCD.

5.2.1 Hard-Scale Matching

The invariant mass of the lepton pair is $q^2 = q^+ q^- - q_T^2 \equiv q_L^2 - q_T^2$, where $q_L^2 \gg q_T^2 \gg \Lambda_{\text{QCD}}^2$ and $q^+ \equiv q \cdot n$ and $q^- = q \cdot \bar{n}$ are the large light-cone components of the external current defined in terms of the lightlike vectors $n^\mu = (1, 0, 0, 1)$ and $\bar{n}^\mu = (1, 0, 0, -1)$. This defines the relevant scales for this process. The incoming state consists of two hadrons; the invariant mass of partons in the same hadron is of order Λ_{QCD} , while the invariant mass of partons in different hadrons is of order q_L . Therefore, at a hard scale $\mu_H \sim q_L$ partons in different hadrons are above one another's cutoff, and QCD is matched onto an EFT in which direct interactions between the sectors have been integrated out. In the SCET formalism used in this thesis, SCET consists of decoupled copies of QCD for each sector which only mutually interact via the external electromagnetic current Eq. (5.6). Only quark and antiquark PDFs are considered in this thesis. Gluon PDFs may be included in the same formalism, and the relevant hard-scattering operators are listed in Appendix 5.A, but the calculation for incoming gluons is beyond the scope of this work. We work in a reference frame where the incoming hard quark is in the n -sector and the antiquark is in the \bar{n} -sector.

The matching of the external vector current from QCD to SCET at subleading power has been considered in a number of papers [77, 91, 120, 121, 123, 179], and is obtained by expanding QCD amplitudes in powers of $p_i \cdot n / q \cdot n$ for particles in the n -sector, and $p_i \cdot \bar{n} / q \cdot \bar{n}$ for particles in the \bar{n} -sector. In addition to the analogues of operators considered in [179] for two incoming partons, there are also operators suppressed by single powers of the net transverse momentum $p_{n_i, T}$ in either sector (which were eliminated by a choice of reference frame in [179]) as well as corrections to the multipole expansion of the energy-momentum conserving delta functions.

The SCET current has the expansion Eq. (5.6). The corresponding scattering operators are constructed from the field building blocks [168, 179]

$$\begin{aligned} \bar{\chi}_{\bar{n}}(x) &= \bar{\psi}_{\bar{n}}(x) \bar{W}_{\bar{n}}(x) P_n \\ \chi_n(x) &= \bar{W}_n^\dagger(x) P_n \psi_n(x) \\ \mathcal{B}_n^{\mu_1 \dots \mu_N}(x) &= \bar{W}_{\bar{n}}^\dagger(x) i D_{\bar{n}}^{\mu_1}(x) \dots i D_{\bar{n}}^{\mu_N}(x) \bar{W}_{\bar{n}}(x) \\ \mathcal{B}_n^{\dagger \mu_1 \dots \mu_N}(x) &= (-1)^N \bar{W}_n^\dagger(x) i \bar{D}_n^{\mu_1}(x) \dots i \bar{D}_n^{\mu_N}(x) \bar{W}_n(x) \end{aligned} \quad (5.15)$$

where we note that $(\mathcal{B}^{\mu_1 \dots \mu_N})^\dagger = \mathcal{B}^{\dagger \mu_N \dots \mu_1}$. The incoming Wilson lines \bar{W} are defined as

$$\begin{aligned} \bar{W}_n^\dagger(x) &= \bar{\mathcal{P}} \exp \left(-ig \int_{-\infty}^0 ds \bar{n} \cdot A_n(x + \bar{n}s) e^{s0^+} \right) \\ \bar{W}_{\bar{n}}(x) &= \mathcal{P} \exp \left(ig \int_{-\infty}^0 ds n \cdot A_{\bar{n}}(x + ns) e^{s0^+} \right). \end{aligned} \quad (5.16)$$

We use the conventions

$$i D_{\bar{n}}^\mu(x) = i \partial^\mu + g A_{\bar{n}}^\mu(x), \quad i \bar{D}_n^\mu(x) = i \bar{\partial}^\mu - g A_n^\mu(x) \quad (5.17)$$

and it is convenient to define the four-vectors introduced in [77]

$$\eta^\mu = \sqrt{\frac{\bar{n} \cdot q}{n \cdot q}} n^\mu, \quad \bar{\eta}^\mu = \sqrt{\frac{n \cdot q}{\bar{n} \cdot q}} \bar{n}^\mu \quad (5.18)$$

which are invariant under the boost reparameterization $n^\mu \rightarrow e^y n^\mu$, $\bar{n}^\mu \rightarrow e^{-y} \bar{n}^\mu$.

At leading power there is a single scattering operator,

$$O_2^{(0)\mu}(x) = [\bar{\chi}_{\bar{n}}(x_{\bar{n}})] \gamma^\mu [\chi_n(x_n)], \quad (5.19)$$

where

$$\begin{aligned} x_n^\mu &\equiv x^+ \frac{\bar{n}^\mu}{2} + x_\perp^\mu, \text{ and} \\ x_{\bar{n}}^\mu &\equiv x^- \frac{n^\mu}{2} + x_\perp^\mu. \end{aligned} \quad (5.20)$$

Note that the fields in the operator are multipole expanded; this is necessary for the energy-momentum conserving delta functions to preserve the correct power counting. For example, if p_n^μ and $p_{\bar{n}}^\mu$ are momenta in the n - and \bar{n} -sectors respectively, we have the expansion

$$\delta(p_n^- + p_{\bar{n}}^- - q^-) = \delta(p_n^- - q^-) + p_{\bar{n}}^- \delta'(p_n^- - q^-) + \dots \quad (5.21)$$

and similarly for the n components. Performing this expansion up to $O(1/q_L^2)$ gives

$$[\bar{\chi}_{\bar{n}}(x)] \gamma^\mu [\chi_n(x)] = O_2^{(0)\mu}(x) + \frac{1}{q_L^2} \left(O_2^{(2\delta^+)\mu}(x) + O_2^{(2\delta^-)\mu}(x) \right), \quad (5.22)$$

where

$$\begin{aligned} O_2^{(2\delta^+)\mu}(x) &= \frac{1}{2} q^- q^+ x^- [\bar{\chi}_{\bar{n}}(x_{\bar{n}})] \gamma^\mu [n \cdot \partial \chi_n(x_n)] \\ O_2^{(2\delta^-)\mu}(x) &= \frac{1}{2} q^- q^+ x^+ [\bar{n} \cdot \partial \bar{\chi}_{\bar{n}}(x_{\bar{n}})] \gamma^\mu [\chi_n(x_n)]. \end{aligned} \quad (5.23)$$

Power counting the multipole-expanded operators is not immediately obvious. In $O_2^{(2\delta^+)}$ for example, $q^+ x^-$ is of order 1 since $x^- \sim \partial/\partial q^+$, whereas $q^- p_n^+ \sim O(p_n^- p_n^+) \sim O(p_{n\perp}^2)$; thus, matrix elements of the operators in Eq. (5.23) are $O(1/q_L^2)$ relative to leading power. Since we are working up to $1/q_L^2$ suppression, the contributions from higher multipole expansions in the fields are only included for the leading power operator $O_2^{(0)}$.

At $O(1/q_L)$, there are two operators suppressed by a single perpendicular derivative,

$$\begin{aligned} O_2^{(1\perp n)\mu}(x) &= [\bar{\chi}_{\bar{n}}(x_{\bar{n}})] \gamma^\mu \frac{\not{q}}{2} \gamma_\alpha^\perp [-i \partial^\alpha \chi_n(x_n)] \\ O_2^{(1\perp \bar{n})\mu}(x) &= [-i \partial^\alpha \bar{\chi}_{\bar{n}}(x_{\bar{n}})] \gamma_\alpha^\perp \frac{\not{q}}{2} \gamma^\mu [\chi_n(x_n)]. \end{aligned} \quad (5.24)$$

These were not required in [77, 179] since they could be removed by a suitable choice of reference frame, while here the presence of initial-state radiation prevents such a choice.

Finally, there are several operators containing factors of $\mathcal{B}_{n,\bar{n}}$ whose matrix elements begin at $O(g_s)$. These operators are labeled by a continuous parameter t which parameterizes the separation of fields along the light-cone [118]. We define the dimensionless parameter $\hat{t} \equiv q^- t$ if the shift occurs in the n -sector, and by $\hat{t} \equiv q^+ t$ if the shift occurs in the \bar{n} -sector. We define the A -type operators in which a

gluon is emitted at leading order in the n -sector,

$$\begin{aligned} O_2^{(1A_1)\mu}(x, \hat{t}) &= [\bar{\chi}_{\bar{n}}(x_{\bar{n}})] \gamma_{\alpha}^{\perp} \frac{\not{q}}{2} \gamma^{\mu} [\mathcal{B}_n^{\dagger\alpha}(x_n - \bar{n}t) \chi_n(x_n)] \\ O_2^{(1A_2)\mu}(x, \hat{t}) &= - [\bar{\chi}_{\bar{n}}(x_{\bar{n}})] \gamma^{\mu} \frac{\not{q}}{2} \gamma_{\alpha}^{\perp} [\mathcal{B}_n^{\dagger\alpha}(x_n - \bar{n}t) \chi_n(x_n)] \\ O_2^{(2A_1)\mu}(x, \hat{t}) &= - 2\pi i \theta(\hat{t}) \otimes [\bar{\chi}_{\bar{n}}(x_{\bar{n}})] \gamma_{\alpha}^{\perp} \gamma_{\beta}^{\perp} \gamma^{\mu} [\mathcal{B}_n^{\dagger\alpha\beta}(x_n - \bar{n}t) \chi_n(x_n)], \end{aligned} \quad (5.25)$$

and the corresponding B -type operators where the gluon is emitted in the \bar{n} -sector,

$$\begin{aligned} O_2^{(1B_1)\mu}(x, \hat{t}) &= - [\bar{\chi}_{\bar{n}}(x_{\bar{n}}) \mathcal{B}_{\bar{n}}^{\alpha}(x_{\bar{n}} - nt)] \gamma^{\mu} \frac{\not{q}}{2} \gamma_{\alpha}^{\perp} [\chi_n(x_n)] \\ O_2^{(1B_2)\mu}(x, \hat{t}) &= [\bar{\chi}_{\bar{n}}(x_{\bar{n}}) \mathcal{B}_{\bar{n}}^{\alpha}(x_{\bar{n}} - nt)] \gamma_{\alpha}^{\perp} \frac{\not{q}}{2} \gamma^{\mu} [\chi_n(x_n)] \\ O_2^{(2B_1)\mu}(x, \hat{t}) &= - 2\pi i \theta(\hat{t}) \otimes [\bar{\chi}_{\bar{n}}(x_{\bar{n}}) \mathcal{B}_{\bar{n}}^{\alpha\beta}(x_{\bar{n}} - nt)] \gamma^{\mu} \gamma_{\alpha}^{\perp} \gamma_{\beta}^{\perp} [\chi_n(x_n)]. \end{aligned} \quad (5.26)$$

Following [118], it is convenient to work with the Fourier-transformed operators

$$\begin{aligned} O_2^{(i)}(x, u) &= \int \frac{d\hat{t}}{2\pi} e^{-iut} O_2^{(i)}(x, \hat{t}) \\ C_2^{(i)}(x, u) &= \int d\hat{t} e^{iut} C_2^{(i)}(x, \hat{t}). \end{aligned} \quad (5.27)$$

We have also defined the convolutions in \hat{t} -space in these definitions as

$$f(\hat{t}) \otimes g(\hat{t}) = \int \frac{dx dy}{2\pi} f(x) g(y) \delta(\hat{t} - x - y). \quad (5.28)$$

Note that the one-gluon matrix element of $O_2^{(2A_1)}(x, u)$ is proportional to $\delta(u + k^-)/u$, where k^{μ} is the gluon momentum. If the convolution with $\theta(\hat{t})$ had not been included in its definition (as was the case in [179]), the matrix element of the operator would instead be proportional to $\delta(u + k^-)$, and the operator would have a factor of $1/u$ in its Wilson coefficient. This is inconvenient because in the DY process studied here, this factor of $1/u \sim 1/k^-$ corresponds to a rapidity divergence, and rapidity renormalizing operator products such as $O_2^{(2A_1)\dagger} O_2^{(0)}$ without the factor of $1/u$ in its matrix element would then give rise to an unregulated rapidity divergence in the final integral over u .² These are similar to the endpoint divergences which have been previously noted at NLP in SCET, in particular in b -mediated $h \rightarrow \gamma\gamma$ decay [87–89]. With the definition given here – which is similar to the modification of SCET operators proposed in [221] – the u integral does not introduce any additional singularities and thus all rapidity divergences are correctly regulated by the pure rapidity regulator. We illustrate this with an example in Section 5.2.4.

Since SCET currents and their products contain operators with zero, one, or two factors of u at this order, we use the notation $\{u\}$ to denote the dependence of a quantity on any number of u 's, as well as $\int d\{u\}$ to indicate integration over any number of u 's (including zero). The expansion of the SCET

²The importance of having a finite integral over convolution variables was stressed in [91, 219, 220].

current may therefore be written

$$\begin{aligned} J_{\text{SCET}}^\mu(x) &= \sum_i \int d\{u\} \frac{1}{q_L^{[i]}} C_2^{(i)}(\{u\}) O_2^{(i)\mu}(x, \{u\}) \\ &= C_2^{(0)} \left[O_2^{(0)\mu}(x) + \frac{1}{q_L} \left(O_2^{(1\perp n)\mu}(x) + O_2^{(1\perp \bar{n})\mu}(x) \right) + \frac{1}{q_L^2} \left(O_2^{(2\delta^+)\mu}(x) + O_2^{(2\delta^-)\mu}(x) \right) \right] \quad (5.29) \\ &\quad + \frac{1}{q_L} \sum_i \int du C_2^{(1i)}(u) O_2^{(1i)\mu}(x, u) + \frac{1}{q_L^2} \sum_i \int du C_2^{(2i)}(u) O_2^{(2i)\mu}(x, u) + O\left(\frac{1}{q_L^3}\right) \end{aligned}$$

where on the first line the sum is over all operators $i = 0, 1\perp n, \dots, 2B_1$, while in the last line the sums are over the operators of the appropriate dimension whose coefficients are not fixed by reparameterization or translation invariance. The operators $O_2^{(1\perp n, \bar{n})}$ are related to $O_2^{(0)}$ through reparameterization invariance (RPI) [83, 218], and so to all orders in α_s we have the equalities $C_2^{(0)} = C_2^{(1\perp n)} = C_2^{(1\perp \bar{n})}$, while translation invariance of QCD ensures that $C_2^{(0)} = C_2^{(2\delta^+)} = C_2^{(2\delta^-)}$. The normalizations of all operators have been chosen so that their tree-level matching coefficient is unity in u -space,

$$C_2^{(i)}(\mu, \{u\}) = 1 + O(\alpha_s). \quad (5.30)$$

The one-gluon matrix elements of the operators $O_2^{(i)}(\mu, \{u\})$ are given in Appendix 5.A.

There are additional operators not included in Eq. (5.25) and Eq. (5.26) which are part of the general SCET current expansion [179], but which do not contribute to $C_{f\bar{f}}$ at the order (in α_s , q_T/Q , or Λ_{QCD}/Q) to which we are working, or which contribute only to the gluon-initiated Drell-Yan sub-process. These operators do not mix under renormalization at one loop with the operators considered here, and so are not included in this analysis, though we list them in Appendix 5.A for completeness.

5.2.2 Renormalization Group Running

The anomalous dimensions of all the required matching coefficients $C_2^{(i)}(\{u\})$ have been calculated previously in [78, 83, 179]. They obey the integro-differential equation

$$\frac{d}{d \log \mu} C_2^{(i)}(\mu, \{u\}) = \int d\{v\} \gamma_2^{(i)}(\{u\}, \{v\}) C_2^{(i)}(\mu, \{v\}), \quad (5.31)$$

where the kernels $\gamma_2^{(i)}$ have the form

$$\gamma_2^{(i)}(\{u\}, \{v\}) = \Gamma_{\text{cusp}}^{(i)}[\alpha_s] \log \frac{-q_L^2 - i0^+}{\mu^2} \delta(\{u\} - \{v\}) + \gamma_{\text{non-cusp}}^{(i)}(\{u\}, \{v\}). \quad (5.32)$$

Working in the leading-log (LL) approximation only the cusp anomalous dimension is required. The one-loop cusp anomalous dimension is universal,

$$\Gamma_{\text{cusp}}^{(0)} = \Gamma_{\text{cusp}}^{(1A_i)} = \Gamma_{\text{cusp}}^{(2A_i)} = \Gamma_{\text{cusp}}^{(1B_i)} = \Gamma_{\text{cusp}}^{(2B_i)} = \frac{\alpha_s C_F}{\pi}. \quad (5.33)$$

With the definition $H_{(i,j)}(\{u\}) = C_2^{(i)\dagger}(\{u\})C_2^{(j)}(\{u\})$, the leading-log running of the hard functions is determined by the RGE

$$\frac{d}{d \log \mu} H_{(i,j)}(\mu, \{u\}) = \left(2\Gamma_{\text{cusp}} \log \frac{q_L^2}{\mu^2} \right) H_{(i,j)}(\mu, \{u\}). \quad (5.34)$$

This gives the LL unitary evolution for all $H_{(i,j)}$

$$H_{(i,j)}(\mu, \{u\}) = U_H^{\text{LL}}(\mu, \mu_H) H_{(i,j)}(\mu_H, \{u\}), \quad (5.35)$$

where, with $\beta[\alpha_s] \equiv d\alpha_s/d \log \mu = -\beta_0 \alpha_s^2/2\pi + \dots$,

$$\begin{aligned} \log U_H^{\text{LL}}(\mu, \mu_H) &= -4 \int_{\alpha_s(\mu_H)}^{\alpha_s(\mu)} \frac{d\alpha}{\beta[\alpha]} \Gamma_{\text{cusp}}[\alpha] \int_{\alpha(q_L)}^{\alpha} \frac{d\alpha'}{\beta[\alpha']} \\ &= \frac{16\pi C_F}{\beta_0^2} \left(\frac{1}{\alpha_s(\mu_H)} - \frac{1}{\alpha(\mu)} - \frac{1}{\alpha(q_L)} \log \frac{\alpha(\mu)}{\alpha(\mu_H)} \right). \end{aligned} \quad (5.36)$$

Beyond LL there will be operator mixing, and the solution to the RGE will be more involved. This sums the RGE logarithms of μ_H/μ in the hard functions.

5.2.3 $T_{(i,j)}$ Definitions

The differential cross section for DY production is given in terms of hadronic matrix elements of products of operators $O_2^{(i)\dagger}(x)O_2^{(j)}(0)$ in Eq. (5.7). Matrix elements of these operator products may be evaluated between partons in perturbation theory to calculate the matching conditions onto light-cone distribution operators (whose matrix elements are the usual PDFs); however, it is convenient to perform a Fierz rearrangement for each operator product to write it as the product of factors in the n - and \bar{n} -sectors, corresponding to the convolution of generalized transverse momentum dependent distribution operators. At leading power, this gives

$$\begin{aligned} \int \frac{d^d x}{2(2\pi)^d} (-g_{\mu\nu}) e^{-iq \cdot x} O_2^{(0)\mu\dagger}(x) O_2^{(0)\nu}(0) &= \frac{1}{N_c} \int \frac{d^d x}{2(2\pi)^d} e^{-iq \cdot x} \Phi_n^{(0)}(x_n) \Phi_{\bar{n}}^{(0)}(x_{\bar{n}}) \\ &\equiv \frac{1}{N_c} T_{(0,0)}(q^-, q^+, \mathbf{q}_T). \end{aligned} \quad (5.37)$$

The leading power position space distribution operators are defined as

$$\Phi_n(x_n) \equiv \bar{\chi}_n(x_n) \frac{\not{q}}{2} \chi_n(0), \quad \Phi_{\bar{n}}(x_{\bar{n}}) \equiv \bar{\chi}_{\bar{n}}(0) \frac{\not{q}}{2} \chi_{\bar{n}}(x_{\bar{n}}), \quad (5.38)$$

where x_n and $x_{\bar{n}}$ are defined in (5.20), and thus consist of quark fields separated in the transverse direction by x_{\perp}^{μ} as well as along the light-cone.

Products of power-suppressed operators may similarly be written as convolutions of higher dimension operators,

$$T_{(i,j)}(q, \{u\}) = \int \frac{d^d x}{2(2\pi)^d} e^{-iq \cdot x} \Phi_n^{(i)}(x_n, \{u\}) \Phi_{\bar{n}}^{(j)}(x_{\bar{n}}, \{u\}), \quad (5.39)$$

where we define the relevant subleading transverse momentum dependent light-cone distribution opera-

tors $\Phi_n^{(i)}(x, \{t\})$ as

$$\begin{aligned}
\Phi_n^{(2_1)}(x_n, \hat{t}) &\equiv (i\partial^\mu \bar{\chi}_n(x_n)) \frac{\not{q}}{2} \gamma_\mu^\perp \gamma_\nu^\perp \mathcal{B}_n^{\dagger\nu}(-\bar{n}t) \chi_n(0) \\
\Phi_n^{(2_2)}(x_n, \hat{t}_1, \hat{t}_2) &\equiv -\bar{\chi}_n(x_n) \mathcal{B}_n^\mu(x_n - \bar{n}t_1) \frac{\not{q}}{2} \gamma_\mu^\perp \gamma_\nu^\perp \mathcal{B}_n^{\dagger\nu}(-\bar{n}t_2) \chi_n(0) \\
\Phi_n^{(2_3)}(x_n, \hat{t}) &\equiv 2\pi i\theta(\hat{t}) \otimes \bar{\chi}_n(x_n) \mathcal{B}_n^{\mu\nu}(x_n - \bar{n}t) \frac{\not{q}}{2} \gamma_\nu^\perp \gamma_\mu^\perp \chi_n(0) \\
\Phi_n^{(2_4)}(x_n) &\equiv q^+ q^- \frac{x^-}{2} (n \cdot \partial \bar{\chi}_n(x_n)) \frac{\not{q}}{2} \chi_n(0).
\end{aligned} \tag{5.40}$$

The corresponding \bar{n} -sector operators $\Phi_{\bar{n}}^{(i)}$ are found by taking the Hermitian conjugate and changing $n \leftrightarrow \bar{n}$. The u -space Fourier conjugates of these building blocks are defined by the transformation in Eq. (5.27) for shifts relative to the origin (since these shifts come from an operator), and by the conjugate transformation for shifts relative to x_n (since these shifts come from the conjugated operator).

Thus, for example,

$$\begin{aligned}
T_{(0,2_1)}(q, u) &= \int \frac{d^d x}{2(2\pi)^d} e^{-iq \cdot x} \Phi_n^{(0)}(x_n) \Phi_{\bar{n}}^{(2_1)}(x_{\bar{n}}, u) \\
&= \int \frac{d^d x}{2(2\pi)^d} \frac{d\hat{t}}{2\pi} e^{-iu\hat{t}} e^{-iq \cdot x} \left[\bar{\chi}_n(x_n) \frac{\not{q}}{2} \chi_n(0) \right] \left[\bar{\chi}_{\bar{n}}(0) \mathcal{B}_{\bar{n}}^\nu(-nt) \gamma_\nu^\perp \gamma_\mu^\perp \frac{\not{q}}{2} (-i\partial^\mu \chi_{\bar{n}}(x_{\bar{n}})) \right].
\end{aligned} \tag{5.41}$$

In general, we can write

$$\int \frac{d^d x}{2(2\pi)^d} (-g_{\mu\nu}) e^{-iq \cdot x} O_2^{(i)\mu\dagger}(x) O_2^{(j)\nu}(0) = \sum_{k,\ell} \frac{1}{N_c} K_{(k,\ell)}^{(i,j)} T_{(k,\ell)} + \text{spin-dependent}, \tag{5.42}$$

where the only non-zero elements of K which are relevant at this order are

$$\begin{aligned}
K_{(2_1,0)}^{(1\perp n, 1A_1)} &= K_{(2_1,0)}^{(1A_1, 1\perp n)} = K_{(2_2,0)}^{(1A_2, 1A_1)} = K_{(2_2,0)}^{(1A_1, 1A_2)} \\
&= K_{(0,2_1)}^{(1\perp \bar{n}, 1B_1)} = K_{(0,2_1)}^{(1B_1, 1\perp \bar{n})} = K_{(0,2_2)}^{(1B_2, 1B_1)} \\
&= K_{(0,2_2)}^{(1B_1, 1B_2)} = K_{(2_3,0)}^{(2A_1, 0)} = K_{(2_3,0)}^{(0,2A_1)} \\
&= K_{(2_4,0)}^{(2\delta^+, 0)} = K_{(0,2_3)}^{(0,2B_1)} = K_{(0,2_3)}^{(2B_1, 0)} = K_{(0,2_4)}^{(2\delta^-, 0)} = 1.
\end{aligned} \tag{5.43}$$

5.2.4 Matrix Elements of Operator Products

Individual n - and \bar{n} -sector graphs contributing to the matrix elements of each $T_{(i,j)}$ are rapidity divergent, and require a regulator to give finite results. We use a version of the pure rapidity regulator introduced in [76]. As discussed in that reference, other commonly-used rapidity regulators such as the δ -regulator [173] or the η -regulator [182] are not suitable for handling the power-law rapidity divergences that arise at NLP. An explicit example of the δ -regulator failing to regulate rapidity divergences at NLP is given in Section 5.2.4.

In what follows we define the pure rapidity regulator by modifying the integration measure of n -sector

and \bar{n} -sector particles as

$$\begin{aligned} d^d k_n &\rightarrow w_n^2 \left(\frac{q_L^2}{\nu_n^2} \right)^{\eta_n/2} \left(\frac{q^-}{q^+} \frac{k_n^+}{k_n^-} \right)^{\eta_n/2} d^d k_n \\ d^d k_{\bar{n}} &\rightarrow w_{\bar{n}}^2 \left(\frac{q_L^2}{\nu_{\bar{n}}^2} \right)^{\eta_{\bar{n}}/2} \left(\frac{q^+}{q^-} \frac{k_{\bar{n}}^-}{k_{\bar{n}}^+} \right)^{\eta_{\bar{n}}/2} d^d k_{\bar{n}}. \end{aligned} \quad (5.44)$$

This regulator has the distinct advantage that – as in dimensional regularization – scaleless integrals vanish, and as a result all overlap integrals evaluate to zero. This greatly simplifies the calculation since, as is discussed in detail in Section 5.3, in a scheme where overlap integrals do not vanish, the overlap subtraction procedure must be carried out to subleading powers.

The regulator in Eq. (5.44) is slightly modified from the form presented in [76]: the factors of q^\pm ensure boost invariance, as in [123], the dimensionless parameter v has been replaced by the equivalent dimensionful parameters ν_i , and distinct parameters η_i , ν_i , and w_i have been introduced for each sector, since the fields in the n - and \bar{n} -sectors are independent. As discussed in [175], rapidity logarithms in SCET correspond to a scheme dependence in defining the sum of individually rapidity divergent graphs in the n - and \bar{n} -sectors. Regulating both sectors (and their corresponding overlap graphs) in the same way and then removing the regulator is equivalent to naïvely adding the individual graphs together before performing the loop integrals, and reproduces the rapidity logarithms of QCD. Since QCD has no rapidity divergences, rapidity divergences cancel for this choice, which corresponds to choosing the parameters $\eta_n = -\eta_{\bar{n}}$, $\nu_n \nu_{\bar{n}} = q_L^2$ and $w_n = w_{\bar{n}}$. This was explicitly demonstrated up to NLP in [76]: these authors showed that if QCD diagrams are first rapidity regulated and then expanded in the n -collinear, \bar{n} -collinear, and soft limits, the leading and subleading power matrix elements reproduce the rapidity-finite QCD results expanded to the same order. A similar cancellation of rapidity divergences will be shown here.

Using different rapidity regulator parameters in the two sectors moves the rapidity logarithm of q_L^2 into the Wilson coefficients of the EFT and allows the scheme dependence of the resulting graphs to be exploited to sum the corresponding rapidity logs. The corresponding rapidity divergences correspond to $1/\eta_i$ singularities which are canceled by introducing the appropriate counterterms into the EFT, and rapidity logarithms are then summed using rapidity renormalization group (RRG) techniques similar to [182]. The bookkeeping constants w_i are taken to formally obey the RRG equation

$$\frac{dw_i}{d \log \nu_i} = \frac{\eta_i}{2} w_i, \quad (5.45)$$

which cancels the scheme dependence in the measure, keeping the bare theory ν_i independent and allowing techniques analogous to those in dimensional regularization to be used to extract the rapidity anomalous dimensions. As in [76, 182], these bookkeeping constants are set to unity at the end of calculation. Rapidity logarithms are minimized by the appropriate choice of the dimensionless parameters $\nu_{n, \bar{n}}$.

As noted in [175], choosing $\nu_n \nu_{\bar{n}} \neq q_L^2$ requires rapidity counterterms for each $T_{(i,j)}$ which are sensitive to the scale q_T . Scale-sensitivities in the counterterm generate the same scale-dependence in the Wilson coefficient through the RGE, and since Wilson coefficients in an EFT must be independent of infrared physics, this adds the constraint that the theory must first be evolved to $\mu \sim q_T$ before running in rapidity. This will be discussed in more detail in Section 5.2.6.

At LP the only operator is $T_{(0,0)}$, so its divergences are absorbed by the renormalization constant

$$Z_{(0,0),(0,0)},$$

$$T_{(0,0)}^B(q^-, q^+, \mathbf{q}_T) = \int \frac{d\omega_1}{\omega_1} \frac{d\omega_2}{\omega_2} d^{d-2} \mathbf{p}_T Z_{(0,0),(0,0)}(\omega_1, \omega_2, \mathbf{p}_T) T_{(0,0)} \left(\frac{q^-}{\omega_1}, \frac{q^+}{\omega_2}, \mathbf{q}_T - \mathbf{p}_T \right), \quad (5.46)$$

where $T_{(i,j)}^B$ and $T_{(i,j)}$ denote the bare and renormalized operators, respectively, and the integral corresponds to summing over the infinite set of operators $T_{(0,0)}(k^-, k^+, \mathbf{k}_T)$. At subleading powers the various operators may mix with one another, so we have the general relation

$$\begin{aligned} T_{(i,j)}^B(q^-, q^+, \mathbf{q}_T, \{u\}) &= \sum_{(k,l)} \int \frac{d\omega_1}{\omega_1} \frac{d\omega_2}{\omega_2} d^{d-2} \mathbf{p}_T d\{v\} Z_{(i,j),(k,l)}(\omega_1, \omega_2, \mathbf{p}_T, \{v\}) \\ &\quad \times T_{(k,l)} \left(\frac{q^+}{\omega_2}, \frac{q^-}{\omega_1}, \mathbf{q}_T - \mathbf{p}_T, \{u - v\} \right), \end{aligned} \quad (5.47)$$

where the sum over operators includes each subleading $T_{(i,j)}$ as well as the leading operator $T_{(0,0)}$ with a power-suppressed coefficient, as will be discussed in the following sections.

Leading Power Example

The leading power calculation of DY production in this formalism was presented in [175] using the δ -regulator; we repeat the calculation here with the pure rapidity regulator. At leading power, there is a single bilocal operator contributing to the rate,

$$T_{(0,0)}(q^-, q^+, \mathbf{q}_T) = \int \frac{d^d x}{2(2\pi)^d} e^{-i\mathbf{q}\cdot\mathbf{x}} \left[\bar{\chi}_n(x_n) \frac{\not{p}}{2} \chi_n(0) \right] \left[\bar{\chi}_{\bar{n}}(0) \frac{\not{p}}{2} \chi_{\bar{n}}(x_{\bar{n}}) \right]. \quad (5.48)$$

With incoming quark and antiquark states $q(p_1)$ and $\bar{q}(p_2)$ the tree-level matrix element of this operator is

$$\begin{aligned} \frac{1}{4} \sum_{\text{spins}} \langle p_1^n p_2^{\bar{n}} | T_{(0,0)} | p_1^n p_2^{\bar{n}} \rangle &= \frac{1}{4} \sum_{\text{spins}} \int \frac{d^d x}{2(2\pi)^d} e^{-i\mathbf{q}\cdot\mathbf{x}} \langle p_1^n | \left[\bar{\chi}_n(x_n) |0\rangle \frac{\not{p}}{2} \langle 0| \chi_n(0) \right] |p_1^n\rangle \\ &\quad \times \langle p_2^{\bar{n}} | \left[\bar{\chi}_{\bar{n}}(0) |0\rangle \frac{\not{p}}{2} \langle 0| \chi_{\bar{n}}(x_{\bar{n}}) \right] |p_2^{\bar{n}}\rangle \\ &= \delta(\bar{z}_1) \delta(\bar{z}_2) \delta^{d-2}(\mathbf{q}_T) \equiv \delta_1 \delta_2 \delta_T, \end{aligned} \quad (5.49)$$

where the superscripts n - and \bar{n} in Eq. (5.49) denote the sector of the corresponding parton. We also use the notation

$$z_1 \equiv \frac{q^-}{p_1^-}, \quad z_2 \equiv \frac{q^+}{p_2^+}, \quad \bar{z}_i \equiv 1 - z_i \quad (5.50)$$

and

$$\delta_i \equiv \delta(\bar{z}_i), \quad \delta'_i \equiv \delta'(\bar{z}_i), \quad \delta_T \equiv \delta^{d-2}(\mathbf{q}_T). \quad (5.51)$$

At $O(\alpha_s)$, the matrix element corresponding to the emission of a real n -sector gluon is given by the three n -sector graphs shown of Figure 5.1. Denoting the spin-averaged one-loop matrix element of $T_{(0,0)}$ by $\mathcal{M}_{(0,0)}$, we write

$$\mathcal{M}_{(0,0)} = \mathcal{M}_{(0,0)}^n + \mathcal{M}_{(0,0)}^{\bar{n}} - \mathcal{M}_{(0,0)}^O, \quad (5.52)$$

where the superscripts n and \bar{n} denote the $O(\alpha_s)$ contribution from a gluon in the corresponding sector, and the O superscript denotes the overlap subtraction. Since these matrix elements correspond to a

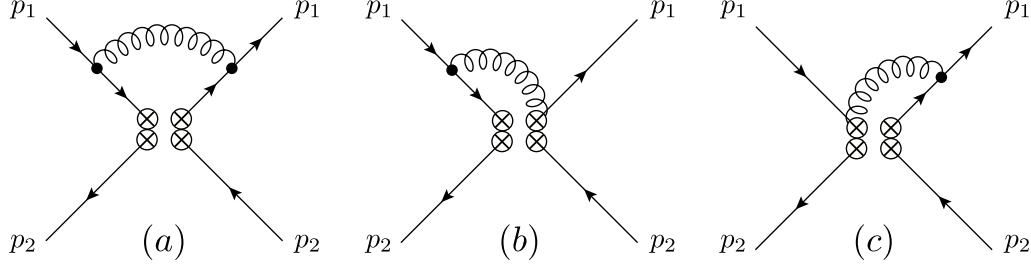


Figure 5.1: Non-vanishing graphs in the n -sector contributing to the matrix element $\langle p_1^n p_2^{\bar{n}} | T_{(0,0)} | p_1^n p_2^{\bar{n}} \rangle$ at $O(\alpha_s)$.

matching calculation at the scale $\mu_S \sim q_T \gg \Lambda_{\text{QCD}}$ we use the initial-state kinematics $p_1^+ = p_{1\perp} = 0 = p_{2\perp} = p_2^-$, and we obtain

$$\begin{aligned} \mathcal{M}_{(0,0)}^n = & -2\pi g^2 C_F \int \frac{d^d k}{(2\pi)^d} w_n^2 \left(\frac{q_L^2}{\nu_n^2} \frac{q^-}{q^+} \frac{k^+}{k^-} \right)^{\eta_n/2} \delta(k^2) \delta(p_1^- - q^- - k^-) \delta(p_2^+ - q^+) \delta^{d-2}(\mathbf{q}_T + \mathbf{k}_T) \\ & \times \text{Tr} \left[\frac{\not{p}_2}{2} \left(\frac{2p_1^\alpha - \gamma^\alpha \not{k}}{-2p_1 \cdot k} + \frac{\bar{n}^\alpha}{k^-} \right) \frac{\not{k}}{2} \times \left(\frac{2p_{1\alpha} - \not{k}\gamma_\alpha}{-2p_1 \cdot k} - \frac{\bar{n}_\alpha}{-k^-} \right) \right] \text{Tr} \left[\frac{\not{p}_2}{2} \frac{\not{k}}{2} \right], \end{aligned} \quad (5.53)$$

which evaluates to

$$\mathcal{M}_{(0,0)}^n = \frac{\bar{\alpha}}{\pi} f_\epsilon w_n^2 \delta_2 \frac{(\mu^2)^{-\eta_n/2}}{(\mathbf{q}_T^2)^{1-\eta_n/2}} \left(\frac{z_1 \mu}{\nu_n} \right)^{\eta_n} \frac{(2 - 2\bar{z}_1 + (1 - \epsilon)\bar{z}_1^2)}{\bar{z}_1^{1+\eta_n}}, \quad (5.54)$$

where

$$\bar{\alpha} \equiv \frac{\alpha_s C_F}{2\pi}, \quad f_\epsilon \equiv (\pi \mu^2 e^\gamma)^\epsilon \quad (5.55)$$

and we work in $d = 4 - 2\epsilon$ dimensions.

To extract the singularity structure of this matrix element at $\bar{z}_1 = 0$ we use the distributional identity

$$\frac{\theta(\bar{z}_1)}{\bar{z}_1^{1+\eta}} = -\frac{\delta(\bar{z}_1)}{\eta} + \left[\frac{\theta(\bar{z}_1)}{\bar{z}_1} \right]_+ + \dots \quad (5.56)$$

for scalars (see Appendix 5.B for definitions) as well as the identity [67]

$$\frac{(\mu^2)^{-\eta/2}}{(\mathbf{q}_T^2)^{1-\eta/2}} = \mu^{-2\epsilon} \frac{S_{d-2}}{2} \left(\frac{\delta_T}{\frac{\eta}{2} - \epsilon} + \mathcal{L}_{0T} + \frac{\eta}{2} \mathcal{L}_{1T} + \dots \right) \quad (5.57)$$

for vectors in $(d-2)$ dimensions, where the \mathcal{L}_{nT} are vector plus distributions [67, 80] defined in Appendix 5.B.2,

$$\mathcal{L}_{nT} \equiv \mathcal{L}_n(\mathbf{q}_T, \mu) = \frac{2\mu^{2\epsilon}}{S_{d-2}} \left[\frac{\log^n \frac{\mathbf{q}_T^2}{\mu^2} \theta(\mathbf{q}_T^2)}{\mathbf{q}_T^2} \right]_+^{\mu^2}, \quad (5.58)$$

and $S_{d-2} = 2\pi^{\frac{d-2}{2}} / \Gamma(\frac{d-2}{2})$. Upon expanding first in η_n then in ϵ , the n -sector contribution to the

matrix element from a single real emission is

$$\begin{aligned} \mathcal{M}_{(0,0)}^n = & \bar{\alpha} w_n^2 \delta_2 \left[\frac{4}{\eta_n} \delta_1 \left(\frac{\delta_T}{\epsilon} - \mathcal{L}_{0T} \right) + \delta_1 \delta_T \left(\frac{2}{\epsilon^2} + \frac{3 - 2 \log \frac{\nu_n^2}{\mu^2}}{\epsilon} \right) \right. \\ & + 2 \left(\mathcal{L}_{0T} - \frac{\delta_T}{\epsilon} \right) \left[\frac{1 + z_1^2}{\bar{z}_1} \right]_+ \delta_T \\ & \left. + 2 \bar{z}_1 \delta_T - \zeta_2 \delta_1 \delta_T - 2 \delta_1 \mathcal{L}_{1T} - \delta_1 \mathcal{L}_{0T} \left(3 - 2 \log \frac{\nu_n^2}{\mu^2} \right) \right]. \end{aligned} \quad (5.59)$$

The \bar{n} -sector contribution is obtained under the replacements $z_1 \rightarrow z_2$, $w_n \rightarrow w_{\bar{n}}$, $\nu_n \rightarrow \nu_{\bar{n}}$ and $\eta_n \rightarrow \eta_{\bar{n}}$.

As in [77], the overlap between the two sectors is obtained by taking the opposite-sector gluon limit of the n - and \bar{n} -sector graphs. As detailed in Section 5.3, the subtraction prescription corresponds to subtracting half the wrong sector limit for the gluon of each sector³, which we denote

$$\mathcal{M}_{(0,0)}^O = \frac{1}{2} \left(\mathcal{M}_{(0,0)}^{n \rightarrow \bar{n}} + \mathcal{M}_{(0,0)}^{\bar{n} \rightarrow n} \right). \quad (5.60)$$

For example, the wrong sector limit of Eq. (5.53) is

$$\begin{aligned} \mathcal{M}_{(0,0)}^{n \rightarrow \bar{n}} = & -2\pi g^2 C_F \int \frac{d^d k}{(2\pi)^d} w_n^2 \left(\frac{q_L^2}{\nu_n^2} \frac{q^-}{q^+} \frac{k^+}{k^-} \right)^{\eta_n/2} \delta(k^2) \delta(p_1^- - q^-) \delta(p_2^+ - q^+) \delta^{d-2}(\mathbf{q}_T + \mathbf{k}_T) \\ & \times \text{Tr} \left[\frac{\not{p}_1}{2} \left(\frac{n^\alpha}{-k^+} + \frac{\bar{n}^\alpha}{k^-} \right) \frac{\not{q}}{2} \left(\frac{n_\alpha}{-k^+} - \frac{\bar{n}_\alpha}{k^-} \right) \right] \text{Tr} \left[\frac{\not{p}_2}{2} \frac{\not{q}}{2} \right] + \dots \end{aligned} \quad (5.61)$$

where the dots indicate terms suppressed by powers of $1/q_L$ relative to leading power. Integrating with respect to \mathbf{k}_T then k^+ , we find the \bar{n} limit of the n -sector graphs is

$$\mathcal{M}_{(0,0)}^{n \rightarrow \bar{n}} = \frac{2\bar{\alpha}}{\pi} f_\epsilon w_n^2 \delta_1 \delta_2 \left(\frac{q_L^2}{\nu_n^2} \frac{q^-}{q^+} \right)^{\eta_n/2} \frac{1}{(q_T^2)^{1-\eta_n/2}} \int_0^\infty \frac{dk^-}{(k^-)^{1+\eta_n}}, \quad (5.62)$$

which is a scaleless divergence and vanishes in this regularization scheme. The overlap subtraction between the two sectors is therefore zero when using the pure rapidity regulator at $O(\alpha_s)$, and this remains true beyond leading power.

Summing the contributions from each sector and subtracting off the (vanishing) overlap, we find the $O(\alpha_s)$ contribution to the matrix element of $T_{(0,0)}$

$$\begin{aligned} \mathcal{M}_{(0,0)} = & \bar{\alpha} \left[2 \left(\frac{w_n^2}{\eta_n} + \frac{w_{\bar{n}}^2}{\eta_{\bar{n}}} \right) \delta_1 \delta_2 \left(\frac{\delta_T}{\epsilon} - \mathcal{L}_{0T} \right) + \delta_1 \delta_2 \delta_T \left(\frac{2}{\epsilon^2} + \frac{3 - 2 \log \frac{\nu_n \nu_{\bar{n}}}{\mu^2}}{\epsilon} \right) \right. \\ & + \left(\mathcal{L}_{0T} - \frac{\delta_T}{\epsilon} \right) \left(\delta_2 \left[\frac{1 + z_1^2}{\bar{z}_1} \right]_+ + \delta_1 \left[\frac{1 + z_2^2}{\bar{z}_2} \right]_+ \right) \\ & \left. - \delta_1 \delta_2 \left[2 \mathcal{L}_{1T} + \mathcal{L}_{0T} \left(3 - 2 \log \frac{\nu_n \nu_{\bar{n}}}{\mu^2} \right) \right] + (\bar{z}_1 \delta_2 + \bar{z}_2 \delta_1 - \delta_1 \delta_2 \zeta_2) \delta_T \right], \end{aligned} \quad (5.63)$$

where we have set $w_{n,\bar{n}} = 1$ for all η_i -independent terms. As discussed earlier, the rapidity divergences appear as the η -divergent terms in the first line. The rapidity-finiteness of the full theory is reflected

³In [77], the limits from either sector were equal.

in the fact that setting $w_n = w_{\bar{n}}$ and $\eta_n = -\eta_{\bar{n}}$ gives a total rate which is free from η -poles, which is to be expected since this scheme corresponds to regulating the n and \bar{n} sectors identically; using different schemes for the two sectors spoils the cancellation of rapidity divergences between the sectors. However, resumming the rapidity logarithms requires keeping the $w_{n,\bar{n}}$ and $\eta_{n,\bar{n}}$ scheme dependence. This introduces explicit rapidity divergences in the matrix elements which require rapidity counterterms, from which the RRG may be derived.

In the scheme where $\nu_n \nu_{\bar{n}} = q_L^2$, the purely ϵ -divergent terms (ultraviolet divergences) in the first line of Eq. (5.63) are canceled by the renormalization constant $Z_{2,(0)}$ for $O_2^{(0)}$

$$Z_{2,(0)} = 1 + \frac{\bar{\alpha}}{2} \left(\frac{2}{\epsilon^2} + \frac{3 - 2 \log \frac{q_L^2}{\mu^2}}{\epsilon} \right), \quad (5.64)$$

which follows the product of renormalized operators $O_{2,(0)}^{\dagger\mu} O_{2,(0)}^{\dagger\nu}$ through the Fierz rearrangement. Since $Z_{2,(0)}$ depends only on $\log(q_L^2/\mu^2)$, the scheme $\nu_n \nu_{\bar{n}} = q_L^2$ is enforced at $\mu \sim q_L$ and throughout the μ -running when $\mu > q_T$. As we later discuss in Section 5.2.6, when $\mu \sim q_T$ then q_T is no longer an infrared scale, and then $\nu_{n,\bar{n}}$ can be evolved with the RRG, allowing for the resummation of rapidity logarithms.

The IR divergent terms in the second line of Eq. (5.63) are the Altarelli-Parisi splitting functions, and are reproduced by the infrared divergences in the light-cone distribution operators in the low-energy theory. The remaining divergences are rapidity divergences, and are absorbed by the counterterm in Eq. (5.46), where

$$Z_{(0,0),(0,0)}(\omega_1, \omega_2, \mathbf{q}_T) = \delta_1 \delta_2 \left(\delta_T + 2\bar{\alpha} \left(\frac{w_n^2}{\eta_n} + \frac{w_{\bar{n}}^2}{\eta_{\bar{n}}} \right) \left(\frac{\delta_T}{\epsilon} - \mathcal{L}_{0T} \right) + 2\bar{\alpha} \frac{\delta_T}{\epsilon} \log \frac{q_L^2}{\nu_n \nu_{\bar{n}}} \right). \quad (5.65)$$

Using the running of the fictional coupling $w_{n,\bar{n}}$ in Eq. (5.45), we can obtain the rapidity anomalous dimension and rapidity evolution equation for $T_{(0,0)}$, which we further discuss in Section 5.2.6.

Note that for $\eta_n = -\eta_{\bar{n}}$ and $\nu_{n,\bar{n}} = q_L^2$ there are no additional ultraviolet (UV) divergences in the matrix element of $T_{(0,0)}$ beyond the renormalization of $O_2^{(0)}(\mu)$, indicating that the phase space integral in SCET is UV finite at $O(\alpha_s)$. Similarly, one-loop matrix elements at NLP will also be found to be UV finite. Additional UV divergences in matrix elements of the $T_{(i,j)}$'s would indicate phase space integrals which were sensitive to the UV scale q_L , in which case the RG running of the corresponding $T_{(i,j)}$ would not simply be given by the running of its constituent SCET operators, but would have additional contributions. It is possible that this could complicate the RG running of the $H_{(i,j)}$'s at higher orders in α_s , where the final state phase space can include multiple gluons with individually large \mathbf{k}_T which largely cancel to contribute at small q_T , but this would not affect the one-loop running or the form of the factorization Eq. (5.14).

Subtracting the counterterms yields the renormalized matrix element

$$\begin{aligned} \langle p_1^n p_2^{\bar{n}} | T_{(0,0)} \left(q^-, q^+, \mathbf{q}_T, \frac{\mu}{q_T}, \frac{\nu_{n,\bar{n}}}{\mu} \right) | p_1^n p_2^{\bar{n}} \rangle_{1\text{-gluon}} &= \bar{\alpha} \left[\left(\mathcal{L}_{0T} - \frac{\delta_T}{\epsilon} \right) \left(\delta_2 \left[\frac{1+z_1^2}{\bar{z}_1} \right]_+ + \delta_1 \left[\frac{1+z_2^2}{\bar{z}_2} \right]_+ \right) \right. \\ &\quad - \delta_1 \delta_2 \left[2\mathcal{L}_{1T} + \mathcal{L}_{0T} \left(3 - 2 \log \frac{\nu_n \nu_{\bar{n}}}{\mu^2} \right) \right] \\ &\quad \left. + (\bar{z}_1 \delta_2 + \bar{z}_2 \delta_1 - \delta_1 \delta_2 \zeta_2) \delta_T \right], \end{aligned} \quad (5.66)$$

which, with the replacement $\nu_n \nu_{\bar{n}} = \nu^2$, also reproduces the result in [175].

Next-to-Leading Power Example: $T_{(24,0)}$

Since $O(\Lambda_{\text{QCD}})$ contributions are not considered, there is no 0-gluon contribution to the matrix element of $T_{(24,0)}$, and there is also no \bar{n} -sector contribution at $O(\alpha_s)$. Thus at first non-trivial order the graphs $T_{(24,0)}$ are those shown in Fig. 5.1, yielding

$$\begin{aligned} \mathcal{M}_{(24,0)}^n &= 2\pi g^2 C_F q^+ q^- \int \frac{d^d k}{(2\pi)^d} w_n^2 \left(\frac{q_L^2}{\nu_n^2} \frac{q^- k^+}{q^+ k^-} \right)^{\eta_n/2} k^+ \delta(k^2) \delta(p_1^- - q^- - k^-) \delta'(p_2^+ - q^+) \delta^{d-2}(\mathbf{q}_T + \mathbf{k}_T) \\ &\quad \times \text{Tr} \left[\frac{\not{p}_2}{2} \left(\frac{2p_1^\alpha - \gamma^\alpha \not{k}}{-2p_1 \cdot k} + \frac{\bar{n}^\alpha}{k^-} \right) \frac{\not{k}}{2} \left(\frac{2p_{1\alpha} - \not{k} \gamma_\alpha}{-2p_1 \cdot k} - \frac{\bar{n}_\alpha}{-k^-} \right) \right] \text{Tr} \left[\frac{\not{p}_2}{2} \frac{\not{k}}{2} \right] \\ &= -\frac{\bar{\alpha}}{\pi} f_\epsilon z_1 z_2 w_n^2 \delta'_2 \left(\frac{z_1 q_T}{\nu_n} \right)^{\eta_n} \frac{(2 - 2\bar{z}_1 + (1 - \epsilon)\bar{z}_1^2)}{\bar{z}_1^{2+\eta_n}}. \end{aligned} \quad (5.67)$$

Here, we use the scalar distributional identity

$$\frac{\theta(\bar{z}_1)}{\bar{z}_1^{2+\eta}} = \frac{\delta'(\bar{z}_1)}{\eta} - \delta(\bar{z}_1) + \left[\frac{\theta(\bar{z}_1)}{\bar{z}_1} \right]_{++} + \dots \quad (5.68)$$

where the double-plus distribution [76] is defined in Appendix 5.B. We also use the usual expansion

$$\frac{(\mu^2)^{-\eta/2}}{(q_T^2)^{-\eta/2}} = 1 - \frac{\eta}{2} \log \frac{\mu^2}{q_T^2} + \dots \quad (5.69)$$

Eq. (5.67) is finite as $\epsilon \rightarrow 0$. Expanding in η_n , we find the bare matrix element of $T_{(24,0)}$

$$\mathcal{M}_{(24,0)}^n = \frac{\bar{\alpha}}{\pi} z_1 z_2 \delta'_2 \left((\delta_1 + \delta'_1) \left(-\frac{2w_n^2}{\eta_n} + \log \frac{\nu_n^2}{q_T^2} \right) - 2 \left[\frac{\theta(\bar{z}_1)}{\bar{z}_1} \right]_{++} + 2 \left[\frac{1}{\bar{z}_1} \right]_+ - 1 \right). \quad (5.70)$$

The $1/\eta_n$ rapidity divergence in (5.70) is similar in form to that found in the study of NLP jet and soft functions in [91, 119, 123, 222]. The divergence is independent of \mathbf{q}_T and may be absorbed through mixing of $T_{(24,0)}$ with the leading-power operator $T_{(0,0)}$, as in Eq. (5.47), with

$$Z_{(24,0),(0,0)}(\omega_1, \omega_2, \mathbf{q}_T) = -2 \frac{\bar{\alpha}}{\pi} \frac{w_n^2}{\eta_n} \omega_1 \omega_2 (\delta(\bar{\omega}_1) + \delta'(\bar{\omega}_1)) \delta'(\bar{\omega}_2). \quad (5.71)$$

This rapidity renormalization factor is suppressed by one power of q_T^2 relative to the leading term $Z_{(0,0),(0,0)}$ in (5.65) since it does not contain a factor of $\delta(q_T^2)$, and so the mixing is consistent with power

counting. Equivalently, the divergence may be absorbed by $O(1)$ mixing with the NLP operator

$$\int d^{d-2} \mathbf{p}_T T_{(0,0)}(q^-, q^+, \mathbf{p}_T). \quad (5.72)$$

This is similar to the cumulant operators introduced in [91, 119, 123, 222] except that Eq. (5.72) has no upper cutoff $|p_T| < \Lambda$ on the integral.

Next-to-Leading Power Example: $T_{(0,2_3)}$

$T_{(0,2_3)}$ provides an example of a matrix element with nontrivial u dependence. Calculating its spin-averaged matrix element, the only contribution comes from an \bar{n} -sector gluon and we find

$$\begin{aligned} \mathcal{M}_{(0,2_3)}^{\bar{n}} = & -2\pi g^2 C_F \int \frac{d^d k}{(2\pi)^d} w_{\bar{n}}^2 \left(\frac{q_L^2}{\nu_{\bar{n}}^2} \frac{q^+ k^-}{q^- k^+} \right)^{\eta_{\bar{n}}/2} \delta(k^2) \delta(p_1^- - q^- - k^-) \delta(p_2^+ - q^+) \delta^{d-2}(\mathbf{q}_T + \mathbf{k}_T) \\ & \times \text{Tr} \left[\frac{\not{p}_2 \not{q}}{2} \right] \text{Tr} \left[\frac{1}{u} \bar{v}(p_2) \left(\frac{2p_{2\alpha} - \gamma_\alpha \not{k}}{-2p_2 \cdot k} - \frac{\bar{n}_\alpha}{-k^-} \right) \frac{\not{q}}{2} \gamma_\nu^\perp \gamma_\mu^\perp \Delta^{\alpha\mu}(k) k^\nu v(p_2) \delta \left(u + \frac{k^+}{q^+} \right) \right]. \end{aligned} \quad (5.73)$$

After using $\delta(u + k^+/q^+)/u = -q^+ \delta(u + k^+/q^+)/k^+$ and integrating over the gluon's phase space, the bare matrix element is

$$\mathcal{M}_{(0,2_3)}^{\bar{n}} = -\frac{\bar{\alpha}}{\pi} f_\epsilon w_{\bar{n}}^2 z_1 z_2 \left(\frac{z_2 q_T}{\nu_{\bar{n}}} \right)^{\eta_{\bar{n}}} \frac{1}{\bar{z}_2^{2-\eta_{\bar{n}}}} \delta_1 \delta \left(u + \frac{\bar{z}_2}{z_2} \right). \quad (5.74)$$

Using distributional identities to extract the pole structure of Eq. (5.74), we expand to find

$$\mathcal{M}_{(0,2_3)}^{\bar{n}} = -\frac{\bar{\alpha}}{\pi} z_1 z_2 \delta_1 \left(\delta'_2 \left(\frac{w_{\bar{n}}^2}{\eta_{\bar{n}}} - \frac{1}{2} \log \frac{\nu_{\bar{n}}^2}{q_T^2} \right) + \left[\frac{\theta(\bar{z}_2)}{\bar{z}_2^2} \right]_{++} \right) \delta \left(u + \frac{\bar{z}_2}{z_2} \right). \quad (5.75)$$

where the rapidity divergence is absorbed by Eq. (5.47) with the renormalization constant

$$Z_{(0,2_3),(0,0)}(\omega_1, \omega_2, \mathbf{q}_T, u) = -\bar{\alpha} \tilde{\theta}(q_T^2) \frac{w_{\bar{n}}^2}{\eta_{\bar{n}}} \omega_1 \omega_2 \delta(\bar{\omega}_1) \delta'(\bar{\omega}_2) \delta \left(u + \frac{\bar{\omega}_2}{\omega_2} \right). \quad (5.76)$$

Note that if the operator definition of $O_2^{(2B_1)}(x, \hat{t})$ had not included the $\theta(\hat{t})$ convolution discussed in Section 5.2.1, then its u -space matching coefficient would instead be $C_2^{(2B_1)} = 1/u$, and the corresponding expression in (5.74) would contain only delta functions and single plus distributions in \bar{z}_2 ,

$$\mathcal{M} \sim \frac{1}{\bar{z}_2^{1-\eta_{\bar{n}}}} \delta \left(u + \frac{\bar{z}_2}{z_2} \right) = \left(\frac{\delta(\bar{z}_2)}{\eta_{\bar{n}}} + \left[\frac{\theta(\bar{z}_2)}{\bar{z}_2^2} \right]_+ + O(\eta_{\bar{n}}) \right) \delta \left(u + \frac{\bar{z}_2}{z_2} \right). \quad (5.77)$$

Multiplying this by the Wilson coefficient $\sim 1/u$ and integrating over u would then give an unregulated divergence at $\bar{z}_2 = 0$. Instead, keeping the singular $1/u$ dependence in the matrix element of the operator gives the properly regulated result in Eq. (5.75) and Eq. (5.76) in terms of δ' and double-plus distributions.

Finally, we can also demonstrate here that the δ -regulator does not regulate all rapidity divergences at NLP. Replacing the previous pure rapidity regulator in Eqs. (5.73) and (5.74) with the δ -regulator,

the same expressions read

$$\begin{aligned}
\mathcal{M}_{(0,2_3)}^{\bar{n}\delta} &= -2\pi g^2 C_F \int \frac{d^d k}{(2\pi)^d} \text{Tr} \left[\frac{\not{p}_2}{2} \frac{\not{k}}{2} \right] \delta \left(u + \frac{k^+}{q^+} \right) \delta(k^2) \delta(p_1^- - q^- - k^-) \delta(p_2^+ - q^+) \delta^{d-2}(\mathbf{q}_T + \mathbf{k}_T) \\
&\quad \times \text{Tr} \left[\frac{1}{u} \bar{v}(p_2) \left(\frac{2p_{2\alpha} - \gamma_\alpha \not{k}}{-2p_2 \cdot k} - \frac{\bar{n}_\alpha}{-k^- - \delta_{\bar{n}}} \right) \frac{\not{k}}{2} \gamma_\nu^\perp \gamma_\mu^\perp \left(g^{\alpha\mu} - \frac{n^\alpha k^\mu}{k^+ + \delta_{\bar{n}}} \right) k^\nu v(p_2) \right] \\
&= -\frac{\bar{\alpha}}{\pi} f_\epsilon w_{\bar{n}}^2 z_1 z_2 \frac{1}{\bar{z}_2(\bar{z}_2 + \delta_{\bar{n}}/p_2^+)} \delta_1 \delta \left(u + \frac{\bar{z}_2}{z_2} \right)
\end{aligned} \tag{5.78}$$

which contains an uncontrolled rapidity divergence when integrated over \bar{z}_2 . Since the unregulated divergence does not originate from a Wilson line propagator, any regulator which only modifies the definition of a Wilson line, such as the η -regulator of [80], will suffer from similar problems.

One Loop Results

As shown in previous examples, matrix elements of the $T_{(i,j)}$'s are rapidity divergent and require subtractions via rapidity counterterms proportional to the leading order operator $T_{(0,0)}$. The renormalization constants for the rest of the subleading $T_{(i,j)}$'s are found to be

$$\begin{aligned}
Z_{(2_1,0),(0,0)}(\omega_1, \omega_2, \mathbf{q}_T, u) &= \frac{\bar{\alpha}}{\pi} \frac{w_n^2}{\eta_n} \delta(\bar{\omega}_1) \delta(\bar{\omega}_2) \delta(u), \\
Z_{(0,2_1),(0,0)}(\omega_1, \omega_2, \mathbf{q}_T, u) &= \frac{\bar{\alpha}}{\pi} \frac{w_{\bar{n}}^2}{\eta_{\bar{n}}} \delta(\bar{\omega}_1) \delta(\bar{\omega}_2) \delta(u),
\end{aligned} \tag{5.79}$$

and

$$\begin{aligned}
Z_{(2_2,0),(0,0)}(\omega_1, \omega_2, \mathbf{q}_T, u_1, u_2) &= -\frac{\bar{\alpha}}{\pi} \frac{w_n^2}{\eta_n} \delta(\bar{\omega}_1) \delta(\bar{\omega}_2) \delta(u_1) \delta(u_2), \\
Z_{(0,2_2),(0,0)}(\omega_1, \omega_2, \mathbf{q}_T, u_1, u_2) &= -\frac{\bar{\alpha}}{\pi} \frac{w_{\bar{n}}^2}{\eta_{\bar{n}}} \delta(\bar{\omega}_1) \delta(\bar{\omega}_2) \delta(u_1) \delta(u_2),
\end{aligned} \tag{5.80}$$

for the operators $T_{(2_1,0)}$ through $T_{(0,2_2)}$, and

$$\begin{aligned}
Z_{(2_3,0),(0,0)}(\omega_1, \omega_2, \mathbf{q}_T, u) &= -\frac{\bar{\alpha}}{\pi} \frac{w_n^2}{\eta_n} \omega_1 \omega_2 \delta'(\bar{\omega}_1) \delta(\bar{\omega}_2) \delta \left(u + \frac{\bar{\omega}_1}{\omega_1} \right), \\
Z_{(0,2_3),(0,0)}(\omega_1, \omega_2, \mathbf{q}_T, u) &= -\frac{\bar{\alpha}}{\pi} \frac{w_{\bar{n}}^2}{\eta_{\bar{n}}} \omega_1 \omega_2 \delta(\bar{\omega}_1) \delta'(\bar{\omega}_2) \delta \left(u + \frac{\bar{\omega}_2}{\omega_2} \right), \\
Z_{(2_4,0),(0,0)}(\omega_1, \omega_2, \mathbf{q}_T) &= -2 \frac{\bar{\alpha}}{\pi} \frac{w_n^2}{\eta_n} \omega_1 \omega_2 (\delta(\bar{\omega}_1) + \delta'(\bar{\omega}_1)) \delta'(\bar{\omega}_2), \\
Z_{(0,2_4),(0,0)}(\omega_1, \omega_2, \mathbf{q}_T, u) &= -2 \frac{\bar{\alpha}}{\pi} \frac{w_{\bar{n}}^2}{\eta_{\bar{n}}} \omega_1 \omega_2 (\delta(\bar{\omega}_2) + \delta'(\bar{\omega}_2)) \delta'(\bar{\omega}_1),
\end{aligned} \tag{5.81}$$

for the remaining operators $T_{(2_3,0)}$ through $T_{(0,2_4)}$.

In contrast to the leading power operator, the matrix elements of the power suppressed operators $T_{(i,j)}$ are individually rapidity divergent even when setting $w_n = w_{\bar{n}} = 1$ and $\eta_n = -\eta_{\bar{n}}$. Nevertheless, these divergences cancel pairwise between $T_{(2_1,0)}$ and $T_{(0,2_1)}$, and $T_{(2_2,0)}$ and $T_{(0,2_2)}$. The divergences also cancel in the sum over the four operators in Eq. (5.81) when weighted and integrated against their appropriate prefactor $H_{(i,j)}(\{u\}) K_{(k,\ell)}^{(i,j)}$. The cancellation of rapidity divergences in the total rate reflects the rapidity-finiteness of the total NLP cross section in SCET and is a non-trivial check on the validity of the EFT expansion. In Section 5.3.2 we will show that this cancellation can be understood without

an explicit regulator, in which case the correct treatment of overlap subtraction graphs, which vanished here when using the pure rapidity regulator, is critical.

The hard-scale matching coefficients of all the subleading operators $T_{(i,j)}$ have the same LL anomalous dimensions [179], so these cancellations are manifestly maintained to all orders in the leading-log approximation. Since the rate must also be finite beyond leading logarithm, finiteness of the theory will place constraints on rapidity divergences, but these constraints are beyond the scope of this thesis.

As in Eq. (5.9), the $T_{(i,j)}$ operators are matched onto a theory solely consisting of light-cone distribution operators, defined as

$$\begin{aligned} O_q(\ell^-) &= \frac{1}{2\pi} \int d\xi e^{-i\xi\ell^-} \bar{\psi}_n(\bar{n}\xi) \frac{\not{q}}{2} W(\bar{n}\xi, 0) \psi_n(0), \\ O_{\bar{q}}(\ell^+) &= \frac{1}{2\pi} \int d\xi e^{-i\xi\ell^+} \bar{\psi}_{\bar{n}}(0) \frac{\not{q}}{2} W(0, n\xi) \psi_{\bar{n}}(n\xi). \end{aligned} \quad (5.82)$$

Since the renormalized partonic matrix element of the product of these soft theory operators is [78, 223]

$$\langle p_1^n p_2^{\bar{n}} | O_q(q^-) O_{\bar{q}}(q^+) | p_1^n p_2^{\bar{n}} \rangle = \left(\delta_1 - \frac{\bar{\alpha}}{\epsilon} \left[\frac{1+z_1^2}{\bar{z}_1} \right]_+ \right) \left(\delta_2 - \frac{\bar{\alpha}}{\epsilon} \left[\frac{1+z_2^2}{\bar{z}_2} \right]_+ \right) + \dots \quad (5.83)$$

and since these IR divergences are precisely reproduced in the renormalized matrix element of $T_{(0,0)}$ (see Eq. (5.63)), the leading-power soft matching coefficient is then

$$\begin{aligned} C_{S,(0,0)} \left(z_1, z_2, \mathbf{q}_T, \frac{\mu}{q_T}, \frac{\nu_n \nu_{\bar{n}}}{\mu} \right) &= \delta_1 \delta_2 \delta_T + \bar{\alpha} \left\{ -\delta_1 \delta_2 \left[2\mathcal{L}_{1T} + \mathcal{L}_{0T} \left(3 - 2 \log \frac{\nu_n \nu_{\bar{n}}}{\mu^2} \right) \right] \right. \\ &\quad \left. + \left(\delta_2 \left[\frac{1+z_1^2}{\bar{z}_1} \right]_+ + \delta_1 \left[\frac{1+z_2^2}{\bar{z}_2} \right]_+ \right) \mathcal{L}_{0T} + (\bar{z}_1 \delta_2 + \bar{z}_2 \delta_1 - \delta_1 \delta_2 \zeta_2) \delta_T \right\}. \end{aligned} \quad (5.84)$$

This also provides the fixed order expansion of $V_{(0,0),(0,0)}$,

$$V_{(0,0),(0,0)} \left(z_1, z_2, \mathbf{q}_T, \frac{\mu}{q_T}, \frac{q_L}{\nu_n \nu_{\bar{n}}} \right) = \delta_1 \delta_2 \delta_T + 2\bar{\alpha} \mathcal{L}_{0T} \log \frac{q_L^2}{\nu_n \nu_{\bar{n}}} + \dots, \quad (5.85)$$

where higher order terms can be generated using the running in Section 5.2.6.

At subleading power the renormalized matrix elements of $T_{(i,j)}$ begin at $\mathcal{O}(\alpha_s)$ and thus match onto the tree level term $\delta(\bar{z}_1)\delta(\bar{z}_2)$ of Eq. (5.83). The renormalized matrix elements of $T_{(i,j)}$ are thus equal to the soft matching coefficients $C_{S,(i,j)}$. Suppressing their scale dependence, the first four NLP soft

matching coefficients are

$$\begin{aligned}
C_{S,(2_1,0)}(z_1, z_2, \mathbf{q}_T) &= -\frac{\bar{\alpha}}{\pi} \delta_2 \left(\left[\frac{\theta(\bar{z}_1)}{\bar{z}_1} \right]_+ + \frac{1}{2} \delta_1 \log \frac{\nu_n^2}{q_T^2} \right) \delta \left(u + \frac{\bar{z}_1}{z_1} \right), \\
C_{S,(0,2_1)}(z_1, z_2, \mathbf{q}_T) &= -\frac{\bar{\alpha}}{\pi} \delta_1 \left(\left[\frac{\theta(\bar{z}_2)}{\bar{z}_2} \right]_+ + \frac{1}{2} \delta_2 \log \frac{\nu_{\bar{n}}^2}{q_T^2} \right) \delta \left(u + \frac{\bar{z}_2}{z_2} \right), \\
C_{S,(2_2,0)}(z_1, z_2, \mathbf{q}_T) &= \frac{\bar{\alpha}}{\pi} \delta_2 \left(\left[\frac{\theta(\bar{z}_1)}{\bar{z}_1} \right]_+ + \frac{1}{2} \delta_1 \log \frac{\nu_n^2}{q_T^2} \right) \delta \left(u_1 + \frac{\bar{z}_1}{z_1} \right) \delta(u_1 - u_2), \\
C_{S,(0,2_2)}(z_1, z_2, \mathbf{q}_T) &= \frac{\bar{\alpha}}{\pi} \delta_1 \left(\left[\frac{\theta(\bar{z}_2)}{\bar{z}_2} \right]_+ + \frac{1}{2} \delta_2 \log \frac{\nu_{\bar{n}}^2}{q_T^2} \right) \delta \left(u_2 + \frac{\bar{z}_2}{z_2} \right) \delta(u_1 - u_2),
\end{aligned} \tag{5.86}$$

and the remaining four matching coefficients are

$$\begin{aligned}
C_{S,(2_3,0)}(z_1, z_2, \mathbf{q}_T) &= \frac{\bar{\alpha}}{\pi} z_1 z_2 \delta_2 \delta \left(u + \frac{\bar{z}_1}{z_1} \right) \left(\frac{1}{2} \delta'_1 \log \frac{\nu_n^2}{q_T^2} - \left[\frac{\theta(\bar{z}_1)}{\bar{z}_1^2} \right]_{++} \right), \\
C_{S,(0,2_3)}(z_1, z_2, \mathbf{q}_T) &= \frac{\bar{\alpha}}{\pi} z_1 z_2 \delta_1 \delta \left(u + \frac{\bar{z}_2}{z_2} \right) \left(\frac{1}{2} \delta'_2 \log \frac{\nu_{\bar{n}}^2}{q_T^2} - \left[\frac{\theta(\bar{z}_2)}{\bar{z}_2^2} \right]_{++} \right), \\
C_{S,(2_4,0)}(z_1, z_2, \mathbf{q}_T) &= \frac{\bar{\alpha}}{\pi} z_1 z_2 \delta'_2 \left((\delta(\bar{z}_1) + \delta'(\bar{z}_1)) \log \frac{\nu_n^2}{q_T^2} - 2 \left[\frac{\theta(\bar{z}_1)}{\bar{z}_1^2} \right]_{++} + 2 \left[\frac{\theta(\bar{z}_1)}{\bar{z}_1} \right]_+ - 1 \right), \\
C_{S,(0,2_4)}(z_1, z_2, \mathbf{q}_T) &= \frac{\bar{\alpha}}{\pi} z_1 z_2 \delta'_1 \left((\delta(\bar{z}_2) + \delta'(\bar{z}_2)) \log \frac{\nu_{\bar{n}}^2}{q_T^2} - 2 \left[\frac{\theta(\bar{z}_2)}{\bar{z}_2^2} \right]_{++} + 2 \left[\frac{\theta(\bar{z}_2)}{\bar{z}_1} \right]_+ - 1 \right).
\end{aligned} \tag{5.87}$$

Matching QCD onto SCET at $\mu = q_L$ and $\nu_{n,\bar{n}} = q_L$, these matrix elements have large logarithms of q_L^2/q_T^2 . We will discuss the resummation of these logarithms using the rapidity renormalization group in Section 5.2.6.

5.2.5 $C_{f\bar{f}}$ at Fixed Order

It is useful at this stage to check the fixed order results for $C_{f\bar{f}}$ by comparing with the corresponding QCD calculation. At leading power, the $O(\alpha_s)$ expression for $C_{f\bar{f}}^{(0)}$ in SCET is given by $C_{S(0,0)}$ in Eq. (5.84) with $\nu_{n,\bar{n}} = q_L$ and multiplied by the hard function $H_{(0,0)} = C_2^{(0)\dagger} C_2^{(0)}$. After integrating $d\Omega_T$, this gives the one-loop expression

$$\begin{aligned}
C_{f\bar{f}}^{(0)}(z_1, z_2, q_L^2, q_T^2) &= \bar{\alpha} \left\{ \delta_1 \delta_2 \delta(q_T^2) \left(-\log^2 \frac{q_L^2}{\mu^2} + 3 \log \frac{q_L^2}{\mu^2} - 8 + 7\zeta_2 \right) \right. \\
&\quad + \left[\frac{1}{q_T^2} \right]_+^{\mu^2} \left(\delta_1 \left[\frac{1+z_2^2}{\bar{z}_2} \right]_+ + \delta_2 \left[\frac{1+z_1^2}{\bar{z}_1} \right]_+ \right) \\
&\quad - \delta_1 \delta_2 \left[2 \left[\frac{\log \frac{q_T^2}{\mu^2}}{q_T^2} \right]_+^{\mu^2} + \left[\frac{1}{q_T^2} \right]_+^{\mu^2} \left(3 - 2 \log \frac{q_L^2}{\mu^2} \right) \right] \\
&\quad \left. + \delta(q_T^2) (\bar{z}_1 \delta_2 + \bar{z}_2 \delta_1 - \zeta_2 \delta_1 \delta_2) \right\}.
\end{aligned} \tag{5.88}$$

At NLP, adding up the contributions from the unsummed matching coefficients in Eq. (5.86) and Eq. (5.87) with $\nu_{n,\bar{n}} = q_L$ weighted by the corresponding coefficients $H_{(i,j)} K_{(k,\ell)}^{(i,j)}$, gives the $O(\alpha_s)$ coefficient function

$$\begin{aligned} C_{f\bar{f}}^{(2)}(z_1, z_2, \mathbf{q}_T) = & \bar{\alpha} z_1 z_2 \left[\left(2 \log \frac{\hat{s}}{q_T^2} - 3 \right) \delta'_1 \delta'_2 + \left(2 \log \frac{\hat{s}}{q_T^2} + 1 \right) (\delta'_1 \delta_2 + \delta_1 \delta'_2) + 4 \delta_1 \delta_2 \right. \\ & - \delta'_1 \left[\frac{2 - 2\bar{z}_2 + \bar{z}_2^2}{\bar{z}_2^2} \right]_{++} - \delta'_2 \left[\frac{2 - 2\bar{z}_1 + \bar{z}_1^2}{\bar{z}_1^2} \right]_{++} \\ & \left. - 2 \left(\delta_1 \left[\frac{1}{\bar{z}_2^2} \right]_{++} + \delta_2 \left[\frac{1}{\bar{z}_1^2} \right]_{++} \right) \right], \end{aligned} \quad (5.89)$$

where, along with $q_L^2 = z_1 z_2 \hat{s}$, we have used the identities

$$\begin{aligned} \left[\frac{\theta(\bar{z})}{\bar{z}} \right]_{++} &= \left[\frac{\theta(\bar{z})}{\bar{z}} \right]_+ + \delta'(\bar{z}), \\ [\theta(\bar{z})]_{++} &= 1 + \frac{1}{2} \delta'(\bar{z}) - \delta(\bar{z}). \end{aligned} \quad (5.90)$$

These results may be compared with the direct QCD calculation. $C_{f\bar{f}}$ is determined in QCD by the partonic rate

$$\begin{aligned} \mathcal{R}_{\text{QCD}} &= - \int \frac{d^d x}{(2\pi)^d} \langle p_1 p_2 | \bar{\psi}(x) \gamma^\mu \psi(x) \bar{\psi}(0) \gamma_\mu \psi(0) | p_1 p_2 \rangle \\ &= \frac{1}{2} \int \frac{d^d x}{(2\pi)^d} \langle p_1 p_2 | \bar{\psi}(x) \gamma^\mu \psi(0) \bar{\psi}(0) \gamma_\mu \psi(x) | p_1 p_2 \rangle. \end{aligned} \quad (5.91)$$

The single gluon real emission contribution evaluates to

$$\mathcal{R}_{\text{QCD}}^{1g} = \frac{\bar{\alpha}}{\pi} f_\epsilon \frac{\delta(\bar{z}_1 \bar{z}_2 \hat{s} - \mathbf{q}_T^2)}{\bar{z}_1 \bar{z}_2} [2 - 2(\bar{z}_1 + \bar{z}_2) + (\bar{z}_1^2 + \bar{z}_2^2) - \epsilon(\bar{z}_1 + \bar{z}_2)^2]. \quad (5.92)$$

Expanding (5.92) in powers of q_T^2/q_L^2 ,

$$\mathcal{R}_{\text{QCD}}^{1g} = \mathcal{R}_{\text{QCD}}^{(0)1g} + \mathcal{R}_{\text{QCD}}^{(2)1g} + \dots, \quad (5.93)$$

is straightforward away from $\bar{z}_1 = \bar{z}_2 = 0$

$$\mathcal{R}_{\text{QCD}}^{1g} \Big|_{\bar{z}_1 \neq 0} = \frac{\bar{\alpha}}{\pi} \frac{f_\epsilon}{\mathbf{q}_T^2} \left[\delta(\bar{z}_2) \left(\frac{2 - 2\bar{z}_1 + \bar{z}_1^2}{\bar{z}_1} \right) - 2 \frac{q_T^2}{\hat{s}} \delta_2 \left(\frac{1}{\bar{z}_1^2} \right) - \frac{q_T^2}{\hat{s}} \delta'_2 \left(\frac{2 - 2\bar{z}_1 + \bar{z}_1^2}{\bar{z}_1^2} \right) + O\left(\frac{q_T^4}{\hat{s}^2}\right) \right] \quad (5.94)$$

(with a similar result for $\bar{z}_2 \neq 0$), but care is required at the singular points. At leading power, \mathcal{R} may be written

$$\mathcal{R}_{\text{QCD}}^{(0)1g} = \frac{\bar{\alpha}}{\pi} \frac{f_\epsilon}{\mathbf{q}_T^2} \left(A^{(0)} \delta_1 \delta_2 + \delta_2 [f_n(\bar{z}_1)]_+ + \delta_1 [f_{\bar{n}}(\bar{z}_2)]_+ \right). \quad (5.95)$$

where, from (5.94),

$$f_{n,\bar{n}}(\bar{z}) = \left(\frac{2 - 2\bar{z} + \bar{z}^2}{\bar{z}} \right) \quad (5.96)$$

and $A^{(0)}$ is determined from the integrated rate

$$A = \frac{q_T^2}{\frac{\bar{\alpha}}{\pi} f_\epsilon} \int_0^1 d\bar{z}_1 d\bar{z}_2 \mathcal{R}_{\text{QCD}}^{1g} = A^{(0)} + \frac{q_T^2}{\hat{s}} A^{(2)} + \dots \quad (5.97)$$

Similarly at NLP the rate has the general form

$$\begin{aligned} \mathcal{R}_{\text{QCD}}^{(2)1g} = & \frac{\bar{\alpha}}{\pi} \frac{f_\epsilon}{\hat{s}} \left(A^{(2)} \delta_1 \delta_2 + B^{(2)} \delta'_1 \delta'_2 + C^{(2)} (\delta'_1 \delta_2 + \delta_1 \delta'_2) \right. \\ & \left. + \delta'_2 [g_n(\bar{z}_1)]_{++} + \delta_2 [h_n(\bar{z}_1)]_{++} + \delta'_1 [g_{\bar{n}}(\bar{z}_2)]_{++} + \delta_1 [h_{\bar{n}}(\bar{z}_2)]_{++} \right), \end{aligned} \quad (5.98)$$

where

$$\begin{aligned} g_{n,\bar{n}}(\bar{z}) &= - \left(\frac{2 - 2\bar{z} + \bar{z}^2}{\bar{z}^2} \right) \\ h_{n,\bar{n}}(\bar{z}) &= -2 \left(\frac{1}{\bar{z}^2} \right) \end{aligned} \quad (5.99)$$

and the constants B and C are given by the appropriate moments of the rate,

$$\begin{aligned} B &= \frac{q_T^2}{\frac{\bar{\alpha}}{\pi} f_\epsilon} \int_0^1 d\bar{z}_1 d\bar{z}_2 \bar{z}_1 \bar{z}_2 \mathcal{R}_{\text{QCD}}^{1g} = B^{(0)} + \frac{q_T^2}{\hat{s}} B^{(2)} + \dots \\ C &= - \frac{q_T^2}{\frac{\bar{\alpha}}{\pi} f_\epsilon} \int_0^1 d\bar{z}_1 d\bar{z}_2 \bar{z}_1 \mathcal{R}_{\text{QCD}}^{1g} \\ &= - \frac{q_T^2}{\frac{\bar{\alpha}}{\pi} f_\epsilon} \int_0^1 d\bar{z}_1 d\bar{z}_2 \bar{z}_2 \mathcal{R}_{\text{QCD}}^{1g} = C^{(0)} + \frac{q_T^2}{\hat{s}} C^{(2)} + \dots \end{aligned} \quad (5.100)$$

The integrals in Eqs. (5.97) and (5.100) give the endpoint constants

$$\begin{aligned} A^{(0)} &= 2 \log \frac{\hat{s}}{q_T^2} - 3 - \epsilon, \\ A^{(2)} &= 4, \\ B^{(2)} &= 2 \log \frac{\hat{s}}{q_T^2} - 3, \\ C^{(2)} &= 2 \log \frac{\hat{s}}{q_T^2} + 1, \end{aligned} \quad (5.101)$$

where we drop the ϵ -dependence in the NLP terms since, unlike the LP rate, the NLP rate contains no infrared divergences stemming from a $1/q_T^2$ prefactor.

At leading power, applying (5.185) and (5.186) gives

$$\begin{aligned} \mathcal{R}_{\text{QCD}}^{(0)1g} &= \frac{\bar{\alpha}}{\pi} \frac{f_\epsilon}{\mathbf{q}_T^2} \left\{ \left(2 \log \frac{\hat{s}}{q_T^2} - 3 - \epsilon \right) \delta_1 \delta_2 + \delta_2 \left[\frac{2 - 2\bar{z}_1 + \bar{z}_1^2}{\bar{z}_1} \right]_+ + \delta_1 \left[\frac{2 - 2\bar{z}_2 + \bar{z}_2^2}{\bar{z}_1} \right]_+ \right\} \\ &= \bar{\alpha} \left[\delta_1 \delta_2 \delta_T \left(\frac{2}{\epsilon^2} + \frac{3 - 2 \log \frac{\hat{s}}{\mu^2}}{\epsilon} \right) + \left(\mathcal{L}_{0T} - \frac{\delta_T}{\epsilon} \right) \left(\delta_2 \left[\frac{1 + z_1^2}{\bar{z}_1} \right]_+ + \delta_1 \left[\frac{1 + z_2^2}{\bar{z}_2} \right]_+ \right) \right. \\ &\quad \left. - \delta_1 \delta_2 \left[2\mathcal{L}_{1T} + \mathcal{L}_{0T} \left(3 - 2 \log \frac{\hat{s}}{\mu^2} \right) \right] + (\bar{z}_1 \delta_2 + \bar{z}_2 \delta_1 - \delta_1 \delta_2 \zeta_2) \delta_T \right]. \end{aligned} \quad (5.102)$$

The LP vertex correction gives an additional contribution

$$\mathcal{R}_{\text{QCD}}^{(0)\text{virt}} = \bar{\alpha} \delta_1 \delta_2 \delta_T \left[- \left(\frac{2}{\epsilon^2} + \frac{3 - 2 \log \frac{\hat{s}}{\mu^2}}{\epsilon} \right) - \log^2 \frac{q_L^2}{\mu^2} + 3 \log \frac{q_L^2}{\mu^2} - 8 + 7\zeta_2 \right]. \quad (5.103)$$

Combining the finite pieces of Eq. (5.103) and Eq. (5.102) then integrating $d\Omega_T$ reproduces the SCET result for $C_{f\bar{f}}^{(0)}$ in (5.88). The remaining divergent terms are equal to the infrared divergences of the light-cone distribution operator matrix elements and thus cancel in the matching onto the soft theory.

QCD virtual corrections do not contribute to the NLP coefficient function at $O(\alpha_s)$, and so $C_{f\bar{f}}^{(2)}$ is determined from Eqs. (5.98)–(5.101). After integrating $d\Omega_T$, this gives

$$\begin{aligned} C_{f\bar{f}}^{(2)}(z_1, z_2, q_L^2, q_T^2) = & \bar{\alpha} z_1 z_2 \left[4\delta_1 \delta_2 + \left(2 \log \frac{\hat{s}}{q_T^2} - 3 \right) \delta'_1 \delta'_2 + \left(2 \log \frac{\hat{s}}{q_T^2} + 1 \right) (\delta'_1 \delta_2 + \delta_1 \delta'_2) \right. \\ & - \left(\delta'_1 \left[\frac{2 - 2\bar{z}_2 + \bar{z}_2^2}{\bar{z}_2^2} \right]_{++} + \delta'_2 \left[\frac{2 - 2\bar{z}_1 + \bar{z}_1^2}{\bar{z}_1^2} \right]_{++} \right) \\ & \left. - 2 \left(\delta_1 \left[\frac{1}{\bar{z}_2^2} \right]_{++} + \delta_2 \left[\frac{1}{\bar{z}_1^2} \right]_{++} \right) \right], \end{aligned} \quad (5.104)$$

in agreement with the SCET result in Eq. (5.89). Thus, the SCET result and the expanded QCD result agree to NLP, as required.

Our fixed order results may also be compared with those obtained in [76].⁴ In that reference, the DY rate was determined up to NLP by expanding the QCD matrix element in the n -collinear, \bar{n} -collinear and soft limits, regulating the ensuing rapidity divergences, and combining the results. The results in that reference are also in agreement with the expanded QCD results in this section, but are presented in different variables which makes the comparison more involved. We have checked that our results are in agreement with theirs; details of this comparison are given in Appendix 5.C.

5.2.6 Rapidity Running

Rapidity logarithms arise in this formalism as a scheme dependence in summing together the individually divergent contributions from the n - and \bar{n} -sectors to a given matrix element. It was argued in [175] that in this formalism rapidity renormalization should be performed at the matching scale onto the light-cone distribution operators in order to ensure that Wilson coefficients in SCET are independent of infrared physics.

As discussed in [175], the rapidity regulators in the two sectors are fixed by matching at the hard scale from QCD onto SCET by the requirement that when $\mu \gg \mu_S$ the Wilson coefficients of SCET are independent of infrared energy scales of order μ_S . In the rapidity regularization scheme used here, this corresponds to choosing $\nu_n \nu_{\bar{n}} = q_L^2$, which, as discussed in Section 5.2.4, corresponds to using the same rapidity regulator in the n - and \bar{n} -sectors, and is required for the rapidity divergences to cancel in the EFT. The necessity of this choice can be seen from the q_T -dependence of the leading-power matrix element of Eq. (5.66), which contains the term

$$\langle p_1^n p_2^{\bar{n}} | T_{(0,0)}(q^-, q^+, \mathbf{q}_T, \nu_n, \bar{n}) | p_1^n p_2^{\bar{n}} \rangle_{1-\text{gluon}} = 2\bar{\alpha} \delta_1 \delta_2 \mathcal{L}_{0T} \log \frac{\nu_n \nu_{\bar{n}}}{\mu^2} + \dots . \quad (5.105)$$

⁴Similar results, integrated over rapidity, were presented in [75].

Since physical quantities are independent of the rapidity regulator, any variation in $\nu_n \nu_{\bar{n}}$ in the matrix element of $T_{(0,0)}$ must be compensated by a Wilson coefficient proportional to \mathcal{L}_{0T} in the EFT. This variation would then introduce non-analytic dependence on the IR scale q_T into the effective Lagrangian through the Wilson coefficient, which is inconsistent with factorization of hard and soft scales.

However, at the soft scale $\mu \sim q_T$ where SCET operators are matched onto light-cone distribution operators, the scale q_T is no longer an infrared scale in the EFT, and the Wilson coefficients are free to have nonanalytic dependence on q_T . The operators $T_{(i,j)}$ may therefore be run in $\nu_{n,\bar{n}}$ to minimize rapidity logarithms in the matching coefficients C_S in Eqs. (5.84), (5.86), and (5.87). These operators obey the RRG equation

$$\frac{d}{d \log \nu_{n,\bar{n}}} T_{(i,j)}(q^-, q^+, \mathbf{q}_T, \nu_{n,\bar{n}}) = \sum_{k,\ell} \left(\gamma_{(i,j),(k,\ell)}^{n,\bar{n}} * T_{(k,\ell)} \right) (q^-, q^+, \mathbf{q}_T, \nu_{n,\bar{n}}) , \quad (5.106)$$

where $\gamma^{n,\bar{n}}$ is the rapidity anomalous dimension for each sector, and we define the convolution $*$ by

$$(f * g)(\lambda_1, \lambda_2, \mathbf{k}_T) \equiv \int \frac{d\omega_1}{\omega_1} \frac{d\omega_2}{\omega_2} d^{d-2} \mathbf{p}_T f(\omega_1, \omega_2, \mathbf{p}_T) g \left(\frac{\lambda_1}{\omega_1}, \frac{\lambda_2}{\omega_2}, \mathbf{k}_T - \mathbf{p}_T \right) . \quad (5.107)$$

The solution to Eq. (5.106) can be written in the form of Eq. (5.13),

$$T_{(i,j)}(q^-, q^+, \mathbf{q}_T, \nu_{n,\bar{n}} = q_L) = \sum_{k,\ell} \left(V_{(i,j),(k,\ell)}(q_L, \nu_{n,\bar{n}}) * T_{(k,\ell)}(\nu_{n,\bar{n}}) \right) (q^-, q^+, \mathbf{q}_T) . \quad (5.108)$$

The explicit form of this solution to the RRG in momentum space can be found using the techniques in [67].

From the counterterm definitions in Eq. (5.46) and Eq. (5.47) relating the bare and renormalized operators, and using the fact that the bare operators are independent of the parameters $\nu_{n,\bar{n}}$ (as guaranteed by the fictional coupling $w_{n,\bar{n}}$), the rapidity anomalous dimensions for the operators $T_{(i,j)}$ may be calculated in terms of the renormalization constants as

$$\gamma_{(i,j),(k,\ell)}^{n,\bar{n}} = - \sum_{\kappa,\lambda} Z_{(i,j),(\kappa,\lambda)}^{-1} * \frac{d}{d \log \nu_{n,\bar{n}}} Z_{(\kappa,\lambda),(k,\ell)} . \quad (5.109)$$

Here, the inverse counterterm satisfies the relation

$$\sum_{\kappa,\lambda} \left(Z_{(i,j),(\kappa,\lambda)}^{-1} * Z_{(\kappa,\lambda),(k,\ell)} \right) (\omega_1, \omega_2, \mathbf{q}_T) = \delta(\bar{\omega}_1) \delta(\bar{\omega}_2) \delta(\mathbf{q}_T) \delta_{ik} \delta_{j\ell} . \quad (5.110)$$

At leading power the rapidity anomalous dimension of $T_{(0,0)}$ is calculated from the renormalization constant in Eq. (5.65), which gives

$$\gamma_{(0,0),(0,0)}^n = \gamma_{(0,0),(0,0)}^{\bar{n}} = 2\bar{\alpha} \delta(\bar{\omega}_1) \delta(\bar{\omega}_2) \mathcal{L}_{0T} . \quad (5.111)$$

The leading-power operator $T_{(0,0)}$ thus obeys the RRG equation

$$\frac{d}{d \log \nu_{n,\bar{n}}} T_{(0,0)}(\omega_1, \omega_2, \mathbf{q}_T, \nu_{n,\bar{n}}) = 2\bar{\alpha} \int d^2 \mathbf{p}_T \mathcal{L}_{0T}(\mathbf{q}_T - \mathbf{p}_T, \mu) T_{(0,0)}(\omega_1, \omega_2, \mathbf{p}_T, \nu_{n,\bar{n}}) , \quad (5.112)$$

similar to the results in [175], and with all the complications of running and scale-setting of vector

distributions described in [67]. Symmetrically, this RRG equation begins in the scheme $\nu_{n,\bar{n}} = q_T$ where the logarithms of $T_{(0,0)}$ are minimized, and runs up to the scheme $\nu_{n,\bar{n}} = q_L$ which, as we have argued, reproduces the QCD result.

At subleading power, the rapidity mixing of each $T_{(i,j)}$ with the leading order $T_{(0,0)}$ may easily be read off from Eqs. (5.79)–(5.81):

$$\begin{aligned}
\gamma_{(2_1,0),(0,0)}^n &= \gamma_{(0,2_1),(0,0)}^{\bar{n}} = -\frac{\bar{\alpha}}{\pi} \delta(\bar{\omega}_1) \delta(\bar{\omega}_2) \delta(u) \\
\gamma_{(2_2,0),(0,0)}^n &= \gamma_{(0,2_2),(0,0)}^{\bar{n}} = \frac{\bar{\alpha}}{\pi} \delta(\bar{\omega}_1) \delta(\bar{\omega}_2) \delta(u_1) \delta(u_2), \\
\gamma_{(2_3,0),(0,0)}^n &= \frac{\bar{\alpha}}{\pi} \omega_1 \omega_2 \delta'(\bar{\omega}_1) \delta(\bar{\omega}_2) \delta\left(u + \frac{\bar{\omega}_1}{\omega_1}\right), \\
\gamma_{(0,2_3),(0,0)}^{\bar{n}} &= \frac{\bar{\alpha}}{\pi} \omega_1 \omega_2 \delta(\bar{\omega}_1) \delta'(\bar{\omega}_2) \delta\left(u + \frac{\bar{\omega}_2}{\omega_2}\right), \\
\gamma_{(2_4,0),(0,0)}^n &= 2 \frac{\bar{\alpha}}{\pi} \omega_1 \omega_2 \delta'(\bar{\omega}_1) (\delta(\bar{\omega}_2) + \delta'(\bar{\omega}_2)), \\
\gamma_{(0,2_4),(0,0)}^{\bar{n}} &= 2 \frac{\bar{\alpha}}{\pi} \omega_1 \omega_2 (\delta(\bar{\omega}_1) + \delta'(\bar{\omega}_1)) \delta'(\bar{\omega}_2).
\end{aligned} \tag{5.113}$$

As noted in [121], since each subleading $T_{(i,j)}$ only has a non-vanishing matrix element beginning at $O(\alpha_s)$, calculating the complete rapidity renormalization for each $T_{(i,j)}$ requires calculating matrix elements at $O(\alpha_s^2)$. There will be some constraints on these rapidity anomalous dimensions because of μ -independence of the final result [80], as discussed in this formalism in [175], but the full calculation is beyond the scope of this thesis and will be the subject of future work.

5.3 Overlap Subtractions at NLP

As discussed in [77, 175], in this formulation of SCET it is necessary to subtract the double-counting of low-energy degrees of freedom which are simultaneously below the cutoff of both the n - and \bar{n} -sectors, analogous to zero-bin subtraction in SCET [172]. Rapidity logarithms in this formulation of SCET arise from the scheme dependence in summing the individually rapidity divergent diagrams in each sector and subtracting the corresponding overlap.

In the previous sections we have used a rapidity renormalization scheme in which overlap subtraction graphs vanish; while this is convenient for calculations, it obscures the cancellations which occur between different operators in different regions of phase space which are required to obtain a rapidity-finite result. In this section we generalize the overlap subtraction prescription to NLP and repeat the calculations without a rapidity regulator in order to explicitly show the cancellation of rapidity divergences due to the overlap subtraction, similar to what was done at LP in [175].

At LP, the zero-bin prescription of [172] has been shown to be equivalent to the nonperturbative subtraction definition of dividing the naïve matrix element by a vacuum expectation value of Wilson lines [188–190]. This equivalence also holds for the overlap prescription of [77, 179]. At subleading power, however, this simple prescription does not hold: matrix elements of the NLP operators $T_{(i,j)}$ begin at $O(\alpha_s)$, and thus dividing by a vacuum expectation value of the form $(1 + O(\alpha_s))$ does not provide the necessary $O(\alpha_s)$ subtraction to regulate their matrix elements. Calculations of probabilities in the effective theory therefore require a systematic way to implement the necessary overlap subtraction. In this section we describe a simple diagram-based prescription to perform the overlap subtraction at

subleading powers, and illustrate in the case of DY at NLP that it is required to obtain the correct, finite, result. This allows us to extend the LP discussion of [175] on the relationship between scheme dependence and rapidity logarithms up to NLP. We show that the previous observation in Section 5.2.4 – that at NLP rapidity divergences do not cancel for matrix elements of individual operators, but instead cancel between distinct operators – occurs because different linear combinations of operators are required to reproduce the correct rate in different regions of phase space.

Consider, for example, the process in Fig. 5.1 in which a gluon is produced in DY annihilation in addition to the lepton pair. In SCET this corresponds to two distinct processes in which the gluon is emitted in the n -sector or the \bar{n} -sector. At NLP, the first receives contributions from the $T_{(2i,0)}$ operators while the second receives contributions from the corresponding $T_{(0,2i)}$ operators. Since in loop graphs all momenta are integrated over, the first class of operators will give non-vanishing spurious contributions in the momentum region described by the second, and vice versa. Thus, the overlap subtraction procedure at NLP necessarily involves cancellations between different operators, and the subtraction required in order to avoid overcounting in each is found by taking the wrong limit of matrix elements in the other sector. In the symmetric process that we are examining in this chapter, this may be achieved by subtracting one half of each of the wrong limits from each sector. Schematically, we have the prescription

$$P_{\text{SCET}} = P_n + P_{\bar{n}} - \frac{1}{2} (P_{n \rightarrow \bar{n}} + P_{\bar{n} \rightarrow n}), \quad (5.114)$$

where P_i is the probability to produce a gluon in the i -sector and the subscripts $i \rightarrow j$ denote the wrong sector limits.

The power counting of these subtractions follows the power counting of the limit in which the gluon is taken. An n -sector gluon has the scaling $k_n^-/q^- \sim O(1)$, $k_n^+/q^+ \sim O(q_T^2/q_L^2)$, while its wrong-sector limit has the scaling $k_{n \rightarrow \bar{n}}^-/q^- \sim O(q_T^2/q_L^2)$ and $k_{n \rightarrow \bar{n}}^+/q^+ \sim O(1)$. This definition of overlap subtraction ensures that probabilities in QCD are properly reproduced to the appropriate order by SCET in all regions of phase space. This prescription is inherently perturbative, and further work is required to determine an operator definition of overlap subtraction which correctly reproduces QCD probabilities both at leading and next-to-leading power.

In the next subsection we review the discussion of overlap subtraction at LP presented in [175] using the prescription (5.114). We then demonstrate that the same prescription may be used to calculate the NLP coefficient function $C_{f\bar{f}}^{(2)}$, and discuss the nature of the overlap subtraction in various regions of phase space.

5.3.1 Overlap Subtraction and Scheme Dependence at LP

The DY cross section at LP is determined by the spin-averaged matrix element of $T_{(0,0)}$, which takes the general form

$$\mathcal{M}_{(0,0)} = \frac{\bar{\alpha}}{\pi} \frac{f_\epsilon}{q_T^2} (A_{(0,0)} \delta_1 \delta_2 + \delta_2 [f_n(\bar{z}_1)]_+ + \delta_1 [f_{\bar{n}}(\bar{z}_2)]_+) \quad (5.115)$$

where as before we define $\delta_1 \equiv \delta(\bar{z}_1)$, $\delta_2 \equiv \delta(\bar{z}_2)$. Away from the singular point $\bar{z}_1 = \bar{z}_2 = 0$ the unregulated n - and \bar{n} -sector contributions to the matrix element of $T_{(0,0)}$ are determined by the graphs in Fig. 5.1 and their \bar{n} -sector equivalents, and are given by Eq. (5.54) (and the corresponding expression in the \bar{n} -sector) with $\omega_n = 1$ and $\eta_n = 0$. This immediately gives the functions $f_n(\bar{z}_1)$ and $f_{\bar{n}}(\bar{z}_2)$ in (5.96) which describe the spectrum away from the endpoint. Since each $f_{n,\bar{n}}$ only receives contributions

from a single sector, there is no overcounting, and these expressions are finite and well-defined without a rapidity regulator.

The constant $A_{(0,0)}$ may be most simply obtained by integrating the rate over \bar{z}_1 and \bar{z}_2 , which receives contributions from both sectors. Adding these contributions overcounts the probability of producing a gluon which lies below the cutoff of both sectors and so must be subtracted using the overlap prescription (5.114), given by taking the wrong limit of the matrix elements in each sector. These are given by Eq. (5.61) with the rapidity regulator set to unity,

$$\begin{aligned} \mathcal{M}_{(0,0)}^{n \rightarrow \bar{n}} &= -2\pi g^2 C_F \int \frac{d^d k}{(2\pi)^d} \delta(p_1^- - q^-) \delta(p_2^+ - q^+) \delta^{d-2}(\mathbf{q}_T + \mathbf{k}_T) \delta(k^2) \\ &\quad \times \text{Tr} \left[\frac{\not{p}_1}{2} \left(\frac{n^\alpha}{-k^+} + \frac{\bar{n}^\alpha}{k^-} \right) \frac{\not{k}}{2} \left(\frac{n_\alpha}{-k^+} - \frac{\bar{n}_\alpha}{k^-} \right) \right] \text{Tr} \left[\frac{\not{p}_2}{2} \frac{\not{k}}{2} \right] + \dots \end{aligned} \quad (5.116)$$

and the corresponding (and identical) wrong limit $\mathcal{M}_{(0,0)}^{\bar{n} \rightarrow n}$ of the \bar{n} matrix element. The dots indicate terms suppressed by powers of $1/q_L$ relative to leading power, which do not contribute at LP but which will be important at NLP. By integrating these graphs with respect to \bar{z}_1 and \bar{z}_2 before integrating over the gluon momentum the contributions to the endpoint constant $A_{(0,0)}$ from each sector and their wrong limit subtractions can be obtained. As discussed in [175], because the individual graphs each have rapidity divergences, the ordering of integration is important; the sum is defined here by performing the \bar{z}_1 , \bar{z}_2 , \mathbf{k}_T and k^+ integrals, leaving only a single rapidity-divergent k^- integral⁵

$$A_{(0,0)} = \int_0^\infty \frac{dk^-}{k^-} \left[\theta(p_1^- - k^-) A_{(0,0)}^n(k^-) + \theta\left(k^- - \frac{q_T^2}{p_2^+}\right) A_{(0,0)}^{\bar{n}}(k^-) - \frac{1}{2} \left(A_{(0,0)}^{n \rightarrow \bar{n}}(k^-) + A_{(0,0)}^{\bar{n} \rightarrow n}(k^-) \right) \right], \quad (5.117)$$

where

$$\begin{aligned} A_{(0,0)}^n(k^-) &= 2 - 2 \left(\frac{k^-}{p_1^-} \right) + (1 - \epsilon) \left(\frac{k^-}{p_1^-} \right)^2, \\ A_{(0,0)}^{\bar{n}}(k^-) &= 2 - 2 \left(\frac{q_T^2}{k^- p_2^+} \right) + (1 - \epsilon) \left(\frac{q_T^2}{k^- p_2^+} \right)^2, \\ A_{(0,0)}^{n \rightarrow \bar{n}}(k^-) &= A_{(0,0)}^{\bar{n} \rightarrow n}(k^-) = 2. \end{aligned} \quad (5.118)$$

Physically, regions of phase space where $k^- \sim O(q^-)$ are properly described in the EFT by n -sector gluons. Regions where $k^+ = k_T^2/k^- \sim O(q^+)$ give spurious contributions in the n -sector, producing the unphysical divergence in $A_{(0,0)}^n(k^-)$ as $k^- \rightarrow 0$. Similarly, the divergence in the \bar{n} -sector as $k^- \rightarrow \infty$ corresponds to the large k^- region which is not properly described by the \bar{n} -sector. Both of these spurious divergent contributions are canceled by the overlap terms, leaving the finite result

$$A_{(0,0)} = 2 \log \frac{\hat{s}}{q_T^2} - 3 - \epsilon. \quad (5.119)$$

This is the same endpoint constant we determined from QCD in (5.101), and so we find the same LP coefficient function $C_{f\bar{f}}^{(0)}$. Equivalently, in Eq. (5.118), the constant terms in $A_n^{(0,0)}$ and $A_{\bar{n}}^{(0,0)}$ are common to both sectors, and so the double-counting is removed by subtracting the overlap on the third line.

As discussed in [175], however, the \hat{s} dependence in $A_{(0,0)}$ is actually a scheme-dependence in the EFT, which allows rapidity divergences to be resummed in SCET. Since each integral represents the momentum of a distinct particle in each sector, the momentum in each integral can be independently

⁵This is equivalent to the prescription in [173] of adding the integrands together before performing any loop integrals.

rescaled, which changes the term in the rapidity logarithm. For example, rescaling $k^- \rightarrow k^- \zeta^2 / \hat{s}$ in the $A_{\bar{n}}$ integral of Eq. (5.118) gives the manifestly scheme-dependent result

$$A_{(0,0)}(\zeta) = 2 \log \frac{\zeta^2}{q_T^2} - 3 - \epsilon. \quad (5.120)$$

In the remainder of this section we will demonstrate a similar origin of rapidity logarithms at NLP.

5.3.2 Overlap Subtraction and Scheme Dependence at NLP

At NLP the overlap subtraction follows the same procedure as at LP, but here more terms are kept in the wrong limit expansion of each operator's matrix elements. The NLP cancellation of divergences is also slightly more involved, since rapidity divergences cancel between different operators, as may be seen in Eqs. (5.79)–(5.81). Similar cancellations between different operators in SCET were also discussed in detail in [89]. There, the endpoint divergences are regulated by explicit hard cutoffs, and expressed in a refactorized form that makes obvious the cancellation between different NLP operators contributing to the observable. Overcounting of hard regions arises from the convolutional structure of the operators with a hard cutoff and thus an “infinity-bin” prescription, distinct from the usual zero-bin prescription, is introduced to correct for this double counting. In this section we will show that the same overlap subtraction required to correct for overcounting in the soft region also properly regulates endpoint divergences. This uniform treatment of divergences is possible because all spurious terms have a common origin, arising from an overcounting of probabilities induced by wrong limit contributions in each individual sector.

The operator products $T_{(2_1,0)}$ through $T_{(0,2_2)}$ come from products of scattering operators $O_{2,(1_i)}^{\dagger\mu} O_{2,(1_j)}^\nu$ whose definitions pick out the longitudinal Lorentz structure $\bar{n}^\mu n^\nu$ or $\bar{n}^\nu n^\mu$, while the remaining operators $T_{(2_3,0)}$ through $T_{(0,2_4)}$, along with the leading order $T_{(0,0)}$, come from products of operators that are proportional to $g_\perp^{\mu\nu}$. It is therefore convenient to classify each $T_{(i,j)}$ according to its Lorentz structure, either as transverse or longitudinal. We consider these two classes of operators in turn.

Longitudinal Class

From Eqs. (5.79) and (5.80), matrix elements of $T_{(2_1,0)}$ and $T_{(0,2_1)}$ are individually rapidity divergent, but the divergences cancel in the sum (and hence in the cross section, since their Wilson coefficients are equal). The same is true for $T_{(2_2,0)}$ and $T_{(0,2_2)}$, and in both cases the cancellation may be understood by examining the unregulated diagrams and corresponding overlaps, as in the previous section.

Taking $T_{(2_1,0)}$ as an example, its unregulated spin-averaged matrix element is

$$\begin{aligned} \mathcal{M}_{(2_1,0)}^n &= -2\pi g^2 C_F \int \frac{d^d k}{(2\pi)^d} \delta(p_1^- - q^- - k^-) \delta(p_2^+ - q^+) \delta^{d-2}(\mathbf{q}_T + \mathbf{k}_T) \delta(k^2) \delta\left(u + \frac{k^-}{q^-}\right) \\ &\quad \times \text{Tr} \left[\frac{\not{p}_2}{2} \frac{\not{q}}{2} \right] \text{Tr} \left[\frac{\not{p}_1}{2} \left(\frac{2p_1^\alpha - \gamma^\alpha \not{k}}{-2p_1 \cdot k} + \frac{\bar{n}^\alpha}{k^-} \right) \frac{\not{q}}{2} \not{k}_\perp \gamma_\mu^\perp \bar{\Delta}^{\alpha\mu}(k) \right] \\ &= -\frac{\bar{\alpha}}{\pi} \delta_2 \int_0^\infty \frac{dk^-}{k^-} p_1^- \delta(p_1^- - q^- - k^-) \delta\left(u + \frac{k^-}{q^-}\right) \\ &= -\frac{\bar{\alpha}}{\pi} \frac{\delta_2}{\bar{z}_1} \delta\left(u + \frac{\bar{z}_1}{z_1}\right), \end{aligned} \quad (5.121)$$

where $\bar{\Delta}$ is defined in Appendix 5.A and its wrong-sector limit is

$$\begin{aligned} \mathcal{M}_{(2_1,0)}^{n \rightarrow \bar{n}} &= -2\pi g^2 C_F \int \frac{d^d k}{(2\pi)^d} \delta(p_1^- - q^-) \delta(p_2^+ - q^+) \delta^{d-2}(\mathbf{q}_T + \mathbf{k}_T) \delta(k^2) \delta\left(u + \frac{k^-}{q^-}\right) \\ &\quad \times \text{Tr} \left[\frac{\not{p}_2}{2} \frac{\not{q}}{2} \right] \text{Tr} \left[\frac{\not{p}_1}{2} \left(\frac{n^\alpha}{-k^+} + \frac{\bar{n}^\alpha}{k^-} \right) \frac{\not{q}}{2} \not{k}_\perp \gamma_\mu^\perp \bar{\Delta}^{\alpha\mu}(k) \right] \\ &= -\frac{\bar{\alpha}}{\pi} \delta(\bar{z}_1) \delta(\bar{z}_2) \int_0^\infty \frac{dk^-}{k^-} \delta\left(u + \frac{k^-}{q^-}\right). \end{aligned} \quad (5.122)$$

Away from $\bar{z}_1 = \bar{z}_2 = 0$ the overlap does not contribute and (5.121) gives a well-defined result; however, it is rapidity divergent at $\bar{z}_1 = 0$. Following the LP approach, the matrix element may be written in the general form

$$\mathcal{M}_{(2_1,0)} = \frac{\bar{\alpha}}{\pi} \delta_2 \left(A_{(2_1,0)} \delta_1 \delta(u) - \left[\frac{1}{\bar{z}_1} \right]_+ \delta\left(u + \frac{\bar{z}_1}{z_1}\right) \right), \quad (5.123)$$

in accordance with Eq. (5.86). The constant $A_{(2_1,0)}$ is determined by integrating with respect to u , \bar{z}_1 , and \bar{z}_2 , which gives

$$A_{(2_1,0)} = \int_0^\infty \frac{dk^-}{k^-} \left[\theta(p_1^- - k^-) A_{(2_1,0)}^n(k^-) - \frac{1}{2} A_{(2_1,0)}^{\bar{n}}(k^-) \right], \quad (5.124)$$

where

$$A_{(2_1,0)}^n(k^-) = A_{(2_1,0)}^{\bar{n}}(k^-) = -1. \quad (5.125)$$

The integral in Eq. (5.124) is divergent: matrix elements of $T_{(2_1,0)}$ alone are not rapidity-finite, in agreement with the result (5.79) using the pure rapidity regular. This is to be expected, since gluons in both the n - and \bar{n} -sectors are required to reproduce the QCD rate, and the corresponding \bar{n} -sector gluon is emitted from the operator $T_{(0,2_1)}$. Including this operator and its corresponding subtraction gives

$$\mathcal{M}_{(2_1,0)} + \mathcal{M}_{(0,2_1)} = \frac{\bar{\alpha}}{\pi} \left\{ A_{2_1} \delta_1 \delta_2 \delta(u) - \delta_2 \left[\frac{1}{\bar{z}_1} \right]_+ \delta\left(u + \frac{\bar{z}_1}{z_1}\right) - \delta_1 \left[\frac{1}{\bar{z}_2} \right]_+ \delta\left(u + \frac{\bar{z}_2}{z_2}\right) \right\} \quad (5.126)$$

where

$$A_{2_1} = \int_0^\infty \frac{dk^-}{k^-} \left[\theta(p_1^- - k^-) A_{(2_1,0)}^n(k^-) + \theta\left(k^- - \frac{q_T^2}{p_2^+}\right) A_{(0,2_1)}^{\bar{n}}(k^-) - \frac{1}{2} \left(A_{(2_1,0)}^{\bar{n}}(k^-) + A_{(0,2_1)}^n(k^-) \right) \right] \quad (5.127)$$

and

$$A_{(0,2_1)}^{\bar{n}}(k^-) = A_{(0,2_1)}^n(k^-) = -1. \quad (5.128)$$

The integral in Eq. (5.127) is finite; as at LP, the spurious divergences from the n -sector as $k^- \rightarrow 0$ and the \bar{n} -sector as $k^- \rightarrow \infty$ have been canceled by the overlap subtraction to give the finite result

$$A_{2_1} = -\log \frac{\hat{s}}{q_T^2}, \quad (5.129)$$

which, by a similar rescaling argument as at leading power, gives a scheme-dependent rapidity logarithm reproducing that in Eq. (5.86).

A similar argument holds for $T_{(2_2,0)}$ and $T_{(0,2_2)}$. Explicitly, we find

$$\mathcal{M}_{(2_2,0)} + \mathcal{M}_{(0,2_2)} = \frac{\bar{\alpha}}{\pi} \left\{ A_{2_2} \delta_1 \delta_2 \delta(u_1) + \delta_2 \left[\frac{1}{\bar{z}_1} \right]_+ \delta \left(u_1 + \frac{\bar{z}_1}{z_1} \right) + \delta_1 \left[\frac{1}{\bar{z}_2} \right]_+ \delta \left(u_1 + \frac{\bar{z}_2}{z_2} \right) \right\} \delta(u_1 - u_2), \quad (5.130)$$

where

$$A_{(2_2,0)}^n(k^-) = A_{(2_2,0)}^{n \rightarrow \bar{n}}(k^-) = A_{(0,2_2)}^{\bar{n}}(k^-) = A_{(0,2_2)}^{\bar{n} \rightarrow n}(k^-) = 1, \quad (5.131)$$

and so

$$A_{2_2} = \log \frac{\hat{s}}{q_T^2}, \quad (5.132)$$

again in agreement with Eq. (5.86). The total fixed-order contribution to the cross section therefore cancels between the four longitudinal operators.

Transverse Class

Matrix elements of the transverse class of operators $T_{(2_3,0)}$ through $T_{(0,2_4)}$ are more complicated because they originate from operator products having the same Lorentz structure as those which produce the leading-power operator $T_{(0,0)}$, and power corrections to the overlap subtraction of $T_{(0,0)}$ must also be included to achieve a rapidity-finite combination. Thus, while in the longitudinal case rapidity divergences canceled between the corresponding n - and \bar{n} -sector operators, here they only cancel in the particular linear combination of transverse operators which contribute to the DY cross section.

The contribution of the transverse operators to the coefficient function $C_{f\bar{f}}^{(2)}$ is calculated from Eq. (5.12) and has the general form

$$C_{f\bar{f}}^{(2)T} = \bar{\alpha} z_1 z_2 \left(A_T^{(2)} \delta_1 \delta_2 + B_T^{(2)} \delta'_1 \delta'_2 + C_T^{(2)} (\delta'_1 \delta_2 + \delta_1 \delta'_2) + \delta'_2 [g_n^T(\bar{z}_1)]_{++} + \delta_2 [h_n^T(\bar{z}_1)]_{++} + \delta'_1 [g_{\bar{n}}^T(\bar{z}_2)]_{++} + \delta_1 [h_{\bar{n}}^T(\bar{z}_2)]_{++} \right). \quad (5.133)$$

Away from the endpoint $\bar{z}_1 = \bar{z}_2 = 0$ there are no rapidity divergences, so the contribution from each operator to $g_{n,\bar{n}}^T$ and $h_{n,\bar{n}}^T$ are the same as in Eqs. (5.86) and (5.87). After summing and integrating over u 's, these combine to give the functions $g_{n,\bar{n}}^T$, $h_{n,\bar{n}}^T$:

$$g_{n,\bar{n}}^T(\bar{z}) = - \left(\frac{2 - 2\bar{z} + \bar{z}^2}{\bar{z}^2} \right), \quad (5.134)$$

$$h_{n,\bar{n}}^T(\bar{z}) = - \frac{2}{\bar{z}^2}.$$

The endpoint region is overcounted in the sum of the two sectors, and must be compensated by subtracting away half the wrong limit of each sector. In contrast with the previous cases, the power counting of the required overlap subtractions is more subtle because the overlap graphs must subtract not only logarithmic, but also linear rapidity divergences.

Consider first the various contributions to $A_T^{(2)}$, which are found by integrating unweighted matrix elements over $\{u\}$, \bar{z}_1 , and \bar{z}_2 . The naïve contributions from $T_{(2_3,0)}$ and $T_{(0,2_3)}$ are calculated to be

$$\int_0^\infty \frac{dk^-}{k^-} \left[\theta(p_1^- - k^-) A_{(2_3,0)}^n(k^-) + \theta \left(k^- - \frac{q_T^2}{p_2^+} \right) A_{(0,2_3)}^{\bar{n}}(k^-) \right], \quad (5.135)$$

where

$$\begin{aligned} A_{(2_3,0)}^n(k^-) &= -2 \left(\frac{p_1^-}{k^-} \right), \\ A_{(0,2_3)}^{\bar{n}}(k^-) &= -2 \left(\frac{k^- p_2^+}{q_T^2} \right). \end{aligned} \quad (5.136)$$

The integral in (5.135) is rapidity divergent. Both terms in Eq. (5.136) are $O(1)$ in their respective correct regions, $k^- \sim O(q^-)$ in the n -sector and $k^+ = q_T^2/k^- \sim O(q^+)$ in the \bar{n} -sector, but are enhanced and give rise to linear rapidity divergences in the regions where this correct momentum scaling is no longer valid. The contributions to $C_{f\bar{f}}$ from these spurious regions are subtracted away by the overlap. There are two sources of overlap subtraction for $A_T^{(2)}$: the wrong limits $A_{(2_3,0)}^{n \rightarrow \bar{n}}$ and $A_{(0,2_3)}^{\bar{n} \rightarrow n}$, and also the subleading wrong limits from the leading power operator $T_{(0,0)}$.

Expanding the Feynman diagrams of $T_{(2_3,0)}$ and $T_{(0,2_3)}$ in their wrong limits gives the same functions as in Eq. (5.136) but are integrated over the region $0 < k^- < \infty$. Explicitly, there are two non-vanishing terms from the wrong limit of the $T_{(2_3,0)}$ matrix element,

$$\begin{aligned} \mathcal{M}_{(2_3,0)}^{n \rightarrow \bar{n}, \text{I}} &= g^2 C_F \int \frac{d^d k}{(2\pi)^d} \delta(p_1^- - q^-) \delta(p_2^+ - q^+) \delta^{d-2}(\mathbf{q}_T + \mathbf{k}_T) 2\pi \delta(k^2) \delta \left(u + \frac{k^-}{q^-} \right) \\ &\quad \times \text{Tr} \left[\frac{\not{p}_2}{2} \frac{\not{q}}{2} \right] \text{Tr} \left[\frac{\not{p}_1}{2} \frac{1}{u} k^\mu \bar{\Delta}(k)^{\alpha\nu} \frac{\not{k}}{2} \gamma_\nu^\perp \gamma_\mu^\perp \left(\frac{n_\alpha}{-k^+} - \frac{\bar{n}_\alpha}{-k^-} \right) \right] \\ &= \frac{\bar{\alpha}}{\pi} \delta_1 \delta_2 \int_0^\infty \frac{dk^-}{k^-} \frac{1}{u} \delta \left(u + \frac{k^-}{q^-} \right), \end{aligned} \quad (5.137)$$

and

$$\begin{aligned} \mathcal{M}_{(2_3,0)}^{n \rightarrow \bar{n}, \text{II}} &= g^2 C_F \int \frac{d^d k}{(2\pi)^d} (-k^-) \delta'(p_1^- - q^-) \delta(p_2^+ - q^+) \delta^{d-2}(\mathbf{q}_T + \mathbf{k}_T) 2\pi \delta(k^2) \delta \left(u + \frac{k^-}{q^-} \right) \\ &\quad \times \text{Tr} \left[\frac{\not{p}_2}{2} \frac{\not{q}}{2} \right] \text{Tr} \left[\frac{\not{p}_1}{2} \frac{1}{u} k^\mu \bar{\Delta}(k)^{\alpha\nu} \frac{\not{k}}{2} \gamma_\nu^\perp \gamma_\mu^\perp \left(\frac{n_\alpha}{-k^+} - \frac{\bar{n}_\alpha}{-k^-} \right) \right] \\ &= -\frac{\bar{\alpha}}{\pi} \delta'(\bar{z}_1) \delta(\bar{z}_2) \int_0^\infty \frac{dk^-}{p_1^-} \frac{1}{u} \delta \left(u + \frac{k^-}{q^-} \right). \end{aligned} \quad (5.138)$$

The wrong-limit expansion is truncated after the terms reach an $O(q_T^2/q_L^2)$ suppression relative to the leading-power operator in the wrong-limit momentum scaling $p_1^- \sim O(q^-)$ and $k^+, p_2^+ \sim O(q^+)$. The subtraction term in Eq. (5.137) contributes to $A_T^{(2)}$ while the term in Eq. (5.138) contributes to $C_T^{(2)}$.

Similarly, expanding the \bar{n} - and n -sector graphs of $T_{(0,0)}$ up to NLP gives the $O(1/k^-)$ term in $A_{(2_3,0)}^n$ and the $O(k^-)$ term in $A_{(0,2_3)}^{\bar{n}}$ in Eq. (5.136), respectively, which are again integrated over all values of k^- . Explicitly, expanding $\mathcal{M}_{(0,0)}^n$ gives two contributions to the subleading overlap,

$$\begin{aligned} \mathcal{M}_{(0,0)}^{n \rightarrow \bar{n}, \text{NLP}_1} &= -2\pi g^2 C_F \int \frac{d^d k}{(2\pi)^d} (-k^-) \delta'(p_1^- - q^-) \delta(p_2^+ - q^+) \delta^{d-2}(\mathbf{q}_T + \mathbf{k}_T) \delta(k^2) \\ &\quad \times \text{Tr} \left[\frac{\not{p}_2}{2} \frac{\not{q}}{2} \right] \text{Tr} \left[\frac{\not{p}_1}{2} \left(\frac{n^\alpha}{-k^+} + \frac{\bar{n}^\alpha}{-k^-} \right) \frac{\not{k}}{2} \left(\frac{n_\alpha}{-k^+} - \frac{\bar{n}_\alpha}{-k^-} \right) \right] \\ &= -2\delta'(\bar{z}_1) \delta(\bar{z}_2) \frac{\bar{\alpha}}{\pi} \int_0^\infty \frac{dk^-}{k^-} \frac{k^- p_2^+}{q_T^2}, \end{aligned} \quad (5.139)$$

and

$$\begin{aligned}
\mathcal{M}_{(0,0)}^{n \rightarrow \bar{n}, \text{NLP}_2} &= -2\pi g^2 C_F \int \frac{d^d k}{(2\pi)^d} \delta(p_1^- - q^-) \delta(p_2^+ - q^+) \delta^{d-2}(\mathbf{q}_T + \mathbf{k}_T) 2\pi \delta(k^2) \\
&\quad \times \text{Tr} \left[\frac{\not{p}_2}{2} \frac{\not{q}}{2} \right] \text{Tr} \left[\frac{\not{p}_1}{2} \left(\frac{n^\alpha}{-k^+} + \frac{\bar{n}^\alpha}{k^-} \right) \frac{\not{q}}{2} \left(\frac{\not{k}_\perp \gamma_\perp^\mu}{p_1^- k^+} \Delta_{\alpha\mu}(k) \right) \right. \\
&\quad \left. + \frac{\not{p}_1}{2} \left(\Delta^{\alpha\mu}(k) \frac{\gamma_\mu^\perp \not{k}_\perp}{p_1^- k^+} \right) \frac{\not{q}}{2} \left(\frac{n_\alpha}{-k^+} - \frac{\bar{n}_\alpha}{-k^-} \right) \right] \\
&= -2 \frac{\bar{\alpha}}{\pi} \delta(\bar{z}_1) \delta(\bar{z}_2) \int_0^\infty \frac{dk^-}{k^-} \frac{k^- p_2^+}{q_T^2},
\end{aligned} \tag{5.140}$$

the first of which comes from higher corrections to the momentum-conserving delta function, while the second comes from higher corrections to the quark propagator expansions. Only the second term contributes here; the first contributes to $C_T^{(2)}$.

Putting these together, we obtain the expression for $A_T^{(2)}$,

$$\begin{aligned}
A_T^{(2)} &= \int_0^\infty \frac{dk^-}{k^-} \left[\theta(p_1^- - k^-) A_{(2_3,0)}^n(k^-) + \theta \left(k^- - \frac{q_T^2}{p_2^+} \right) A_{(0,2_3)}^{\bar{n}}(k^-) \right. \\
&\quad \left. - \frac{1}{2} \left(A_{(0,0)}^{n \rightarrow \bar{n}, \text{NLP}}(k^-) + A_{(0,0)}^{\bar{n} \rightarrow n, \text{NLP}}(k^-) \right) - \frac{1}{2} \left(A_{(2_3,0)}^{n \rightarrow \bar{n}}(k^-) + A_{(0,2_3)}^{\bar{n} \rightarrow n}(k^-) \right) \right],
\end{aligned} \tag{5.141}$$

where the contributions from $T_{(2_4,0)}$ and $T_{(0,2_4)}$ all vanish, and explicitly

$$\begin{aligned}
A_{(2_3,0)}^{n \rightarrow \bar{n}}(k^-) &= A_{(0,0)}^{\bar{n} \rightarrow n, \text{NLP}}(k^-) = -2 \left(\frac{p_1^-}{k^-} \right), \\
A_{(0,2_3)}^{\bar{n} \rightarrow n}(k^-) &= A_{(0,0)}^{n \rightarrow \bar{n}, \text{NLP}}(k^-) = -2 \left(\frac{k^- p_2^+}{q_T^2} \right).
\end{aligned} \tag{5.142}$$

This gives the finite result

$$A_T^{(2)} = 4. \tag{5.143}$$

Next consider the contributions to the endpoint constant $C_T^{(2)}$, which are obtained by integrating the various matrix elements weighted with \bar{z}_1 (or equivalently \bar{z}_2). The naïve contributions to the \bar{z}_1 moment give

$$\int_0^\infty \frac{dk^-}{k^-} \left[\theta(p_1^- - k^-) C_{(2_3,0)}^n(k^-) + \theta \left(k^- - \frac{q_T^2}{p_2^+} \right) C_{(0,2_4)}^{\bar{n}}(k^-) \right], \tag{5.144}$$

where

$$\begin{aligned}
C_{(2_3,0)}^n(k^-) &= 2, \\
C_{(0,2_4)}^{\bar{n}}(k^-) &= -2 \left(\frac{k^- p_2^+}{q_T^2} \right) + 2 - \left(\frac{q_T^2}{k^- p_2^+} \right).
\end{aligned} \tag{5.145}$$

This is again is rapidity divergent: $C_{(2_3,0)}^n(k^-)$ gives a logarithmically divergent contribution as $k^- \rightarrow 0$, while $C_{(0,2_4)}^{\bar{n}}(k^-)$ gives contributions which are both logarithmically and linearly divergent as $k^- \rightarrow \infty$. As with $A_T^{(2)}$, taking the wrong limit of the Feynman diagrams contributing to Eq. (5.145) gives the $k^- \rightarrow 0$ and $k^- \rightarrow \infty$ expansions of these terms. For example, the wrong-limit expansion of $\mathcal{M}_{(0,2_4)}^{\bar{n}}$ gives three terms which correspond almost exactly to the overlaps of $T_{(0,0)}$ in Eqs. (5.116), (5.139), and (5.140), except they have a different momentum-conserving delta function structure. These give the

contributions

$$C_{(0,24)}^{\bar{n} \rightarrow n}(k^-) = -2 \left(\frac{k^- p_2^+}{q_T^2} \right) + 2 , \quad (5.146)$$

while from the $T_{(23,0)}$ overlap given in Eq. (5.138) is the contribution

$$C_{(23,0)}^{n \rightarrow \bar{n}}(k^-) = 2 . \quad (5.147)$$

The overlap term from $T_{(0,24)}$ contains two terms: the leading term is proportional to k^- and cancels a linear rapidity divergence, while the $O(1)$ term contributes to the cancellation of a logarithmic divergence.

We also have the contribution from the NLP overlap of $T_{(0,0)}$ in Eq. (5.139),

$$C_{(0,0)}^{n \rightarrow \bar{n}, \text{NLP}}(k^-) = -2 \left(\frac{k^- p_2^+}{q_T^2} \right) , \quad (5.148)$$

with the sum of all contributions giving the result

$$\begin{aligned} C_T^{(2)} &= \int_0^\infty \frac{dk^-}{k^-} \left[\theta(p_1^- - k^-) C_{(23,0)}^n(k^-) + \theta \left(k^- - \frac{q_T^2}{p_2^+} \right) C_{(0,24)}^{\bar{n}}(k^-) \right. \\ &\quad \left. - \frac{1}{2} \left(C_{(0,0)}^{n \rightarrow \bar{n}, \text{NLP}}(k^-) \right) - \frac{1}{2} \left(C_{(23,0)}^{\bar{n} \rightarrow n}(k^-) + C_{(0,24)}^{\bar{n} \rightarrow n}(k^-) \right) \right] \\ &= 2 \log \frac{\hat{s}}{q_T^2} + 1 . \end{aligned} \quad (5.149)$$

Once again there is a precise interplay between naïve matrix elements and overlap subtractions required to obtain the same finite result as using the pure rapidity regulator. Rescaling the integrals for $C_{(0,24)}^{\bar{n}}(k^-)$, $C_{(0,24)}^{\bar{n} \rightarrow n}(k^-)$, and $C_{(0,0)}^{n \rightarrow \bar{n}, \text{NLP}}(k^-)$ as $k^- \rightarrow k^- \zeta^2 / \hat{s}$ replaces the \hat{s} -dependence in the result of Eq. (5.149) with ζ^2 scheme dependence. This correlation between the rescaling of individual integrals is necessary to maintain a finite result, and is a general feature of power-law divergences.

Finally, the endpoint constant B_T is found by weighting the integrals by $\bar{z}_1 \bar{z}_2$, giving

$$\begin{aligned} B_T^{(2)} &= \int_0^\infty \frac{dk^-}{k^-} \left[\theta(p_1^- - k^-) B_{(24,0)}^n(k^-) + \theta \left(k^- - \frac{q_T^2}{p_2^+} \right) B_{(0,24)}^{\bar{n}}(k^-) \right. \\ &\quad \left. - \frac{1}{2} \left(B_{(24,0)}^{\bar{n} \rightarrow n}(k^-) + B_{(0,24)}^{\bar{n} \rightarrow n}(k^-) \right) \right] \end{aligned} \quad (5.150)$$

where explicitly

$$\begin{aligned} B_{(24,0)}^n(k^-) &= 2 - 2 \left(\frac{k^-}{p_1^-} \right) + \left(\frac{k^-}{p_1^-} \right)^2 , \\ B_{(0,24)}^{\bar{n}}(k^-) &= 2 - 2 \left(\frac{q_T^2}{k^- p_2^+} \right) + \left(\frac{q_T^2}{k^- p_2^+} \right)^2 , \end{aligned} \quad (5.151)$$

and the overlap terms cancel just the logarithmic divergences,

$$B_{(24,0)}^{\bar{n} \rightarrow n}(k^-) = B_{(0,24)}^{\bar{n} \rightarrow n}(k^-) = 2 . \quad (5.152)$$

This gives

$$B_T^{(2)} = 2 \log \frac{\hat{s}}{q_T^2} - 3 , \quad (5.153)$$

where rescaling the second line of Eq. (5.151) as $k^- \rightarrow k^- \zeta^2 / \hat{s}$ replaces the \hat{s} -dependence in Eq. (5.153) with ζ^2 scheme dependence.

This concludes the calculation of all the endpoint constants $A_{L,T}$, $B_{L,T}$, and $C_{L,T}$. In each case, these constants agree with those of QCD as calculated in Section 5.2.5. We have thus demonstrated an overlap subtraction prescription that allows us to properly calculate probabilities at NLP without an explicit rapidity regulator, providing a non-trivial crosscheck of our results using different rapidity regularization schemes.

5.4 Conclusion

In this chapter we have shown that factorization of the Drell-Yan production cross section into hard matching coefficients, rapidity evolution factors, soft matching coefficients and PDFs occurs naturally in a formulation of SCET in which the low energy degrees of freedom are not separated into distinct fields for each mode relevant to the process. The DY rate is given by the matrix element of the nonlocal product of two external currents in SCET. Usually in SCET observables are factorized into jet and soft factors which are separately renormalized and run to the appropriate scales; here, the EFT is first run in μ down to the soft matching scale $\mu \sim q_T$, at which point the product of currents is renormalized in rapidity space. After resumming the rapidity logs at the soft matching scale, the operator products are then matched onto a product of light-cone distribution operators, whose hadronic matrix elements are the usual PDFs. At $O(\alpha_s)$, our EFT cross section reproduces the fixed-order QCD cross section at NLP, as well as the equivalent fixed-order cross section calculated using the pure rapidity regulator in [76]. Off-diagonal rapidity anomalous dimensions were calculated and rapidity divergences were shown to cancel in the cross section. The resummation of rapidity logarithms at NLP requires the complete rapidity anomalous dimension matrix for the subleading operators $T_{(i,j)}$, which is beyond the scope of this thesis, and will be the subject of future work.

The factorization and resummation of the DY process is particularly simple in this approach: it does not depend on proving factorization at a given order in the SCET expansion or in the leading-log approximation, but instead is a straightforward consequence of the usual EFT approach of matching and running. By not explicitly factorizing modes in the Lagrangian, the complication of power corrections coupling different modes in the Lagrangian is avoided, as is the necessity to re-factorize the result to make individual jet and soft functions well-defined. Divergences analogous to the endpoint divergences arising at NLP in other approaches arise, but are regulated by the rapidity regulator and systematically canceled by the same overlap subtraction procedure required to avoid double counting at leading power.

Rapidity divergences were considered in detail, and the cancellation of rapidity divergences in the rate was shown in two ways. Using the pure rapidity regulator, it was shown that all rapidity poles canceled between the different linear combinations of subleading operators arising in the expression for the differential rate, as was found in previous analyses [87–89, 123]. In Section 5.3 it was shown that even without an explicit rapidity regulator, rapidity divergences in the DY cross section cancel between particular linear combinations of operators, and that these linear combinations could be understood by requiring that SCET reproduce the correct differential rate in different regions of phase space. A consistent treatment of subleading overlap subtractions from the leading order operator was shown to be necessary for this cancellation.

Acknowledgements

We would like to thank Christian Bauer for useful comments on the manuscript. This work was supported in part by the Natural Sciences and Engineering Research Council of Canada.

5.A Summary of Matrix Elements of Hard Scattering Operators

In the following equations we list all relevant u -space matrix elements of scattering operators which contribute to the quark-induced DY process through the emission of an n -sector gluon. We use the soft-scale matching kinematics $p_1^+ = p_{1\perp} = 0 = p_2^- = p_{2\perp}$, and define the non-common factor $\mathcal{A}_{n,\bar{n}}^{(i)}$ of these matrix elements through the relation

$$\int \frac{d^d x}{2(2\pi)^d} e^{-iq \cdot x} \langle k^{n,\bar{n}} | O_2^{(i)\mu}(x, \{u\}) | p_1^n p_2^{\bar{n}} \rangle \equiv g T_{cc'}^a \bar{v}^c(p_2^{\bar{n}}) \mathcal{A}_{n,\bar{n}}^{(i)} u^{c'}(p_1^n) \epsilon_\nu^*, \quad (5.154)$$

where \mathcal{A} is tensor-valued with implied Lorentz indices μ and ν . We find for the n -gluon emissions

$$\begin{aligned} \mathcal{A}_n^{(0)} &= -P_n \gamma^\mu P_n \left(\frac{2p_1^\nu - \not{k}\gamma^\nu}{-2p_1 \cdot k} - \frac{\bar{n}^\nu}{-k^-} \right) \delta_n^- \delta_n^+ \delta_\perp \\ \mathcal{A}_n^{(1\perp n)} &= -P_n \gamma^\mu \frac{\not{\gamma}}{2} \not{k}_\perp \left(\frac{2p_1^\nu - \not{k}\gamma^\nu}{-2p_1 \cdot k} - \frac{\bar{n}^\nu}{-k^-} \right) \delta_n^- \delta_n^+ \delta_\perp, \\ \mathcal{A}_n^{(1A_1)} &= \gamma_\alpha^\perp \frac{\not{\gamma}}{2} \gamma^\mu P_n \bar{\Delta}^{\nu\alpha}(k) \delta_n^- \delta_n^+ \delta_\perp \delta(u + \hat{k}^-), \\ \mathcal{A}_n^{(1A_2)} &= -P_n \gamma^\mu \frac{\not{\gamma}}{2} \gamma_\alpha^\perp \bar{\Delta}^{\nu\alpha}(k) \delta_n^- \delta_n^+ \delta_\perp \delta(u + \hat{k}^-), \\ \mathcal{A}_n^{(2\delta^+)} &= q^+ q^- P_n \gamma^\mu P_n \left(\frac{2p_1^\nu - \not{k}\gamma^\nu}{-2p_1 \cdot k} - \frac{\bar{n}^\nu}{-k^-} \right) k^+ \delta_n^- \delta_n^+ \delta_\perp, \\ \mathcal{A}_n^{(2A_1)} &= -\frac{1}{u} \gamma_\alpha^\perp \gamma_\beta^\perp P_n \gamma^\mu P_n \bar{\Delta}^{\nu\alpha}(k) k^\beta \delta_n^- \delta_n^+ \delta_\perp \delta(u + \hat{k}^-), \end{aligned} \quad (5.155)$$

while for the \bar{n} -gluon emissions we find

$$\begin{aligned} \mathcal{A}_{\bar{n}}^{(0)} &= \left(\frac{2p_2^\nu - \gamma^\nu \not{k}}{-2p_2 \cdot k} - \frac{n^\nu}{-k^+} \right) P_n \gamma^\mu P_n \delta_{\bar{n}}^- \delta_{\bar{n}}^+ \delta_\perp, \\ \mathcal{A}_{\bar{n}}^{(1\perp \bar{n})} &= \left(\frac{2p_2^\nu - \gamma^\nu \not{k}}{-2p_2 \cdot k} - \frac{n^\nu}{-k^+} \right) \not{k}_\perp \frac{\not{\gamma}}{2} \gamma^\mu P_n \delta_{\bar{n}}^- \delta_{\bar{n}}^+ \delta_\perp, \\ \mathcal{A}_{\bar{n}}^{(1B_1)} &= -P_n \gamma^\mu \frac{\not{\gamma}}{2} \gamma_\alpha^\perp \bar{\Delta}^{\nu\alpha}(k) \delta_{\bar{n}}^- \delta_{\bar{n}}^+ \delta_\perp \delta(u + \hat{k}^+), \\ \mathcal{A}_{\bar{n}}^{(1B_2)} &= \gamma_\alpha^\perp \frac{\not{\gamma}}{2} \gamma^\mu P_n \bar{\Delta}^{\nu\alpha}(k) \delta_{\bar{n}}^- \delta_{\bar{n}}^+ \delta_\perp \delta(u + \hat{k}^+), \\ \mathcal{A}_{\bar{n}}^{(2\delta^-)} &= q^+ q^- \left(\frac{n^\nu}{-k^+} - \frac{2p_2^\nu - \gamma^\nu \not{k}}{-2p_2 \cdot k} \right) P_n \gamma^\mu P_n k^- \delta_{\bar{n}}^- \delta_{\bar{n}}^+ \delta_\perp, \\ \mathcal{A}_{\bar{n}}^{(2B_1)} &= \frac{1}{u} P_n \gamma^\mu P_n \gamma_\alpha^\perp \gamma_\beta^\perp k^\alpha \bar{\Delta}^{\nu\beta}(k) \delta_{\bar{n}}^- \delta_{\bar{n}}^+ \delta_\perp \delta(u + \hat{k}^+). \end{aligned} \quad (5.156)$$

The 1-gluon matrix elements of the scattering operators defined in Eqs. (5.155) and (5.156) use the

following definitions

$$\bar{\Delta}^{\alpha\mu}(k) = g^{\alpha\mu} - \frac{\bar{n}^\alpha k^\mu}{\bar{n} \cdot k}, \quad \Delta^{\alpha\mu}(k) = g^{\alpha\mu} - \frac{n^\alpha k^\mu}{n \cdot k}. \quad (5.157)$$

These are common structures associated with the covariant derivative. We also define the dimensionless quantities

$$\hat{\ell}^- = \frac{\ell^-}{q^-}, \quad \hat{\ell}^+ = \frac{\ell^+}{q^+} \quad (5.158)$$

and we have we used the shorthand notation $\delta_1^- = \delta(p_1^- - k^- - q^-)$, $\delta_n^+ = \delta(p_2^+ - q^+)$, $\delta_{\bar{n}}^- = \delta(p_1^- - q^-)$, $\delta_{\bar{n}}^+ = \delta(p_2^+ - k^+ - q^+)$, and $\delta_{\perp} = \delta^{(d-2)}(k_{\perp} + q_{\perp})$.

There are additional operators which are present from the hard-scale matching [83, 162, 163, 169, 179], but which do not contribute to the quark-initiated DY process to the order at which we are working. Up to a $1/q_L^2$ suppression, these include an operator with two perpendicular derivatives

$$O_2^{(2\perp\perp)\mu}(x) = [i\partial^\alpha \bar{\chi}_{\bar{n}}(x_{\bar{n}})] \gamma_\alpha^\perp \frac{\not{q}}{2} \gamma^\mu \frac{\not{\ell}}{2} \gamma_\beta^\perp [i\partial^\beta \chi_n(x_n)], \quad (5.159)$$

the A -type operators

$$\begin{aligned} O_2^{(2A_2)\mu}(x, \hat{t}) &= 2\pi i \theta(\hat{t}) \otimes [\bar{\chi}_{\bar{n}}(x)] \gamma_\alpha^\perp \frac{\not{q}}{2} \gamma^\mu \frac{\not{\ell}}{2} \gamma_\beta^\perp [\mathcal{B}_n^{\dagger\alpha\beta}(x) \chi_n(x - \bar{n}t)] \\ O_2^{(2A_3)\mu}(x, \hat{t}) &= 2\pi i \theta(\hat{t}) \otimes [\bar{\chi}_{\bar{n}}(x)] \gamma_\beta^\perp \frac{\not{q}}{2} \gamma^\mu \frac{\not{\ell}}{2} \gamma_\alpha^\perp [i\partial^\alpha \mathcal{B}_n^{\dagger\beta}(x) \chi_n(x - \bar{n}t)] \\ O_2^{(2A_4)\mu}(x, \hat{t}) &= -2\pi i \theta(\hat{t}) \otimes [i\partial^\beta \bar{\chi}_{\bar{n}}(x - nt)] \gamma_\beta^\perp \frac{\not{q}}{2} \gamma^\mu \frac{\not{\ell}}{2} \gamma_\alpha^\perp [\mathcal{B}_n^{\dagger\alpha}(x) \chi_n(x)] \\ O_2^{(2A_5)\mu}(x, \hat{t}) &= 2\pi i \theta(\hat{t}) \otimes [i\partial^\alpha \bar{\chi}_{\bar{n}}(x)] \gamma^\mu \{\gamma_\alpha^\perp, \gamma_\beta^\perp\} [\mathcal{B}_n^{\dagger\beta}(x - \bar{n}t) \chi_n(x)], \end{aligned} \quad (5.160)$$

and the corresponding B -type operators

$$\begin{aligned} O_2^{(2B_2)\mu}(x, \hat{t}) &= 2\pi i \theta(\hat{t}) \otimes [\bar{\chi}_{\bar{n}}(x - nt) \mathcal{B}_{\bar{n}}^{\alpha\beta}(x)] \gamma_\alpha^\perp \frac{\not{q}}{2} \gamma^\mu \frac{\not{\ell}}{2} \gamma_\beta^\perp [\chi_n(x)] \\ O_2^{(2B_3)\mu}(x, \hat{t}) &= 2\pi i \theta(\hat{t}) \otimes [i\partial^\alpha \bar{\chi}_{\bar{n}}(x - nt) \mathcal{B}_{\bar{n}}^\beta(x)] \gamma_\alpha^\perp \frac{\not{q}}{2} \gamma^\mu \frac{\not{\ell}}{2} \gamma_\beta^\perp [\chi_n(x)] \\ O_2^{(2B_4)\mu}(x, \hat{t}) &= -2\pi i \theta(\hat{t}) \otimes [\bar{\chi}_{\bar{n}}(x) \mathcal{B}_{\bar{n}}^\alpha(x - \bar{n}t)] \gamma_\alpha^\perp \frac{\not{q}}{2} \gamma^\mu \frac{\not{\ell}}{2} \gamma_\beta^\perp [i\partial^\beta \chi_n(x)] \\ O_2^{(2B_5)\mu}(x, \hat{t}) &= 2\pi i \theta(\hat{t}) \otimes [\bar{\chi}_{\bar{n}}(x) \mathcal{B}_{\bar{n}}^\alpha(x - \bar{n}t)] \gamma^\mu \{\gamma_\alpha^\perp, \gamma_\beta^\perp\} [i\partial^\beta \chi_n(x)]. \end{aligned} \quad (5.161)$$

There are also the C -type operators, which are only relevant for gluon-induced Drell-Yan

$$\begin{aligned} O_2^{(1C_1)\mu}(x, \hat{t}) &= -2\pi i \theta(\hat{t}) \otimes [\mathcal{B}_n^{\alpha cc'}(x)] [\bar{\chi}_{\bar{n}}^c(x) \gamma^\mu \frac{\not{q}}{2} \gamma_\alpha^\perp \chi_{\bar{n}}^{c'}(x - nt)] \\ O_2^{(1C_2)\mu}(x, \hat{t}) &= 2\pi i \theta(\hat{t}) \otimes [\mathcal{B}_n^{\alpha cc'}(x)] [\bar{\chi}_{\bar{n}}^c(x - nt) \gamma_\alpha^\perp \frac{\not{q}}{2} \gamma^\mu \chi_{\bar{n}}^{c'}(x)]. \end{aligned} \quad (5.162)$$

5.B Plus Distribution Identities

5.B.1 Single Variable Plus Distributions

The familiar plus distribution may be written as

$$[\theta(x)f(x)]_+ = \lim_{\beta \rightarrow 0} [F(\beta) - F(1)] \delta(x - \beta) + \theta(x - \beta)f(x), \quad (5.163)$$

where $f(x) = dF(x)/dx$, and has the properties

$$\begin{aligned} \int_0^1 dx [\theta(x)f(x)]_+ &= 0 \\ [\theta(x)f(x)]_+ &= f(x) , \quad x > 0 . \end{aligned} \tag{5.164}$$

Rearranging these equations gives the differential relation

$$\frac{d}{dx} [\theta(x)F(x)] = \left[\theta(x) \frac{dF(x)}{dx} \right]_+ + \delta(x)F(1) \tag{5.165}$$

which is useful for expanding rapidity divergent integrals in terms of plus functions. For example, taking $f(x) = x^{-1-\eta}$ gives $F(x) = -x^{-\eta}/\eta$, and so

$$\frac{d}{dx} \left[\frac{-\theta(x)}{\eta x^\eta} \right] = \frac{\theta(x)}{x^{1+\eta}} - \frac{\delta(x)}{\eta x^\eta} = \left[\frac{\theta(x)}{x^{1+\eta}} \right]_+ - \frac{\delta(x)}{\eta} . \tag{5.166}$$

The factor of $\delta(x)x^{-\eta}$ vanishes by analytic continuation, so expanding about $\eta = 0$ gives

$$\begin{aligned} \frac{\theta(x)}{x^{1+\eta}} &= -\frac{\delta(x)}{\eta} + \left[\frac{\theta(x)}{x} - \eta \frac{\log(x)\theta(x)}{x} + \dots \right]_+ \\ &= -\frac{\delta(x)}{\eta} + \left[\frac{\theta(x)}{x} \right]_+ - \eta \left[\frac{\log(x)\theta(x)}{x} \right]_+ + \dots . \end{aligned} \tag{5.167}$$

Matrix elements at next-to-leading power involve higher-order poles that are more singular than the usual plus distributions. As in [76], we define double-plus distributions which satisfy

$$\begin{aligned} \int_0^1 dx [\theta(x)f(x)]_{++} &= 0 , \\ \int_0^1 dx x [\theta(x)f(x)]_{++} &= 0 , \\ [\theta(x)f(x)]_{++} &= f(x) , \quad x > 0 . \end{aligned} \tag{5.168}$$

They are related to the single-plus distributions by

$$[\theta(x)f(x)]_{++} - [\theta(x)f(x)]_+ = \lim_{\beta \rightarrow 0} \delta'(x - \beta) \int_\beta^1 dy (y - \beta) f(y) . \tag{5.169}$$

For example, taking $f(x) = x^{-2-\eta}$, then $F(x) = -x^{-1-\eta}/(1 + \eta)$, and we obtain

$$\frac{\theta(x)}{x^{2+\eta}} = \left[\frac{\theta(x)}{x^{2+\eta}} \right]_+ - \frac{\delta(x)}{1 + \eta} . \tag{5.170}$$

Since $\left[\frac{\theta(x)}{x^2} \right]_+$ is not well-defined, we convert to a double-plus distribution before expanding in η ,

$$\begin{aligned} \left[\frac{\theta(x)}{x^{2+\eta}} \right]_+ &= \left[\frac{\theta(x)}{x^{2+\eta}} \right]_{++} - \delta'(x) \int_0^1 dx \frac{1}{x^{1+\eta}} \\ &= \left[\frac{\theta(x)}{x^{2+\eta}} \right]_{++} + \frac{\delta'(x)}{\eta} \end{aligned} \tag{5.171}$$

to obtain the expansion

$$\frac{1}{x^{2+\eta}} = \frac{\delta'(x)}{\eta} - \frac{\delta(x)}{1+\eta} + \left[\frac{\theta(x)}{x^2} \right]_{++} - \eta \left[\frac{\log(x)\theta(x)}{x^2} \right]_{++} \quad (5.172)$$

as in Eq. (2.40) of [76].

5.B.2 Vector Plus Distributions

The same techniques may be applied to divergent vector-valued functions. Since our operators $T_{(i,j)}$ live in $d \neq 4$ spacetime dimensions, we define the vector plus distribution (which we also call the ξ^2 -distribution) by the relations

$$\int_{q_T^2 < \xi^2} d^{d-2} \mathbf{q}_T [\theta(q_T^2) (f(\mathbf{q}_T))]_+^{\xi^2} = 0, \quad (5.173)$$

$$[\theta(q_T^2) f(\mathbf{q}_T)]_+^{\xi^2} = f(\mathbf{q}_T), \quad q_T^2 > 0.$$

When $f(\mathbf{q}_T) = f(q_T^2)$ is a rotationally symmetric function, we have

$$\int d^{d-2} \mathbf{q}_T f(q_T^2) = \int J_{q_T}^\epsilon f(q_T^2) dq_T^2. \quad (5.174)$$

where

$$J_{q_T}^\epsilon \equiv \frac{S_{2-2\epsilon}}{2} q_T^{-2\epsilon} \quad (5.175)$$

and $S_{d-2} = 2\pi^{\frac{d-2}{2}}/\Gamma(\frac{d-2}{2})$, e.g. $S_2 = 2\pi$. We also note that a $(d-2)$ -dimensional delta function at the origin may be written as

$$\delta(\mathbf{q}_T) = \frac{\delta(q_T^2)}{J_{q_T}^\epsilon}. \quad (5.176)$$

Therefore if

$$g(q_T^2) = \int_{\mathbf{p}_T^2 < q_T^2} d^{d-2} \mathbf{p}_T f(\mathbf{p}_T) \quad (5.177)$$

for some rotationally invariant function $f(\mathbf{p}_T)$, then

$$f(q_T^2) = \frac{1}{J_{q_T}^\epsilon} \frac{d}{dq_T^2} g(q_T^2). \quad (5.178)$$

which is useful for converting between distributions and their cumulants.

The vector plus distribution may be written as the limit

$$[f(\mathbf{q}_T)]_+^{\xi^2} = \lim_{\beta \rightarrow 0} A(\beta, \epsilon, \xi) \delta(\mathbf{q}_T) + \theta(q_T^2 - \beta^2) f(\mathbf{q}_T), \quad (5.179)$$

where, from (5.173),

$$A(\beta, \epsilon, \xi) = - \int_{\beta^2 < q_T^2 < \xi^2} d^{d-2} \mathbf{q}_T f(\mathbf{q}_T). \quad (5.180)$$

For example, we have the explicit form of the ξ^2 -distribution

$$\left[\frac{1}{\mathbf{q}_T^2} \right]_+^{\xi^2} = \xi^{-2\epsilon} \left(1 - \left(\frac{\beta^2}{\xi^2} \right)^{-\epsilon} \right) \frac{S_{d-2}}{2\epsilon} \delta(\mathbf{q}_T) + \frac{\theta(q_T^2 - \beta^2)}{\mathbf{q}_T^2}, \quad (5.181)$$

(where the limit $\beta \rightarrow 0$ is implicit). We can also derive the analogue of (5.165) [67],

$$\frac{1}{J_{q_T}^\epsilon} \frac{d}{dq_T^2} \theta(q_T^2) F(q_T^2) = \left[\theta(q_T^2) \frac{1}{J_{q_T}^\epsilon} \frac{dF(q_T^2)}{dq_T^2} \right]_+^{\xi^2} + \delta(\mathbf{q}_T) F(\xi^2). \quad (5.182)$$

As in Appendix 5.B.1, we may then derive the expansion

$$\frac{(\nu^2)^{-\eta/2}}{(\mathbf{q}_T^2)^{1-\eta/2}} = J_\xi^\epsilon \left(\frac{\nu^2}{\xi^2} \right)^{-\eta/2} \frac{\delta(\mathbf{q}_T)}{\frac{\eta}{2} - \epsilon} + \left[\frac{\theta(q_T^2)}{q_T^2} \right]_+^{\xi^2} + \frac{\eta}{2} \left[\frac{\log \frac{q_T^2}{\nu^2} \theta(q_T^2)}{q_T^2} \right]_+^{\xi^2} + \dots. \quad (5.183)$$

The choice of ξ in these identities is entirely arbitrary. However, since each diagram comes with an overall $\mu^{2\epsilon}$, and since these identities put all the ϵ -dependence into the delta-function prefactor $J_\xi^\epsilon \propto \xi^{-2\epsilon}$, the canonical choice that avoids spurious logarithms is $\xi = \mu$.

It is convenient to rescale the vector plus distributions to have the same scaling dimensions and π -counting as $\delta(\mathbf{q}_T)$. Borrowing from the generalized-log notation of [67], we define

$$\mathcal{L}_n(\mathbf{q}_T, \mu) = \frac{1}{J_\mu^\epsilon} \left[\frac{\log^n \frac{\mathbf{q}_T^2}{\mu^2} \theta(q_T^2)}{\mathbf{q}_T^2} \right]_+^{\mu^2}. \quad (5.184)$$

With these definitions, and taking $\nu = \mu = \xi$, we have

$$\frac{(\mu^2)^{-\eta/2}}{(\mathbf{q}_T^2)^{1-\eta/2}} = J_\mu^\epsilon \left(\frac{\delta(\mathbf{q}_T)}{\frac{\eta}{2} - \epsilon} + \mathcal{L}_0^{(0)}(\mathbf{q}_T, \mu) + \frac{\eta}{2} \mathcal{L}_1^{(0)}(\mathbf{q}_T, \mu) + \dots \right). \quad (5.185)$$

Finally, we also need the identity

$$\frac{\log \frac{\mathbf{q}_T^2}{\mu^2}}{\mathbf{q}_T^2} = J_\mu^\epsilon \left(-\frac{\delta(\mathbf{q}_T)}{\epsilon^2} + \mathcal{L}_1^{(0)}(\mathbf{q}_T, \mu) \right) \quad (5.186)$$

which appears in the context of calculations without a regulator.

5.C Fixed-Order Comparison

In this section we compare our results to that of [76]. In that reference, the QCD cross section for the process $N_1 N_2 \rightarrow V + X$ up to NLP is decomposed into a sum of convolutions of coefficient functions

multiplied by PDFs and their first derivatives, so that

$$\begin{aligned} \frac{1}{\sigma_0} \frac{d\sigma}{dq^2 dy d^2 \mathbf{q}_T} = & \int \frac{dz_a}{z_a} \frac{dz_b}{z_b} \left[C_{f_q f_{\bar{q}}}^{(0)}(z_a, z_b, q^2, q_T^2) f\left(\frac{x_a}{z_a}\right) f\left(\frac{x_b}{z_b}\right) \right. \\ & + \frac{1}{q^2} C_{f_q f_{\bar{q}}}^{(2)}(z_a, z_b, q^2, q_T^2) f\left(\frac{x_a}{z_a}\right) f\left(\frac{x_b}{z_b}\right) \\ & + \frac{1}{q^2} C_{f_q' f_{\bar{q}}}^{(2)}(z_a, z_b, q^2, q_T^2) \frac{x_a}{z_a} f'\left(\frac{x_a}{z_a}\right) f\left(\frac{x_b}{z_b}\right) \\ & + \frac{1}{q^2} C_{f_q f_{\bar{q}}'}^{(2)}(z_a, z_b, q^2, q_T^2) f\left(\frac{x_a}{z_a}\right) \frac{x_b}{z_b} f'\left(\frac{x_b}{z_b}\right) \\ & \left. + \frac{1}{q^2} C_{f_q' f_{\bar{q}}'}^{(2)}(z_a, z_b, q^2, q_T^2) \frac{x_a}{z_a} f'\left(\frac{x_a}{z_a}\right) \frac{x_b}{z_b} f'\left(\frac{x_b}{z_b}\right) \right], \end{aligned} \quad (5.187)$$

where at one loop

$$\begin{aligned} C_{f_q f_{\bar{q}}}^{(0)} = & \bar{\alpha} \left\{ \delta(\bar{z}_a) \delta(\bar{z}_b) \delta(q_T^2) \left(-\log^2 \frac{q^2}{\mu^2} + 3 \log \frac{q^2}{\mu^2} - 8 + 7\zeta_2 \right) \right. \\ & + \left[\frac{1}{q_T^2} \right]_+^{\mu^2} \left(\delta(\bar{z}_a) \left[\frac{1+z_b^2}{\bar{z}_b} \right]_+ + \delta(\bar{z}_b) \left[\frac{1+z_a^2}{\bar{z}_a} \right]_+ \right) \\ & - \delta(\bar{z}_a) \delta(\bar{z}_b) \left(2 \left[\frac{\log q_T^2/q^2}{q_T^2} \right]_+^{\mu^2} + 3 \left[\frac{1}{q_T^2} \right]_+^{\mu^2} \right) \\ & \left. + \delta(q_T^2) (\bar{z}_a \delta(\bar{z}_b) + \bar{z}_b \delta(\bar{z}_a) - \zeta_2 \delta(\bar{z}_a) \delta(\bar{z}_b)) \right\}, \end{aligned} \quad (5.188)$$

at LP, and

$$\begin{aligned} C_{f_q f_{\bar{q}}}^{(2)} = & \bar{\alpha} \left[-4\delta(\bar{z}_a) \delta(\bar{z}_b) - \delta(\bar{z}_a) \frac{1+z_b^2-4z_b^3}{z_b} - \frac{1+z_a^2-4z_a^3}{z_a} \delta(\bar{z}_b) \right] \\ C_{f_q' f_{\bar{q}}}^{(2)} = & \bar{\alpha} \left[\left(-\log \frac{q^2}{q_T^2} - 1 \right) \delta(\bar{z}_a) \delta(\bar{z}_b) \right. \\ & + \delta(\bar{z}_a) \left(\frac{1+3z_b+2z_b^2}{2z_b} - \left[\frac{1}{\bar{z}_b} \right]_+ \right) - \left(\frac{1+z_a+2z_a^3}{2z_a} + \left[\frac{1}{\bar{z}_a} \right]_+ \right) \delta(\bar{z}_b) \left. \right] \\ C_{f_q f_{\bar{q}}'}^{(2)} = & \bar{\alpha} \left[\left(-\log \frac{q^2}{q_T^2} - 1 \right) \delta(\bar{z}_a) \delta(\bar{z}_b) \right. \\ & - \delta(\bar{z}_a) \left(\frac{1+z_b+2z_b^3}{2z_b} + \left[\frac{1}{\bar{z}_b} \right]_+ \right) + \left(\frac{1+3z_a+2z_a^2}{2z_a} - \left[\frac{1}{\bar{z}_a} \right]_+ \right) \delta(\bar{z}_b) \left. \right] \\ C_{f_q' f_{\bar{q}}'}^{(2)} = & \bar{\alpha} \left[\left(2 \log \frac{q^2}{q_T^2} + 4 \right) \delta(\bar{z}_a) \delta(\bar{z}_b) \right. \\ & - \delta(\bar{z}_a) \left(\frac{1-2z_b-z_b^2}{2z_b} + 2 \left[\frac{1}{\bar{z}_b} \right]_+ \right) + \left(\frac{1-2z_a-z_a^2}{2z_a} + 2 \left[\frac{1}{\bar{z}_a} \right]_+ \right) \delta(\bar{z}_b) \left. \right] \end{aligned} \quad (5.189)$$

at NLP.

Since the $x_{a,b}$ in Eq. (5.187) differ from the $\xi_{1,2}$ used in Eq. (5.11) at $O(q_T^2/q_L^2)$, and since our results are expressed entirely in terms of PDFs instead of PDFs and their first derivatives, the results in Eq. (5.188) and Eq. (5.189) are related to Eq. (5.88) and Eq. (5.89) by a change of variables, integration by parts and a few distributional identities. Working in the hadronic center-of-mass frame for simplicity,

where $P_1^- = \sqrt{s} = P_2^+$, the variables $x_{a,b}$ may be written in terms of $\xi_{1,2}$ as

$$\begin{aligned} x_a &= \xi_1 \left(1 - \frac{1}{2} \frac{q_T^2}{q_L^2} + \dots \right), \\ x_b &= \xi_2 \left(1 - \frac{1}{2} \frac{q_T^2}{q_L^2} + \dots \right). \end{aligned} \quad (5.190)$$

Expanding (5.187)–(5.189) up to $O(q_T^2/q_L^2)$ gives

$$\begin{aligned} \frac{1}{\sigma_0} \frac{d\sigma}{dq^2 dy d^2\mathbf{q}_T} &= \sigma_0 \int \frac{dz_1}{z_1} \frac{dz_2}{z_2} \left[C_{f_q f_{\bar{q}}}^{(0)}(z_1, z_2, q_L^2, q_T^2) f\left(\frac{\xi_1}{z_1}\right) f\left(\frac{\xi_2}{z_2}\right) \right. \\ &\quad + \frac{1}{q_L^2} \left(C_{f_q f_{\bar{q}}}^{(2)}(z_1, z_2, q_L^2, q_T^2) + \delta C_{f_q f_{\bar{q}}}^{(0)}(z_1, z_2, q_L^2, q_T^2) \right) f\left(\frac{\xi_1}{z_1}\right) f\left(\frac{\xi_2}{z_2}\right) \\ &\quad + \frac{1}{q_L^2} \left(C_{f_q f_{\bar{q}}}^{(2)}(z_1, z_2, q_L^2, q_T^2) - \frac{1}{2} \frac{q_T^2}{q_L^2} C_{ff}^{(0)}(z_1, z_2) \right) \frac{\xi_1}{z_1} f'\left(\frac{\xi_1}{z_1}\right) f\left(\frac{\xi_2}{z_2}\right) \\ &\quad + \frac{1}{q_L^2} \left(C_{f_q f_{\bar{q}}}^{(2)}(z_1, z_2, q_L^2, q_T^2) - \frac{1}{2} \frac{q_T^2}{q_L^2} C_{ff}^{(0)}(z_1, z_2) \right) f\left(\frac{\xi_1}{z_1}\right) \frac{\xi_2}{z_2} f'\left(\frac{\xi_2}{z_2}\right) \\ &\quad \left. + \frac{1}{q_L^2} C_{f_q f_{\bar{q}}}^{(2)}(z_1, z_2, q_L^2, q_T^2) \frac{\xi_1}{z_1} f'\left(\frac{\xi_1}{z_1}\right) \frac{\xi_2}{z_2} f'\left(\frac{\xi_2}{z_2}\right) \right], \end{aligned} \quad (5.191)$$

where $C_{f_q f_{\bar{q}}}^{(0)}(z_1, z_2, q_L^2, q_T^2) = C_{ff}^{(0)}(z_1, z_2, q_L^2; q_T^2)$ in Eq. (5.88), and

$$\begin{aligned} C_{f_q f_{\bar{q}}}^{(2)} + \delta C_{f_q f_{\bar{q}}}^{(0)} &= \bar{\alpha} \left[-6\delta_1\delta_2 - \delta_1 \frac{1+z_2^2-4z_2^3}{z_2} - \frac{1+z_1^2-4z_1^3}{z_1} \delta_2 \right] \\ C_{f_q f_{\bar{q}}}^{(2)} - \frac{1}{2} \frac{q_T^2}{q_L^2} C_{f_q f_{\bar{q}}}^{(0)} &= \bar{\alpha} \left[\left(-2 \log \frac{q_L^2}{q_T^2} - 1 \right) \delta_1 \delta_2 \right. \\ &\quad \left. + \delta_1 \left(\frac{1+4z_2+3z_2^2}{2z_2} - 2 \left[\frac{1}{\bar{z}_2} \right]_+ \right) - \left(\frac{1-z_1^2+2z_1^3}{2z_1} + 2 \left[\frac{1}{\bar{z}_1} \right]_+ \right) \delta_2 \right] \\ C_{f_q f_{\bar{q}}}^{(2)} - \frac{1}{2} \frac{q_T^2}{q_L^2} C_{f_q f_{\bar{q}}}^{(0)} &= \bar{\alpha} \left[\left(-2 \log \frac{q_L^2}{q_T^2} - 1 \right) \delta_1 \delta_2 \right. \\ &\quad \left. - \delta_1 \left(\frac{1-z_2^2+2z_2^3}{2z_2} + 2 \left[\frac{1}{\bar{z}_2} \right]_+ \right) + \left(\frac{1+4z_1+3z_1^2}{2z_1} - 2 \left[\frac{1}{\bar{z}_1} \right]_+ \right) \delta_2 \right] \\ C_{f_q f_{\bar{q}}}^{(2)} &= \bar{\alpha} \left[\left(2 \log \frac{q_L^2}{q_T^2} + 4 \right) \delta_1 \delta_2 \right. \\ &\quad \left. - \delta_1 \left(\frac{1-2z_2-z_2^2}{2z_2} + 2 \left[\frac{1}{\bar{z}_2} \right]_+ \right) + \left(\frac{1-2z_1-z_1^2}{2z_1} + 2 \left[\frac{1}{\bar{z}_1} \right]_+ \right) \delta_2 \right]. \end{aligned} \quad (5.192)$$

Finally, the comparison is completed by applying the following integration by parts identities, valid when

$f(x/z) = 0$ for $x \geq z$,

$$\begin{aligned}
 \int \frac{dz}{z} \delta(\bar{z}) \frac{x}{z} f' \left(\frac{\xi}{z} \right) &= \int \frac{dz}{z} [-z \delta'(\bar{z})] f \left(\frac{\xi}{z} \right) \\
 \int \frac{dz}{z} z^n \frac{x}{z} f' \left(\frac{\xi}{z} \right) &= \int \frac{dz}{z} [nz^n - z \delta(\bar{z})] f \left(\frac{\xi}{z} \right) \\
 \int \frac{dz}{z} \left[\frac{1}{\bar{z}} \right]_+ \frac{x}{z} f' \left(\frac{\xi}{z} \right) &= \int \frac{dz}{z} \left(z \left[\frac{1}{\bar{z}^2} \right]_{++} + z \delta'(\bar{z}) \right. \\
 &\quad \left. - z \delta(\bar{z}) \right) f \left(\frac{\xi}{z} \right).
 \end{aligned} \tag{5.193}$$

These identities transform the coefficient functions in Eq. (5.192) from acting on derivatives of PDFs to the equivalent form of coefficient functions acting only on PDFs, and in doing so reproduces the NLP coefficient function in Eq. (5.89).

Chapter 6

Conclusions

In this thesis we have continued to develop a recent formulation of Soft-Collinear Effective Theory without modes, and have used this formalism to study power corrections to the Drell-Yan process when $q_T^2 \ll q^2$. The work presented here will provide a better understanding of power corrections in collider processes, which will provide increasingly narrow uncertainties when predicting observables measured at the LHC, and will help in the pursuit of new physics and in the measurement of the properties of the recently discovered Higgs boson.

In Chapter 2 we explained how EFTs are structured, how their factorization structure allows for the disentanglement of relevant energy scales, and how their RGE properties allow the logarithms of widely separated energy scales to be summed and brought under theoretical control. We demonstrated this at one-loop in the 4-Fermi Effective Theory, which we then used as an analogy to motivate the ideas behind our construction Soft-Collinear Effective Theory.

In Chapter 3 we derived an operator basis that is sufficient for describing QCD amplitudes up to $O(g_s)$ in the strong coupling and up to $O(1/Q^2)$ in the power counting. We used the spinor helicity formalism to expand QCD amplitudes, and matched these QCD amplitudes onto the operator basis at tree level. The $O(1/Q^2)$ operators we found were then renormalized, providing a renormalization group equation that, in the future, can be solved to find an all-orders form of the operator linking the hard scale Q and any arbitrary scale μ . In the derivation of the operator basis we assumed that the total transverse momentum \mathbf{p}_T of each sector vanished, eliminating the need for some operators which depend on this total \mathbf{p}_T . Since these total- \mathbf{p}_T operators are related through RPI to operators which are less suppressed by $1/Q$, the anomalous dimensions of these total- \mathbf{p}_T operators are also known. Thus, even for processes for which the total- \mathbf{p}_T of each sector can not be set to zero, the one-loop renormalization of the hard-scattering operator basis at $O(g_s, 1/Q^2)$ is now complete.

In Chapter 4, we analyzed two SCET_{II} observables in our formulation of SCET without modes. Starting with the massive Sudakov form factor, we found that the appearance of Q^2 in the effective theory is actually a hidden scheme dependence ν^2 brought about by the existence of rapidity divergences. Without an explicit regulator there are unregulated rapidity divergences in each sector and the overlap, which when summed together amount to a difference of infinities; interpreting this difference of infinities as a finite number is inherently a scheme-dependent process. Similarly with the δ -regulator, a separate δ for each sector and the overlap produces logarithms of the scheme-dependent ratio $\delta_n \delta_{\bar{n}} / \delta_o^2$. The existence of this scheme dependence was also shown to exist for the Drell-Yan process. We inferred

from these calculations that without reference to QCD, the effective theory does not involve dynamical dependence on the scale Q^2 , and that it is only when matching onto QCD at the hard scale that the hard scale can enter into the effective theory. In these calculations we also showed that our formulation of SCET reproduces the same leading-power resummation formulae found in the literature. The key point is that the scheme dependence, while fixed by matching at scales $\mu \gg q_T$, becomes free when $\mu \sim q_T$, allowing for a rapidity renormalization group to be used at the soft matching scale.

In Chapter 5, we demonstrated how our formalism can calculate and factorize the NLP cross section of the quark-induced Drell-Yan process when $\Lambda_{\text{QCD}}^2 \ll q_T^2 \ll q^2$, which had previously not been factorized at NLP in the perturbative ratio q_T^2/q^2 . We showed that, just as at LP, the NLP factorization naturally arises from a sequence of successive matching stages: we match QCD amplitudes onto SCET operators, we run these operators from q^2 down to q_T^2 , and finally we evolve the product of operators in rapidity space before matching onto PDFs. We have thus shown that the simplicity and straightforwardness of our formalism is useful for achieving factorization, and in the future, resummation, of observables at NLP.

From this point, there are many research directions to be explored in the future. While we have achieved a factorization for the NLP Drell-Yan process, we have still not attained an all-orders resummation for this observable. The operator products defined for the factorization have only been partially renormalized, and determining the full rapidity anomalous dimension matrix is necessary for correctly resumming the rapidity logarithms¹.

There are also many observables which remain to be studied in this formalism at next-to-leading power. With varying degrees of interest and urgency, one such list might include thrust (for measuring α_s), or deep-inelastic scattering (for measuring PDFs), or N-jettiness (for N-jettiness IR-divergence subtractions in numerical fixed-order cross section calculations), or Higgs decays through QCD diagrams (for measuring its properties more precisely).

Developing the factorization and resummation structure of thrust at NLP was the original aim of this thesis, but various complications pushed this goal to the side in favor of further developing the formalism. After completing the three works contained in this thesis, it seems likely that the complications are understood, and that the factorization can continue unhindered. The overlap subtraction of real emissions is now understood at NLP, so it should be possible to integrate over all of phase space for the emissions from each operator, where previously a hard boundary had to be placed to constrain an operator to only its own region of validity. Divergences which previously arose from integrating over matching coefficients $C_{2,i}(u) \sim 1/u$ are now accounted for by placing the $1/u$ into the operator, which allows the divergence to be controlled in dimensional regularization. The LL summation of thrust has already been demonstrated by the authors of [119], but we believe that if the full u -space RGE for the dijet operators can be solved, even numerically, then a NLL summation of thrust at NLP is possible.

Regarding the last item in the list of possible observables to study at NLP, studying bottom-mediated $h \rightarrow \gamma\gamma$ decay has already been initiated in SCET using the method-of-regions approach [87–90]. There, the use of non-standard subtraction notation, infinity-bins, and the lack of a renormalized factorization formula leads us to believe that our formalism might provide further clarity to the factorization structure of this NLP observable.

¹Some authors [67] count the vector plus-distributions $\mathcal{L}_{0T} \sim \log q_T^2/\mu^2$ as large logarithms and thus in their log-counting they can partition their anomalous dimensions into LL and NLL pieces. These LL pieces are related to the cusp anomalous dimension via consistency relations, and are thus known (even in our formalism) for every NLP operator product. However in our formalism the rapidity running is performed at $\mu \sim q_T$, so we do not consider $\mathcal{L}_{0T} \sim \log q_T^2/\mu^2$ to be large, and thus we find no benefit to using these consistency relations.

Finally, there are still some leading-power theoretical foundations which are well understood in SCET's usual formulation which have not been studied in our formalism. Namely, the existence and/or necessity for Glauber modes [177, 178] in our formulation of SCET has not been established, and if they are required it has not been shown how they should be treated in our formalism. Referring to the mode picture in SCET, since $p_n \sim Q(\lambda^2, 1, \lambda)$ and $p_{\text{Glauber}} \sim Q(\lambda^2, \lambda^2, \lambda)$, then the invariant mass of a collinear-Glauber interaction is $(p_n + p_{\text{Glauber}})^2 \sim \lambda^2 Q^2 \ll Q^2$. The collinear-Glauber interactions are thus below the cutoff Q^2 of the EFT, and therefore Glauber modes should not be treated as a separate degree of freedom until a lower energy scale is reached. It will be left for future work, however, to decide how Glauber modes are to be handled.

6.1 Epilogue

Graduate school is a long exploration into the unknown, requiring years of deep thought, spurts of frenetic work, and many inevitable failures. This cyclic process needs a vast well of motivation to draw upon, so I think it appropriate for me to bookend this journey with a verse that has often provided a place of still quietude through which my mind may wander.

*O*verhead the albatross hangs motionless upon the air
And deep beneath the rolling waves in labyrinths of coral caves
The echo of a distant time comes willowing across the sand
And everything is green and submarine

*A*nd no one showed us to the land
And no one knows the where's or why's
But something stirs and something tries
And starts to climb toward the light

– Pink Floyd, *Echoes*

Appendix A

QCD Expansion up to $O(1/Q^2)$

In this Appendix we complete the Section 2.3.1 expansion of QCD 1-gluon amplitudes up to $O(1/Q^2)$, which is necessary for the tree-level matching of QCD onto SCET operators which are relevant for dijet production (and DY and DIS) up to $O(g_s)$. This was also done in the spinor-helicity formalism in Chapter 3, but it should also be helpful to collect the various formulae in the much more prevalent Dirac notation. From Eqs. (2.24) and (2.25), the amplitude to be expanded is

$$i\mathcal{M}_{a+b} = igT_{cc'}^a \bar{u}^c(p_1) \left(P_{\bar{n}} - \frac{\not{p}_{1\perp} \not{k}}{p_1^-/2} \right) \left(-\frac{2p_1^\alpha + \gamma^\alpha \not{k}}{2p_1 \cdot k} \gamma^\mu + \gamma^\mu \frac{2p_2^\alpha + \not{k} \gamma^\alpha}{2p_2 \cdot k} \right) \left(P_{\bar{n}} - \frac{\not{p} \not{p}_{2\perp}}{2 p_2^+} \right) v^{c'}(p_2) \epsilon_\alpha^*. \quad (\text{A.1})$$

Following the same methods of [163], there are six distinct topologies of these three final state particle into collimated jets. A quark and a gluon forming jet 1 (jet 2) is called *A*-type (\bar{A} -type), a quark by itself forming jet 1 (jet 2) is called *B*-type (\bar{B} -type), while a quark and an antiquark forming jet 1 (jet 2) is called *C*-type (\bar{C} -type). The barred groupings are related to the unbarred grouping by interchanging $n \leftrightarrow \bar{n}$, while the *A*- and *B*-type grouping are related by CP (Hermitian conjugation $+ n \leftrightarrow \bar{n}$). Thus the full operator basis up to $O(g_s)$ may be entirely determined by considering only the *A*-type and the *C*-type expansions, which we do in the following subsections.

Before expanding momentum components, it is useful to apply a topology non-specific manipulation of the above matrix element which places the projection operators adjacent to the central gamma matrix γ^μ . It can be shown with much effort that the spinor expansions obey the commutation relations

$$\epsilon_\alpha^* \bar{u}(p) \left[P_{\bar{n}} - \frac{\not{p}_{\perp} \not{k}}{p^-/2}, 2p^\alpha + \gamma^\alpha \not{k} \right] = \epsilon_\alpha^* \bar{u}(p) \left(\frac{2p \cdot k}{p^+ + k^-} \bar{\Delta}^{\alpha\sigma}(p) - \frac{2p^\alpha + \not{k} \gamma^\alpha}{p^- + k^-} \bar{\Delta}^{\rho\sigma}(p) k_\rho \right) \gamma_\sigma^\perp \frac{\not{k}}{2}, \quad (\text{A.2})$$

and

$$\left[2p^\alpha + \not{k} \gamma^\alpha, P_{\bar{n}} - \frac{\not{p} \not{p}_{\perp}}{2 p^+} \right] v_{\bar{n}}(p) \epsilon_\alpha^* = \frac{\not{p}}{2} \gamma_\sigma^\perp \left(\frac{2p \cdot k}{p^+ + k^+} \Delta^{\alpha\sigma}(p) - \frac{2p^\alpha + \not{k} \gamma^\alpha}{p^+ + k^+} \Delta^{\rho\sigma}(p) k_\rho \right) v_{\bar{n}}(p) \epsilon_\alpha^*, \quad (\text{A.3})$$

so that after applying these relations the amplitude reads

$$i\mathcal{M}_{a+b} = igT_{cc'}^a \bar{u}^c(p_1) \left\{ - \left[\frac{2p_1^\alpha + \gamma^\alpha \not{k}}{2p_1 \cdot k} \left(P_{\bar{n}} - \frac{\not{p}_{1\perp} + \not{k}_\perp \not{k}}{p_1^- + k^-/2} \right) + \frac{\bar{\Delta}^{\alpha\sigma}(p_1)}{p_1^- + k^-} \gamma_\sigma^\perp \frac{\not{k}}{2} \right] \gamma^\mu \left(P_{\bar{n}} - \frac{\not{p} \not{p}_{2\perp}}{2 p_2^+} \right) \right. \\ \left. + \left(P_{\bar{n}} - \frac{\not{p}_{1\perp} \not{k}}{p_1^-/2} \right) \gamma^\mu \left(P_{\bar{n}} - \frac{\not{p} \not{p}_{2\perp} + \not{k}_\perp}{2 p_2^+ + k^+} \right) \frac{2p_2^\alpha + \not{k} \gamma^\alpha}{2p_2 \cdot k} + \frac{\not{p}}{2} \gamma_\sigma^\perp \frac{\Delta^{\alpha\sigma}(p_2)}{p_2^+ + k^+} \right\} v^{c'}(p_2) \epsilon_\alpha^*(q), \quad (\text{A.4})$$

From this point, we expand with topology-specific momentum scalings.

A-Type Expansion

In the case that both the gluon and quark are n -collinear and recoil against an \bar{n} -collinear antiquark, the amplitudes in eq. (A.1) can be expanded in inverse powers of the hard scale q_L . If SCET is a valid effective field theory, i.e. $p_n^2, p_{\bar{n}}^2, \mathbf{p}_{1T}^2, \mathbf{p}_{2T}^2, \mathbf{k}_T^2 \ll q_L^2$, then in this topology we can derive that

$$\begin{aligned}\bar{\eta} \cdot p_n &= \bar{\eta} \cdot (q - p_{\bar{n}}) = \sqrt{q^+ q^-} \left(1 - \frac{p_{\bar{n}}^2 + \mathbf{p}_{\bar{n}T}^2}{\eta \cdot p_{\bar{n}} \bar{\eta} \cdot q} \right) \sim q_L + \dots, \text{ and} \\ \eta \cdot p_{\bar{n}} &= \bar{\eta} \cdot (q - p_n) = \sqrt{q^+ q^-} \left(1 - \frac{p_n^2 + \mathbf{p}_{nT}^2}{\bar{\eta} \cdot p_n \eta \cdot q} \right) \sim q_L + \dots.\end{aligned}\quad (\text{A.5})$$

The expanded amplitude to produce the A-type final state is then

$$i\mathcal{M}_{a+b}^{\text{Type A}} = igT_{cc'}^a \bar{u}^c(p_1) \left(\mathcal{A}^{(0)} + \frac{1}{q_L} \mathcal{A}^{(1)} + \frac{1}{q_L^2} \mathcal{A}^{(2)} + \dots \right) v^{c'}(p_2) \epsilon_{\alpha}^*, \quad (\text{A.6})$$

where the order-by-order amplitudes (with implied Lorentz indices μ and α) are¹

$$\begin{aligned}\mathcal{A}^{(0)} &= - \left(\frac{2p_1^{\alpha} + \gamma^{\alpha} \not{k}}{2p_1 \cdot k} - \frac{\bar{n}^{\alpha}}{k^-} \right) P_{\bar{n}} \gamma^{\mu} P_{\bar{n}} \\ \mathcal{A}^{(1)} &= \left(\frac{2p_1^{\alpha} + \gamma^{\alpha} \not{k}}{2p_1 \cdot k} - \frac{\bar{n}^{\alpha}}{k^-} \right) \left(\not{p}_{n\perp} \frac{\not{\eta}}{2} \gamma^{\mu} P_{\bar{n}} + P_{\bar{n}} \gamma^{\mu} \frac{\not{\eta}}{2} \not{p}_{\bar{n}\perp} \right) \\ &\quad + \bar{\Delta}^{\alpha\rho}(k) \left(P_{\bar{n}} \gamma^{\mu} \frac{\not{\eta}}{2} \gamma_{\rho}^{\perp} - \gamma_{\rho}^{\perp} \frac{\not{\eta}}{2} \gamma^{\mu} P_{\bar{n}} \right) \\ \mathcal{A}^{(2)} &= - \left(\frac{2p_1^{\alpha} + \gamma^{\alpha} \not{k}}{2p_1 \cdot k} - \frac{\bar{n}^{\alpha}}{k^-} \right) \not{p}_{1\perp} \frac{\not{\eta}}{2} P_{\bar{n}} \gamma^{\mu} \frac{\not{\eta}}{2} \not{p}_{\bar{n}\perp} \\ &\quad + \frac{p_{\bar{n}}^-}{k^-} P_{\bar{n}} \gamma^{\mu} P_{\bar{n}} \gamma_{\rho}^{\perp} \gamma_{\sigma}^{\perp} k^{\rho} \bar{\Delta}^{\alpha\sigma}(k) + \frac{p_{\bar{n}}^-}{p_1^-} \gamma_{\rho}^{\perp} \frac{\not{\eta}}{2} \gamma^{\mu} \frac{\not{\eta}}{2} \gamma_{\sigma}^{\perp} k^{\rho} \bar{\Delta}^{\alpha\sigma}(k) \\ &\quad - \bar{\Delta}^{\alpha\rho}(k) \left(\frac{p_{\bar{n}}^-}{p_1^-} \not{p}_{n\perp} \frac{\not{\eta}}{2} \gamma^{\mu} \frac{\not{\eta}}{2} \gamma_{\rho}^{\perp} - \gamma_{\rho}^{\perp} \frac{\not{\eta}}{2} \gamma^{\mu} \frac{\not{\eta}}{2} \not{p}_{\bar{n}\perp} \right) \\ &\quad + 2g_{\rho\sigma}^{\perp} \frac{p_{\bar{n}}^-}{k^-} \bar{\Delta}^{\alpha\rho}(k) P_{\bar{n}} \gamma^{\mu} P_{\bar{n}} p_{\bar{n}}^{\sigma},\end{aligned}\quad (\text{A.7})$$

and we have defined the net momenta contributing to the n - and \bar{n} -jets as $p_n = p_1 + k$ and $p_{\bar{n}} = p_2$.

The leading-power amplitude $\mathcal{A}^{(0)}$ is reproduced by the operator $O_{2(0)}$

$$O_{2(0)}^{\mu}(x) = [\bar{\chi}_n(x)] \gamma^{\mu} [\chi_{\bar{n}}(x)] \quad (\text{A.8})$$

along with an insertion of the QCD Lagrangian in the n -sector, where we have defined $\chi_{\bar{n}} = \bar{\psi}_n W_n P_{\bar{n}}$, $\chi_n = P_{\bar{n}} W_n^{\dagger} \psi_{\bar{n}}$. The first lines of $\mathcal{A}^{(1)}$ and $\mathcal{A}^{(2)}$ are similarly reproduced by the operators

$$\begin{aligned}O_{2(1\perp_1)}^{\mu}(x) &= [i\partial^{\rho} \bar{\chi}_n(x)] \gamma_{\rho}^{\perp} \frac{\not{\eta}}{2} \gamma^{\mu} [\chi_{\bar{n}}(x)] \\ O_{2(1\perp_2)}^{\mu}(x) &= [\bar{\chi}_n(x)] \gamma^{\mu} \frac{\not{\eta}}{2} \gamma_{\rho}^{\perp} [i\partial^{\rho} \chi_{\bar{n}}(x)] \\ O_{2(2\perp_1\perp_2)}^{\mu}(x) &= [i\partial^{\rho} \bar{\chi}_n(x)] \gamma_{\rho}^{\perp} \frac{\not{\eta}}{2} \gamma^{\mu} \frac{\not{\eta}}{2} \gamma_{\sigma}^{\perp} [i\partial^{\sigma} \chi_{\bar{n}}(x)],\end{aligned}\quad (\text{A.9})$$

again with an insertion of the QCD Lagrangian in the n -sector.

¹Technical detail: Power counting lightcone components of polarization vectors is a difficult topic. Perhaps the most formal method is to write the polarization of a gluon with momentum k as $\epsilon_{L,R}^{\mu}(k,r) = \mp \frac{\bar{u}_{L,R}(r) \gamma_{\mu} u_{L,R}(k)}{\sqrt{2} \bar{u}_{R,L}(r) u_{L,R}(k)}$, where r is an arbitrary lightlike 4-vector with $r \cdot k \neq 0$ which acts as a gauge parameter that must drop out of the equation for any observable [169]. Through the application of the spinor expansion in Eq. (2.25), the power counting of the lightcone components of ϵ^{μ} then follow the same power counting as k^{μ} .

The second line of $\mathcal{A}^{(1)}$ is reproduced by the operators

$$\begin{aligned} O_{2(1A_1)}^\mu(x, \hat{t}) &= [\bar{\chi}_n(x) \mathcal{B}_n^\rho(x + \bar{n}t)] \gamma^\mu \frac{\not{q}}{2} \gamma_\rho^\perp [\chi_{\bar{n}}(x)] \\ O_{2(1A_2)}^\mu(x, \hat{t}) &= -[\bar{\chi}_n(x) \mathcal{B}_n^\rho(x + \bar{n}t)] \gamma_\rho^\perp \frac{\not{q}}{2} \gamma^\mu [\chi_{\bar{n}}(x)] , \end{aligned} \quad (\text{A.10})$$

while the second line of $\mathcal{A}^{(2)}$ is reproduced by the operators

$$\begin{aligned} O_{2(2A_1)}^\mu(x, \hat{t}) &= -2\pi i \theta(\hat{t}) \otimes [\bar{\chi}_n(x) \mathcal{B}_n^{\rho\sigma}(x + \bar{n}t)] \gamma^\mu \gamma_\rho^\perp \gamma_\sigma^\perp [\chi_{\bar{n}}(x)] \\ O_{2(2A_2)}^\mu(x, \hat{t}) &= -2\pi i \theta(\hat{t}) \otimes [\bar{\chi}_n(x + \bar{n}t) \mathcal{B}_n^{\rho\sigma}(x)] \gamma_\rho^\perp \frac{\not{q}}{2} \gamma^\mu \frac{\not{q}}{2} \gamma_\sigma^\perp [\chi_{\bar{n}}(x)] \end{aligned} \quad (\text{A.11})$$

and the third and fourth lines of $\mathcal{A}^{(2)}$ are reproduced by the operators

$$\begin{aligned} O_{2(2A_3)}^\mu(x, \hat{t}) &= 2\pi i \theta(\hat{t}) \otimes [i \partial^\rho \bar{\chi}_n(x + \bar{n}t) \mathcal{B}_n^\sigma(x)] \gamma_\rho^\perp \frac{\not{q}}{2} \gamma^\mu \frac{\not{q}}{2} \gamma_\sigma^\perp [\chi_{\bar{n}}(x)] \\ O_{2(2A_4)}^\mu(x, \hat{t}) &= -[\bar{\chi}_n(x) \mathcal{B}_n^\rho(x + \bar{n}t)] \gamma_\rho^\perp \frac{\not{q}}{2} \gamma^\mu \frac{\not{q}}{2} \gamma_\sigma^\perp [i \partial^\sigma \chi_{\bar{n}}(x)] \\ O_{2(2A_5)}^\mu(x, \hat{t}) &= -2\pi i \theta(\hat{t}) \otimes [\bar{\chi}_n(x) \mathcal{B}_n^\rho(x + \bar{n}t)] \gamma^\mu \{\gamma_\rho^\perp, \gamma_\sigma^\perp\} [i \partial^\sigma \chi_{\bar{n}}(x)] . \end{aligned} \quad (\text{A.12})$$

Shifts and convolutions are defined in Chapter 5. In that chapter the quarks are incoming rather than outgoing so while the overall structure of these operators are largely the same the definitions here are slightly different.

The operators we renormalized in Chapter 3 do not contain the \hat{t} convolutional structure appearing in these definitions (the importance of which is discussed in Chapter 5), meaning that the matching coefficients in Chapter 3 have a $\theta(\hat{t}) \rightarrow 1/u$ functional dependence rather than a $\delta(\hat{t}) \rightarrow 1$ functional dependence. While this difference in definitions will change the anomalous dimensions derived in Chapter 3, since the operator definitions differ by a simple scaling $O_2(u) \rightarrow O_2(u)/u$, the change in the anomalous dimension is directly calculable without performing the calculation anew. Depending on conventions, this should be as simple as $\gamma(u, v) \rightarrow (v/u)\gamma(u, v)$.

C-Type Expansion

In the case that only the gluon is n -collinear, recoiling against an \bar{n} -collinear quark and antiquark, the amplitude in Eq. (A.4) is

$$i\mathcal{M}_{a+b}^{\text{Type C}} = ig T_{cc'}^a \bar{u}^c(p_1) \left(\frac{1}{q_L} \mathcal{C}^{(1)} + \dots \right) v^{c'}(p_2) \epsilon_\alpha^* , \quad (\text{A.13})$$

We can stop the expansion at $O(1/q_L)$ – since observables involve squared amplitudes, and since there are no leading-power terms in this expansion, no higher-order terms are required for the observable to achieve $O(1/q_L^2)$ accuracy.

The $O(1/q_L)$ amplitude is found to be

$$\mathcal{C}^{(1)} = \bar{\Delta}^{\alpha\rho}(k) \left(\frac{p_{\bar{n}}^\perp}{p_2^\perp} P_n \gamma^\mu \frac{\not{q}}{2} \gamma_\rho^\perp - \frac{p_{\bar{n}}^\perp}{p_1^\perp} \gamma_\rho^\perp \frac{\not{q}}{2} \gamma^\mu P_n \right) , \quad (\text{A.14})$$

where we have defined the net momenta $p_n = k$ and $p_{\bar{n}} = p_1 + p_2$.

These terms are reproduced by the operators

$$\begin{aligned} O_{2(1C_1)}^\mu(x, \hat{t}) &= 2\pi i \theta(\hat{t}) \otimes [\mathcal{B}_n^\rho(x)]^{cc'} [\bar{\chi}_{\bar{n}}^c(x) \gamma^\mu \frac{\not{q}}{2} \gamma_\rho^\perp \chi_{\bar{n}}^{c'}(x + nt)] \\ O_{2(1C_2)}^\mu(x, \hat{t}) &= -2\pi i \theta(\hat{t}) \otimes [\mathcal{B}_n^\rho(x)]^{cc'} [\bar{\chi}_{\bar{n}}^c(x + nt) \gamma_\rho^\perp \frac{\not{q}}{2} \gamma^\mu \chi_{\bar{n}}^{c'}(x)] . \end{aligned} \quad (\text{A.15})$$

Bibliography

- [1] SUPER-KAMIOKANDE collaboration, Y. Fukuda et al., *Evidence for oscillation of atmospheric neutrinos*, *Phys. Rev. Lett.* **81** (1998) 1562–1567, [[hep-ex/9807003](#)].
- [2] SNO collaboration, Q. R. Ahmad et al., *Direct evidence for neutrino flavor transformation from neutral current interactions in the Sudbury Neutrino Observatory*, *Phys. Rev. Lett.* **89** (2002) 011301, [[nucl-ex/0204008](#)].
- [3] M. Hirsch, R. Srivastava and J. W. F. Valle, *Can one ever prove that neutrinos are Dirac particles?*, *Phys. Lett. B* **781** (2018) 302–305, [[1711.06181](#)].
- [4] G. 't Hooft and M. J. G. Veltman, *One loop divergencies in the theory of gravitation*, *Ann. Inst. H. Poincaré Phys. Theor. A* **20** (1974) 69–94.
- [5] M. H. Goroff and A. Sagnotti, *The Ultraviolet Behavior of Einstein Gravity*, *Nucl. Phys. B* **266** (1986) 709–736.
- [6] SUPERNOVA SEARCH TEAM collaboration, A. G. Riess et al., *Observational evidence from supernovae for an accelerating universe and a cosmological constant*, *Astron. J.* **116** (1998) 1009–1038, [[astro-ph/9805201](#)].
- [7] SUPERNOVA COSMOLOGY PROJECT collaboration, S. Perlmutter et al., *Measurements of Ω and Λ from 42 high redshift supernovae*, *Astrophys. J.* **517** (1999) 565–586, [[astro-ph/9812133](#)].
- [8] F. Zwicky, *On the Masses of Nebulae and of Clusters of Nebulae*, *Astrophys. J.* **86** (1937) 217–246.
- [9] S. Profumo, L. Giani and O. F. Piattella, *An Introduction to Particle Dark Matter*, *Universe* **5** (2019) 213, [[1910.05610](#)].
- [10] S. Dodelson, *The Real Problem with MOND*, *Int. J. Mod. Phys. D* **20** (2011) 2749–2753, [[1112.1320](#)].
- [11] MINIBOONE collaboration, A. A. Aguilar-Arevalo et al., *Updated MiniBooNE neutrino oscillation results with increased data and new background studies*, *Phys. Rev. D* **103** (2021) 052002, [[2006.16883](#)].
- [12] LSND collaboration, C. Athanassopoulos et al., *Evidence for $\bar{\nu}_\mu \rightarrow \bar{\nu}_e$ oscillations from the LSND experiment at LAMPF*, *Phys. Rev. Lett.* **77** (1996) 3082–3085, [[nucl-ex/9605003](#)].
- [13] MUON G-2 collaboration, B. Abi et al., *Measurement of the Positive Muon Anomalous Magnetic Moment to 0.46 ppm*, *Phys. Rev. Lett.* **126** (2021) 141801, [[2104.03281](#)].
- [14] MUON G-2 collaboration, G. W. Bennett et al., *Final Report of the Muon E821 Anomalous Magnetic Moment Measurement at BNL*, *Phys. Rev. D* **73** (2006) 072003, [[hep-ex/0602035](#)].
- [15] LHCb collaboration, R. Aaij et al., *Test of lepton universality in beauty-quark decays*, [2103.11769](#).

- [16] ATLAS collaboration, G. Aad et al., *Observation of a new particle in the search for the Standard Model Higgs boson with the ATLAS detector at the LHC*, *Phys. Lett. B* **716** (2012) 1–29, [[1207.7214](#)].
- [17] CMS collaboration, S. Chatrchyan et al., *Observation of a New Boson at a Mass of 125 GeV with the CMS Experiment at the LHC*, *Phys. Lett. B* **716** (2012) 30–61, [[1207.7235](#)].
- [18] ATLAS, CMS collaboration, A. Sopczak, *Precision measurements in Higgs sector at ATLAS and CMS*, *Pos FFK2019* (2020) 006, [[2001.05927](#)].
- [19] S. D. Drell and T.-M. Yan, *Massive Lepton Pair Production in Hadron-Hadron Collisions at High-Energies*, *Phys. Rev. Lett.* **25** (1970) 316–320.
- [20] H. D. Politzer, *STILL QCD-ing*, *Proceedings of the Eighth Hawaii Topical Conference in Particle Physics* (1979) 268–375.
- [21] J. R. Oppenheimer, B. Rossi, A. Pais, Collins and Dalitz, *Elementary particles*, in *5th Annual Rochester Conference on High-Energy Nuclear Physics*, pp. 241–269, 1955.
- [22] J. R. Oppenheimer, C. N. Yang, C. Wentzel, R. E. Marshak, R. H. Dalitz, M. Gell-Mann et al., *Theoretical interpretation of new particles*, in *6th Annual Rochester Conference on High-Energy Nuclear Physics*, pp. VIII.1–36, 1956.
- [23] M. Gell-Mann, *The Eightfold Way: A Theory of Strong Interaction Symmetry*, *CTSL-20, TID-12608* (1961) .
- [24] Y. Ne'eman, *Derivation of strong interactions from a gauge invariance*, *Nucl. Phys.* **26** (1961) 222–229.
- [25] M. Gell-Mann, *A Schematic Model of Baryons and Mesons*, *Phys. Lett.* **8** (1964) 214–215.
- [26] E. D. Bloom et al., *High-Energy Inelastic e-p Scattering at 6-Degrees and 10-Degrees*, *Phys. Rev. Lett.* **23** (1969) 930–934.
- [27] C. G. Callan, Jr. and D. J. Gross, *High-energy electroproduction and the constitution of the electric current*, *Phys. Rev. Lett.* **22** (1969) 156–159.
- [28] R. P. Feynman, *Very high-energy collisions of hadrons*, *Phys. Rev. Lett.* **23** (Dec, 1969) 1415–1417.
- [29] J. D. Bjorken and E. A. Paschos, *Inelastic Electron Proton and gamma Proton Scattering, and the Structure of the Nucleon*, *Phys. Rev.* **185** (1969) 1975–1982.
- [30] GARGAMELLE NEUTRINO collaboration, H. Deden et al., *Experimental Study of Structure Functions and Sum Rules in Charge Changing Interactions of Neutrinos and Anti-Neutrinos on Nucleons*, *Nucl. Phys. B* **85** (1975) 269–288.
- [31] C.-N. Yang and R. L. Mills, *Conservation of Isotopic Spin and Isotopic Gauge Invariance*, *Phys. Rev.* **96** (1954) 191–195.
- [32] G. 't Hooft, *Renormalization of Massless Yang-Mills Fields*, *Nucl. Phys. B* **33** (1971) 173–199.
- [33] H. D. Politzer, *Reliable Perturbative Results for Strong Interactions?*, *Phys. Rev. Lett.* **30** (1973) 1346–1349.
- [34] D. J. Gross and F. Wilczek, *Ultraviolet Behavior of Nonabelian Gauge Theories*, *Phys. Rev. Lett.* **30** (1973) 1343–1346.

- [35] H. Fritzsch, M. Gell-Mann and H. Leutwyler, *Advantages of the Color Octet Gluon Picture*, *Phys. Lett. B* **47** (1973) 365–368.
- [36] J. Ellis, *The Discovery of the Gluon*, *Int. J. Mod. Phys. A* **29** (2014) 1430072, [[1409.4232](#)].
- [37] TASSO collaboration, R. Brandelik et al., *Evidence for Planar Events in e^+e^- Annihilation at High-Energies*, *Phys. Lett. B* **86** (1979) 243–249.
- [38] K. G. Wilson, *Confinement of quarks*, *Phys. Rev. D* **10** (Oct, 1974) 2445–2459.
- [39] C. Davies, *Lattice QCD: A Guide for people who want results*, in *58th Scottish Universities Summer School in Physics (SUSSP58): A NATO Advanced Study Institute and EU Hadron Physics 13 Summer Institute*, pp. 233–272, 9, 2005, [hep-lat/0509046](#).
- [40] X. Ji, *Parton Physics on a Euclidean Lattice*, *Phys. Rev. Lett.* **110** (2013) 262002, [[1305.1539](#)].
- [41] X. Ji, *Parton Physics from Large-Momentum Effective Field Theory*, *Sci. China Phys. Mech. Astron.* **57** (2014) 1407–1412, [[1404.6680](#)].
- [42] M. A. Ebert, S. T. Schindler, I. W. Stewart and Y. Zhao, *One-loop Matching for Spin-Dependent Quasi-TMDs*, *JHEP* **09** (2020) 099, [[2004.14831](#)].
- [43] A. V. Manohar, *Effective field theories*, *Lect. Notes Phys.* **479** (1997) 311–362, [[hep-ph/9606222](#)].
- [44] S. Weinberg, *Dynamical approach to current algebra*, *Phys. Rev. Lett.* **18** (1967) 188–191.
- [45] K. G. Wilson, *The Renormalization Group: Critical Phenomena and the Kondo Problem*, *Rev. Mod. Phys.* **47** (1975) 773.
- [46] S. Weinberg, *Phenomenological Lagrangians*, *Physica A* **96** (1979) 327–340.
- [47] S. Weinberg, *Effective Gauge Theories*, *Phys. Lett. B* **91** (1980) 51–55.
- [48] H. D. Politzer and M. B. Wise, *Effective Field Theory Approach to Processes Involving Both Light and Heavy Fields*, *Phys. Lett. B* **208** (1988) 504–507.
- [49] J. C. Collins, D. E. Soper and G. F. Sterman, *Transverse Momentum Distribution in Drell-Yan Pair and W and Z Boson Production*, *Nucl. Phys. B* **250** (1985) 199–224.
- [50] J. C. Collins, D. E. Soper and G. F. Sterman, *Factorization for Short Distance Hadron - Hadron Scattering*, *Nucl. Phys. B* **261** (1985) 104–142.
- [51] J. Collins, *Foundations of perturbative QCD*, vol. 32. Cambridge University Press, 2013, [10.1017/CBO9780511975592](#).
- [52] W. Bizon, P. F. Monni, E. Re, L. Rottoli and P. Torrielli, *Momentum-space resummation for transverse observables and the Higgs p_\perp at $N^3LL+NNLO$* , *JHEP* **02** (2018) 108, [[1705.09127](#)].
- [53] V. Bertone, I. Scimemi and A. Vladimirov, *Extraction of unpolarized quark transverse momentum dependent parton distributions from Drell-Yan/Z-boson production*, *JHEP* **06** (2019) 028, [[1902.08474](#)].
- [54] A. Bacchetta, V. Bertone, C. Bissolotti, G. Bozzi, F. Delcarro, F. Piacenza et al., *Transverse-momentum-dependent parton distributions up to N^3LL from Drell-Yan data*, *JHEP* **07** (2020) 117, [[1912.07550](#)].

- [55] M. A. Ebert, J. K. L. Michel, I. W. Stewart and F. J. Tackmann, *Drell-Yan q_T resummation of fiducial power corrections at $N^3 LL$* , *JHEP* **04** (2021) 102, [[2006.11382](#)].
- [56] T. Becher and T. Neumann, *Fiducial q_T resummation of color-singlet processes at $N^3 LL + NNLO$* , *JHEP* **03** (2021) 199, [[2009.11437](#)].
- [57] S. Camarda, L. Cieri and G. Ferrera, *Drell-Yan lepton-pair production: q_T resummation at $N^3 LL$ accuracy and fiducial cross sections at $N^3 LO$* , [2103.04974](#).
- [58] E. Re, L. Rottoli and P. Torrielli, *Fiducial Higgs and Drell-Yan distributions at $N^3 LL' + NNLO$ with RadISH*, *JHEP* **09** (2021) 108, [[2104.07509](#)].
- [59] R. K. Ellis, W. Furmanski and R. Petronzio, *Power Corrections to the Parton Model in QCD*, *Nucl. Phys. B* **207** (1982) 1–14.
- [60] R. K. Ellis, W. Furmanski and R. Petronzio, *Unraveling Higher Twists*, *Nucl. Phys. B* **212** (1983) 29.
- [61] R. L. Jaffe, *Parton Distribution Functions for Twist Four*, *Nucl. Phys. B* **229** (1983) 205–230.
- [62] J.-W. Qiu, *Twist Four Contributions to the Parton Structure Functions*, *Phys. Rev. D* **42** (1990) 30–44.
- [63] J.-W. Qiu and G. F. Sterman, *Power corrections in hadronic scattering (1). Leading $1/Q^2$ corrections to the Drell-Yan cross-section*, *Nucl. Phys. B* **353** (1991) 105–136.
- [64] T. Becher and M. Neubert, *Drell-Yan Production at Small q_T , Transverse Parton Distributions and the Collinear Anomaly*, *Eur. Phys. J. C* **71** (2011) 1665, [[1007.4005](#)].
- [65] M. G. Echevarria, A. Idilbi and I. Scimemi, *Factorization Theorem For Drell-Yan At Low q_T And Transverse Momentum Distributions On-The-Light-Cone*, *JHEP* **07** (2012) 002, [[1111.4996](#)].
- [66] J. C. Collins and T. C. Rogers, *Equality of Two Definitions for Transverse Momentum Dependent Parton Distribution Functions*, *Phys. Rev. D* **87** (2013) 034018, [[1210.2100](#)].
- [67] M. A. Ebert and F. J. Tackmann, *Resummation of Transverse Momentum Distributions in Distribution Space*, *JHEP* **02** (2017) 110, [[1611.08610](#)].
- [68] C. W. Bauer, S. Fleming and M. E. Luke, *Summing Sudakov logarithms in $B \rightarrow X_s \gamma$ in effective field theory*, *Phys. Rev. D* **63** (2000) 014006, [[hep-ph/0005275](#)].
- [69] C. W. Bauer, S. Fleming, D. Pirjol and I. W. Stewart, *An Effective field theory for collinear and soft gluons: Heavy to light decays*, *Phys. Rev. D* **63** (2001) 114020, [[hep-ph/0011336](#)].
- [70] C. W. Bauer and I. W. Stewart, *Invariant operators in collinear effective theory*, *Phys. Lett. B* **516** (2001) 134–142, [[hep-ph/0107001](#)].
- [71] C. W. Bauer, D. Pirjol and I. W. Stewart, *Soft collinear factorization in effective field theory*, *Phys. Rev. D* **65** (2002) 054022, [[hep-ph/0109045](#)].
- [72] C. W. Bauer, S. Fleming, D. Pirjol, I. Z. Rothstein and I. W. Stewart, *Hard scattering factorization from effective field theory*, *Phys. Rev. D* **66** (2002) 014017, [[hep-ph/0202088](#)].
- [73] M. Beneke, A. P. Chapovsky, M. Diehl and T. Feldmann, *Soft collinear effective theory and heavy to light currents beyond leading power*, *Nucl. Phys. B* **643** (2002) 431–476, [[hep-ph/0206152](#)].
- [74] M. Beneke and T. Feldmann, *Multipole-expanded soft collinear effective theory with non-Abelian gauge symmetry*, *Phys. Lett. B* **553** (2003) 267–276, [[hep-ph/0211358](#)].

- [75] L. Cieri, C. Oleari and M. Rocco, *Higher-order power corrections in a transverse-momentum cut for colour-singlet production at NLO*, *Eur. Phys. J. C* **79** (2019) 852, [[1906.09044](#)].
- [76] M. A. Ebert, I. Moult, I. W. Stewart, F. J. Tackmann, G. Vita and H. X. Zhu, *Subleading power rapidity divergences and power corrections for q_T* , *JHEP* **04** (2019) 123, [[1812.08189](#)].
- [77] R. Goerke and M. Luke, *Power Counting and Modes in SCET*, *JHEP* **02** (2018) 147, [[1711.09136](#)].
- [78] A. V. Manohar, *Deep inelastic scattering as $x \rightarrow 1$ using soft collinear effective theory*, *Phys. Rev. D* **68** (2003) 114019, [[hep-ph/0309176](#)].
- [79] C. W. Bauer, D. Pirjol and I. W. Stewart, *Factorization and endpoint singularities in heavy to light decays*, *Phys. Rev. D* **67** (2003) 071502, [[hep-ph/0211069](#)].
- [80] J.-y. Chiu, A. Jain, D. Neill and I. Z. Rothstein, *A Formalism for the Systematic Treatment of Rapidity Logarithms in Quantum Field Theory*, *JHEP* **05** (2012) 084, [[1202.0814](#)].
- [81] C. W. Bauer, F. J. Tackmann, J. R. Walsh and S. Zuberi, *Factorization and Resummation for Dijet Invariant Mass Spectra*, *Phys. Rev. D* **85** (2012) 074006, [[1106.6047](#)].
- [82] M. Beneke and V. A. Smirnov, *Asymptotic expansion of Feynman integrals near threshold*, *Nucl. Phys. B* **522** (1998) 321–344, [[hep-ph/9711391](#)].
- [83] S. M. Freedman and R. Goerke, *Renormalization of Subleading Dijet Operators in Soft-Collinear Effective Theory*, *Phys. Rev. D* **90** (2014) 114010, [[1408.6240](#)].
- [84] J.-y. Chiu, F. Golf, R. Kelley and A. V. Manohar, *Electroweak Corrections in High Energy Processes using Effective Field Theory*, *Phys. Rev. D* **77** (2008) 053004, [[0712.0396](#)].
- [85] T. Becher, G. Bell and M. Neubert, *Factorization and Resummation for Jet Broadening*, *Phys. Lett. B* **704** (2011) 276–283, [[1104.4108](#)].
- [86] T. Becher and G. Bell, *Enhanced nonperturbative effects through the collinear anomaly*, *Phys. Rev. Lett.* **112** (2014) 182002, [[1312.5327](#)].
- [87] Z. L. Liu and M. Neubert, *Factorization at subleading power and endpoint-divergent convolutions in $h \rightarrow \gamma\gamma$ decay*, *JHEP* **04** (2020) 033, [[1912.08818](#)].
- [88] Z. L. Liu, B. Mecaj, M. Neubert and X. Wang, *Factorization at subleading power, Sudakov resummation, and endpoint divergences in soft-collinear effective theory*, *Phys. Rev. D* **104** (2021) 014004, [[2009.04456](#)].
- [89] Z. L. Liu, B. Mecaj, M. Neubert and X. Wang, *Factorization at subleading power and endpoint divergences in $h \rightarrow \gamma\gamma$ decay. Part II. Renormalization and scale evolution*, *JHEP* **01** (2021) 077, [[2009.06779](#)].
- [90] X. Wang, *Next-to-leading power SCET in Higgs amplitudes induced by light quarks*, in *15th International Symposium on Radiative Corrections: Applications of Quantum Field Theory to Phenomenology AND LoopFest XIX: Workshop on Radiative Corrections for the LHC and Future Colliders*, 10, 2021, [2110.05174](#).
- [91] I. Moult, I. W. Stewart and G. Vita, *Subleading Power Factorization with Radiative Functions*, *JHEP* **11** (2019) 153, [[1905.07411](#)].
- [92] G. T. Bodwin, J.-H. Ee, J. Lee and X.-P. Wang, *Renormalization of the radiative jet function*, [2107.07941](#).

- [93] J. Polchinski, *Effective field theory and the Fermi surface*, in *Theoretical Advanced Study Institute (TASI 92): From Black Holes and Strings to Particles*, 1992, [hep-th/9210046](#).
- [94] H. Georgi, *Effective field theory*, *Ann. Rev. Nucl. Part. Sci.* **43** (1993) 209–252.
- [95] D. B. Kaplan, *Effective field theories*, in *7th Summer School in Nuclear Physics Symmetries*, 1995, [nucl-th/9506035](#).
- [96] I. Z. Rothstein, *TASI lectures on effective field theories*, 8, 2003, [hep-ph/0308266](#).
- [97] A. V. Manohar, *Introduction to Effective Field Theories*, *Les Houches Lect. Notes* **108** (2020) , [[1804.05863](#)].
- [98] A. F. Falk, H. Georgi, B. Grinstein and M. B. Wise, *Heavy Meson Form-factors From QCD*, *Nucl. Phys. B* **343** (1990) 1–13.
- [99] A. F. Falk and B. Grinstein, *Power corrections to leading logs and their application to heavy quark decays*, *Physics Letters B* **247** (1990) 406–411.
- [100] A. F. Falk, M. Neubert and M. E. Luke, *The Residual mass term in the heavy quark effective theory*, *Nucl. Phys. B* **388** (1992) 363–375, [[hep-ph/9204229](#)].
- [101] M. Neubert, *Heavy quark symmetry*, *Phys. Rept.* **245** (1994) 259–396, [[hep-ph/9306320](#)].
- [102] M. B. Wise, *HQET and exclusive B decays*, *Nucl. Instrum. Meth. A* **408** (1998) 1–6, [[hep-ph/9803247](#)].
- [103] R. Abbate, M. Fickinger, A. H. Hoang, V. Mateu and I. W. Stewart, *Thrust at N^3LL with Power Corrections and a Precision Global Fit for $\alpha_s(m_Z)$* , *Phys. Rev. D* **83** (2011) 074021, [[1006.3080](#)].
- [104] R. Brüser, Z. L. Liu and M. Stahlhofen, *Three-loop soft function for heavy-to-light quark decays*, *JHEP* **03** (2020) 071, [[1911.04494](#)].
- [105] C. W. Bauer and A. V. Manohar, *Shape function effects in $B \rightarrow X_s \gamma$ and $B \rightarrow X_u \ell \bar{\nu}$ decays*, *Phys. Rev. D* **70** (2004) 034024, [[hep-ph/0312109](#)].
- [106] M. Neubert, *Renormalization-group improved calculation of the $B \rightarrow X_s \gamma$ branching ratio*, *Eur. Phys. J. C* **40** (2005) 165–186, [[hep-ph/0408179](#)].
- [107] S. W. Bosch, B. O. Lange, M. Neubert and G. Paz, *Factorization and shape function effects in inclusive B meson decays*, *Nucl. Phys. B* **699** (2004) 335–386, [[hep-ph/0402094](#)].
- [108] J.-y. Chiu, R. Kelley and A. V. Manohar, *Electroweak Corrections using Effective Field Theory: Applications to the LHC*, *Phys. Rev. D* **78** (2008) 073006, [[0806.1240](#)].
- [109] T. Becher and M. D. Schwartz, *A precise determination of α_s from LEP thrust data using effective field theory*, *JHEP* **07** (2008) 034, [[0803.0342](#)].
- [110] A. H. Hoang, D. W. Kolodrubetz, V. Mateu and I. W. Stewart, *State-of-the-art predictions for C-parameter and a determination of α_s* , *Nucl. Part. Phys. Proc.* **273-275** (2016) 2015–2021, [[1501.04753](#)].
- [111] T. Becher, M. Neubert and G. Xu, *Dynamical Threshold Enhancement and Resummation in Drell-Yan Production*, *JHEP* **07** (2008) 030, [[0710.0680](#)].
- [112] G. Das, S.-O. Moch and A. Vogt, *Soft corrections to inclusive DIS at four loops and beyond*, *PoS DIS* **2019** (2019) 010, [[1908.03071](#)].

- [113] A. H. Hoang, D. W. Kolodrubetz, V. Mateu and I. W. Stewart, *C-parameter distribution at $N^3 LL$ including power corrections*, *Phys. Rev. D* **91** (2015) 094017, [[1411.6633](#)].
- [114] A. F. Falk and B. Grinstein, *Power corrections to leading logs and their application to heavy quark decays*, *Phys. Lett. B* **247** (1990) 406–411.
- [115] A. F. Falk, B. Grinstein and M. E. Luke, *Leading mass corrections to the heavy quark effective theory*, *Nucl. Phys. B* **357** (1991) 185–207.
- [116] M. E. Luke, *Effects of subleading operators in the heavy quark effective theory*, *Phys. Lett. B* **252** (1990) 447–455.
- [117] D. Pirjol and I. W. Stewart, *A Complete basis for power suppressed collinear ultrasoft operators*, *Phys. Rev. D* **67** (2003) 094005, [[hep-ph/0211251](#)].
- [118] R. J. Hill, T. Becher, S. J. Lee and M. Neubert, *Sudakov resummation for subleading SCET currents and heavy-to-light form-factors*, *JHEP* **07** (2004) 081, [[hep-ph/0404217](#)].
- [119] I. Moult, I. W. Stewart, G. Vita and H. X. Zhu, *First Subleading Power Resummation for Event Shapes*, *JHEP* **08** (2018) 013, [[1804.04665](#)].
- [120] M. Beneke, A. Broggio, M. Garny, S. Jaskiewicz, R. Szafron, L. Vernazza et al., *Leading-logarithmic threshold resummation of the Drell-Yan process at next-to-leading power*, *JHEP* **03** (2019) 043, [[1809.10631](#)].
- [121] M. Beneke, M. Garny, S. Jaskiewicz, R. Szafron, L. Vernazza and J. Wang, *Leading-logarithmic threshold resummation of Higgs production in gluon fusion at next-to-leading power*, *JHEP* **01** (2020) 094, [[1910.12685](#)].
- [122] A. Bhattacharya, I. Moult, I. W. Stewart and G. Vita, *Helicity Methods for High Multiplicity Subleading Soft and Collinear Limits*, *JHEP* **05** (2019) 192, [[1812.06950](#)].
- [123] I. Moult, G. Vita and K. Yan, *Subleading power resummation of rapidity logarithms: the energy-energy correlator in $\mathcal{N} = 4$ SYM*, *JHEP* **07** (2020) 005, [[1912.02188](#)].
- [124] M. Kramer, E. Laenen and M. Spira, *Soft gluon radiation in Higgs boson production at the LHC*, *Nucl. Phys. B* **511** (1998) 523–549, [[hep-ph/9611272](#)].
- [125] A. A. Penin, *High-Energy Limit of Quantum Electrodynamics beyond Sudakov Approximation*, *Phys. Lett. B* **745** (2015) 69–72, [[1412.0671](#)].
- [126] N. Bahjat-Abbas, D. Bonocore, J. Sinnenhe Damsté, E. Laenen, L. Magnea, L. Vernazza et al., *Diagrammatic resummation of leading-logarithmic threshold effects at next-to-leading power*, *JHEP* **11** (2019) 002, [[1905.13710](#)].
- [127] M. van Beekveld, E. Laenen, J. Sinnenhe Damsté and L. Vernazza, *Next-to-leading power threshold corrections for finite order and resummed colour-singlet cross sections*, *JHEP* **05** (2021) 114, [[2101.07270](#)].
- [128] C. Oleari and M. Rocco, *Power corrections in a transverse-momentum cut for vector-boson production at NNLO: the $q\bar{q}$ -initiated real-virtual contribution*, *Eur. Phys. J. C* **81** (2021) 183, [[2012.10538](#)].
- [129] R. Boughezal, A. Isgrò and F. Petriello, *Next-to-leading power corrections to $V + 1$ jet production in N -jettiness subtraction*, *Phys. Rev. D* **101** (2020) 016005, [[1907.12213](#)].

- [130] E. Laenen, J. Sinnenhe Damst , L. Vernazza, W. Waalewijn and L. Zoppi, *Towards all-order factorization of QED amplitudes at next-to-leading power*, *Phys. Rev. D* **103** (2021) 034022, [[2008.01736](#)].
- [131] CMS collaboration, A. M. Sirunyan et al., *Measurements of differential Z boson production cross sections in proton-proton collisions at $\sqrt{s} = 13$ TeV*, *JHEP* **12** (2019) 061, [[1909.04133](#)].
- [132] A. H. Hoang, D. W. Kolodrubetz, V. Mateu and I. W. Stewart, *Precise determination of α_s from the C-parameter distribution*, *Phys. Rev. D* **91** (2015) 094018, [[1501.04111](#)].
- [133] M. E. Peskin and D. V. Schroeder, *An Introduction to quantum field theory*. Addison-Wesley, Reading, USA, 1995.
- [134] M. Luke, *Bottom Quark Physics and the Heavy Quark Expansion, Particle Physics and Cosmology: The Quest for Physics Beyond the Standard Model (TASI 2002)* (2002) .
- [135] A. Ali and G. Kramer, *Jets and QCD: A Historical Review of the Discovery of the Quark and Gluon Jets and its Impact on QCD*, *Eur. Phys. J. H* **36** (2011) 245–326, [[1012.2288](#)].
- [136] G. Marchesini and B. R. Webber, *Simulation of QCD Jets Including Soft Gluon Interference*, *Nucl. Phys. B* **238** (1984) 1–29.
- [137] G. Hanson et al., *Evidence for Jet Structure in Hadron Production by e^+e^- Annihilation*, *Phys. Rev. Lett.* **35** (1975) 1609–1612.
- [138] T. Sjostrand and P. Z. Skands, *Transverse-momentum-ordered showers and interleaved multiple interactions*, *Eur. Phys. J. C* **39** (2005) 129–154, [[hep-ph/0408302](#)].
- [139] M. L. Mangano and T. J. Stelzer, *Tools for the simulation of hard hadronic collisions*, *Ann. Rev. Nucl. Part. Sci.* **55** (2005) 555–588.
- [140] D. M. Binnie et al., *The Tasso Vertex Detector*, *Nucl. Instrum. Meth. A* **228** (1985) 267.
- [141] B. H. Wiik, *First Results from PETRA*, *Conf. Proc. C* **7906181** (1979) 113–154.
- [142] W. M.-Y. Cheung, M. Luke and S. Zuberi, *Phase Space and Jet Definitions in SCET*, *Phys. Rev. D* **80** (2009) 114021, [[0910.2479](#)].
- [143] S. D. Ellis, C. K. Vermilion, J. R. Walsh, A. Hornig and C. Lee, *Jet Shapes and Jet Algorithms in SCET*, *JHEP* **11** (2010) 101, [[1001.0014](#)].
- [144] N. Brown and W. J. Stirling, *Jet cross-sections at leading double logarithm in e^+e^- annihilation*, *Phys. Lett. B* **252** (1990) 657–662.
- [145] Y. L. Dokshitzer, G. D. Leder, S. Moretti and B. R. Webber, *Better jet clustering algorithms*, *JHEP* **08** (1997) 001, [[hep-ph/9707323](#)].
- [146] M. D. Schwartz, *Resummation and NLO matching of event shapes with effective field theory*, *Phys. Rev. D* **77** (2008) 014026, [[0709.2709](#)].
- [147] B. D. Pecjak, *Non-factorizable contributions to deep inelastic scattering at large x* , *JHEP* **10** (2005) 040, [[hep-ph/0506269](#)].
- [148] T. Becher, M. Neubert and B. D. Pecjak, *Factorization and Momentum-Space Resummation in Deep-Inelastic Scattering*, *JHEP* **01** (2007) 076, [[hep-ph/0607228](#)].

- [149] A. V. Manohar, *Infrared scales and factorization in QCD*, *Phys. Lett. B* **633** (2006) 729–733, [[hep-ph/0512173](#)].
- [150] C. W. Bauer, D. Pirjol and I. W. Stewart, *On Power suppressed operators and gauge invariance in SCET*, *Phys. Rev. D* **68** (2003) 034021, [[hep-ph/0303156](#)].
- [151] A. J. Larkoski, I. Moult and D. Neill, *Toward Multi-Differential Cross Sections: Measuring Two Angularities on a Single Jet*, *JHEP* **09** (2014) 046, [[1401.4458](#)].
- [152] M. Procura, W. J. Waalewijn and L. Zeune, *Resummation of Double-Differential Cross Sections and Fully-Unintegrated Parton Distribution Functions*, *JHEP* **02** (2015) 117, [[1410.6483](#)].
- [153] A. J. Larkoski, I. Moult and D. Neill, *Non-Global Logarithms, Factorization, and the Soft Substructure of Jets*, *JHEP* **09** (2015) 143, [[1501.04596](#)].
- [154] P. Pietrulewicz, F. J. Tackmann and W. J. Waalewijn, *Factorization and Resummation for Generic Hierarchies between Jets*, *JHEP* **08** (2016) 002, [[1601.05088](#)].
- [155] M. Procura, W. J. Waalewijn and L. Zeune, *Joint resummation of two angularities at next-to-next-to-leading logarithmic order*, *JHEP* **10** (2018) 098, [[1806.10622](#)].
- [156] R. Abbate, M. Fickinger, A. H. Hoang, V. Mateu and I. W. Stewart, *Precision Thrust Cumulant Moments at $N^3 LL$* , *Phys. Rev. D* **86** (2012) 094002, [[1204.5746](#)].
- [157] S. Bethke, *World summary of α_s* , *Nuclear Physics B - Proceedings Supplements* **234** (2013) 229 – 234.
- [158] G. Kramer and B. Lampe, *Jet Cross-Sections in e^+e^- Annihilation*, *Fortsch. Phys.* **37** (1989) 161.
- [159] Y.-T. Chien and M. D. Schwartz, *Resummation of heavy jet mass and comparison to LEP data*, *JHEP* **08** (2010) 058, [[1005.1644](#)].
- [160] I. Moult, L. Rothen, I. W. Stewart, F. J. Tackmann and H. X. Zhu, *Subleading Power Corrections for N-Jettiness Subtractions*, *Phys. Rev. D* **95** (2017) 074023, [[1612.00450](#)].
- [161] R. Boughezal, X. Liu and F. Petriello, *Power Corrections in the N-jettiness Subtraction Scheme*, *JHEP* **03** (2017) 160, [[1612.02911](#)].
- [162] S. M. Freedman, *Subleading Corrections To Thrust Using Effective Field Theory*, [1303.1558](#).
- [163] S. M. Freedman and M. Luke, *SCET, QCD and Wilson Lines*, *Phys. Rev. D* **85** (2012) 014003, [[1107.5823](#)].
- [164] I. Feige and M. D. Schwartz, *An on-shell approach to factorization*, *Phys. Rev. D* **88** (2013) 065021, [[1306.6341](#)].
- [165] I. Feige and M. D. Schwartz, *Hard-Soft-Collinear Factorization to All Orders*, *Phys. Rev. D* **90** (2014) 105020, [[1403.6472](#)].
- [166] A. Hornig, C. Lee, I. W. Stewart, J. R. Walsh and S. Zuberi, *Non-global Structure of the $O(\alpha_s^2)$ Dijet Soft Function*, *JHEP* **08** (2011) 054, [[1105.4628](#)].
- [167] I. Moult, I. W. Stewart, F. J. Tackmann and W. J. Waalewijn, *Employing Helicity Amplitudes for Resummation*, *Phys. Rev. D* **93** (2016) 094003, [[1508.02397](#)].
- [168] D. W. Kolodrubetz, I. Moult and I. W. Stewart, *Building Blocks for Subleading Helicity Operators*, *JHEP* **05** (2016) 139, [[1601.02607](#)].

- [169] I. Feige, D. W. Kolodrubetz, I. Moult and I. W. Stewart, *A Complete Basis of Helicity Operators for Subleading Factorization*, *JHEP* **11** (2017) 142, [[1703.03411](#)].
- [170] C. W. Bauer, C. Lee, A. V. Manohar and M. B. Wise, *Enhanced nonperturbative effects in Z decays to hadrons*, *Phys. Rev.* **D70** (2004) 034014, [[hep-ph/0309278](#)].
- [171] R. N. Lee, A. V. Smirnov and V. A. Smirnov, *Analytic Results for Massless Three-Loop Form Factors*, *JHEP* **04** (2010) 020, [[1001.2887](#)].
- [172] A. V. Manohar and I. W. Stewart, *The Zero-Bin and Mode Factorization in Quantum Field Theory*, *Phys. Rev.* **D76** (2007) 074002, [[hep-ph/0605001](#)].
- [173] J.-y. Chiu, A. Fuhrer, A. H. Hoang, R. Kelley and A. V. Manohar, *Soft-Collinear Factorization and Zero-Bin Subtractions*, *Phys. Rev.* **D79** (2009) 053007, [[0901.1332](#)].
- [174] L. F. Abbott, *Introduction to the Background Field Method*, *Acta Phys. Polon.* **B13** (1982) 33.
- [175] M. Inglis-Whalen, M. Luke and A. Spourdalakis, *Rapidity logarithms in SCET without modes*, *Nucl. Phys. A* **1014** (2021) 122260, [[2005.13063](#)].
- [176] M. Procura, W. J. Waalewijn and L. Zeune, *Joint resummation of two angularities at next-to-next-to-leading logarithmic order*, *JHEP* **10** (2018) 098, [[1806.10622](#)].
- [177] I. Z. Rothstein and I. W. Stewart, *An Effective Field Theory for Forward Scattering and Factorization Violation*, *JHEP* **08** (2016) 025, [[1601.04695](#)].
- [178] C. W. Bauer, B. O. Lange and G. Ovanesyan, *On Glauber modes in Soft-Collinear Effective Theory*, *JHEP* **07** (2011) 077, [[1010.1027](#)].
- [179] R. Goerke and M. Inglis-Whalen, *Renormalization of dijet operators at order $1/Q^2$ in soft-collinear effective theory*, *JHEP* **05** (2018) 023, [[1711.09147](#)].
- [180] V. A. Smirnov, *Asymptotic expansions of two loop Feynman diagrams in the Sudakov limit*, *Phys. Lett. B* **404** (1997) 101–107, [[hep-ph/9703357](#)].
- [181] M. Beneke and T. Feldmann, *Factorization of heavy to light form-factors in soft collinear effective theory*, *Nucl. Phys. B* **685** (2004) 249–296, [[hep-ph/0311335](#)].
- [182] J.-y. Chiu, A. Jain, D. Neill and I. Z. Rothstein, *The Rapidity Renormalization Group*, *Phys. Rev. Lett.* **108** (2012) 151601, [[1104.0881](#)].
- [183] J.-y. Chiu, F. Golf, R. Kelley and A. V. Manohar, *Electroweak Sudakov corrections using effective field theory*, *Phys. Rev. Lett.* **100** (2008) 021802, [[0709.2377](#)].
- [184] A. H. Mueller, *Perturbative QCD*. WORLD SCIENTIFIC, 1989, [10.1142/0494](#).
- [185] T. Becher and G. Bell, *NNLL Resummation for Jet Broadening*, *JHEP* **11** (2012) 126, [[1210.0580](#)].
- [186] J. Chay, C. Kim, Y. G. Kim and J.-P. Lee, *Soft Wilson lines in soft-collinear effective theory*, *Phys. Rev. D* **71** (2005) 056001, [[hep-ph/0412110](#)].
- [187] C. M. Arnesen, J. Kundu and I. W. Stewart, *Constraint equations for heavy-to-light currents in SCET*, *Phys. Rev. D* **72** (2005) 114002, [[hep-ph/0508214](#)].
- [188] C. Lee and G. F. Sterman, *Momentum Flow Correlations from Event Shapes: Factorized Soft Gluons and Soft-Collinear Effective Theory*, *Phys. Rev. D* **75** (2007) 014022, [[hep-ph/0611061](#)].

- [189] A. Idilbi and T. Mehen, *On the equivalence of soft and zero-bin subtractions*, *Phys. Rev. D* **75** (2007) 114017, [[hep-ph/0702022](#)].
- [190] A. Idilbi and T. Mehen, *Demonstration of the equivalence of soft and zero-bin subtractions*, *Phys. Rev. D* **76** (2007) 094015, [[0707.1101](#)].
- [191] Y. Li, D. Neill and H. X. Zhu, *An Exponential Regulator for Rapidity Divergences*, [1604.00392](#).
- [192] I. W. Stewart, F. J. Tackmann and W. J. Waalewijn, *Factorization at the LHC: From PDFs to Initial State Jets*, *Phys. Rev. D* **81** (2010) 094035, [[0910.0467](#)].
- [193] M. G. Echevarria, A. Idilbi and I. Scimemi, *Definition and Evolution of Transverse Momentum Distributions*, *Int. J. Mod. Phys. Conf. Ser.* **20** (2012) 92–108, [[1209.3892](#)].
- [194] J. Chay and C. Kim, *Structure of divergences in Drell-Yan process with small transverse momentum*, *Phys. Rev. D* **86** (2012) 074011, [[1208.0662](#)].
- [195] T. Becher and X. Garcia i Tormo, *Factorization and resummation for transverse thrust*, *JHEP* **06** (2015) 071, [[1502.04136](#)].
- [196] C. W. Bauer, N. D. Dunn and A. Hornig, *Factorization of Boosted Multijet Processes for Threshold Resummation*, *Phys. Rev. D* **82** (2010) 054012, [[1002.1307](#)].
- [197] M. Inglis-Whalen, M. Luke, J. Roy and A. Spourdalakis, *Factorization of Power Corrections in the Drell-Yan Process in EFT*, *Phys. Rev. D* **104** (2021) 076018, [[2105.09277](#)].
- [198] J. C. Collins, D. E. Soper and G. F. Sterman, *Factorization of Hard Processes in QCD*, *Adv. Ser. Direct. High Energy Phys.* **5** (1989) 1–91, [[hep-ph/0409313](#)].
- [199] R. K. Ellis, W. J. Stirling and B. R. Webber, *QCD and Collider Physics*. Cambridge Monographs on Particle Physics, Nuclear Physics and Cosmology. Cambridge University Press, 1996, [10.1017/CBO9780511628788](#).
- [200] Y. L. Dokshitzer, D. Diakonov and S. I. Troian, *Hard Processes in Quantum Chromodynamics*, *Phys. Rept.* **58** (1980) 269–395.
- [201] Y. L. Dokshitzer, D. Diakonov and S. I. Troian, *On the Transverse Momentum Distribution of Massive Lepton Pairs*, *Phys. Lett. B* **79** (1978) 269–272.
- [202] G. Parisi and R. Petronzio, *Small Transverse Momentum Distributions in Hard Processes*, *Nucl. Phys. B* **154** (1979) 427–440.
- [203] G. Curci, M. Greco and Y. Srivastava, *QCD Jets From Coherent States*, *Nucl. Phys. B* **159** (1979) 451–468.
- [204] R. K. Ellis and S. Veseli, *W and Z transverse momentum distributions: Resummation in q_T space*, *Nucl. Phys. B* **511** (1998) 649–669, [[hep-ph/9706526](#)].
- [205] S. Frixione, P. Nason and G. Ridolfi, *Problems in the resummation of soft gluon effects in the transverse momentum distributions of massive vector bosons in hadronic collisions*, *Nucl. Phys. B* **542** (1999) 311–328, [[hep-ph/9809367](#)].
- [206] C. T. H. Davies and W. J. Stirling, *Nonleading Corrections to the Drell-Yan Cross-Section at Small Transverse Momentum*, *Nucl. Phys. B* **244** (1984) 337–348.

- [207] C. T. H. Davies, B. R. Webber and W. J. Stirling, *Drell-Yan cross sections at small transverse momentum*, *Nucl. Phys. B* **256** (1984) 413–433.
- [208] D. de Florian and M. Grazzini, *Next-to-next-to-leading logarithmic corrections at small transverse momentum in hadronic collisions*, *Phys. Rev. Lett.* **85** (2000) 4678–4681, [[hep-ph/0008152](#)].
- [209] G. Bozzi, S. Catani, G. Ferrera, D. de Florian and M. Grazzini, *Production of Drell-Yan lepton pairs in hadron collisions: Transverse-momentum resummation at next-to-next-to-leading logarithmic accuracy*, *Phys. Lett. B* **696** (2011) 207–213, [[1007.2351](#)].
- [210] S. Catani, D. de Florian, G. Ferrera and M. Grazzini, *Vector boson production at hadron colliders: transverse-momentum resummation and leptonic decay*, *JHEP* **12** (2015) 047, [[1507.06937](#)].
- [211] R. K. Ellis, G. Martinelli and R. Petronzio, *Lepton Pair Production at Large Transverse Momentum in Second Order QCD*, *Nucl. Phys. B* **211** (1983) 106–138.
- [212] R. J. Gonsalves, J. Pawłowski and C.-F. Wai, *QCD Radiative Corrections to Electroweak Boson Production at Large Transverse Momentum in Hadron Collisions*, *Phys. Rev. D* **40** (1989) 2245.
- [213] C. W. Bauer, A. V. Manohar and P. F. Monni, *Disentangling observable dependence in SCETI and SCETII anomalous dimensions: singularities at two loops*, [2012.09213](#).
- [214] J. C. Collins and A. Metz, *Universality of soft and collinear factors in hard-scattering factorization*, *Phys. Rev. Lett.* **93** (2004) 252001, [[hep-ph/0408249](#)].
- [215] M. Diehl, J. R. Gaunt, D. Ostermeier, P. Plößl and A. Schäfer, *Cancellation of Glauber gluon exchange in the double Drell-Yan process*, *JHEP* **01** (2016) 076, [[1510.08696](#)].
- [216] K. S. M. Lee and I. W. Stewart, *Factorization for power corrections to $B \rightarrow X_s \gamma$ and $B \rightarrow X_u \ell \bar{\nu}$* , *Nucl. Phys. B* **721** (2005) 325–406, [[hep-ph/0409045](#)].
- [217] J. Chay and C. Kim, *Collinear effective theory at subleading order and its application to heavy - light currents*, *Phys. Rev. D* **65** (2002) 114016, [[hep-ph/0201197](#)].
- [218] A. V. Manohar, T. Mehen, D. Pirjol and I. W. Stewart, *Reparameterization invariance for collinear operators*, *Phys. Lett. B* **539** (2002) 59–66, [[hep-ph/0204229](#)].
- [219] I. Moult, I. W. Stewart, G. Vita and H. X. Zhu, *The Soft Quark Sudakov*, *JHEP* **05** (2020) 089, [[1910.14038](#)].
- [220] M. Beneke, A. Broggio, S. Jaskiewicz and L. Vernazza, *Threshold factorization of the Drell-Yan process at next-to-leading power*, *JHEP* **07** (2020) 078, [[1912.01585](#)].
- [221] M. Beneke, M. Garny, R. Szafron and J. Wang, *Violation of the Kluberg-Stern-Zuber theorem in SCET*, *JHEP* **09** (2019) 101, [[1907.05463](#)].
- [222] G. Paz, *Subleading Jet Functions in Inclusive B Decays*, *JHEP* **06** (2009) 083, [[0903.3377](#)].
- [223] J. C. Collins and D. E. Soper, *Parton Distribution and Decay Functions*, *Nucl. Phys. B* **194** (1982) 445–492.